

NASA/TP-2005-213537



Third Generation Wireless Phone Threat Assessment for Aircraft Communication and Navigation Radios

*Truong X. Nguyen, Sandra V. Koppen,
Laura J. Smith and Reuben A. Williams
Langley Research Center, Hampton, Virginia*

*Maria Theresa P. Salud
Lockheed Martin, Hampton, Virginia*

March 2005

The NASA STI Program Office ... in Profile

Since its founding, NASA has been dedicated to the advancement of aeronautics and space science. The NASA Scientific and Technical Information (STI) Program Office plays a key part in helping NASA maintain this important role.

The NASA STI Program Office is operated by Langley Research Center, the lead center for NASA's scientific and technical information. The NASA STI Program Office provides access to the NASA STI Database, the largest collection of aeronautical and space science STI in the world. The Program Office is also NASA's institutional mechanism for disseminating the results of its research and development activities. These results are published by NASA in the NASA STI Report Series, which includes the following report types:

- TECHNICAL PUBLICATION. Reports of completed research or a major significant phase of research that present the results of NASA programs and include extensive data or theoretical analysis. Includes compilations of significant scientific and technical data and information deemed to be of continuing reference value. NASA counterpart of peer-reviewed formal professional papers, but having less stringent limitations on manuscript length and extent of graphic presentations.
- TECHNICAL MEMORANDUM. Scientific and technical findings that are preliminary or of specialized interest, e.g., quick release reports, working papers, and bibliographies that contain minimal annotation. Does not contain extensive analysis.
- CONTRACTOR REPORT. Scientific and technical findings by NASA-sponsored contractors and grantees.
- CONFERENCE PUBLICATION. Collected papers from scientific and technical conferences, symposia, seminars, or other meetings sponsored or co-sponsored by NASA.
- SPECIAL PUBLICATION. Scientific, technical, or historical information from NASA programs, projects, and missions, often concerned with subjects having substantial public interest.
- TECHNICAL TRANSLATION. English-language translations of foreign scientific and technical material pertinent to NASA's mission.

Specialized services that complement the STI Program Office's diverse offerings include creating custom thesauri, building customized databases, organizing and publishing research results ... even providing videos.

For more information about the NASA STI Program Office, see the following:

- Access the NASA STI Program Home Page at <http://www.sti.nasa.gov>
- E-mail your question via the Internet to help@sti.nasa.gov
- Fax your question to the NASA STI Help Desk at (301) 621-0134
- Phone the NASA STI Help Desk at (301) 621-0390
- Write to:
NASA STI Help Desk
NASA Center for Aerospace Information
7121 Standard Drive
Hanover, MD 21076-1320

NASA/TP-2005-213537



Third Generation Wireless Phone Threat Assessment for Aircraft Communication and Navigation Radios

*Truong X. Nguyen, Sandra V. Koppen,
Laura J. Smith and Reuben A. Williams
Langley Research Center, Hampton, Virginia*

*Maria Theresa P. Salud
Lockheed Martin, Hampton, Virginia*

National Aeronautics and
Space Administration

Langley Research Center
Hampton, Virginia 23681-2199

March 2005

Acknowledgments

This work was funded by the Federal Aviation Administration as part of FAA/NASA Interagency Agreement DFTA03-96-X-90001, Revision 9, as well as the NASA Aviation Safety Program (Single Aircraft Accident Prevention Project)

The authors wish to express their gratitude to Dave Walen, John Dimtroff, and Tony Wilson of the Federal Aviation Administration for their continuing support and technical direction.

The authors are grateful to Paul Guckian, John Forrester, Faraz Faheem, Hussein Hachem, and others at Qualcomm for providing tutorials on basic wireless phone technologies and on the use of the Agilent 8960 for controlling the phones. They also helped in troubleshooting the connectivity problems between the Agilent 8960 and the wireless phones that were critical in the timely completion of this report.

Special thanks are extended to United Airlines and Eagle Wings Incorporated for the Boeing 737-200 full-aircraft path-loss data collected in collaboration with members from NASA LaRC. Full aircraft path loss data were used in the multiple-equipment-factor analysis.

The authors are also indebted to Dominick Marciano, Kalpesh Patel and Louis LaMedica of Verizon Wireless for allowing us to visit their phone test facility and for their guidance in using the Agilent 8960.

The authors also received assistance from:

- Richard Larios of Cingular for help in buying GSM phones without service contracts.
- David Shively of Cingular, Joseph Morrissey of Motorola, and Kwok Chan of the FCC for providing guidance in selecting the Base-Station Simulator for the testing efforts.
- David Burch of Research-In-Motion for the loan of a CDMA Blackberry for testing. We were allowed to retain the unit for several months while learning to use the base-station simulator and refine our test process.

Their help is greatly appreciated.

The authors offer their appreciation to Dr. John Beggs for serving as liaison to the NASA LaRC Financial Accounting Services Branch and development of an Estimated Price Report for the FAA/NASA Interagency Agreement.

The authors would also like to thank Jay Ely, Celeste Belcastro, Robin Cravey and Courtney Rollins for their assistance in technical and editorial editing.

Disclaimer: The authors alone made all the decisions in the selection of phone models, test modes and test procedures. The selections reflect the authors' understanding of the wireless technology at the time. At no time during the process did the authors receive any special influence that negatively affected the test process and the results.

<p>The use of trademarks or names of manufacturers in this report is for accurate reporting and does not constitute an official endorsement, either expressed or implied, of such products or manufacturers by the National Aeronautics and Space Administration.</p>

Available from:

NASA Center for AeroSpace Information (CASI)
7121 Standard Drive
Hanover, MD 21076-1320
(301) 621-0390

National Technical Information Service (NTIS)
5285 Port Royal Road
Springfield, VA 22161-2171
(703) 605-6000

Table of Contents

Table of Contents	iii
Acronyms	v
List of Symbols	vii
Abstract	ix
1 Executive Summary	ix
2 Introduction	1
2.1 <i>Objective</i>	2
2.2 <i>Scope</i>	2
2.3 <i>Approach</i>	2
2.3.1 Emission Measurements of Wireless Phones	3
2.3.2 Path Loss Measurements.....	4
2.3.3 Safety Margin Calculations.....	5
2.3.4 Multiple Equipment Factor Calculations	5
2.4 <i>Report Organization</i>	5
3 Wireless Phones and Radio RF Emissions	6
3.1 <i>Wireless Phone Overview and Phone Settings</i>	6
3.1.1 GSM/GPRS Overview	6
3.1.2 CDMA2000 Overview	10
3.2 <i>Wireless Phone Test Modes Selection</i>	14
3.2.1 Phone Controls.....	15
3.2.2 GSM/GPRS Phone Test Modes	16
3.2.3 CDMA Phone Test Modes.....	19
3.3 <i>Measurement Process</i>	22
3.3.1 Measurement Method	22
3.3.2 Device-Focused Testing.....	28
3.3.3 Data Reduction.....	35
3.4 <i>Wireless Phone Measurement Results</i>	36
3.4.1 GSM/GPRS phones	37
3.4.2 CDMA phones	44
3.4.3 Summary of Emission Data	52
3.5 <i>Baseline Emissions from Standard Laptop Computers and PDA</i>	57
3.6 <i>Summary of Maximum Emissions from Wireless Phones</i>	62
3.6.1 Summary of Maximum Emission Results	62
3.6.2 Emission Limits	63
3.6.3 Measurement Results and Spurious Emission Limit Comparison.....	65
3.6.4 Device Expected Directivity	66
4 Aircraft Interference Path Loss	67
4.1 <i>IPL Measurement Method</i>	68
4.2 <i>Interference Path Loss Results</i>	72
4.2.1 Recent Measured Results	72

4.2.2	Other Interference Path Loss Data.....	73
4.3	<i>Summary of Minimum Interference Path Loss Data</i>	86
5	Interference Analysis	87
5.1	<i>Published Receiver Susceptibility</i>	87
5.1.1	RTCA/DO-233.....	87
5.1.2	RTCA/DO-199.....	87
5.2	<i>Safety Margin Calculations</i>	88
6	Multiple Equipment Cumulative Effects	92
6.1	<i>Approach</i>	92
6.1.1	MEF Formulation.....	92
6.1.2	Assumptions.....	94
6.2	<i>Aircraft Path Loss Measurement</i>	94
6.2.1	Method.....	95
6.2.2	Measurement Results	95
6.3	<i>MEF Based on IPL Measurements</i>	98
6.4	<i>Results of MEF Calculations</i>	99
6.5	<i>Observations</i>	106
7	Summary and Conclusions	107
8	Recommended Future Work.....	108
9	References	109
Appendix A:	CDMA Phone Test Results.....	111
A.1	<i>Band 1</i>	111
A.2	<i>Band 2</i>	119
A.3	<i>Band 3</i>	127
A.4	<i>Band 4</i>	135
A.5	<i>Band 5</i>	144
Appendix B:	GSM Phone Test Results	153
B.1	<i>Band 1</i>	153
B.2	<i>Band 2</i>	162
B.3	<i>Band 3</i>	170
B.4	<i>Band 4</i>	179
B.5	<i>Band 5</i>	187
Appendix C:	Comparisons of MEF Using Window IPL.....	197

Acronyms

1xRTT	1x (one time the number of 1.25 MHz channels) Radio Transmission Technology
1xEV-DO	1xEvolution Data Optimized
1xEV-DV	1xEvolution for Data and Voice
2G, 3G	Second Generation, Third Generation
ATCRBS	Air Traffic Control Radar Beacon System
B737, B747	Boeing 737, 747 Aircraft
BSS	Base Station Simulator
CD	Compact Disc
CDMA	Code Division Multiple Access
CDMA2000	also known as IMT-CDMA Multi-Carrier or 1xRTT
CS	Coding Scheme
CW	Continuous-wave
dB	Decibel
dBi	dB relative to isotropic reference pattern
dBm	dB relative to 1 milliwatt
dB μ V/m	Field strength unit in dB relative to one μ V/m
DME	Distance Measuring Equipment
DUT	Device-Under-Test
DVD	Digital Versatile Disc or Digital Video Disc
EDGE	Enhanced Data rates for Global Evolution
EE	Emergency Exit
EGPRS	Enhanced GPRS (i.e. GPRS protocol with EDGE (8PSK) modulation)
EIRP	Effective Isotropic Radiated Power
EMI	Electromagnetic Interference
ERP	Effective Radiated Power
EWI	Eagle Wings Inc.
FAA	Federal Aviation Administration
FCC	Federal Communications Commission
FDMA	Frequency Division Multiple Access
GHz	Gigahertz

GPRS	General Packet Radio Service
GPS	Global Positioning System
GS	Glideslope
GSM	Global System for Mobile Communication
ICAO	International Civil Aviation Organisation
ILS	Instrument Landing System
IPL	Interference Path Loss
ITU	International Telecommunication Union
kbps	Kilobits per second
LAP1-8	Laptop computers 1-8
LaRC	Langley Research Center
LOC	Localizer
MAX, Max	Maximum
MCC	Mobile Country Code
MNC	Mobile Network Code
MEF	Multiple Equipment Factor calculated using path loss data for aircraft seats
MEF _{window}	Multiple Equipment Factor calculated using window path loss data
MHz	Megahertz
Min	Minimum
MIPL	Minimum Interference Path Loss
MLS	Microwave Landing Systems
MOPS	Minimum Operating Performance Standards
MS	Mobile Station
NASA	National Aeronautics and Space Administration
PCMCIA	Personal Computer Memory Card Interface Adapter Card
PCS	Personal Communications Services
PDA	Personal Digital Assistant
PED(s)	Portable Electronic Device(s)
PRN	Printer
PRBS	Pseudo-Random Binary Sequences
RC	Radio Configuration
RF	Radio Frequency

RFID	Radio Frequency Identification
RTCA	RTCA, Inc.
SAC	Semi-anechoic Chamber
SatCom	Satellite Communication (Aeronautical Mobile Satellite Service)
SIM	Subscriber Identity Module
SO	Service Option
StDev	Standard Deviation
TCAS	Traffic Collision Avoidance System
TDMA	Time Division Multiple Access
T-PED(s)	Transmitting Portable Electronic Device(s)
TRP	Total Radiated Power
UAL	United Airlines
US	United States
VHF-Com 1	VHF-Com radio no. 1
VHF-Com	Very High Frequency Voice Communication
VOR	VHF Omnidirectional Range
WLAN	Wireless Local Area Network

List of Symbols

π	Universal constant = 3.141592654
η_{Tx}	Transmit antenna efficiency factor
A	Device emission power
B	Interference coupling factor, negative of interference path loss in dB
C	Receiver susceptibility threshold
C_i^n	Interference Coupling Factor for aircraft seat n
CF	Chamber Calibration Factor (dB)
CLF	Chamber Loading Factor
D_G	Directivity
E	Electric Field Intensity (V/m)
$EIRP$	Effective Isotropic Radiated Power (W)
IL	Empty chamber Insertion Loss

$L_{Chmbr}(dB)$	Chamber loss (dB), or = $-10\log_{10}(CLF * IL)$
$L_{RecCable}(dB)$	Receive cable loss (dB)
$L_{XmitCable}(dB)$	Transmit cable loss (dB)
P_c	Carrier frequency power
P_{input}	Input power
P_{MaxRec}	Maximum received power measured over one paddle rotation
$P^R(2), P^R(3)$	Power received at points (2) and (3), respectively, in dBm
$P_{SAMeas}(dBm)$	Maximum receive power measured at the spectrum analyzer (dBm) over one stirrer revolution
$P^T(1),$	Power transmitted at point (1), in dBm
P_{TotRad}	Total radiated power within measurement resolution bandwidth
$P_{Xmit}(dBm)$	Power transmitted from source (dBm)
P_{rec}^n	Power at aircraft receiver due to PED transmitter at aircraft seat n
P_{xmit}^n	PED transmitted power at aircraft seat n
R	Distance (m)
Rx	Receive
S/I	Signal-to-Interference Ratio
TRP	Total Radiated Power (within measurement resolution bandwidth)

Abstract

Radiated emissions in aircraft communication and navigation bands are measured from third generation (3G) wireless mobile phones. The two wireless technologies considered are the latest available to general consumers in the US. The measurements are conducted using reverberation chambers. The results are compared against baseline emissions from laptop computers and personal digital assistant devices that are currently allowed to operate on aircraft. Using existing interference path loss data and receivers' interference threshold, a risk assessment is performed for several aircraft communication and navigation radio systems. In addition, cumulative interference effects of multiple similar devices are conservatively estimated or bounded. The effects are computed by summing the interference power from individual devices that is scaled according to the interference path loss at its location.

1 Executive Summary

Wireless technologies have experienced a phenomenal growth in the last several years. Two of the technologies that saw the most growth are wireless phones and wireless local area networks (WLANs). These technologies enabled a revolution in accessibility and productivity. They enable consumers to have convenient access to the internet, email, instant messaging and numerous other applications.

For various reasons, use of wireless phones is currently prohibited by most airlines while the aircraft is in the air. However, with a high percentage of travelers owning wireless phones, occasional unintended use, as well as unauthorized intended use is possible. In addition, vendors are very interested in providing wireless phone service (legally) on airplanes. Recent flight demonstrations show that wireless phone use on airplanes is technically possible. This was achieved through the use of low power wireless phone base-stations, forming picocells inside the airplanes. On-board wireless phones communicated with the on-board picocell base-stations rather than with the ground towers, thereby reducing the possibility of interfering with the ground cellular networks. Airplane to ground communications were provided through satellite links.

Unlike aircraft installed equipment, passenger carry-on devices are not required to pass the rigorous aircraft radiated field emission limits. It is therefore of interest to measure the emissions from wireless phones in aviation bands and to assess interference risks to aircraft systems.

With the support of the Federal Aviation Administration (FAA) Aircraft Certification Office and the National Aeronautics and Space Administration (NASA) - Aviation Safety Program - Single Aircraft Accident Prevention Project, radio frequency (RF) emissions from the latest portable wireless phones were measured. Utilizing the results from earlier efforts, the new results are compared against the baseline emissions from laptop computers. Combining the emission data with interference path loss and radio receiver interference threshold data, potential risks to aircraft systems were assessed.

An earlier report [1] documented the measurement of spurious emissions and the results of multiple Code Division Multiple Access (CDMA) wireless phones operating in the US cellular band and Global System for Mobile Communication (GSM) phones in the European 900 MHz band. One of the goals of

the study was to develop and demonstrate the measurement process for intentional transmitters. Data were reported in multiple aircraft radio bands. The work was extended the following year to include several WLAN devices (Institute of Electrical and Electronics Engineers 802.11b, 802.11a, Bluetooth) and of several pairs of two-way radios [2, 3]. Also reported were the measurements and results of aircraft interference path loss (IPL) between the passenger cabin and various aircraft communication and navigation antennas. From the data, interference safety margins were computed for many aircraft radio systems.

Built upon the process and results from the previous efforts, this effort revisits the phone emissions topic. The current effort addresses the latest generation of phones that are more data-capable. Specifically, two of the latest and most popular technologies used in the US are the CDMA2000 1xRTT (1x Radio Transmission Technology) and the GSM/GPRS (General Packet Radio Service). In addition, phones operating in the higher frequency 1900 MHz band are addressed. Many more phone models are considered in this study. Testing in both voice and data modes are conducted.

This document also repeats the previously compiled and reported IPL summary data due to the relevancy to the current analysis. Interference safety margins are calculated.

This report also attempts to provide a conservative bound for the multiple-equipment-factor (MEF). This factor is an estimate of the cumulative interference effects to aircraft radios if there are multiple similar devices present on the airplane.

Radiated Emission Measurement

Radiated emissions from the wireless phones were measured in two reverberation chambers at NASA LaRC. The test phones included 16 CDMA (CDMA2000 1xRTT) and 17 GSM (GPRS data capable) of the latest models. A base-station simulator (BSS) was used for controlling the test phones.

The reverberation chamber emission measurement method used was adopted from the earlier wireless phones and WLAN test efforts [2]. The method was efficient, accurate, and repeatable. It also provided results directly in terms of effective peak radiated power, rather than electric field strength, so that an approximate conversion from field strengths to radiated power was not needed. Filters were used to block intentional high power transmission from the wireless phones from reaching the receiver, preventing undesirable receiver overloading and intermodulation. Filters were also used to block spurious emissions from the BSS, if any, from radiating into the chamber resulting in false measurements.

Interference Path Loss Measurement

Aircraft IPL data are repeated from the earlier report [2] for completeness and relevancy to the analysis. IPL represents the attenuation to the interference signals as they propagate from the portable electronic device (PED) in the passenger cabin to the aircraft system antenna and into its receivers.

As reported in [2], the IPL data were summarized from several sources, including standards, and NASA cooperative efforts with industry partners. Data were available for several aircraft systems including Localizer (LOC), Glideslope (GS), Very High Frequency Omnidirectional Range (VOR), Very High Frequency Voice Communication (VHF-Com), Global Positioning Systems (GPS), Traffic Collision Avoidance System (TCAS), and Satellite Communication (SatCom). The measurements were typically conducted with a radiating antenna positioned at windows and doors, while a spectrum analyzer recorded the maximum signals coupled into aircraft antennas.

Interference Safety Margin

The emissions results for the wireless phones were compared against the emissions from laptop computers and personal digital assistants (PDAs) that are currently allowed for use on aircraft.

Interference analysis was also conducted using the emission results, the IPL data, and the receiver interference thresholds from a standard document. Safety margins were calculated for each combination of wireless phones operating in cellular or PCS bands, the minimum or average IPL, and the interference threshold. The resulting safety margin can be positive or negative depending on whether the minimum or average IPL, and the typical or minimum interference thresholds were used. In most cases, the wireless phones were seen to have better safety margins than laptops and PDAs due to their lower emissions.

Multiple Equipment Factor

The cumulative interference effects on aircraft receivers due to multiple devices were not well addressed previously. This document establishes a conservative bound for the MEF by taking advantage of the available full-aircraft IPL data. Devices' spurious emission power in aircraft radio bands are scaled according to their locations' IPLs, and the results are summed to determine the total interference power. This total interference power is normalized to the worst case single device interference power to determine the effects of multiple devices, in dB. Calculations were made for LOC/VOR, TCAS, and VHF-Com systems where full-aircraft IPL data were available. The results show MEF for the systems can vary between 10 and 14 dB.

Window IPL (IPL collected with the source located near a window rather than at a seat) data are normally easier to acquire than full-aircraft IPL data due to fewer windows on an airplane. In addition, they are often more relevant with respect to aircraft minimum IPL, since the worst case interference coupling is typically near a window or a door. Based on these facts, this paper compares the MEF collected using the window IPL and the MEF computed from the seat data. The comparisons show that they come within one dB of each other. Further validations and including more aircraft systems are needed to establish guidelines for estimating MEF when using only window IPL data.

Conclusions

Emission measurements were conducted on 33 wireless phones of various design configurations by different manufacturers. These mobile phones were more representative of those available in today's market place than the mobile phones tested previously by NASA [1]. The following observations were made:

- The 33 wireless phones tested did not generate higher emissions in most aircraft radio bands than standard laptop computers. An exception is the MLS band, where the emissions from the phone exceeded the emissions from the laptop computers. However, the safety margins in this band were positive for all devices. It is noted that operation of non-intentionally transmitting laptop computers is currently allowed during certain parts of flight.
- Spurious emissions from the wireless phones tested were below the aircraft installed equipment emission limits (RTCA/DO-160 Category M). They were also below the FCC Part 15 limits for unintentional transmitters such as laptop computers.

- The calculated safety margins can be negative or positive depending upon the interference thresholds (minimum or typical) and the minimum IPL data (the lowest or the average) used. The safety margins are based on the measured emission data, the existing IPL and interference threshold data.
- It is generally observed that in lower frequency bands (VHF-Com, LOC, VOR and GS), each mobile phone's maximum emissions are similar regardless whether it is operating in the cellular or PCS bands. This is not the case for higher frequency bands (TCAS, DME, GPS or MLS).
- The measured emissions in the voice and data modes are generally similar for any single device (within 2-5 dB) in most cases.

An approach was developed to provide an estimate of the upper bound on the front-door interference effects of multiple PEDs. This approach sums the interference powers at the receivers after scaling each device's emission by the IPL corresponding to its location. Using full-aircraft B737 IPL data, conservative upper bounds were derived for LOC, VHF and TCAS on a B737 airplane. The following observations were made:

- MEF determined using the windows-only IPL data were within one dB of the MEF determined using full-aircraft seat data.
- Conservative bounds for MEF for the systems measured were between 10 dB and 14 dB for LOC, VHF-Com, VOR and GS.
- The effects of additional seats on the MEF calculation diminished rapidly with the increased distance between the seat locations and the windows/doors.

Recommended Future Work:

- Additional receiver interference threshold data are needed for greater confidence level. Tests on multiple receivers from different manufacturers are recommended. Signal modulation and types should be considered.
- Assessment should be performed for software-defined-radios, active and passive RFID (radio-frequency-identification) tags, and the latest portable music playing devices (non-intentional transmitters).
- Assessment of the potential for emerging radio technologies that overlay existing spectrum (such as Ultra Wideband) to cause interference to aircraft systems.
- Conduct additional IPL measurements on different types of aircraft where minimal data currently exists. Cargo-bay IPL data are also desirable.
- Conduct additional assessment of multiple equipment effects.

2 Introduction

Wireless phones are pervasive in today's society. With their ever expanding network coverage, increased reliability, capabilities and affordability, wireless phones are considered a "must have" for most people. They help to maintain contact between people and their families or businesses while affording the mobility demanded by daily activities.

New phone designs are produced at a very fast pace to incorporate new capabilities and market trends. Newer wireless phones and networks are capable of, and increasingly cater to, data intensive applications rather than just voice communication. Sending and receiving short text messages and emails, downloading musical ring tones, tracking stocks, etc. are very popular in today's phones. Phones that can play games and download music over the wireless network are already available. In fact, wireless phones of the future may be considered more as an integrated personal communicator and entertainment device, and many of today's designs are starting to reflect that trend.

Most intentional-transmitting personal electronic devices (referred to as "T-PEDs" in this report) are prohibited from use while on-board an aircraft. With the popularity of wireless phones, intended as well as unintended use is inevitable. Unintended use includes email or text messages being "pushed" to the phones, or phones trying to register with the ground networks without any action by their owners. In addition, as customers are demanding alternatives to pricey seat-back phones for voice and data communication, airlines and vendors are increasingly interested in "picocell" technologies. With a picocell, an on-board low power base-station forms a small cell serving the passengers on the airplane. Thus, on-board wireless phones communicate with a picocell base-station rather than with the ground networks, therefore reducing interference with the ground networks.

Typical consumer wireless phones are not required to pass the emission requirements specified for aircraft installed equipment. It is, therefore, of great interest that these are tested to determine their spurious emission levels in the aircraft radio bands. The results are compared against aircraft emission limits and emissions from other portable electronic devices (PEDs) that are allowed for use during flights.

An earlier test effort, started in the year 2000, measured the emissions from eight wireless phones using GSM and CDMA technologies [1]. The GSM phones were designed to operate using the European 900 MHz spectrum, whereas the CDMA phones operate on US 850 MHz cellular band. The measurements were conducted at several aircraft radio bands. The final report was published [1] and considered aircraft path loss interference, aircraft radio receiver susceptibility thresholds, and intermodulation products when multiple devices were operating near one another.

In early 2004, [4] documented the emission measurement in the GPS band from a wireless phone that reportedly interfered with GPS receivers on a small general aviation aircraft. Measurement data show high emissions from the device in the GPS band, and a calculated negative interference safety margin for large commercial aircraft. However, the report also showed that the emission levels are not much higher (within 5 dB) than the worst case emissions from eight standard laptop computers measured using the same method and facility.

This current effort is an extension of the earlier work. As newer phones are more data friendly, the new tests include testing in data modes in addition to the voice modes. Phones operating in the US PCS band are also included. In addition, GSM phones designed for use using the US wireless spectrums are now available and used in this testing. In all, 33 wireless phones are considered in this study. Utilizing

interference path loss data (IPL) from the earlier efforts [2] and radio receiver's interference thresholds from RTCA/DO-199, interference safety margins are calculated and reported.

Cumulative interference effects of multiple devices in the aircraft to radio receivers are also a concern due to the large number of devices that may potentially be used on an aircraft if permitted. This report estimates an upper bound for the effects by applying IPL to a device's emission data to determine an individual device's interference power at the receiver. The cumulative effect is the sum of power contributed by individual devices, normalized to the worst-case single device interference power. This report also uses the worst case polarization and measurement at each PED location for a conservative bound.

The following subsections describe the objectives, the approach to measure spurious emissions, and the report organization.

2.1 Objective

The primary objectives of this report are to describe the measurement of unintended radiated emissions from the latest available wireless phones, and to assess interference risks to aircraft communication and navigation radios.

2.2 Scope

In this report, measurements are restricted to unintentional (spurious) emissions in and near the aircraft radio spectrum. Intentional wireless emissions, or desired emissions for the purpose of voice and data communication, are typically known or easily determined and, therefore, are not considered in this measurement.

The large number and the fast changing pace of worldwide wireless phone technologies, and the diverse allocation of frequency bands globally make it necessary to limit the scope of this study. As a result, this study only considers devices intended for use in the US. In addition, the devices use either CDMA or GSM technologies, which are the two dominant wireless technologies in the US. Since a study on second generation phones was conducted earlier [1], this study focuses on newer and more data capable third generation (3G) wireless phones. CDMA devices use CDMA2000 1xRTT protocol (often referred to as CDMA2000, or 1xRTT, or simply "1X"). The latest commonly available GSM devices use GPRS protocols for data communication in addition to the standard GSM protocols for voice.

For simplicity, the terms CDMA and GSM in this report are often used to address a wireless device using the specific technology. The term CDMA should be expanded to CDMA2000 1xRTT technology and devices, unless otherwise noted. Likewise, the GSM term should be expanded to GSM/GPRS. The distinction is made when GSM refers to voice communication mode, while GPRS refers to data mode.

2.3 Approach

Assessment of aircraft radio receiver interference is typically accomplished by addressing the source – path loss – victim elements of the equation:

$$A + B \geq C, \tag{Eq. 2.3-1}$$

at any frequency in the aircraft radio communication and navigation bands, where

“*A*” is the maximum RF emission from a PED in dBm,

“*B*” is the maximum interference coupling factor in dB; “-*B*”, in dB, is commonly referred to as the minimum IPL,

“*C*” is the receiver’s minimum in-band, on-channel interference threshold in dBm.

If the minimum interference threshold, “*C*”, is lower than the maximum interference signal level at the receiver’s antenna port, “(*A* + *B*)”, there is a potential for interference.

A primary focus of this effort was to measure the maximum RF emission, “*A*”, from wireless phones.

The minimum IPL, “-*B*”, were previously reported [2]. These IPL data are summarized in this report for the interference risk analysis.

Receiver interference thresholds “*C*” were not measured in this effort. Rather, test data from RTCA/DO-199 were used in evaluating interference risks to aircraft systems. DO-199 provided receiver interference threshold data on a limited number of receivers.

Sections 2.3.1 and 2.3.2 discuss in more detail the emission and path loss measurement approaches.

2.3.1 Emission Measurements of Wireless Phones

Similar to the earlier efforts [1]-[3], various aircraft radio bands were grouped into five measurement bands to reduce the number of measurements and test time. Aircraft radio bands that overlapped, or were near one another were grouped together, and emissions were measured across the entire combined band simultaneously. Five frequency groups, designated as measurement Band 1 to Band 5, covered many aircraft radio bands of interest, including LOC, VOR, GS, VHF-Com, TCAS, Air Traffic Control Radar Beacon System (ATCRBS), Distance Measuring Equipment (DME), GPS, and MLS. Table 2.3-1 shows the relationship between the measurement bands and aircraft radio bands.

Table 2.3-1: Emission Measurement Band Designations and Corresponding Aircraft Radio Bands.

Measurement Band Designation	Measurement Freq. Range (MHz)	Aircraft Systems Covered	Spectrum (MHz)
Band 1	105 – 140	LOC	108.1 – 111.95
		VOR	108 – 117.95
		VHF-Com	118 - 138
Band 2	325 – 340	GS	328.6 – 335.4
Band 3	960 – 1250	TCAS	1090
		ATCRBS	1030
		DME	962 - 1213
		GPS L2	1227.60
		GPS L5	1176.45
Band 4	1565 – 1585	GPS L1	1575.42 ± 2
Band 5	5020 - 5100	MLS	5031 – 5090.7

It is implied that high emissions anywhere in a measurement band potentially affect all systems grouped in that band. No effort is made to distinguish whether the emissions were on any specific radio band or channel.

Two reverberation chambers were used to conduct the measurements, producing results in *total radiated power* (TRP) [5]. This method differs from the approach used in RTCA/DO-199 [6], where the TRP was estimated from the electric field measured at a given distance from a device-under-test (DUT). Further details about conducting emission measurements in a reverberation chamber are found in Section 3.

The wireless phones were tested individually, and were controlled using a BSS. Located outside the test chamber, the BSS communicated with a phone under test inside the test chamber via a filter network and a wideband antenna. The BSS commanded the phones to operate in various, voice/data communication modes, frequency channels and data rates while emission data were being collected.

The devices considered include 17 phones using GSM technology and 16 phones using CDMA technology. These devices were mostly acquired at local stores and through internet purchases, with one CDMA device on loan from the manufacturer. Most devices did not have an active service subscription, as it was not required to communicate with a BSS.

Each device was tested in voice mode and at several data transfer rates. The devices were also tested while operating on five wireless frequency channels in each of the cellular and PCS bands, if the band was supported in the phone. The channels were selected such that their frequencies were equally spaced spanning across the cellular or PCS bands. Each device was also tested in idle mode (in the presence of a BSS signal) and in “no-signal” mode. “No-signal” mode is the condition where there was no signal from the BSS, as it is often the case at certain locations on the airplane while in the air.

The results are compared against the emissions from common computer laptops and PDAs measured in [2]. Emission data of the laptop computers established a baseline for devices that are currently allowed onboard an aircraft. The results are also compared against the relevant FCC and RTCA aircraft installed equipment emission limits.

A simple filter network, with PCS and cellular band filters in parallel, was used in the BSS antenna path to allow only the intended wireless signal to radiate for communication with the phone under test, while blocking any spurious emissions from BSS. A filter network with parallel PCS and cellular band filters permits signal hand-off between the two bands while communicating with the wireless phone under test. This hand-off is necessary in testing dual-band phones (true for most tested devices) as many devices only allow initial connection in one specific band (PCS or cellular) and not the other. Additional filters were also used in the measurement path to prevent the wireless signals (from the phones and BSS) from overloading the pre-amplifier in the measurement path. Further details are discussed in Section 3.

2.3.2 Path Loss Measurements

An earlier effort [2] supplemented existing IPL data with measurements on four B747-400 and six B737-200 aircraft. Three separate measurement trips were made to an aircraft storage facility in Victorville, California to obtain measurements on VHF-Com system, along with LOC, VOR, GS, TCAS, SatCom and GPS systems (if available on the airplanes). The measurements were conducted using a source antenna simulating an interference device. The antenna was positioned at different windows along each aircraft, and the *minimum* path losses for the aircraft systems were registered, summarized and reported. Much of the existing and publicly available IPL is summarized in [2] for reference.

Section 4 repeats the IPL summary tables, and the results are used in assessing interference risks from the tested devices. The measurement process is also briefly described.

2.3.3 Safety Margin Calculations

Interference thresholds were previously measured and reported in [6] and [7]. With device emission “*A*”, IPL “*-B*” and interference threshold “*C*” known, the safety margin is calculated as:

$$\text{Safety Margin} = C - (A + B) \quad (\text{Eq. 2.3-2})$$

Results of the safety margin calculations are reported in Section 5.

2.3.4 Multiple Equipment Factor Calculations

This report also conservatively assesses the cumulative effects of multiple devices operating inside the passenger cabin. The approach taken utilizes existing “full-aircraft” (all seat locations) IPL data available through an earlier cooperative effort between United Airlines (UAL), Eagle Wings Inc., and NASA Langley Research Center (LaRC).

In this approach, individual IPL at different aircraft cabin locations is applied to the interference signal strength to determine its contribution at the receiver. Conservative approaches are used, by assuming one PED for every passenger seat, all PEDs having the same emission levels in aircraft radio bands, and choosing the worst case IPL (lowest) value among several measurements for any given seats. The total interference power is the sum of all individual contributions, reasonably assuming that signals are non-coherent (all devices operate independently). Application of this approach is demonstrated in Section 6 for VHF, LOC, GS and GPS where full-aircraft data are available on a B737 model.

2.4 Report Organization

Section 3 describes the wireless phone emission measurement and results. Sections 3.1 - 3.2 provides a brief overview of the wireless phone technology considered, namely CDMA2000 1xRTT and GSM/GPRS. Common test modes selected are discussed. Section 3.3 details the measurement and data reduction process. Section 3.4 provides a summary of the test results extracted from Appendices A and B. Section 3.5 repeats the previously reported data concerning emissions from standard laptops and PDAs. These data serve as baseline emissions for PEDs devices that are currently allowed on aircraft. Section 3.6 compares the emissions from the wireless phones to the PEDs emission baseline.

Section 4 summarizes the IPL data previously reported that are used in this report for risk analysis.

Section 5 reports radio receiver interference thresholds reported in RTCA documents. These documents include RTCA/DO-199 [6] and RTCA/DO-235A [7].

Section 6 presents an approach to quantify the effects of multiple equipment. It also shows initial findings of a possible alternative approach to using full-aircraft IPL data. This alternative approach uses windows IPL data rather than seats data. With fewer windows than seats, the alternative approach would save test time if it can be further proven.

The Summary and Conclusions are in Section 7. In addition, more detailed test results are in the Appendices.

3 Wireless Phones and Radio RF Emissions

3.1 Wireless Phone Overview and Phone Settings

Wireless mobile technology is a very broad area. Detailed discussions of any specific technology are beyond the scope for this report. This section focuses narrowly on the two most widely used wireless technologies in the US: GSM/GPRS and CDMA2000. The discussions will be brief and general, but with sufficient details to explain the specific phone settings used during tests. In this report, a wireless phone is also referred to as a mobile station (MS), which is a term widely used in mobile phone standard documents.

3.1.1 GSM/GPRS Overview

GSM is the world's most widely adopted second generation wireless system. It claims to represent over 60% of the digital cellular market worldwide. The standard was set by major players in the European telecommunication industry in early 1990.

The GSM standard, originally aimed at 900 MHz band in Europe, has been adopted for service at 1800 MHz in Europe, and later for the 1900 MHz PCS services in North America. GSM is also being introduced into existing bands where analog networks are being phased out, including 450/480 MHz in Europe and Asia, and 850 MHz cellular band in North America.

The major advantage of GSM is its capacity for global roaming. The system was originally intended to ensure that Europeans could roam their continent and use their handset wherever they chose to travel. As other parts of the world adopt GSM, global roaming capacity is a major advantage. Other benefits of GSM compared to older analog technologies include better speech quality, low operational and service costs, better security, and low-power support.

The following subsections discuss the basic phone, channel utilization, speech transmission, data transmission, GPRS coding, frequency bands, and power classes associated with GSM technology.

GSM Phone

The GSM phone can be divided into two parts, the mobile handset and the Subscriber Identity Module (SIM) card. The SIM card identifies the subscriber to the network. Subscriber information is stored in the SIM, which is a smart card with a processor and memory chip permanently installed. In addition, personal data such as personal phone directory can also be stored on the SIM.

GSM Channel Utilization

In GSM, Frequency Division Multiple Access (FDMA) is used to divide the wireless bands into 200 kHz wide RF channels. Within each 200 kHz channel, Time Division Multiple Access (TDMA) is used to separate data streams into time frames, each with eight time slots. This allows up to eight simultaneous calls on one frequency channel. One frame-duration is *4.615 msec*, which consists of eight time slots of *0.5769 msec* in duration. A mobile station may only transmit data during the time slot assigned to it. Otherwise, it must not emit any power during the remaining time slot. As a result, the radio pulse is simply called a "burst". When a call is made, the information is compressed into one of these time slots. The data are transported to the other caller, and the information is then decompressed.

Speech Transmission

There are three different algorithms in use for speech transmission.

- Full-Rate Speech: This was the first method used for speech transfer over a digital GSM channel. The data rate is 13 kilobits per second (kbps) before channel encoding.
- Half-Rate Speech: This method multiplexes two calls into one time slot, thereby more calls can be made on the same number of carriers. It can also help to save battery power. The bit rate is 5.6 kbps.
- Enhanced-Full-Rate Speech: This method yields superior voice quality. The bit rate is 12.2 kbps.

The testing in the voice mode was restricted to Full-Rate Speech only.

Data Transmission

Standard GSM mobile phones may also be able to transmit data. The standard rate supported is 9.6 kbps, which is inadequate in today's high-speed communication demands. A higher data rate of 14.4 kbps has been introduced; however, the higher data rate is achievable only under ideal conditions.

GPRS provides faster data transmission to the GSM network. Using the GPRS, one or more channels are available to all users for data transfer. In GSM and GPRS operation, a channel is determined by combinations of frequency channel and time slot. Compared to GSM, GPRS is cost and bandwidth efficient in that the data channels are dynamically shared by all users and a time slot is assigned only if there is data to transfer. This setting is called "channel sharing". In addition, since GPRS uses radio resources only when there is data to be transmitted, the protocol allows a device to be "always connected", which is useful in data and web applications.

While GSM uses a single slot for data transmission, the GPRS protocol can use multiple time-slots, resulting in a speed gain equal to the number of time slots used. If multi-slot operation is used, the time slots must be on the same frequency carrier. Depending on channel coding and radio channel situation, a data rate of 9 to 22 kbps per time slot is achievable. Thus for two slots a data transfer rate of 18 to 44 kbps data rate is possible.

GPRS is often considered as "2.5G", which means that the technology is newer than the second generation (or "2G") GSM. However, it does not have the high data rates required for third generation "3G" protocols.

GPRS Coding

A base-station can choose between four "Coding Schemes" to tailor/optimize data throughput or connection quality. The coding schemes and achievable data rates are shown in Table 3.1-1.

Table 3.1-1: Coding Schemes and Maximum Achievable Data Rates

Coding Scheme	Max Data Rate (kbps)			
	One Time Slot	Two Time Slots	Four Time Slots	Eight Time Slots
CS-1	8.0	16	32	64
CS-2	12.0	24	48	96
CS-3	14.4	28.8	57.6	115.2
CS-4	20.0	40	80	160

From Table 3.1-1, the maximum achievable data rate is 160 kbps, using all eight time slots and the CS-4. However, assigning all eight slots to one phone is not realistic. A more reasonable number of time slots is between 1 and 4. Also, the channels may be shared among multiple users. The higher the number of users, the lower the data rate per user will be.

Not all networks are able to handle increased data rates associated with CS-3 and CS-4. In those cases, CS-1 and CS-2 are more appropriate, reducing data rate to 8 kbps to 12 kbps per time slot.

Higher coding schemes result in higher achievable data rates; however, there is less protection against interference. CS-4 provides the least protection against interference. Lower coding schemes provide much better protection, with the cost of reduced data rates.

The phones are also classified into “multislot classes”, which defines the capabilities of the phone. The classes identify the number of slots that can be used for downlink and for uplink. There are 29 multislot classes. However, most current phones are of class 10 or below, including those acquired for testing. It is noted that there are available devices on the market that belong to class 12. Most phones are designed with multi-slot *receive* capability. Many of them may not, however, *transmit* on multiple time slots.

Table 3.1-2 lists the multi-slot classes up to class 12. The maximum number of time slots for downlinks and for uplinks are listed, along with the maximum sum. The number of time slots permitted for use in a connection can be no greater than the uplink or downlink limits, and as long as their sum does not exceed the maximum sum. For example, a mobile station with multislot class 10 can have up to 4 downlink slots and up to 2 uplink slots. However, the total number for both cannot exceed 5, the maximum sum. A few other options for this class include 4 downlink and 1 uplink slots, or 3 downlink and 2 uplink slots. However, it cannot have 4 downlink and 2 uplink slots since the total exceeds 5 for the maximum sum.

Most popular handheld phones can handle only one service at a time, either voice traffic or data traffic, but not both concurrently. However, they can simultaneously attach, and can automatically switch between GSM and GPRS.

These coding schemes and multi-slot classes are relevant in choosing phone test modes, which are discussed in a later section.

Table 3.1-2: GPRS Multislot Classes for Mobile Stations

Multislot Class	Max. Number of Time Slots		
	Downlink	Uplink	Maximum Sum
1	1	1	2
2	2	1	3
3	2	2	3
4	3	1	4
5	2	2	4
6	3	2	4
7	3	3	4
8	4	1	5
9	3	2	5
10	4	2	5
11	4	3	5
12	4	4	5

Frequency Bands

Table 3.1-3 describes different GSM band designations and the associated uplink/downlink frequency bands. Of the bands listed, GSM 850 and GSM 1900 are currently used in the US. Table 3.1-4 shows the frequency channel assignment for the two US bands.

Table 3.1-3: GSM/GPRS bands designation

Band Description	Uplink (MS Transmit) Freq Range (MHz)	Downlink (MS Receive) Freq Range (MHz)	Duplex Spacing (MHz)
GSM 450	450.4 – 457.6	460.4 – 467.6	10
GSM 480	478.8 – 486	488.8 – 496	10
GSM 850	824 – 849	869 – 894	45
GSM 900 (Standard GSM)	890 – 915	935 – 960	45
E-GSM (Extended GSM 900, Includes GSM 900)	880 - 915	925 – 960	45
R-GSM (Railway GSM 900, Includes standard and extended GSM 900)	876 – 915	921 – 960	45
GSM 1800	1710.0 – 1785.0	1805.0 – 1880.0	95
GSM 1900	1850 – 1910	1930 - 1990	80

Table 3.1-4: GSM/GPRS Channel Assignment

Band Description	Channel Number	Uplink Channel Frequency (MHz)	Downlink Channel Frequency (MHz)
GSM 850	$128 \leq n \leq 251$	$824.2 + 0.2(n - 128)$	$869.2 + 0.2(n - 128)$
GSM 1900	$512 \leq n \leq 810$	$1850.2 + 0.2(n - 512)$	$1930.2 + 0.2(n - 512)$

Power Class

A phone's power class determines its maximum output power. Table 3.1-5 shows the maximum output power for different power classes for various GSM bands. A typical GSM phone operating in the US belongs to power class 4 in the Cellular band (GSM 850) and power class 1 in the PCS band (GSM 1900).

Table 3.1-5: GSM MS Maximum Output Power

MS Power Class	GSM 850 GSM 900 GSM 400	GSM 1900	GSM 1800
1		30 dBm (1 W)	30 dBm (1 W)
2	39 dBm (8 W)	24 dBm (0.25 W)	24 dBm (0.25 W)
3	37 dBm (5 W)	33 dBm (2 W)	36 dBm (4 W)
4	33 dBm (2 W)		
5	29 dBm (0.8 W)		

3.1.2 CDMA2000 Overview

CDMA technology uses a different approach to air-interface-design than GSM. With CDMA, all users share the same 1.25 MHz wide carrier. CDMA uses unique and orthogonal codes to differentiate transmissions in the same frequency channel, rather than dividing a frequency carrier into time slots as in GSM. These codes are called "pseudo-random code sequences" and are shared by both the mobile station (i.e. phone) and the base station. Different base-stations in the same system transmit time-offset versions of the same pseudo-random code to differentiate from one another.

CDMA is unique in that there is not a set limit to the number of phone calls that can be handled simultaneously by a base-station. The number of concurrent connections a base-station can handle is the result of a trade-off with the base-station's range and the quality of each connection. A standard CDMA (CDMA IS-95) connection has a digital transfer rate of 9.6 kbps, with the voice data part transmitted at a rate of 8 kbps.

Privacy is also intrinsic to CDMA since a simple radio receiver will not be able to decode individual transmissions out of the remaining transmissions in the band. With the wide bandwidth of a spread spectrum signal, it is also difficult to identify, interfere, and jam.

CDMA2000 General Description

CDMA2000 built upon CDMA IS-95 to improve network capability and high-speed data services, and is backward compatible with the IS-95. CDMA2000 is a family of International Telecommunication Union approved 3G standards that includes CDMA2000 1xRTT and CDMA2000 1xEV technologies. In addition to voice, the standards make available a host of advance services, such as web browsing, games, and multimedia messaging services. The specifications for this standard are developed by the 3G Partnership Project Number 2 (3GPP2) [8].

The first 3G implementation of CDMA2000 is referred to as CDMA2000 1X, which uses the 1.25 MHz narrowband carriers to transmit data in both the forward and reverse links. This characteristic enables IS-95 carriers for CDMA2000. Future implementations may use several carriers together for increased data rates (term “multicarrier”). One release of CDMA2000 may use three such carriers, and is called “3X” mode. The RF channel bandwidth for “3X” is 5 MHz which includes 3 times 1.25 MHz for the three carriers, plus guard bands.

The early implementation of CDMA2000 1X, 1xRTT (1x Radio Transmission Technology), has peak data rates up to 307 kbps in the forward link and 144 kbps in the reverse link. 1xEV-DO (1xEvolution Data Optimized) is the next evolutionary step and is optimized specifically for high speed packet data services. 1xEV-DO and its enhancements can have peak data rates of 2.4 – 3.1 Mbps in the forward link and 1.8 Mbps in the reverse link. The next implementation after the 1xEV-DO is 1xEV-DV (1xEvolution for Data and Voice), which is capable of up to 3.1 Mbps, and is optimized for both voice and data.

Currently, 1xRTT technology is implemented in most new phones, as older IS-95 phones are becoming obsolete in the US. On the other hand, the next evolutionary step 1xEV-DO devices are still very limited in number and therefore not considered in this study. Since 1xEV-DO is optimized for data transmission, devices using the technology are generally available in one of the computer card formats. However, there are indications that several wireless phone models may soon incorporate 1xEV-DO (for data) in addition to 1xRTT (for voice). 1xEV-DO services are currently still limited to a few metropolitan areas, but there is a push for widespread implementation by major wireless service providers. 1xEV-DV is also planned for implementation in the near future by a major US wireless service provider. At this time, however, there are no existing services or mobile devices available to the public.

In the CDMA part of this study, the report focuses exclusively on 1xRTT technology and devices, as this technology is the latest available to *most* consumers in the US. For ease of reference, 1X, 1xRTT, CDMA and CDMA2000 are used interchangeably in the remainder of this document except where explicitly noted. All the terms generally refer to CDMA2000 1xRTT as a technology or a device using the technology. This is to avoid lengthy descriptions, and is especially useful in the large number of charts presented.

CDMA2000 Air Interface Characteristics

This section briefly discuss a few of the RF characteristics of a CDMA2000 1X system relevant to this study. These characteristics include frequency bands, frequency channel assignments, and power rating. In addition, it also discuss different Radio Configuration settings that define the wireless device’s transmission formats, such as modulation characteristic, data rates and channel encoding.

Band Class and Channel Assignment

Table 3.1-6 shows a partial list of the current Band Class designations. Band Classes 0 and 1 are used in the US. Band Class 0 is also commonly referred to as US cellular band, or simply cellular band. Band Class 1 is commonly referred to as US PCS band, or simply PCS band. Table 3.1-7 shows the channel arrangements for the two bands.

Table 3.1-6: CDMA2000 Band Class Designation [9]

Band Class	Band Description	Reverse Link (MS Transmit) Freq Range (MHz)	Forward Link (MS Receive) Freq Range (MHz)	Duplex Spacing (MHz)
0	US Cellular	824 – 849	869 – 894	45
1	North American PCS	1850 – 1910	1930 – 1990	80
2	TACS Band	872 – 915	917 – 960	45
3	Japan JTACS Band	887 – 925	832 – 870	45
4	Korean PCS	1750 – 1780	1840 – 1870	90
5	NMT-450, CDMA450	411 – 484	421 – 494.0	10
6	IMT-2000	1920 – 1980	2110 – 2170	190
7	700 MHz	776 – 794	746 – 764	30
8	1800 MHz	1710 – 1785	1805 – 1880	95
9	900 MHz	880 – 915	925 – 960	45

Table 3.1-7: CDMA Channel Assignment for Cellular and PCS Bands

Band	CDMA Channel No.	Reverse Link	Forward Link
0 (US Cellular)	$1 \leq n \leq 799$	$0.030 n + 825.000$	$0.030 n + 870.000$
	$991 \leq n \leq 1023$	$0.030 (n-1023) + 825.000$	$0.030 (n-1023) + 870.000$
1 (PCS)	$0 \leq n \leq 1199$	$0.050 n + 1850.000$	$0.050 n + 1930.000$

From Table 3.1-7, the channel spacing is 30 kHz for Band 0 and 50 kHz for Band 1. CDMA2000 1X supports RF channel bandwidths of 1.25 MHz.

Power Class

Table 3.1-8 defines the maximum output power for different MS Classes. Effective Radiated Power (ERP) is typically used for the cellular band, and Effective Isotropic Radiated Power (EIRP) is for the PCS band. When registered with a BSS, most of the tested phones show 23 dBm EIRP in both cellular and PCS bands as reported on the BSS’s display.

Table 3.1-8: Mobile Station Maximum Output Power [10][11]

Band Class	Mobile Station Class	Measurement	Lower Limit (dBm)	Upper Limit (dBm)
0 (US Cellular)	Class I	ERP	31 (1.25 W)	38 (6.3 W)
	Class II	ERP	27 (0.5 W)	34 (2.5 W)
	Class III	ERP	23 (0.2 W)	30 (1.0 W)
1 (US PCS)	Class I	EIRP	28 (0.63 W)	33 (2.0 W)
	Class II	EIRP	23 (0.2 W)	30 (1.0 W)
	Class III	EIRP	18 (63 mW)	27 (0.5 W)
	Class IV	EIRP	13 (20 mW)	24 (0.25 W)
	Class V	EIRP	8 (6.3 mW)	21 (0.13 W)

Radio Configurations

A Radio Configuration (RC) is a set of Forward Traffic Channel and Reverse Traffic Channel transmission formats that are characterized by parameters such as data rates, modulation characteristics and channel encoding. Collectively, there are six RCs for the reverse link and nine RCs for the forward link. In the reverse link, RCs 1 to 4 are for Spreading Rate 1 (1X), and RCs 5 to 6 are for Spreading Rate 3 (3X). In the forward link, RCs 1 to 5 are for Spreading Rate 1 (1X) and RCs 6 to 9 are for Spreading Rate 3 (3X). Also, RC 1 and 2 in the forward and reverse links are specified to be backward compatible with IS-95.

Table 3.1-9 shows a brief set of capabilities and characteristics associated with each RC. Typical 1xRTT phones support RCs 1 to 5 in the forward link and 1 to 4 in the reverse link. Different digital modulations are used for different RCs in the forward links and reverse links.

The CDMA standard also provides different standard test configuration combinations that include nine test modes and the mapping to the RCs. For CDMA 1X, the test modes are shown in Table 3.1-10.

High data rates are supported in different RCs, through the use of Supplemental Channels and/or Dedicated Control Channels. Since Dedicated Control Channels are not supported in the BSS, they are not considered for possible test modes. In contrast, at least one Supplemental Channel is supported in all tested devices as well as in the BSS.

References [10] and [11] provide additional guidance on phone settings for Conducted Spurious Emissions tests. Based on these documents, the capabilities of the phones and of the BSS, Test Mode 3 (RC3 for both forward and reverse links) was chosen as the default BSS setting for data and voice testing. The BSS allows up to 153.6 kbps using the supplemental channel in the RC3. As a result, the specific data rates selected for this testing include 9.6, 38.4, and 153.6 kbps, all of which are supported in RC3.

To select specific capabilities allowed in a RC, such as voice and data rates, different Service Options can be selected and their parameters are set on the BSS.

Table 3.1-9: Radio Configurations for CDMA-2000 1xRTT systems

Reverse Link			
RC	Data Rates (kpbs)	9.6 kbps based	14.4 kbps based
RC 1*	1.2, 2.4, 4.8, 9.6	x	
RC 2*	1.8, 3.6, 7.2, 14.4		x
RC 3	1.2, 1.35, 1.5, 2.4, 2.7, 4.8, 9.6, 19.2, 38.4, 76.8, 153.6, 307.2	x	
RC 4	1.8, 3.6, 7.2, 14.4, 28.8, 57.6, 115.2, 230.4		x
Forward Link			
RC	Data Rates (kpbs)	9.6 kbps based	14.4 kbps based
RC 1*	1.2, 2.4, 4.8, 9.6	x	
RC 2*	1.8, 3.6, 7.2, 14.4		x
RC 3	1.2, 1.35, 1.5, 2.4, 2.7, 4.8, 9.6, 19.2, 38.4, 76.8, 153.6, 307.2	x	
RC 4	1.2, 1.35, 1.5, 2.4, 2.7, 4.8, 9.6, 19.2, 38.4, 76.8, 153.6	x	
RC 5	1.8, 3.6, 7.2, 14.4, 28.8, 57.6, 115.2, 230.4		x

* RC 1 and RC 2 are for backward compatibility with IS-95

Table 3.1-10: CDMA Standard Test Modes and the RC Mapping

Test Mode	Forward Traffic Channel RC	Reverse Traffic Channel RC
1	1	1
2	2	2
3	3	3
4	4	3
5	5	4

3.2 Wireless Phone Test Modes Selection

Multi-path interference in a reverberation chamber can inhibit making wireless connections or cause dropped calls. As a result, manual control of the phone is required to provide the maximum flexibility dealing with those situations. To limit test time to a reasonable level, the phone test modes were carefully selected to represent the most common operating modes. At the same time, a few test modes were chosen to stress the devices to utilize their maximum data transmission capabilities.

It was not the intention in this report to compare the CDMA technology handsets against those using the GSM technology. However, due to the different design features and the test modes selected, the testing and the results were grouped into two distinct groups. All the GSM phones were tested using a

similar set of test modes, whereas the CDMA phones were tested using a completely different set of test modes. However, the test modes selected share these common guidelines:

- Voice mode
- Data modes, utilizing three different data rates or more
- Both cellular and PCS bands (if supported by the phone)
- Five frequency channels, equally spaced, spanning across each of the cellular and PCS bands
- Maximum phone transmission power
- Idle mode
- No BSS signal mode

In most cases, the testing was performed while the devices were in “steady-state” mode, ie. measuring the emissions while a call was in progress. However, it was observed that several models emitted spurious components during transitions that did not exist in steady-state modes. These “transient” modes, such as making initial network connections or switching channels, are more difficult to measure reliably using the current technique, and are, therefore, excluded from the current testing. However, these transient behaviors tend to be short lived and are not expected to be a major interference concern.

In the events where the phones’ wireless connections to the BSS were unintentionally disconnected, the tests were simply repeated after re-establishing the connection. In more challenging situations, re-booting the phones, or re-arranging the distance between the BSS antenna and the phone were required. In rare cases, the problematic test modes were skipped to save time.

Additional details for the CDMA and GSM phone test modes are discussed in the following subsections.

3.2.1 Phone Controls

There are typically three options for controlling a wireless phone for the purpose of testing: keypad entry, software, or using a wireless base-station simulator. The keypad entry and software methods typically require having access to proprietary information and software. The large variety of phone models considered made these two methods impractical, as separate agreements must be negotiated with different manufacturers. The base-station simulator option was adopted for the maximum flexibility. However, a typical BSS can control only one device at a time, and test modes are limited compared to the other methods.

A high performance Agilent 8960 Series 10 Wireless Communication Test Set, Model E5515C, and multi-format E1991B Mobile Test Application Suite [12] were acquired for the testing. This hardware and software combination allows test capabilities for phones of various technologies, including CDMA2000 (1xRTT) and GSM/GPRS needed for this study. In addition, the set-up also provides test capabilities for IS-95, W-CDMA, EGPRS, AMPS, TIA/EIA-136, 1xEV-DO. These other technologies are not considered for this study since they are either outdated (IS-95, AMPS, TIA/EIA-136) or phones using these technologies are not widely available in the US (W-CDMA, EGPRS, 1xEV-DO).

For the CDMA2000 1xRTT and GSM/GPRS phones, test modes are determined considering a number of factors. These factors include 1) typical usage, 2) typical phone’s capabilities, and 3) the BSS’s

capabilities. In addition, the number of test modes was chosen so that the total test time remained manageable.

3.2.2 GSM/GPRS Phone Test Modes

With the exception of one device, all GSM phones acquired were capable of GPRS data transmission. For simplicity, GSM is used loosely to refer to a device or technology that uses GSM protocol. A “GPRS-capable” phone is referred to as a GSM phone, since GPRS is simply an extension of GSM. This helps to simplify annotations in charts.

It is important to note that this report makes a distinction between GSM phone and GSM *mode*. The GSM mode refers to the circuit-switched mode that is used primarily for voice. Likewise, GPRS mode refers to the packet-switched mode that is used strictly for data transmission. A GSM phone can have both the GSM mode (voice) and GPRS mode (data).

The following subsections discuss many of the relevant settings on the BSS that help establish and maintain connections with the phones.

Mobile Country Code and Mobile Network Code

Setting the correct Mobile Country Code (MCC) and Mobile Network Code (MNC) on the BSS is required to establish a connection between the BSS and a phone. The MCC-MNC combination uniquely identifies the home network of the mobile station. By correctly setting the MNC and MCC, the BSS can simulate the networks that a phone is programmed to use.

Many of the test phones recognized the 001-01 codes as the MCC-MNC for test purposes, allowing the testing to proceed without problems. In other cases, valid codes were needed. Since most of the acquired devices were programmed to operate on networks operated by AT&T Wireless Service Inc., Cingular Wireless and T-Mobile USA, the following MCC-MNC codes were used. These MCC-MNC codes were publicly available on the internet [13].

Test:	001-01
AT&T Wireless Service Inc:	310-38
Cingular Wireless:	310-15, 310-17, 310-18
T-Mobile USA:	310-16, 310-20, 310-21

Connection Types

For GSM and GPRS, there are six connection types available on the BSS for the active cell operating modes. However, one of the six connection types is only for EDGE capable phones which are not considered in this study. The remaining five types are explained below [14].

- AUTO: Primarily for GSM voice call, but a GPRS data connection can also be initiated by the MS.
- ETSI Type B (Unack): Test mode B as defined in ETSI 04.14 or 3GPP 44.014. Downlink traffic data is generated and the mobile loops back the downlink data on the uplink.

- ETSI Type B (Ack): Downlink traffic data is generated and the mobile station loops back the downlink data on the uplink. MS is in Radio Link Control acknowledgement mode.
- ETSI Type A: Test mode A as defined in ETSI 04.14 or 3GPP 44.014. The down link is terminated once the uplink has been established.
- BLER: Agilent-proprietary data connection with the primary purpose of calculating block-error-rates.

With the exception of AUTO, the remaining four types are for GPRS connection. Generally, by selecting one of five types, a connection between the BSS and the MS is established, and data are exchanged. These different connection types determine how test data patterns are generated, coded, routed (i.e. data loopback), and the types of error rate measurements that can be made on the BSS [14].

In this study, attempts were made so that the same connection type was used in all GPRS test modes. In actual testing, however, not all connection types were uniformly supported by a MS. Certain connection types were supported only in certain configurations (i.e. data rates). As a result, it was sometimes required to change connection types to allow further testing on a device. The order of preference was:

- ETSI Type B (Unack)
- ETSI Type B (Ack)
- BLER
- ETSI Type A

The GPRS connection types are listed in order of priority for establishing a connection. ETSI Type B (Unack) was the default connection type for most of the testing. If the connection failed to establish, the next one on the list was attempted until a connection was established. In all cases, a spectrum analyzer was used to monitor the MS's output to ensure the desired and expected signals.

Coding Scheme

As discussed earlier, coding schemes (CS) available are CS-1, CS-2, CS-3 and CS-4. CS affects the reliability of the data transmission by changing the allocation of redundancy bit rates versus data bit rates. The overall bit rate per slot does not change, and therefore is not expected to affect the spurious emission level. CS-1 was selected to ensure maximum connection reliability.

Multislot Configuration

As stated earlier, multiple time slots in a data frame are used to increase data rates over the data rate for one time slot. Since using more than one slot physically affects the RF characteristics of the transmission, ie. one burst versus multiple bursts in a frame, change in multislot (MS) configuration is considered for different test modes.

The number of slots in the downlink and uplink supported by the phone is specified by its MS Class. The MS Class for the phones being tested were generally observed between Class 8 and 10, with a few as low as Class 6. There were also Class 12 devices available on the market. However, the BSS supported only up to Class 10 testing.

In this document, the number of downlink and uplink slots in a connection is denoted as MS[downlink, uplink]. For example, 3 downlink slots and 2 uplink slots are denoted as MS[3,2]. For this test, the MS configurations selected included: MS[1,1], MS[2,1], MS[4,1] and MS[2,2]. These selections were supported in most devices. MS[1,1] was to compare the test result against single-slot GSM voice mode. MS[2,1] was a typical transmission currently in use, while MS[4,1] and MS[2,2] were used to stress test the phones performance in the downlink and uplink, respectively.

Other Test Modes

- *Idle*: This is the mode when the phone is ON and is attached to the network via the broadcast channel (BCH), but little or no data transmission. This is the case for most phones while not in use.
- *Idle-No Signal*: This is the mode where there is no BS signal into the test chamber. This is relevant as many devices are left on during high altitude part of a flight, or if the phones are ON and located in luggage compartment.

Another desirable phone test mode is “*Flight Mode*” or “*Airplane Mode*”. An Airplane Mode is used to turn off the RF transmission capability and leave the rest of phone available for other uses such as games. However, this mode is not available on all devices and, therefore, not considered at this time.

Power Output

For all tests, the MSs were commanded to radiate at the maximum level. Generally, the maximum output power for a GSM phone is 2W (33 dBm) in the cellular band, and 1W (30 dBm) in PCS band.

GSM Test Modes Summary

The Table 3.2-1 summarizes different test modes for GSM phone testing. Table 3.2-2 describes the channels used and the corresponding frequencies.

Table 3.2-1: Test modes for each GSM phone testing

Test No.	Test Modes	GPRS Multi-Slot Config. [Down, Up]	No. of Channels (Cellular)	No. of Channels (PCS)	Test Time (minutes)
1	Voice		5	5	2 per channel
2	GPRS	[1,1]	5	5	5 per 5 channels
3		[2,1]	5	5	5 per 5 channels
4		[4,1]	5	5	5 per 5 channels
5		[2,2]	5	5	5 per 5 channels
6	Idle		1	1	2 per channel
7	Idle (no BSS signal)		None	None	2

Table 3.2-2: GSM Phone Test Channels and Corresponding Link Frequencies

Relative Band Position	GSM 850 (US Cellular Band)			GSM 1900 (US PCS Band)		
	Test Channels	Frequency (MHz)		Test Channels	Frequency (MHz)	
		Uplink	Downlink		Uplink	Downlink
Low	128	824.2	869.2	512	1850.2	1930.2
	159	830.4	875.4	587	1865.2	1945.2
Mid	190	836.6	881.6	661	1880.0	1960.0
	220	842.6	887.6	736	1895.0	1975.0
High	251	848.8	893.8	810	1909.8	1989.8

3.2.3 CDMA Phone Test Modes

CDMA is a complex technology and in-depth discussions are far beyond the scope of this study. However, certain terminologies and settings are described for clarity. The explanations are not intended to be comprehensive. Further and more extensive details about the technologies can be found in [10] and [11].

This section discusses details relevant to the CDMA phone testing. Discussed are Service Options, Radio Configurations, Frequency Channels, and other BSS settings during the tests.

Service Options

A Service Option is a service capability of the system. Service Options may be applications such as voice, data, or facsimile etc. The list below shows many of the available Service Options:

Voice Service Options:

- SO1: Basic Variable Rate Voice Service (9600 kbps)
- SO3: Enhanced Variable Rate Voice Service (9600 kbps). Using dynamically variable data rate speech codec algorithm.
- SO17: High Rate Voice Service (14400 kbps)
- SO32768: Basic Variable Rate Voice Service (14400 kbps)

Data Service Options:

- SO2: Mobile Station Data Loopback (9600 kbps) (using Forward Fundamental (Code) Channel)
- SO9: Mobile Station Data Loopback (14400 kbps)

- SO32: TDSO – Test Data Service Option. Supplemental Channel settings for higher data rates can be set on the BSS under this option.
- SO55: Radio Configuration 1/2/3/4/5 Data Loopback

SO1 and SO55 are available on the BSS, but are not supported by all phones.

For voice mode testing, SO3 was selected as it was supported in all phones. In addition, SO2 was used to test the data mode using Fundamental Channel, and SO32 was used for data mode testing using the Supplemental Channel. Higher data rates were achieved by changing data parameters under SO32 (TDSO).

Radio Configurations

Most typical phones support RCs 1-5 downlink (base-station to phone) and 1-4 uplink (phone to base-station). One can relate a Service Option as a capability, and a RC as a pre-defined set of Service Options or capabilities.

RC3 was universally supported by all the phones tested and therefore was adopted as the standard setting on the BSS. On the BSS, RC3 included SO1 (voice), SO2 (data loopback), SO3 (voice), SO9, SO55 and SO32 (data).

Frequency Channels

The phone channels were chosen such that their corresponding frequencies were spaced evenly across the wireless bands. The channels selected and the corresponding frequencies are show in Table 3.2-3:

Table 3.2-3: CDMA Phone Test Channels and Corresponding Link Frequencies

Relative Band Position	Band Class 0 (US Cellular)			Band Class 1 (US PCS)		
	Test Channels	Frequency (MHz)		Test Channels	Frequency (MHz)	
		Reverse Link	Forward Link		Reverse Link	Forward Link
Low	991	824.04	869.04	0	1850.00	1930.00
	176	830.28	875.28	300	1865.00	1945.00
Mid	384	836.52	881.52	600	1880.00	1960.00
	591	842.73	887.73	900	1895.00	1975.00
High	799	848.97	893.97	1199	1909.95	1989.95

Additional Settings

Additional BSS settings include:

- Reverse power (power output from the phone) was set to maximum (“All Up Bits”)
- Voice Service Option Mode: “Swept Sinewave”
- Variable Rate: set to full
- Supplemental Channel Parameters:
 - Encoder Type: Convolutional (the BSS default) was selected as it was supported in all devices. Turbo Coding was the other option available on the BSS. For data transmission, turbo coding scheme was very efficient, and provided better link performance and power savings. However, since the reverse power was set to the maximum, it was not expected that emission characteristics are significantly different.
 - Data Source: PRBS (Pseudo-Random Binary Sequences)

Additional phone settings include:

- GPS Location Service setting was “ON”. This was the default for most phones.
- Antenna length extended to the maximum if possible
- Phone in normal operating conditions – i.e. open configuration if it was a “flip” phone

CDMA Test Modes Summary

Table 3.2-4 summarizes the test modes for the CDMA phones. The specific test channels and the corresponding carrier frequencies are shown in Table 3.2-3. Test results are shown in Section 3.4.

Table 3.2-4: Test modes for each CDMA testing

Test No.	Test Modes	BSS Service Option	No. of Channels (Cellular)	No. of Channels (PCS)	Test Time (minutes)
1	Voice	SO3	5	5	2 per channel (10 per five hannels)
2	Data (Fundamental Channel)	SO2	5	5	5 per five channels
3	Data - 9.6 kbps	SO32 (TDSO)	5	5	5 per five channels
4	38.4 kbps		5	5	5 per five channels
5	153.6 kbps (Supplemental Channel)		5	5	5 per five channels
6	Idle	None	1	1	2 per channel
7	Idle (no BSS signal)	None	None	None	2

3.3 Measurement Process

This section discusses emission measurements of wireless phones located in the test reverberation chambers. Discussed are test parameters that include procedures, filter networks, frequency band settings, resolution bandwidths, setup, and instrumentation.

The reverberation chamber test facility is discussed as well as test procedure, including calibration and emission measurement methods. Test matrices are also presented to illustrate test modes. Finally, the data reduction process is presented.

3.3.1 Measurement Method

Overview

Performing conducted power measurement at the antenna port is the most direct and the easiest approach to measuring emissions from a wireless phone. However, this approach fails to account for the presence of the antenna and for radiated emissions from components other than the antenna. As a result, a radiated emission test chamber is preferred to provide a more comprehensive measurement. In this study, the measurement approach and data analysis process previously developed [1][2] were used. The approach utilized reverberation chambers because of their excellent repeatability, field uniformity, aspect independence, and measurement speed. The results are in the form of total radiated power, rather than in field strength. This makes it easier to apply Eq. 2.3-1 directly for interference risk assessment.

Establishing and maintaining connectivity with a wireless DUT can be difficult in a reverberation chamber due to severe multipath interference, however. In addition, measurement of very fast pulses can be problematic. Additional discussions on multipath interference and fast pulse measurement are discussed in a later subsection.

Test Facility Description

The NASA LaRC High Intensity Radiated Fields Laboratory has three separate reverberation chambers located adjacent to one another. This facility is capable of performing radiated susceptibility and emission measurements using either one chamber at a time or in two or three chambers simultaneously. Using multiple chambers allows for distributed testing of systems, creating different electromagnetic environments in each chamber utilized. The National Institute of Standards and Technology has characterized the field uniformity of these chambers, and the results indicated a high degree of electromagnetic field uniformity performance within the stated usable frequencies. Details regarding their performance are located in [15].

A chamber's lowest usable frequency is determined by its construction and geometry, and a sufficient mode density within the chamber to provide a uniform electromagnetic environment [16]. The largest chamber of the three is labeled as Chamber A. Due to its larger size, Chamber A is the only one capable of conducting measurements in Band 1. The lowest usable frequency for Chamber A is approximately 100 MHz with +/-2 dB field uniformity [15]. Figure 3.3-1 shows the inside of the Chamber A. The smallest chamber, Chamber C, was also used for testing higher frequencies. The lowest usable frequency for Chamber C is approximately 350 MHz.

The reverberation chamber method, however, may not be appropriate for measuring emission signals with very short pulse durations [17]. Due to high chamber quality factor, the chamber time-constant

should not be greater than 0.4 of the pulse-width of the modulated signal. This requirement ensures that once a pulsed signal is turned on, the field environment in the chamber has the sufficient time to reach (near) steady-state level before the pulse is turned off.



Figure 3.3-1: Inside Reverberation Chamber A.

RF absorber can be added to the chamber to lower the time-constant if needed; however, emission signal characteristics must be known in advance for all DUTs in all measurement bands. In addition, measurement sensitivity is reduced due to higher chamber loss. No absorber were added to the chamber for this study.

The chamber time-constants vary with frequency, and are about 0.6 microsecond near 100 MHz for an empty Chamber A. The measurement results are therefore accurate for continuous-wave (CW) signals, or modulated signals of 1.5 microseconds ($= 0.6 \text{ microseconds} / 0.4$) or longer. A method for measuring chamber quality factor and time-constant is described in [17].

Description of Measurement Method

Figure 3.3-2 shows the emission test setup in a reverberation chamber. Tests conducted in reverberation chambers rely on several different methods to produce a statistically uniform and isotropic electromagnetic environment (field statistics measured over one stirrer revolution are isotropic and spatially uniform). Two of these methods are mode-stirred and mode-tuned [17]. Stirrers with reflective surfaces are rotated continuously during mode-stirring, or stepped at equal intervals for a complete rotation during mode-tuning.

The mode-stirred method was adopted in this study due to ease of setup, implementation, and significant speed advantage over the mode-tuned method. While the mode-tuned method can be more accurate in immunity testing applications (especially for DUTs with slow response time), the mode-stirred method is superior for most emission measurement applications due to speed. With a spectrum analyzer being used for measuring receive power, the emission measurement system can respond very fast to the changing fields caused by the continuously rotated stirrers. Settling-time delays for stirrer stepping in mode-tuned operations are eliminated, resulting in significant speed improvements. In addition,

combining mode-stirred operations with continuous frequency sweeping can further expedite the measurements.

In typical reverberation chamber applications, measurement uncertainty levels can be lowered by selecting the number of measurement points in a stirrer revolution approximately equal to the number of calibration points. In addition, the number of measurements during one stirrer revolution should be as large as possible within constraints of instrument capabilities and test time. Using the mode-stirred method, several thousand measurements per stirrer revolution are easily achievable using a spectrum analyzer. On the other hand, the mode-tuned method with the number of measurements exceeding 100 per stirrer revolution is typically considered impractical due to excessive test time.

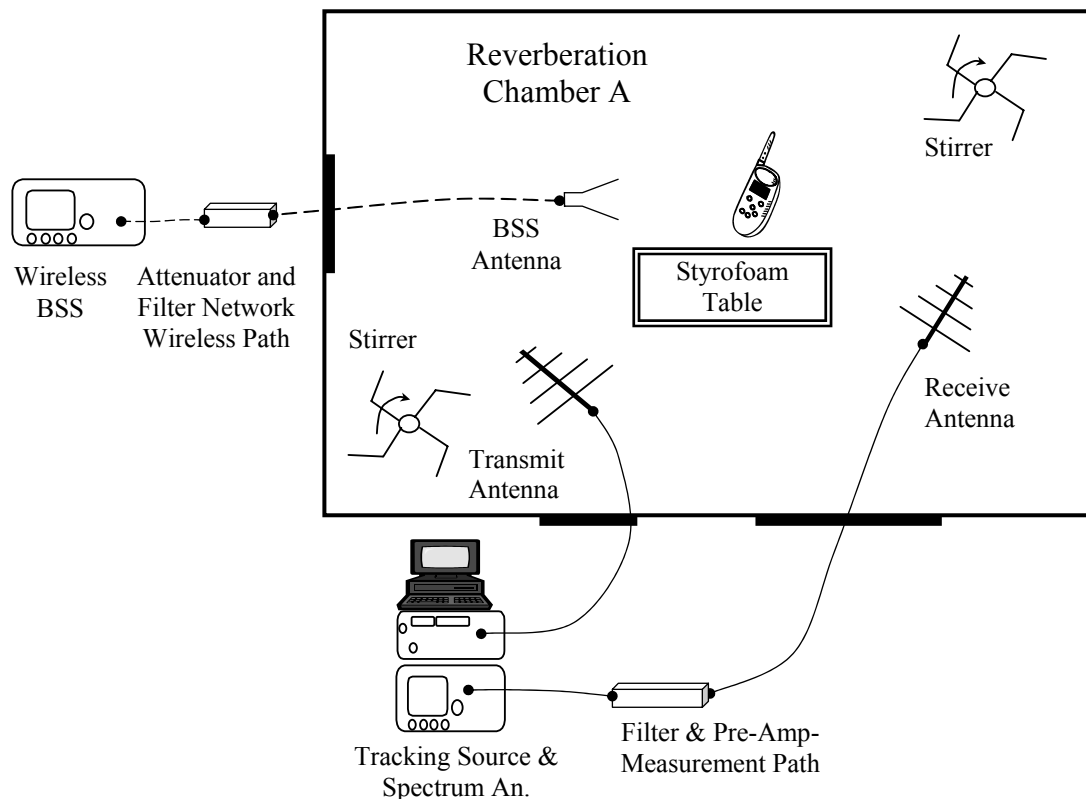


Figure 3.3-2: Reverberation chamber and wireless phone emission test configuration.

Figure 3.3-2 shows the position of a BSS antenna and a wireless phone in the center of the chamber. Utilizing the mode-stirred method, the two stirrers located in the corners of the chamber were continuously rotated at 5 rpm during chamber calibrations and emissions testing. Also illustrated is the control and data acquisition system. RF filters and a preamplifier are indicated in the receive path.

The wireless network is illustrated outside the chamber, and includes a BSS and a bandpass filter network inline with the BSS antenna. A 20 dB attenuator is used at the BSS antenna to reduce signal overload caused by the close proximity of the BSS antenna and wireless phone radiating at the maximum power. This close proximity is necessary to overcome multipath interference, and help maintain the wireless connection.

Emission measurements using the mode-stirred method typically involve [17]:

- 1) Empty chamber insertion loss measurement;
- 2) Measurement of chamber loading, caused by the presence of test devices inside the chamber; and
- 3) Measurement of maximum receive power over a paddle rotation of the stirrer with the DUT powered on in various test modes.

The total radiated power within the measurement resolution bandwidth can be calculated using [18]:

$$P_{TotRad} = (P_{MaxRec} * \eta_{Tx}) / (CLF * IL) , \quad (\text{Eq. 3.3-1})$$

where

P_{TotRad}	=	total radiated power within the measurement resolution bandwidth,
P_{MaxRec}	=	maximum received power measured over one complete paddle rotation,
CLF	=	chamber loading factor, or the additional loading effects caused by the presence of objects in the test chamber,
η_{Tx}	=	efficiency factor of the transmit antenna used in chamber calibration and assumed to be unity for the antennas used,
IL	=	empty chamber insertion loss, pre-determined during chamber calibration.

IL is measured during chamber calibration, and is defined as the ratio of the maximum receive power and the transmit power in a stirrer revolution [18]:

$$IL = P_{MaxRec} / P_{Input} , \quad (\text{Eq. 3.3-2})$$

where P_{MaxRec} and P_{Input} are the maximum received power and the transmit power at the antennas, respectively.

In [17], IL is first measured and averaged over multiple locations for improved uncertainties. CLF is then measured once (one location) when test objects or personnel are introduced into the test chamber. Correction for CLF is applied only when the values exceed a given threshold (3 dB is specified in [17]).

$CLF \approx 1$ in this study since each individual phone is small and has little effect on overall chamber loading. Thus ($CLF * IL$) is simply (IL). In addition, IL was measured at one location rather than averaged over multiple locations. The effect is an acceptable small increase in uncertainty of about two dB or less, based on past measurements and the results of a detailed study reported in [15].

In an actual setup, it is often convenient to include transmit and receive path losses in the chamber calibration measurements. These path losses account for the presence of test cables, in-line amplifiers, attenuators and filters for various purposes. Transmit path losses are associated with components connecting the source output and the transmit antenna, whereas receive path losses are associated with

components connecting the receive antenna and the spectrum analyzer input. As a result, chamber calibration factor (CF), in dB, is introduced:

$$\begin{aligned} CF &= (P_{Xmit(dBm)} - P_{SAMeas(dBm)}) \\ &= L_{Chmbr(dB)} + L_{RecCable(dB)} + L_{XmitCable(dB)}, \end{aligned} \quad (\text{Eq. 3.3-3})$$

where

$$\begin{aligned} CF &= \text{chamber Calibration Factor (dB),} \\ L_{Chmbr(dB)} &= \text{chamber loss (dB), or} \\ &= -10 * \log_{10}(CLF * IL), \\ L_{RecCable(dB)} &= \text{receive cable loss (dB),} \\ L_{XmitCable(dB)} &= \text{transmit cable loss (dB),} \\ P_{SAMeas(dBm)} &= \text{maximum receive power measured at the spectrum analyzer (dBm) over one} \\ &\quad \text{stirrer revolution,} \\ P_{Xmit(dBm)} &= \text{power transmitted from source (dBm).} \end{aligned}$$

Passive losses (not to include amplifier gains) are defined to be positive in dB. The total radiated power in dBm can be computed using:

$$P_{TotRad(dBm)} = P_{SAMeas(dBm)} - L_{XmitCable(dB)} + CF. \quad (\text{Eq. 3.3-4})$$

As shown in Figure 3.3-2, measurement instrumentation included a spectrum analyzer, a tracking source (frequency-coupled with the spectrum analyzer), a data acquisition computer, transmit and receive antennas, RF filters and pre-amplifiers. The measurement procedure begins by performing a transmit path loss measurement. This step is performed at each frequency by injecting a known power from the tracking source through the cable to the antenna connector and using a spectrum analyzer for the measurement.

Next, a chamber calibration is performed. A known level of power is delivered from the source into the chamber through the transmit antenna while the stirrer(s) are continuously rotated at a predetermined rate. The spectrum analyzer is used to record the maximum power coupled into the receive antenna (and the receive path) while performing synchronized frequency sweeps with the tracking source across the measurement bands. Eq. 3.3-3 is applied to determine the CF [2].

During the emission measurements, the spectrum analyzer is set on maximum hold mode while continuously sweeping over the measurement frequency band. The DUT is exercised through different operating modes. Eq. 3.3-4 is applied to normalize the measurement data with the calibration data to arrive at the final total radiated power [2]. In addition, the source is disconnected during the measurements to avoid RF leakage from the source into the test chamber, and the transmit cable path is utilized to provide a communication path between the wireless phone and the BSS. The measurement noise floor is also measured in each band, with the DUT powered off.

Filters and Amplifiers, and Equipment Settings

Proper filtering is required for accurate measurement of spurious emissions from the wireless phones. Several custom-built filters were used for this study. Two separate sets of filters were used, one in the wireless path and the other in the measurement path.

Filters in the *wireless path* are positioned between the BSS and its antenna. These filters pass the wireless signals between the BSS and the wireless phone, while blocking any spurious emissions from the BSS that might contaminate the test chamber. Filters with the pass band covering US cellular and US PCS bands were connected in parallel to pass both bands simultaneously, allowing the BSS to switch between bands as necessary to test dual band phones. Figure 3.3-3 and Table 3.3-1 illustrate the filters used in the wireless path.

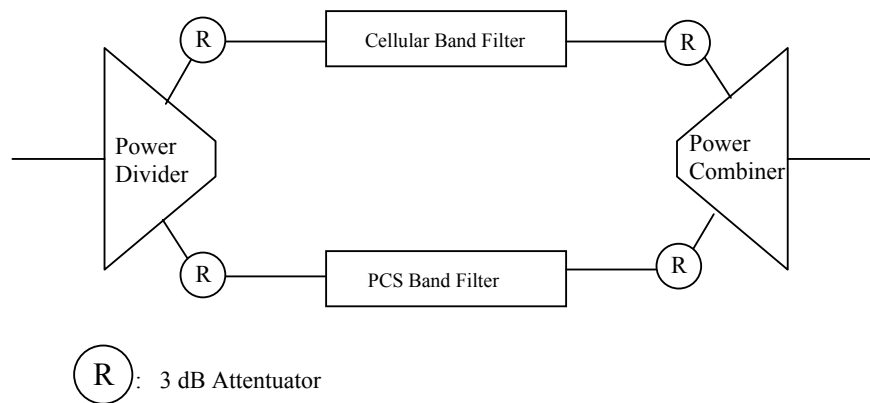


Figure 3.3-3: Parallel filters in the wireless path. The 3 dB attenuators are for improved impedance matching.

Table 3.3-1: Filters Used in the BSS Wireless Path

Wireless Band	Bandpass Filter Pass Band (MHz)	Model
Cellular	820-900	K&L Microwave 6B120-860/X80
PCS	1710-1990	K&L Microwave 9B120-1850/X280

Filters in the *measurement path* help to block the cellular and PCS wireless signals from overloading the preamplifiers and the spectrum analyzer. Different sets of highpass, bandpass and lowpass filters were used for different aircraft radio bands. Both lowpass and highpass filters were also used in combination to create a wideband bandpass filter. Table 3.3-2 shows the different filter sets used for different aircraft radio bands. Also shown are high gain pre-amplifiers and receive antennas used during the tests.

Table 3.3-2: Filters, Amplifiers and Antennas in the Measurement Path

Test Freq. Band	Test Chamber	Pre-Amplifier	Filters – Measurement Path	Receive Antenna
1	A	Miteq AU-1291-N-1103-1179-WP; 60 dB; 0.01-500 MHz	K&L Lowpass 8IL40-336/U468 Cutoff Freq. 336 MHz (2 each)	A&H SAS-200/514 Log-Periodic
2	A	HP8491B Attenuator, 10 dB		
3	C	Miteq AMF-4F-00800250-06-13P; 60 dB; 800-2500 MHz	K&L High Pass 5IH10-960/T1600 Cutoff Freq =960MHz (2 each)	A&H SAS-571 Dual Ridge Horn
4	C		K&L Low Pass 7IL10-1600/X1710 Cutoff Freq=1600MHz (2 each)	
5	C	Miteq AMF-5F-02600520-06-10P; 53 dB; 2600-5200 MHz	K&L Band Pass 4FV30-5050/X100 5000-5100 MHz	

3.3.2 Device-Focused Testing

Overview

Measurements of spurious radiated emissions were conducted on wireless phone devices for all five measurement bands, with each device operating in both US cellular and PCS bands if possible (not at the same time). This section discusses 1) the descriptions of the GSM and CDMA devices tested, 2) the measurement settings, 3) radiated emission measurement test details, and 4) the data reduction process.

GSM and CDMA Phone Tested

Tables 3.3-3, 3.3-4 and Figures 3.3-4, 3.3-5 show the GSM and CDMA phones tested in this effort.

Table 3.3.-3: GSM Devices Tested

DUT Designation	Manufacturer	Model
GSM01	Motorola	V400
GSM02	Nokia	6800
GSM03	LG	G4050
GSM04	LG	G4010
GSM05	Motorola	T720
GSM06	Samsung	SGH-s307
GSM07	Nokia	3100
GSM08	Siemens	SL56
GSM09	Sony Ericsson	T616
GSM10	Motorola	V525
GSM11	Palm	Tungsten W
GSM12	Handspring	Treo 600
GSM13	Research In Motion	Blackberry 6280
GSM14	Siemens	A56
GSM15	Samsung	SGH-E715
GSM16	Sony Ericsson	T610
GSM17	Motorola	V300

Table 3.3-4: CDMA Devices Tested

DUT Designation	Manufacturer	Model
CDM1	Sanyo	SCP-5400
CDM2	Toshiba	CDM9950
CDM3	Nokia	35851
CDM4	Audiovox	CDM8600
CDM5	LG	VX3100
CDM6	Samsung	SCH-A530
CDM7	Motorola	V60p
CDM8	Kyocera	SE47
CDM9	Audiovox	CDM-8500VM
CDM10	Research In Motion	Blackberry 6750
CDM11	Sanyo	SCP-7300(K)
CDM12	Nokia	6225
CDM13	Samsung	SPH-A620
CDM14	Kyocera	KE433
CDM15	Motorola	V710
CDM16	LG	VX6000



Figure 3.3-4: GSM/GPRS Phones Tested (not to scale).



Figure 3.3-5: CDMA Phones Tested (not to scale).

Measurement Settings

Test parameters used in spurious radiated emission testing for this report, such as measurement bandwidth and scan time, were based upon those used in [2]. The selected parameters are shown in Table 3.3-5.

Table 3.3-5: Measurement Bandwidths and Sweep Times for Measuring Spurious Radiated Emissions in Aircraft Radio Frequency Bands

Frequency Band Designation & (Chamber)	Aircraft Systems	MHz	Resolution Bandwidth kHz	Spectrum Analyzer Sweep Time (ms) (HP8561E)
1 (A)	VOR, ILS-LOC, VHF-COM	105 – 140	10	880
2 (A)	ILS GS	325 – 340	10	375
3 (C)	DME, TCAS, ATCRBS, GPS L2	960 – 1250	100	73
4 (C)	GPS L1	1565 – 1585	10	500
5 (C)	MLS	5020 - 5100	30	230

Wireless Phones Radiated Emission Measurements

The previously described measurement method (Section 3.2) was utilized for all calibrations and radiated emission tests. The positions of a wireless phone device and the BSS antenna were similar to that indicated in Figure 3.3-2. Using the control software, power measurements were automatically normalized with the calibrated data and the results were recorded for each frequency within the test band.

The test chamber configuration and test instrumentation used during calibration and emission measurements are illustrated in Figure 3.3-2. Test instrumentation consisted of an HP8561E Spectrum Analyzer, an HP85644A Tracking Source, RF filters, pre-amplifiers, transmit and receive antennas, and a data acquisition computer. A pair of in-band log-periodic antennas were used as transmit and receive antennas for Band 1 and Band 2. Dual-Ridge-Horn antennas were used for Band 3, 4 and 5. RF filters and preamplifiers were included in the receive path to obtain a lower noise floor, amplify signals, and to block out-of-band signals relative to the wireless device transmission frequencies.

Noise floor measurements were conducted to determine the ambient environment with the BSS powered on (the output to the BSS antenna was filtered). These measurements were used to verify a quiet RF environment before proceeding with radiated emissions tests.

Emission test dwell times varied depending on the number of channels accessed during a test. The test dwell time is two minutes per frequency channel for voice, and one minute per channel for data mode due to the large number of data test modes. Reverberation chamber and receive path calibration measurements were conducted for a dwell time of two minutes.

Figure 3.3-6 illustrates the control and data acquisition hardware located outside the reverberation chamber. Pictured are the HP8561E Spectrum Analyzer and the HP85664A Tracking Source. The local oscillators and four other ports of the spectrum analyzer and tracking source were connected in order to synchronize frequencies. The picture also illustrates the receive path including cable, filters and preamplifier. Agilent Visual Engineering Environment software was used to develop control and data-

recording software that was run on a laptop computer. Figure 3.3.7 illustrates the phone testing inside the small test chamber.

Tables 3.3-6 and 3.3-7 illustrate the test matrices used for radiated emissions measurements conducted. DUT numbers, test modes, and frequency band are included. In addition, Table 3.3.8 provides an estimate of the total number of measurements performed.

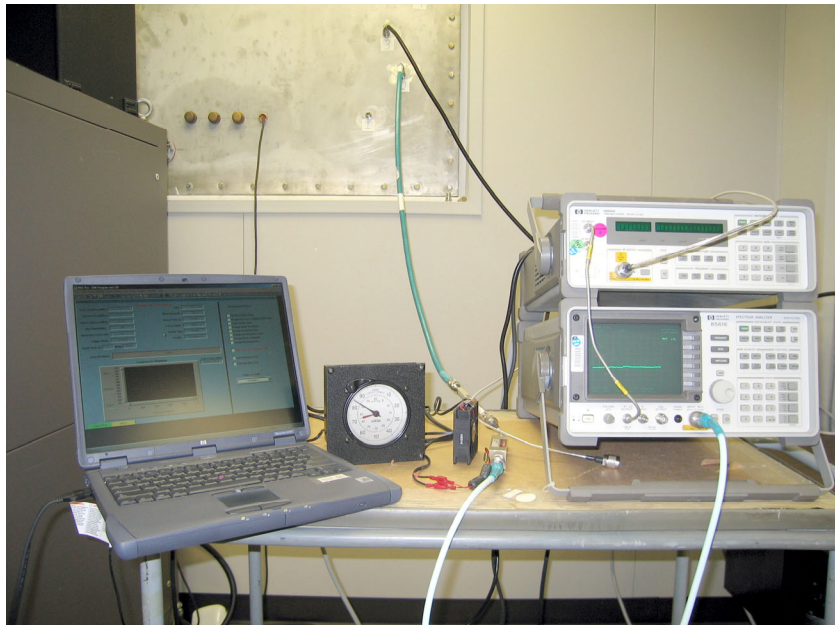


Figure 3.3-6: Control and data acquisition setup outside the reverberation chamber.



Figure 3.3-7: Phone testing inside small test chamber. The lower antenna was for communicating with the phone. The upper antenna pointing at the stirrer was used as the measurement antenna.

Table 3.3-6: Example GSM Test Matrix (for one device)

Device Under Test	Test Modes and Channels	Bands
GSM01	Cell Voice ch 128	1-5
GSM01	Cell Voice ch 159	1-5
GSM01	Cell Voice ch 190	1-5
GSM01	Cell Voice ch 220	1-5
GSM01	Cell Voice ch 251	1-5
GSM01	Cell Data 5 Channels Mult-Slot 1 Down x 1 Up	1-5
GSM01	Cell Data 5 Channels Mult-Slot 2 Down x 1 Up	1-5
GSM01	Cell Data 5 Channels Mult-Slot 4 Down x 1 Up	1-5
GSM01	Cell Data 5 Channels Mult-Slot 2 Down x 2 Up	1-5
GSM01	Cell Data Idle Attached BCH 160	1-5
GSM01	PCS Voice ch 512	1-5
GSM01	PCS Voice ch 587	1-5
GSM01	PCS Voice ch 661	1-5
GSM01	PCS Voice ch 736	1-5
GSM01	PCS Voice ch 810	1-5
GSM01	PCS Data 5 Channels Mult-Slot 1 Down x 1 Up	1-5
GSM01	PCS Data 5 Channels Mult-Slot 2 Down x 1 Up	1-5
GSM01	PCS Data 5 Channels Mult-Slot 4 Down x 1 Up	1-5
GSM01	PCS Data 5 Channels Mult-Slot 2 Down x 2 Up	1-5
GSM01	PCS Data Idle Attached BCH 660	1-5
GSM01	Idle – No Signal	1-5

Table 3.3-7: Example CDMA Test Matrix (for one device)

Device Under Test	Test Modes and Channels	Bands
CDMA01	Cell Voice ch 991	1-5
CDMA01	Cell Voice ch 176	1-5
CDMA01	Cell Voice ch 384	1-5
CDMA01	Cell Voice ch 591	1-5
CDMA01	Cell Voice ch 799	1-5
CDMA01	Cell Data LoopBack - 5 Channels	1-5
CDMA01	Cell Data Reverse Channel 9.6kbps- 5 Channels	1-5
CDMA01	Cell Data Reverse Channel 38.4kbps- 5 Channels	1-5
CDMA01	Cell Data Reverse Channel 153.6kbps- 5 Channels	1-5
CDMA01	Cell Data Idle	1-5
CDMA01	PCS Voice ch 0	1-5
CDMA01	PCS Voice ch 300	1-5
CDMA01	PCS Voice ch 600	1-5
CDMA01	PCS Voice ch 900	1-5
CDMA01	PCS Voice ch 1199	1-5
CDMA01	PCS Data LoopBack - 5 Channels	1-5
CDMA01	PCS Data Reverse Channel 9.6 kbps - 5 Channels	1-5
CDMA01	PCS Data Reverse Channel 38.4 kbps - 5 Channels	1-5
CDMA01	PCS Data Reverse Channel 153.6 kbps - 5 Channels	1-5
CDMA01	PCS Data Idle	1-5
CDMA01	Idle – No Signal	1-5

Table 3.3-8: Approximate Total Number of Phone Test Cases

Wireless Technology	Number of Devices	Number of Test Cases Per Device	Number of Test Bands	Total Test Cases
GSM	17	21	5	1785
CDMA	16	21	5	1680

Dealing with Difficulties in Maintaining Wireless Communication

Similar to the previous efforts [2] and [3], multipath interference occasionally affected communications between BSS and the wireless test devices during testing in the reverberation chambers. When interference occurred, it caused disconnection, making it necessary to repeat tests. Every effort was made to maintain communication for an adequate dwell time in order to collect a complete data set of measurements. Implementing one or more of the following methods helped to overcome many of the multipath interference affects:

- 1) The BSS antenna was placed closer to the test phone, but no closer than approximately 20 centimeters apart.

- 2) A 20 dB attenuator was inserted inline with the BSS antenna to reduce overloading due to the proximity with the wireless phone.
- 3) Metal shielding was placed around the DUT (not closer than approximately 0.5 meters) to block direct paths between the phone and the stirrers.

The test mode was skipped if all attempts to maintain communication failed.

3.3.3 Data Reduction

Figure 3.3-8 illustrates the data reduction process and results. The same process was applied to the PED baseline test data set and wireless devices emission data set in each frequency band. For the purpose of comparison and analysis, large amounts of data were reduced by creating data envelopes, which are representative of the maximum measurements for each wireless phone device. These data envelopes were further reduced to composite envelope that represents the maximum emissions of all devices. The same data reduction was used in the earlier effort to derive the PEDs composite maximum envelope. The comparison plots are shown in Sections 3.4, 3.5, and 3.6.

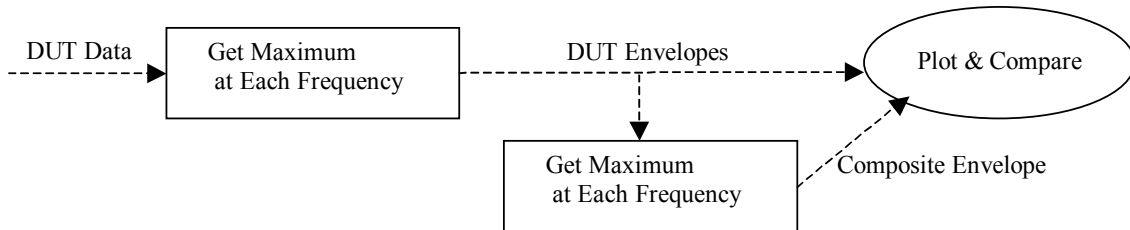


Figure 3.3-8: Data reduction process.

A limited set of wireless phone measurement data are illustrated in Appendices A and B for the GSM and CDMA phones. The reduction of this data followed the general process illustrated in Figure 3.3-8.

The following algorithms summarize the generation of data envelopes. DUT refers to either PEDs or wireless phones.

For each frequency band, and for each DUT,

$$\text{Max} [DUT \text{ Emissions}]_{All_Modes} \Rightarrow DUT \text{ Envelope}$$

For each frequency band,

$$\text{Max} [DUT \text{ Envelope}]_{All_DUT} \Rightarrow All_DUT \text{ Composite_Env}$$

Conforming to the data reduction process, individual DUT envelopes along with their composite envelopes were generated. Wireless phone envelopes are plotted and shown in Section 3.4.

3.4 Wireless Phone Measurement Results

This section reports the measurement results for the 17 GSM and 16 CDMA phones. The measurement process used and the test mode selections were reported in Sections 3.2 and 3.3. The devices tested are shown in Tables 3.3-3, 3.3-4 and Figures 3.3-4, 3.3-5.

Due to the large volume of collected data, the results in this section are the final emission envelope for each of the phones. Each phone emission envelope is determined by retaining the maximum value at each frequency for all phone test modes. The phone test modes include idle mode, voice mode, various data rates, frequency channels, and operating bands (cellular or PCS).

The results are grouped into CDMA and GSM subsections, due to different test modes used for the two technologies. Emissions in each measurement band are organized in groups of five or six phones for ease of viewing and comparisons. In addition, a noise floor is plotted which represents the instrument's (spectrum analyzer's) noise level which was processed and calibrated in the same way as the data. This noise floor establishes the sensitivity of the measurement system. Sixth harmonics of the GSM and CDMA cellular band transmissions are identified in the graphs for Band 5. Appendices A and B show additional test result details.

Section 3.4.1 reports the results for the GSM phones, and Section 3.4.2 for the CDMA phones. Section 3.4.3 further reduces the data reported in Sections 3.4.1, 3.4.2, Appendix A and Appendix B by presenting scattered plots of the peak emission values for each phone operating in voice mode, data mode, cellular band and PCS band. These summary charts help to quickly identify phones that have certain characteristics, such as large emission difference between cellular versus PCS band operations.

In most cases, phone emission levels were significantly lower in idle modes (with and without BSS signal) than in active modes. Idle-mode emissions were usually not observed above the measurement noise floor. The exceptions included three phones that had their maximum idle modes emissions as high as their active mode emissions. Band 3 and Band 5 were the measurement bands in these cases. However, this finding is still preliminary due to the limited number of idle modes considered. In any case, the idle mode emissions were included in determining the phone maximum emission results presented in 3.4.1 and 3.4.2.

3.4.1 GSM/GPRS phones

Band 1

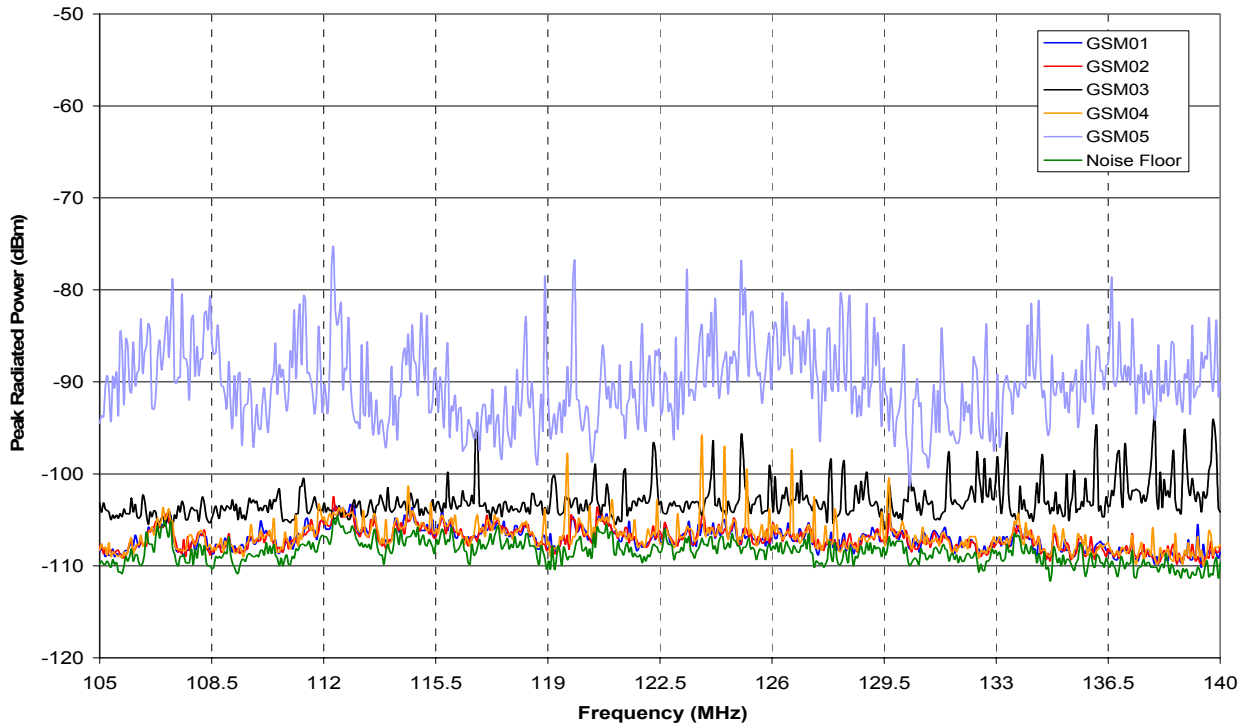


Figure 3.4-1: Individual phone emission envelopes. GSM phones 1 through 5. Band 1.

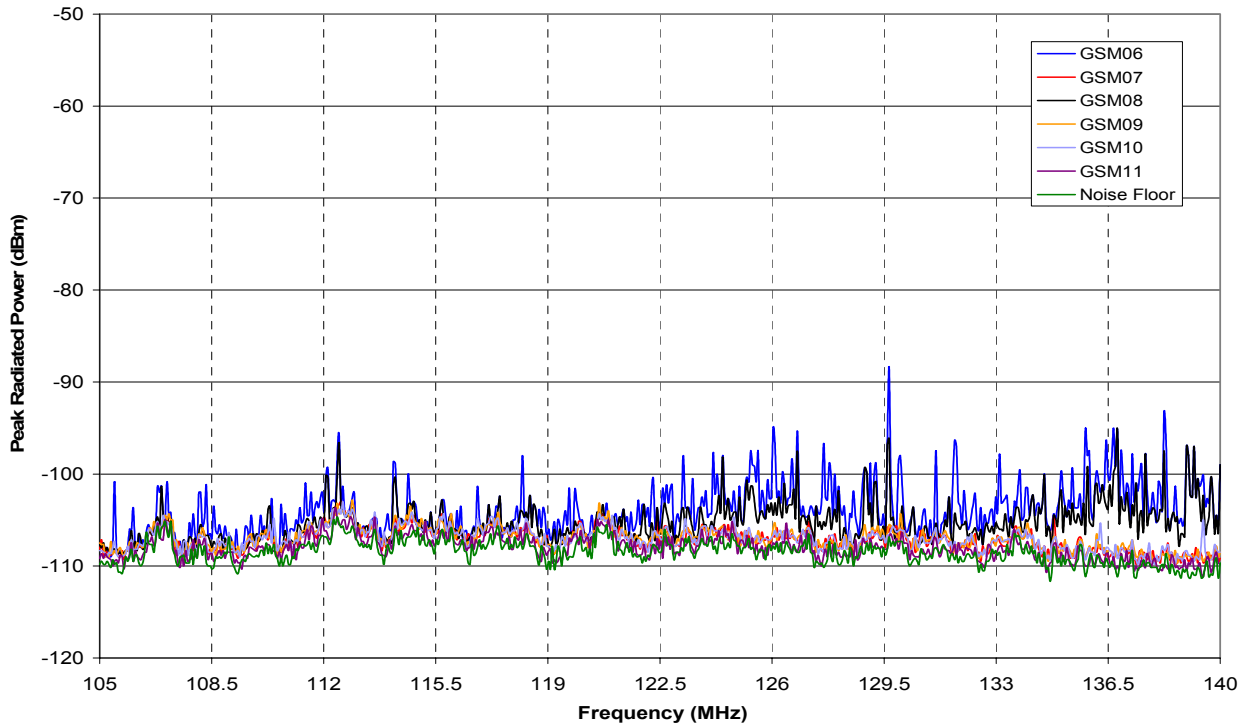


Figure 3.4-2: Individual phone emission envelopes. GSM phones 6 through 11. Band 1.

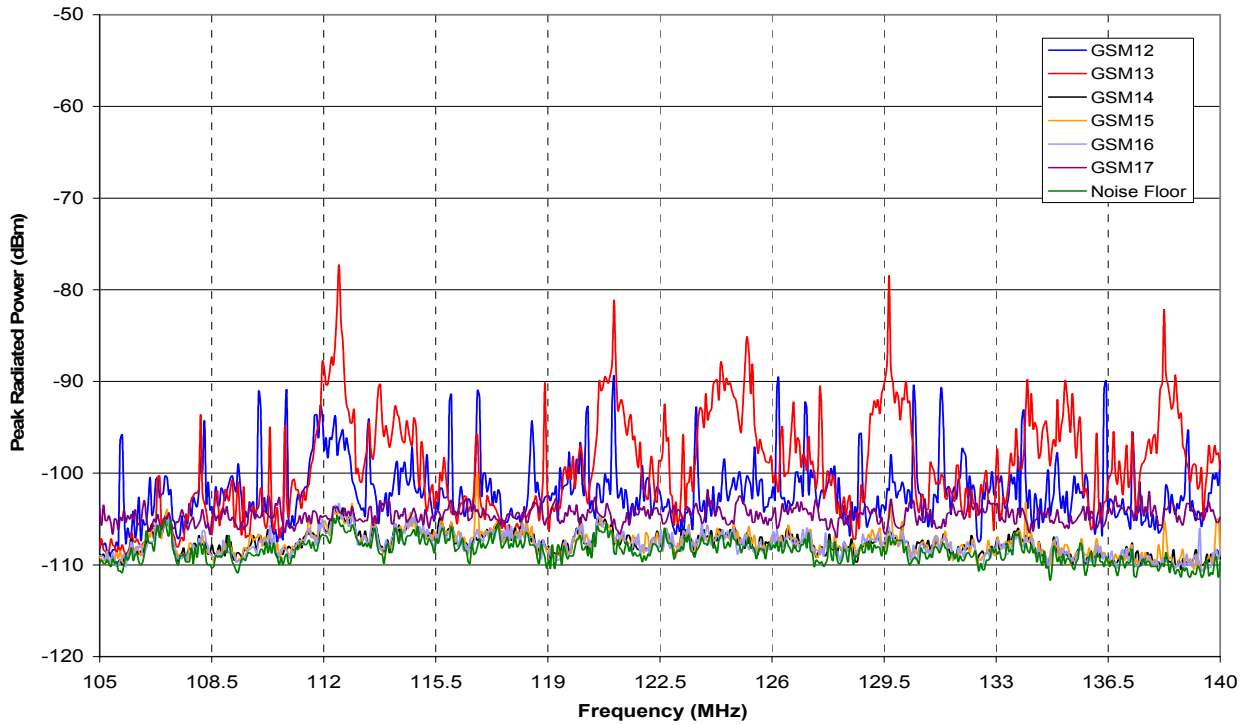


Figure 3.4-3: Individual phone emission envelopes. GSM phones 12 through 17. Band 1.

Band 2

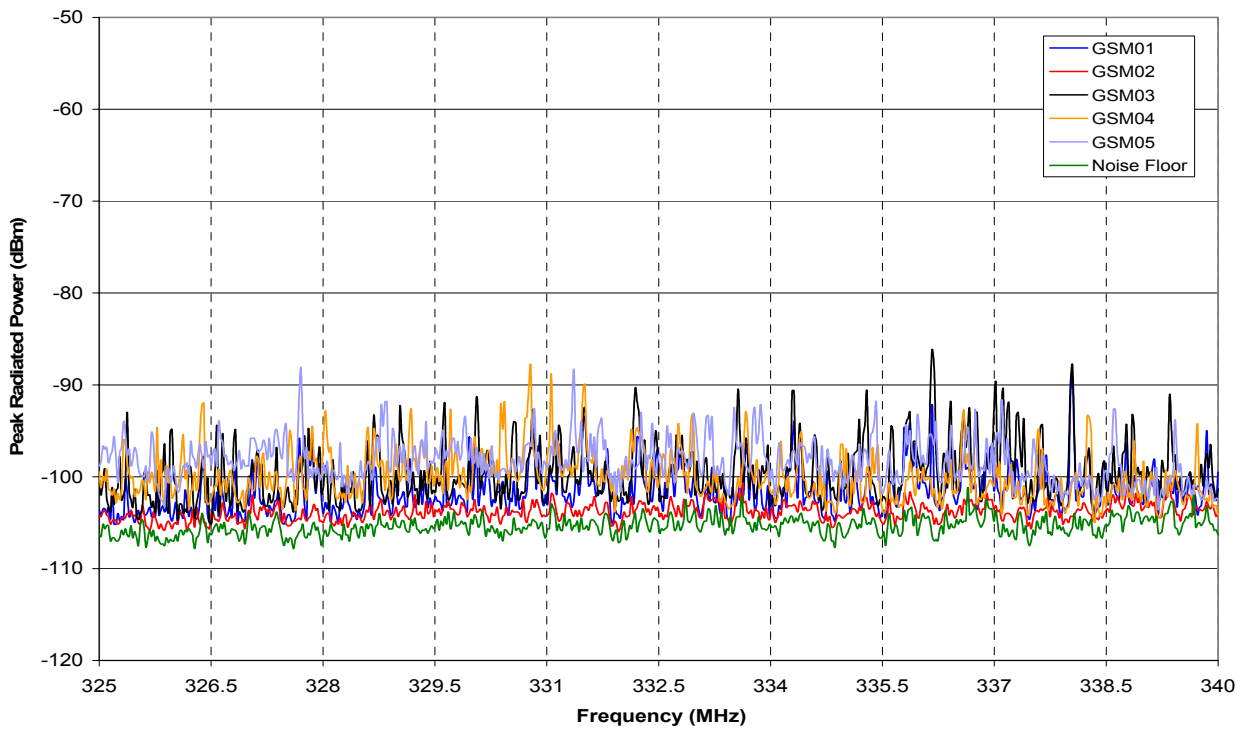


Figure 3.4-4: Individual phone emission envelopes. GSM phones 1 through 5. Band 2.

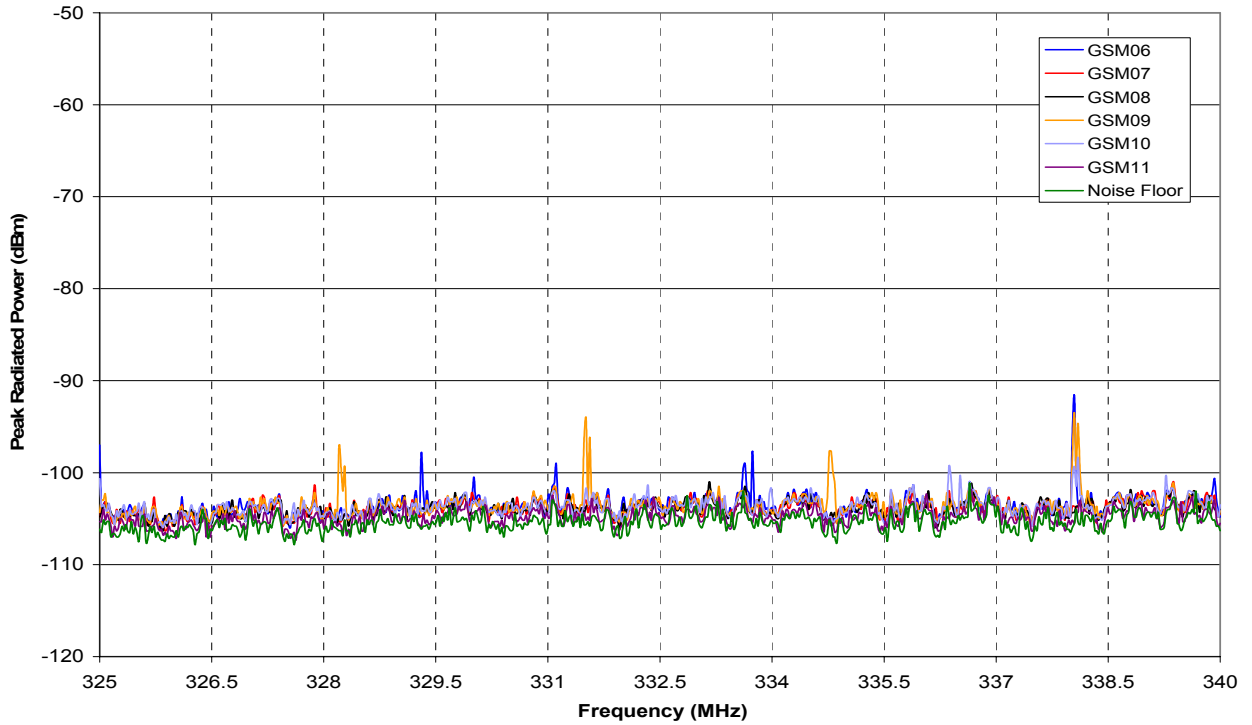


Figure 3.4-5: Individual phone emission envelopes. GSM phones 6 through 11. Band 2.

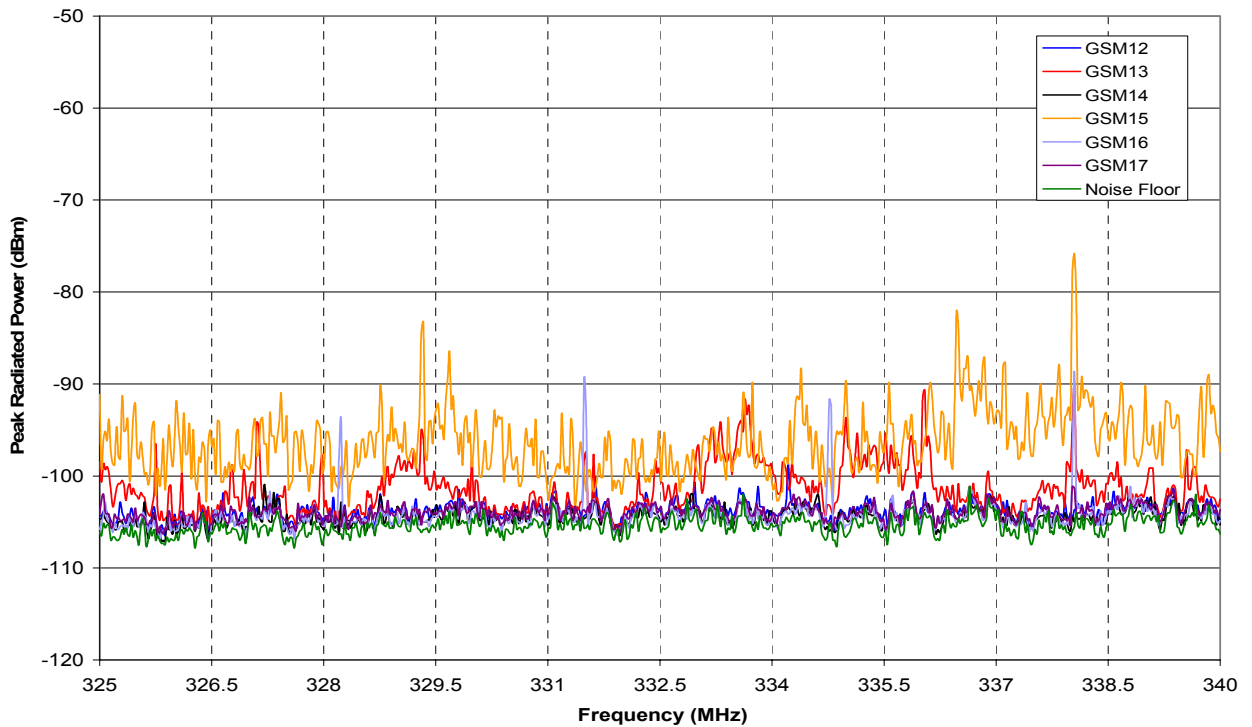


Figure 3.4-6: Individual phone emission envelopes. GSM phones 12 through 17. Band 2.

Band 3

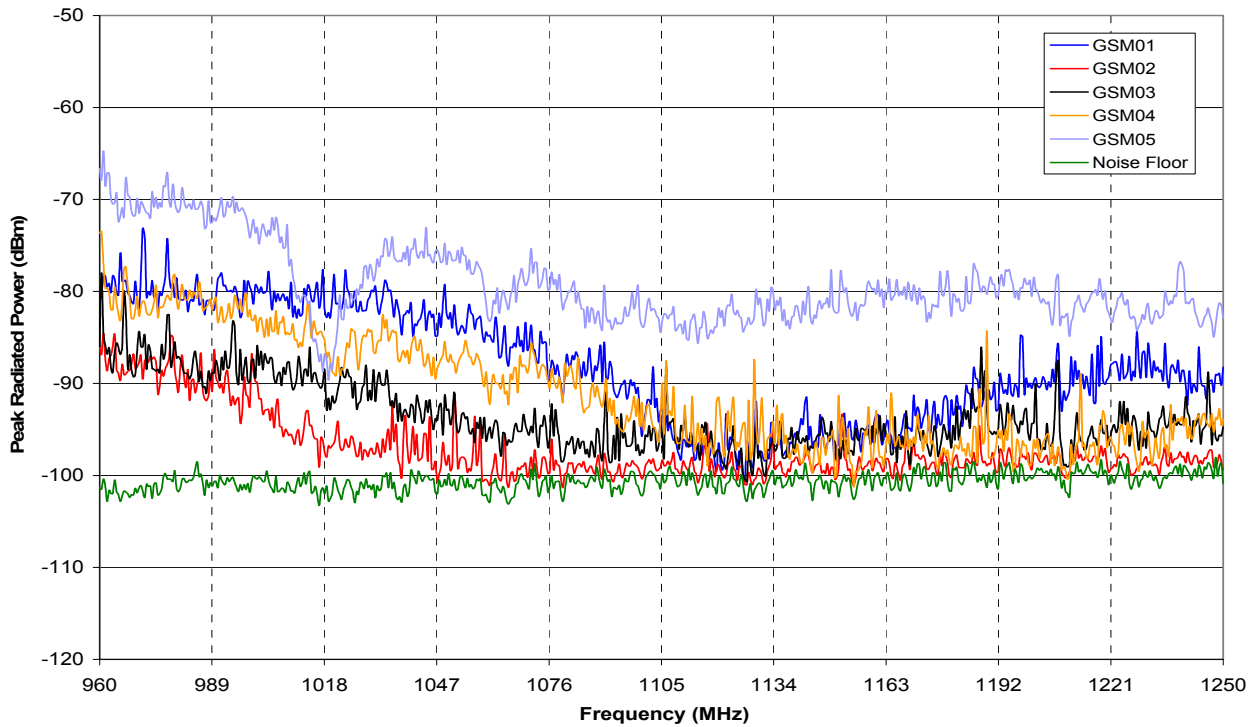


Figure 3.4-7: Individual phone emission envelopes. GSM phones 1 through 5. Band 3.

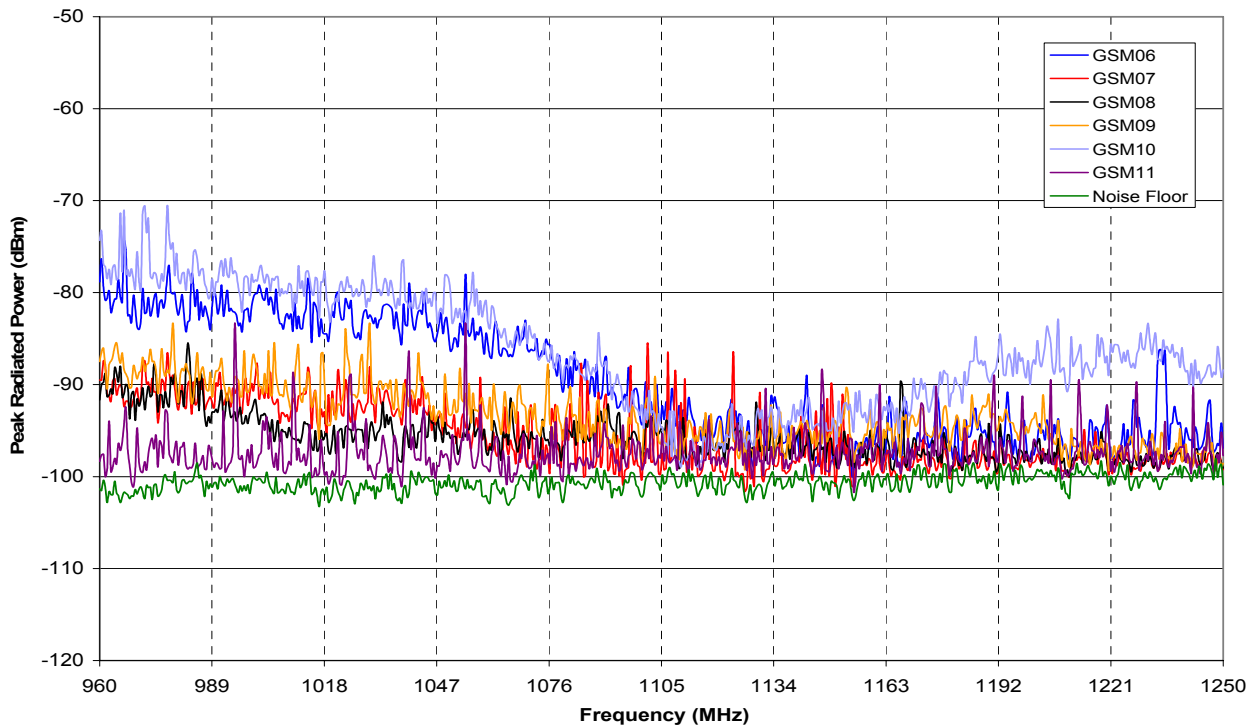


Figure 3.4-8: Individual phone emission envelopes. GSM phones 6 through 11. Band 3.

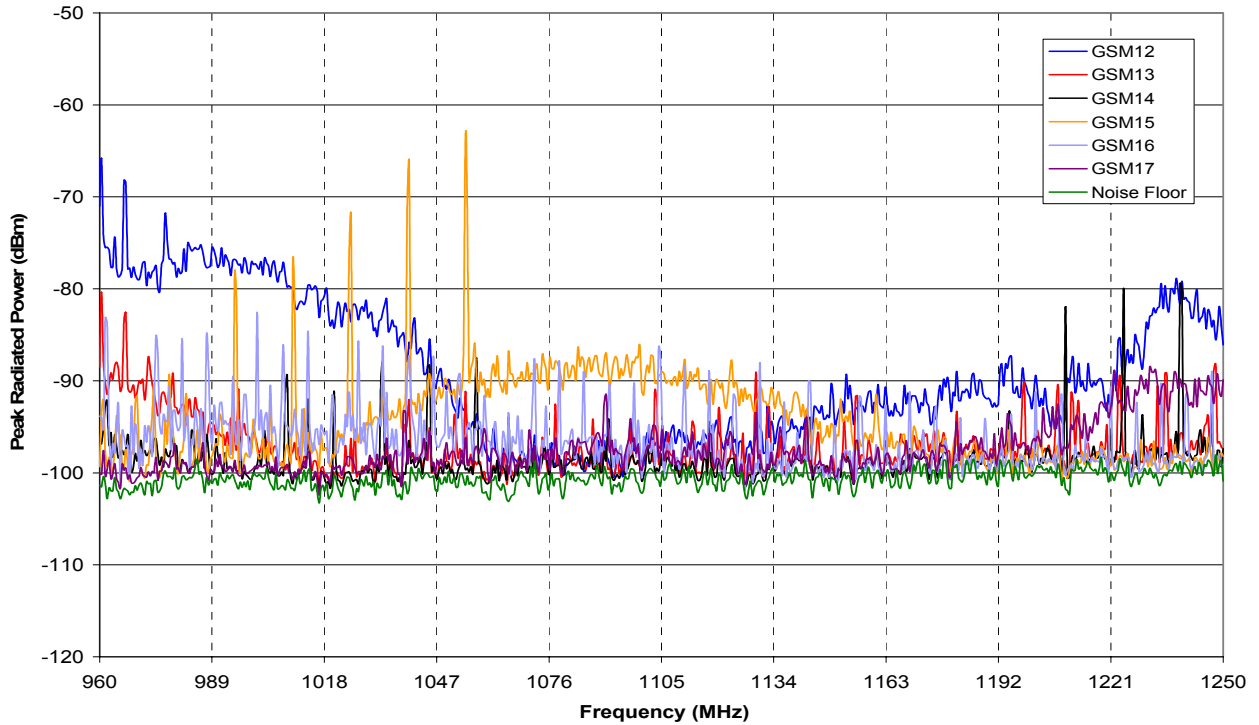


Figure 3.4-9: Individual phone emission envelopes. GSM phones 12 through 17. Band 3.

Band 4

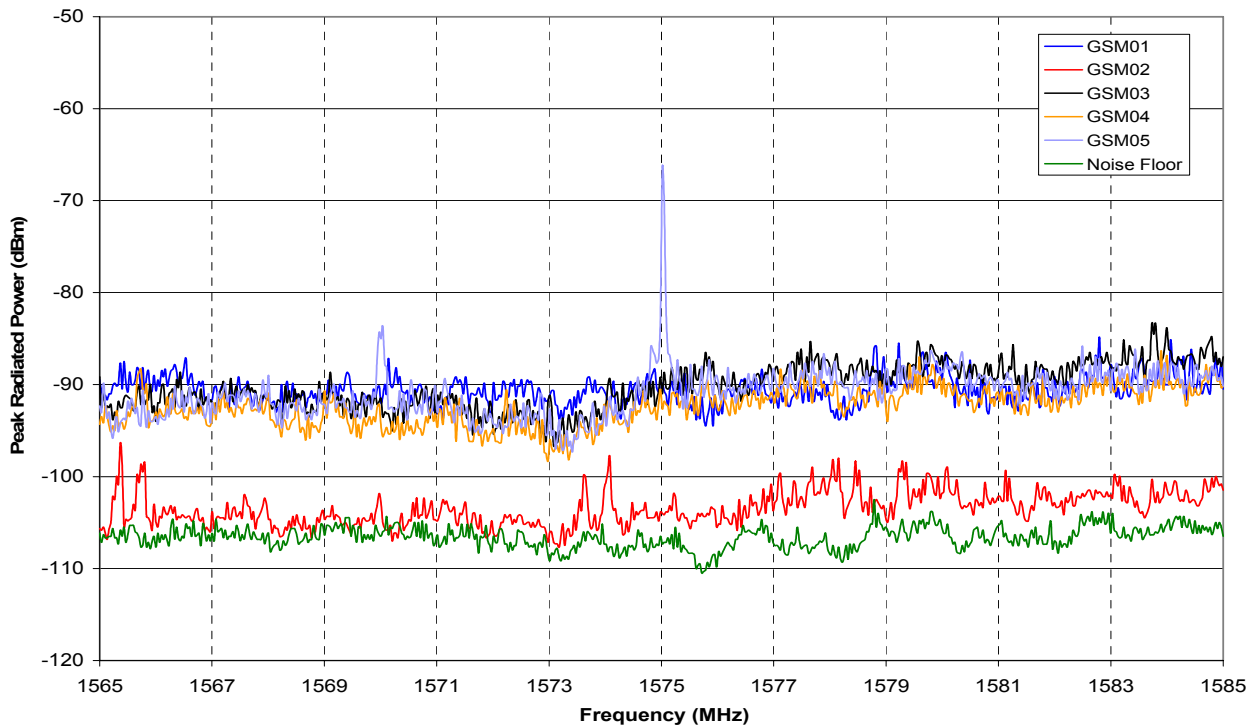


Figure 3.4-10: Individual phone emission envelopes. GSM phones 1 through 5. Band 4.

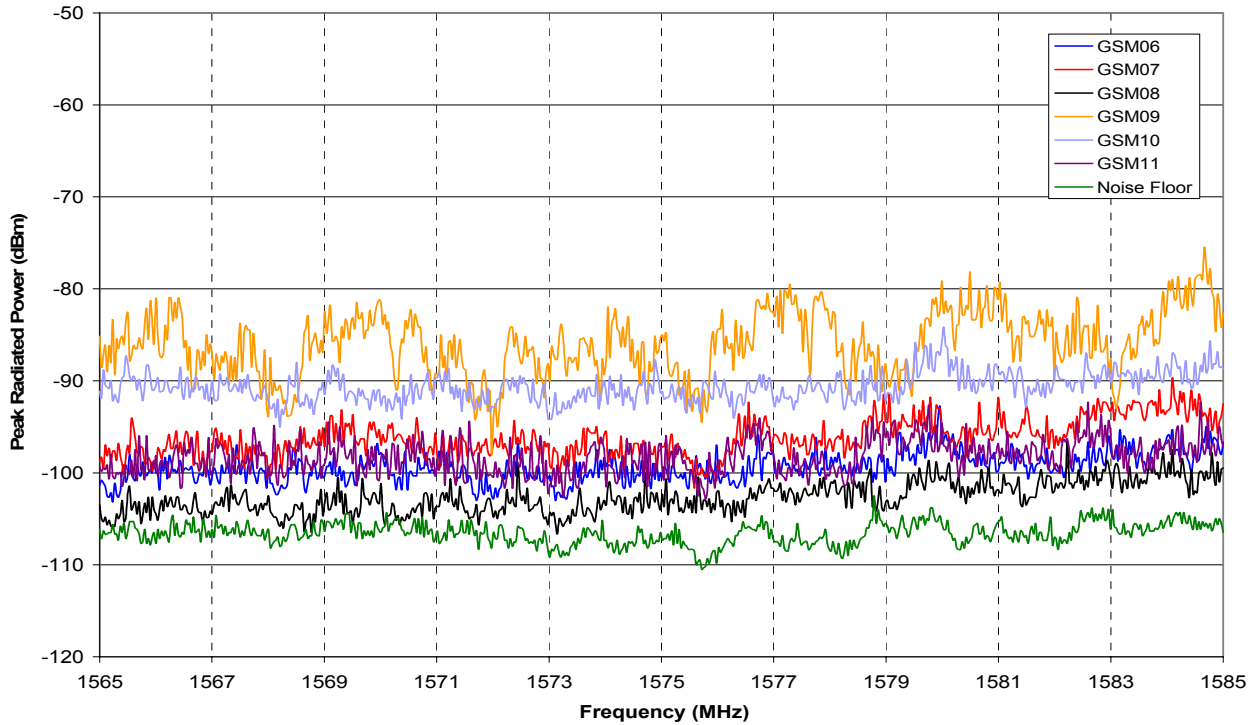


Figure 3.4-11: Individual phone emission envelopes. GSM phones 6 through 11. Band 4.

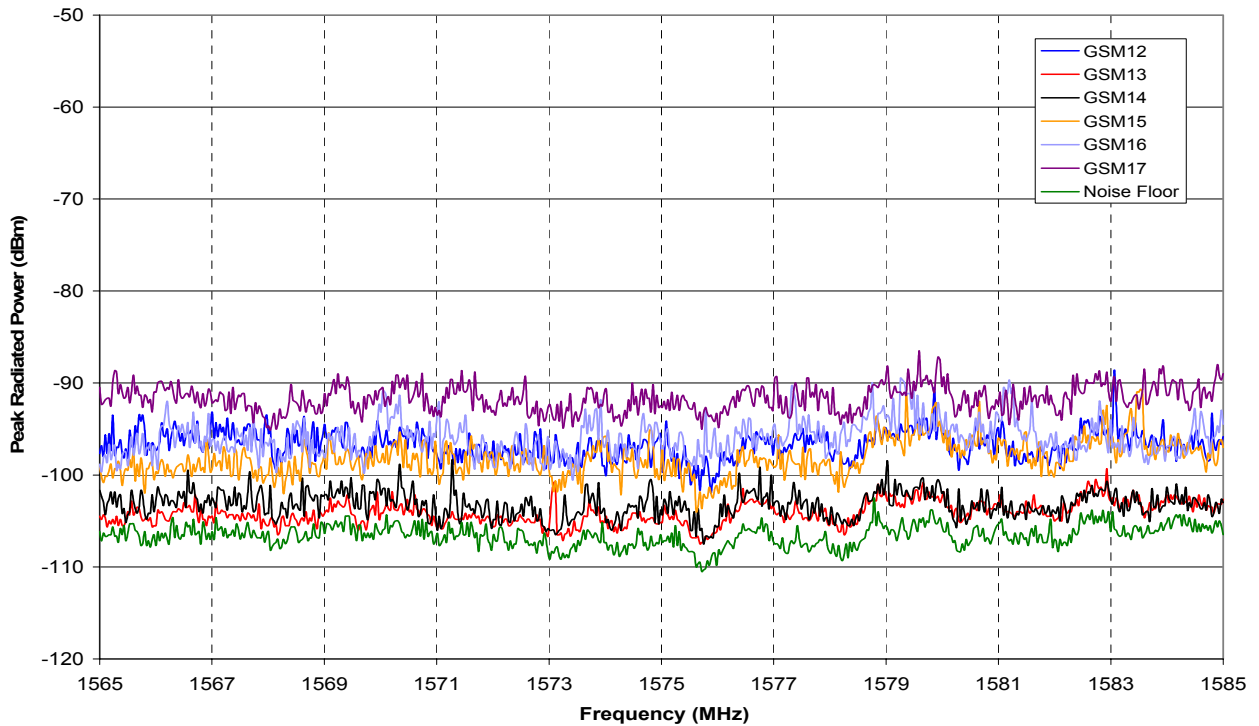


Figure 3.4-12: Individual phone emission envelopes. GSM phones 12 through 17. Band 4.

Band 5

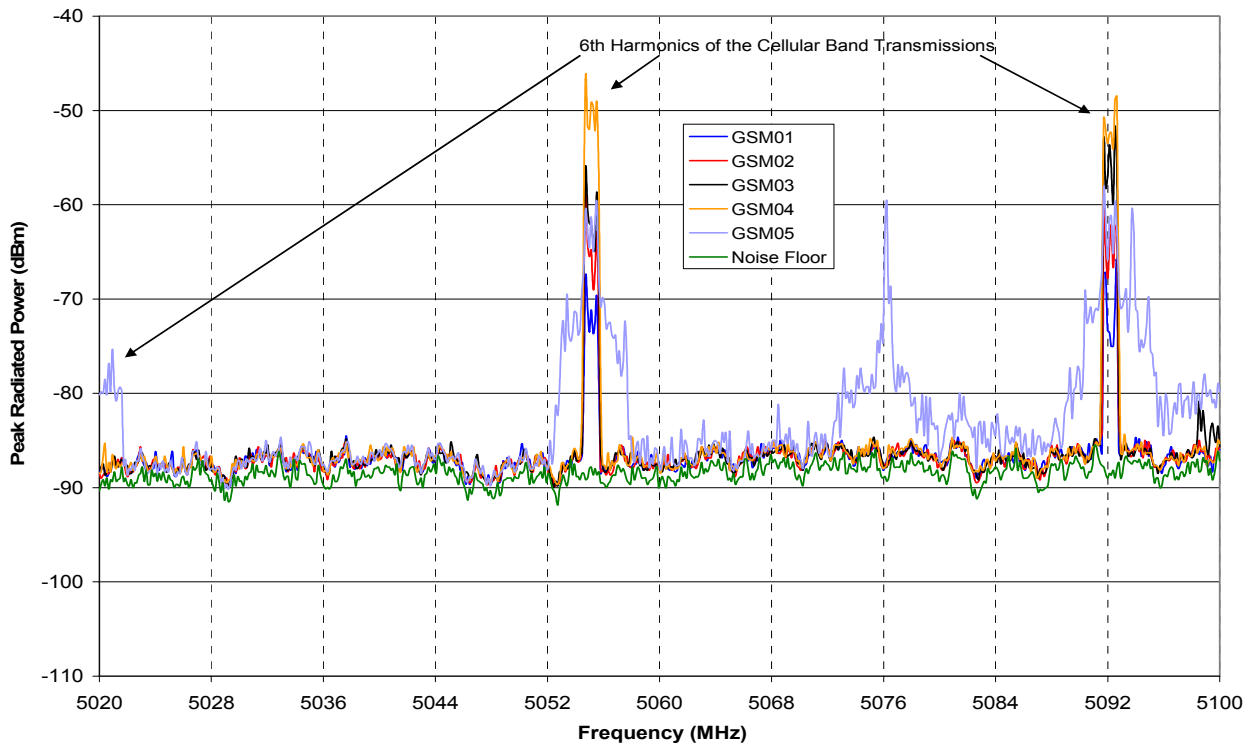


Figure 3.4-13: Individual phone emission envelopes. GSM phones 1 through 5. Band 5.

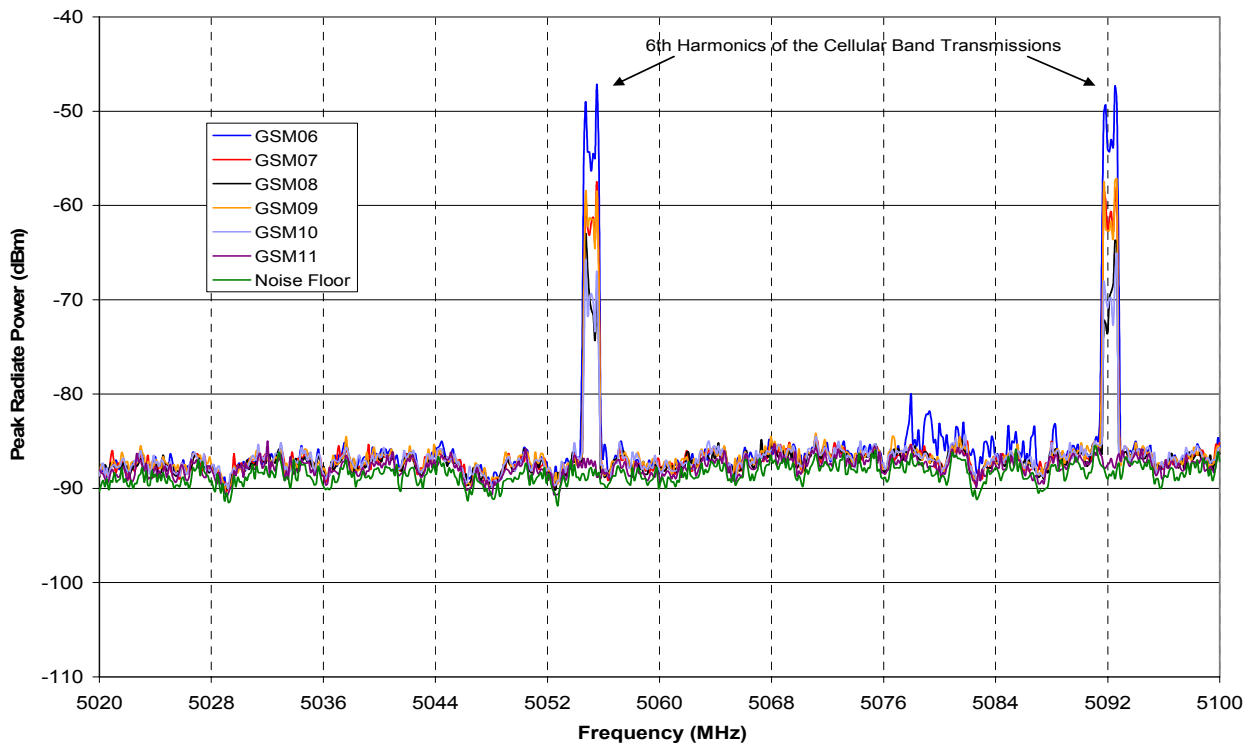


Figure 3.4-14: Individual phone emission envelopes. GSM phones 6 through 11. Band 5.

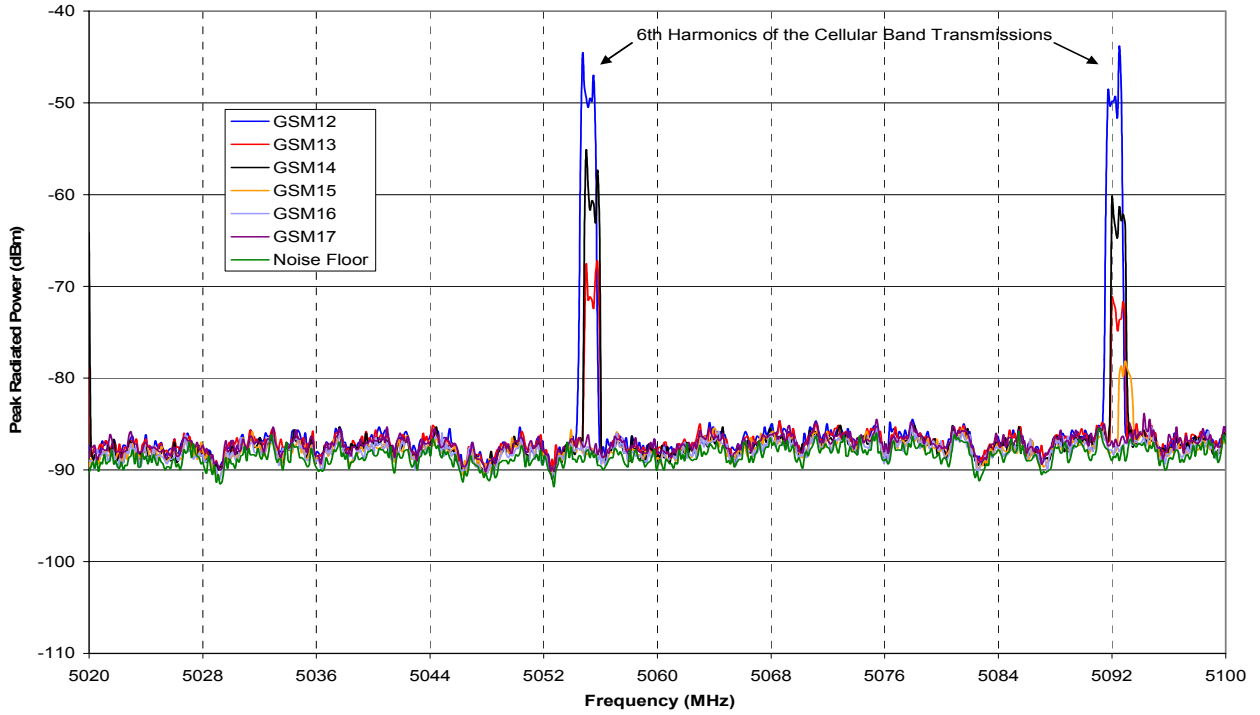


Figure 3.4-15: Individual phone emission envelopes. GSM phones 12 through 17. Band 5.

3.4.2 CDMA phones

Band 1

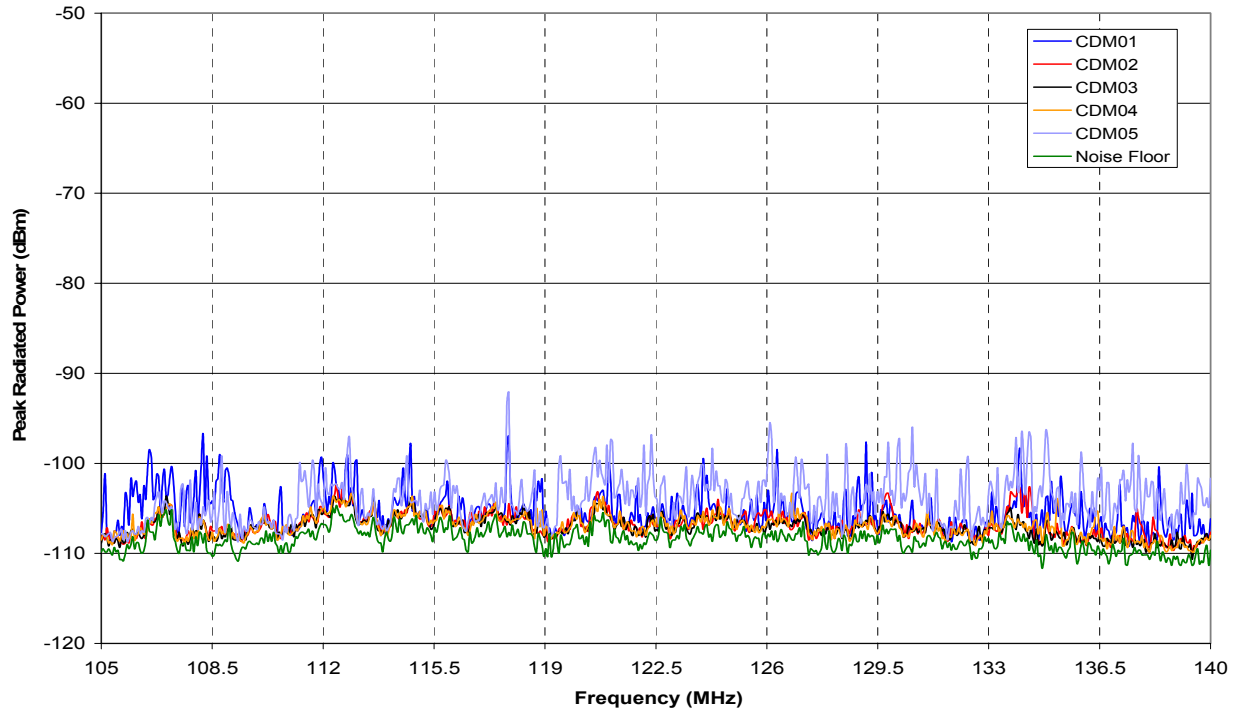


Figure 3.4-16: Individual phone emission envelopes. CDMA phones 1 through 5. Band 1.

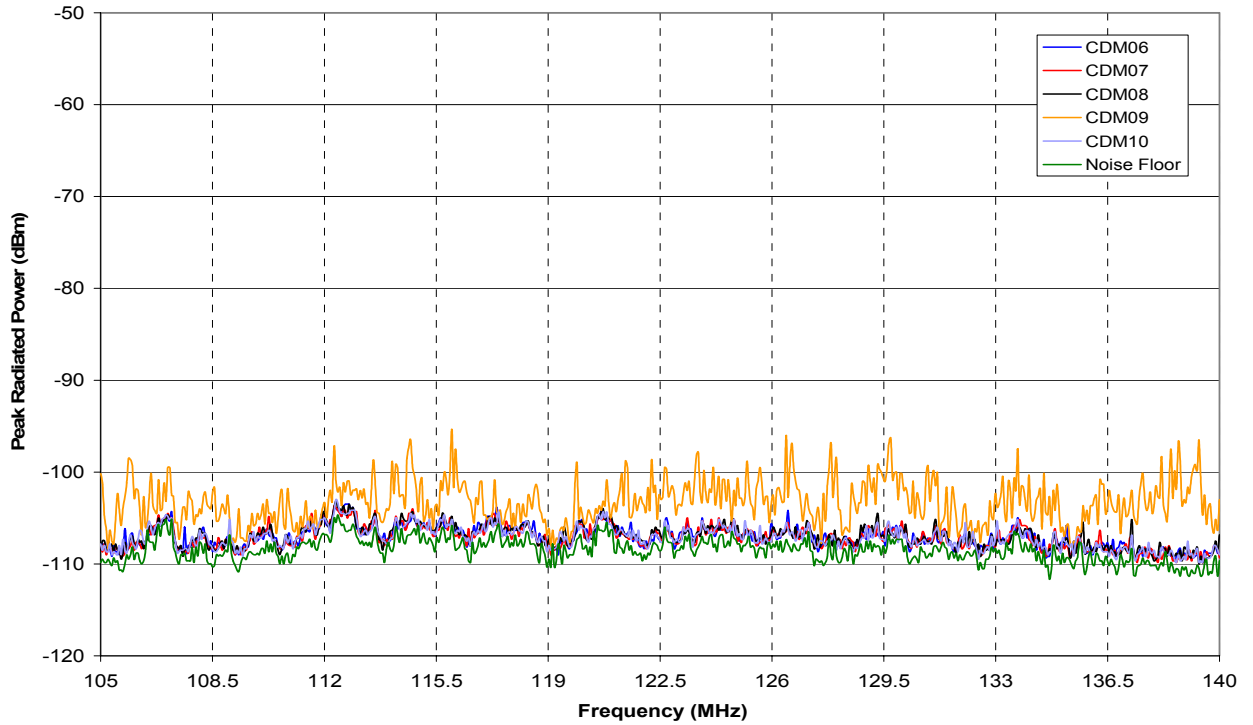


Figure 3.4-17: Individual phone emission envelopes. CDMA phones 6 through 10. Band 1.

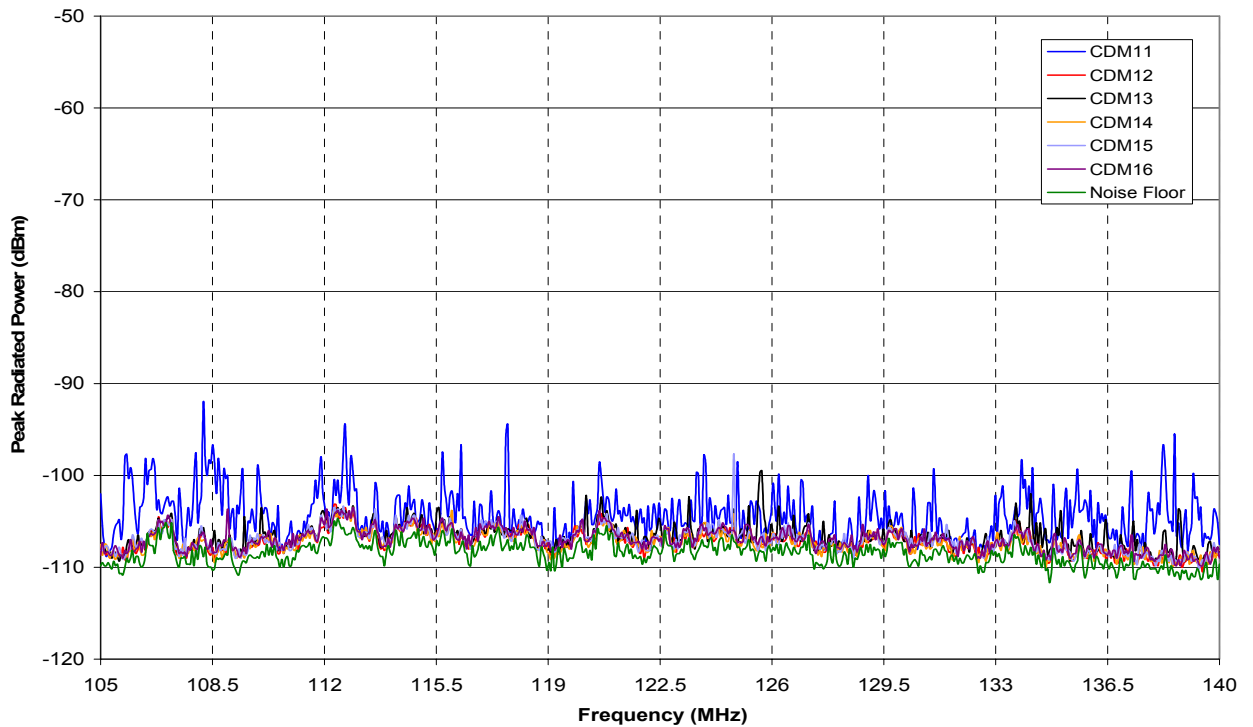


Figure 3.4-18: Individual phone emission envelopes. CDMA phones 11 through 16. Band 1.

Band 2

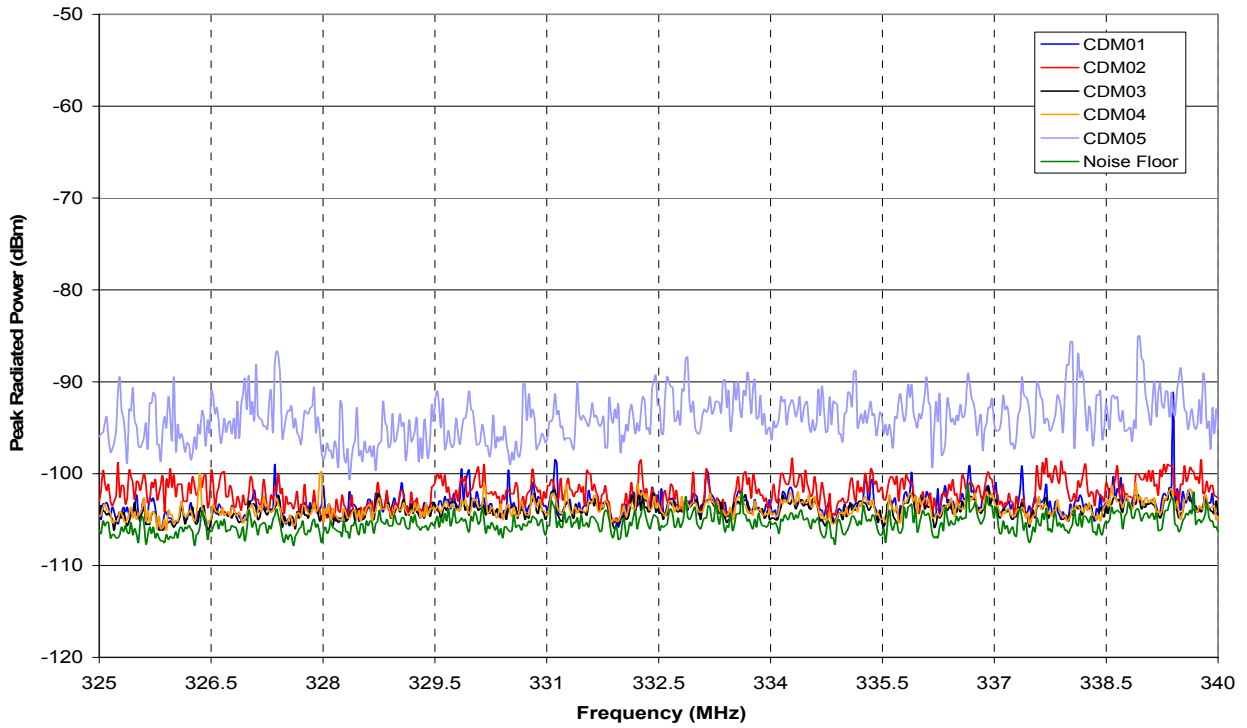


Figure 3.4-19: Individual phone emission envelopes. CDMA phones 1 through 5. Band 2.

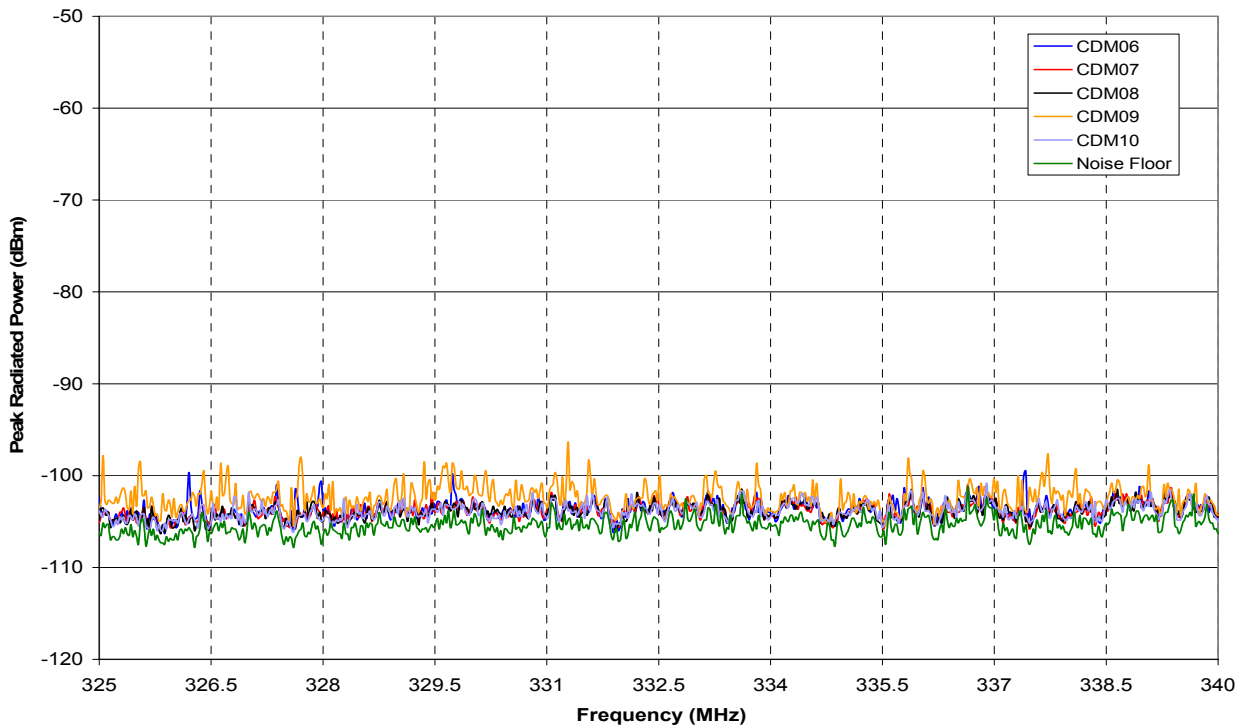


Figure 3.4-20: Individual phone emission envelopes. CDMA phones 6 through 10. Band 2.

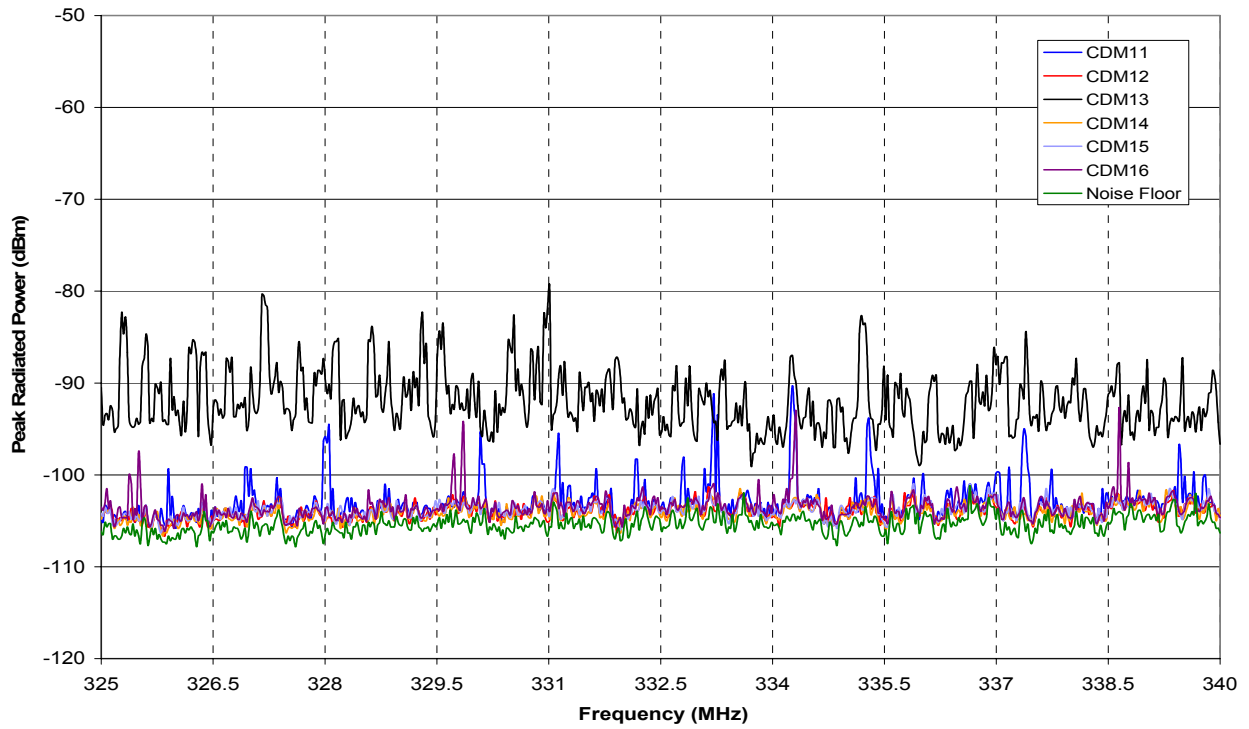


Figure 3.4-21: Individual phone emission envelopes. CDMA phones 11 through 16. Band 2.

Band 3

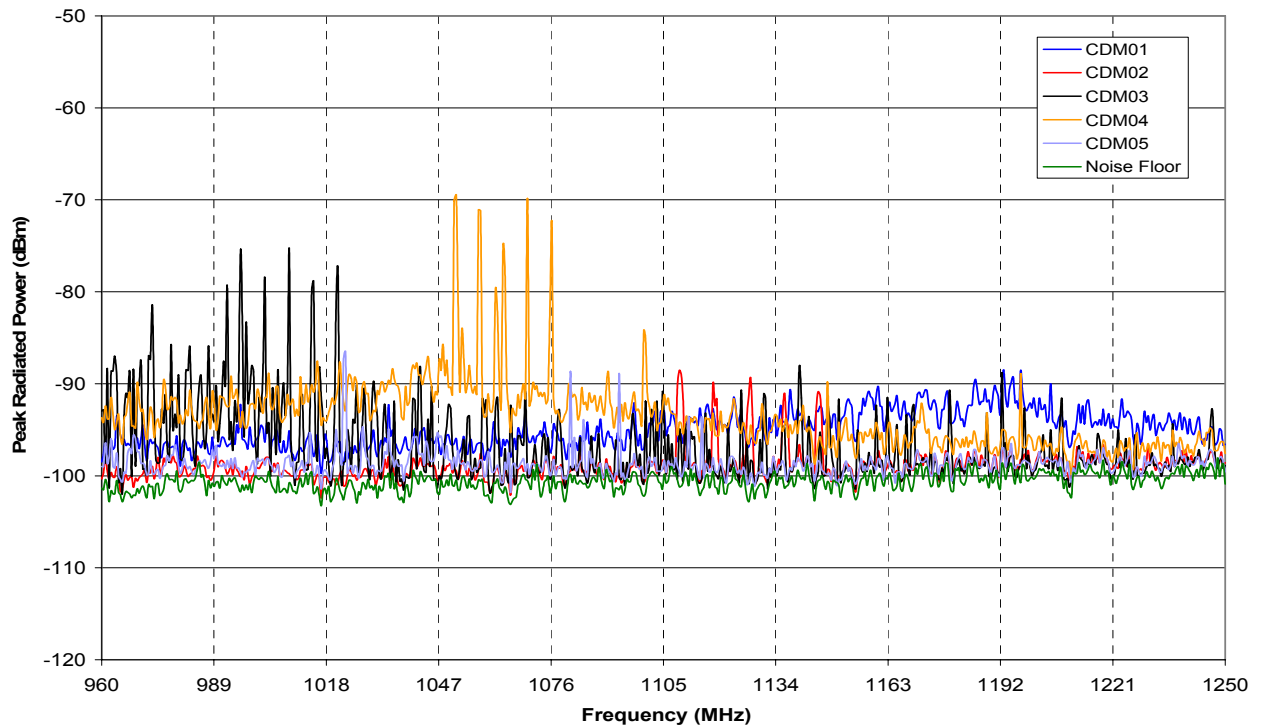


Figure 3.4-22: Individual phone emission envelopes. CDMA phones 1 through 5. Band 3.

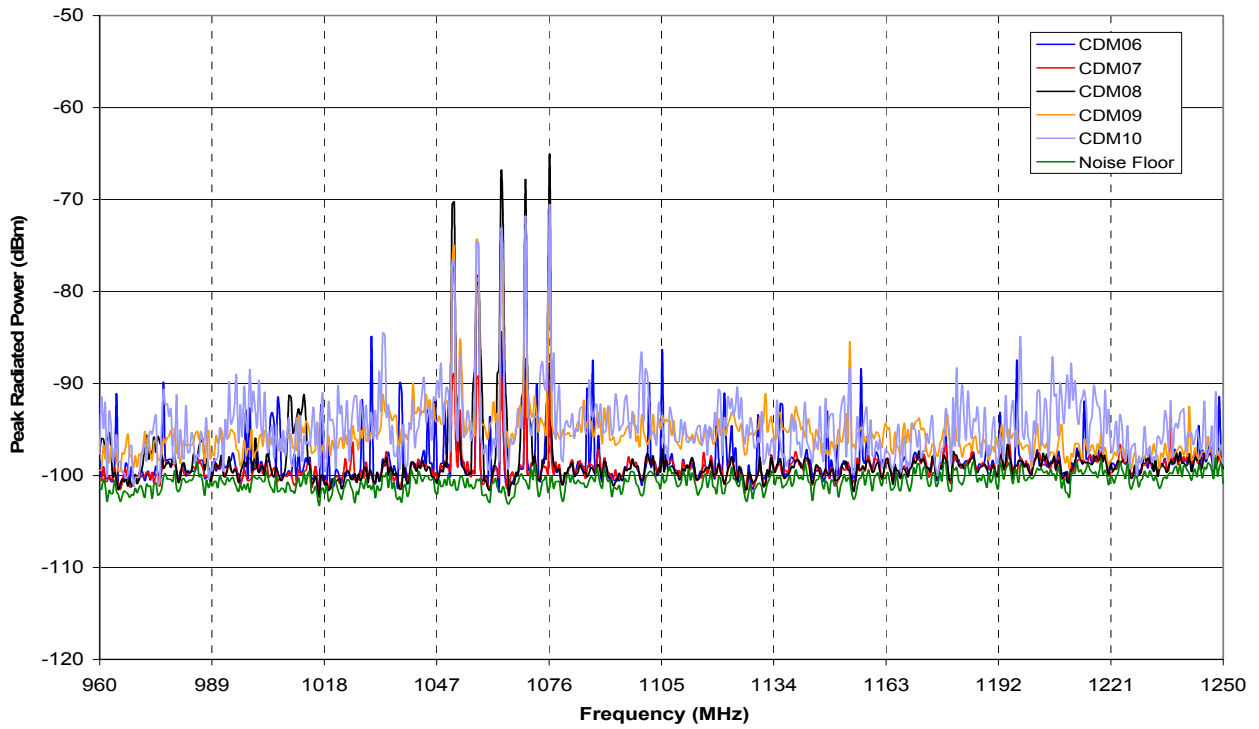


Figure 3.4-23: Individual phone emission envelopes. CDMA phones 6 through 10. Band 3.

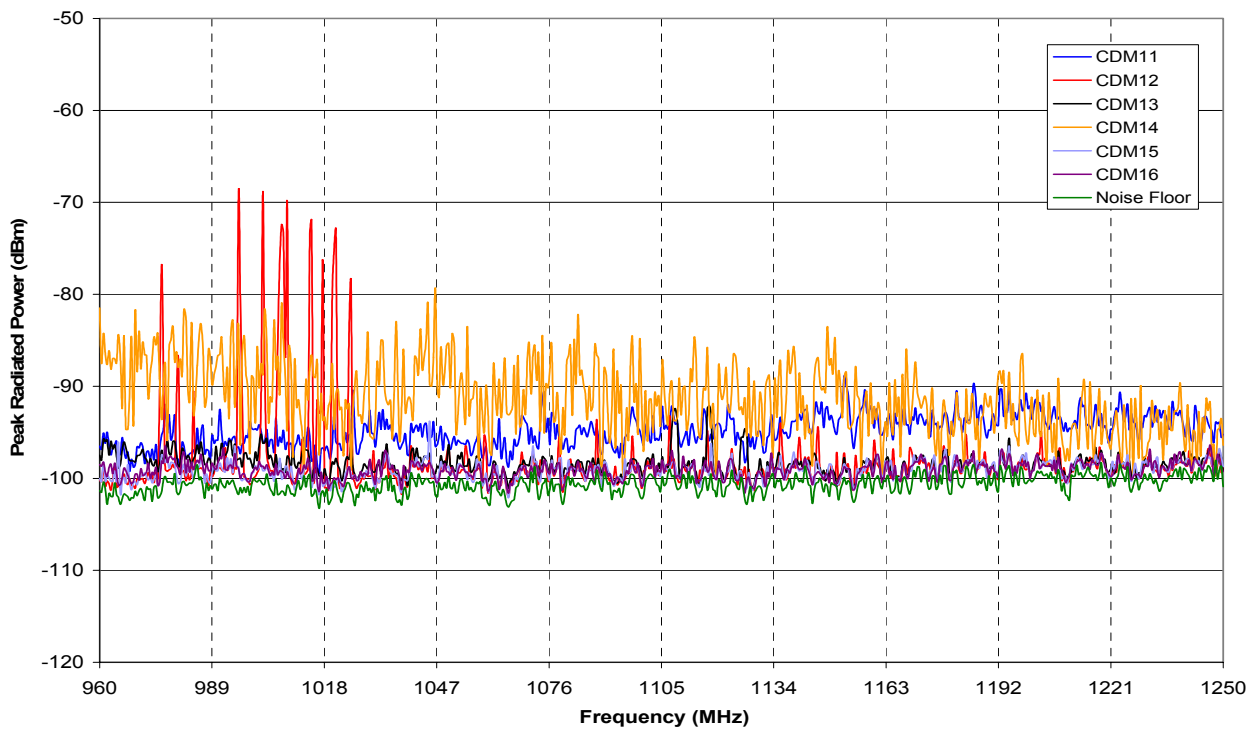


Figure 3.4-24: Individual phone emission envelopes. CDMA phones 11 through 16. Band 3.

Band 4

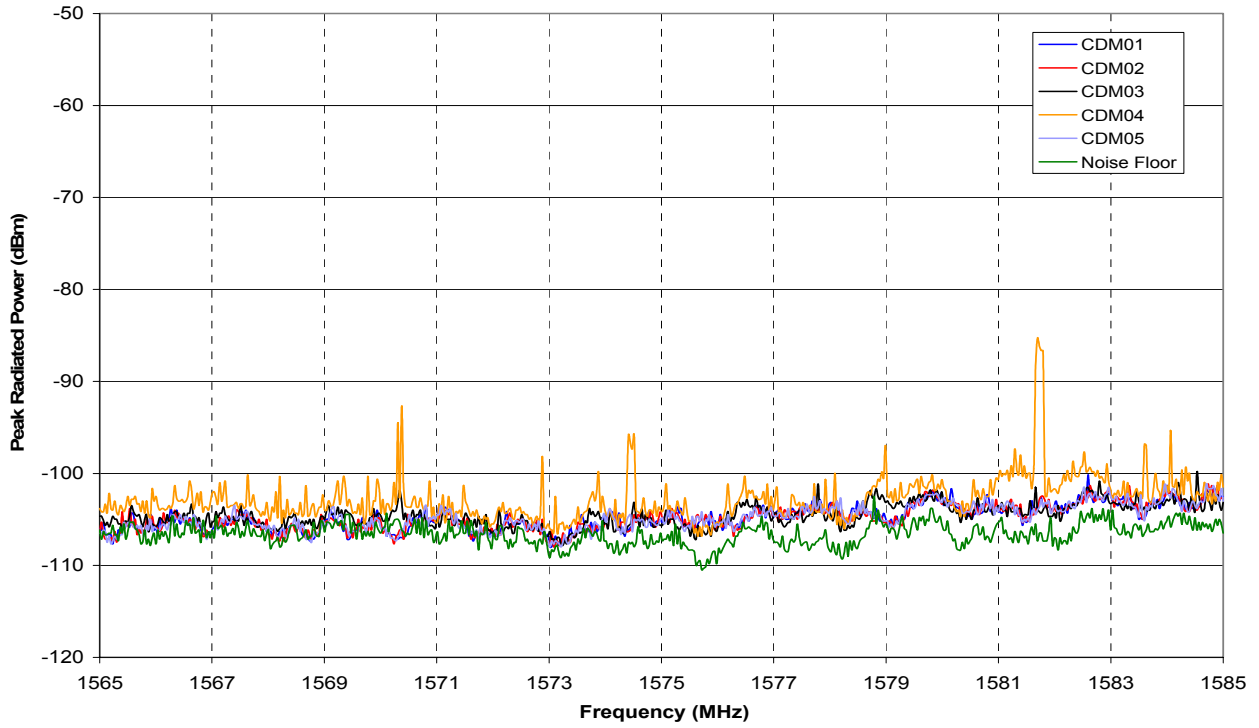


Figure 3.4-25: Individual phone emission envelopes. CDMA phones 1 through 5. Band 4.

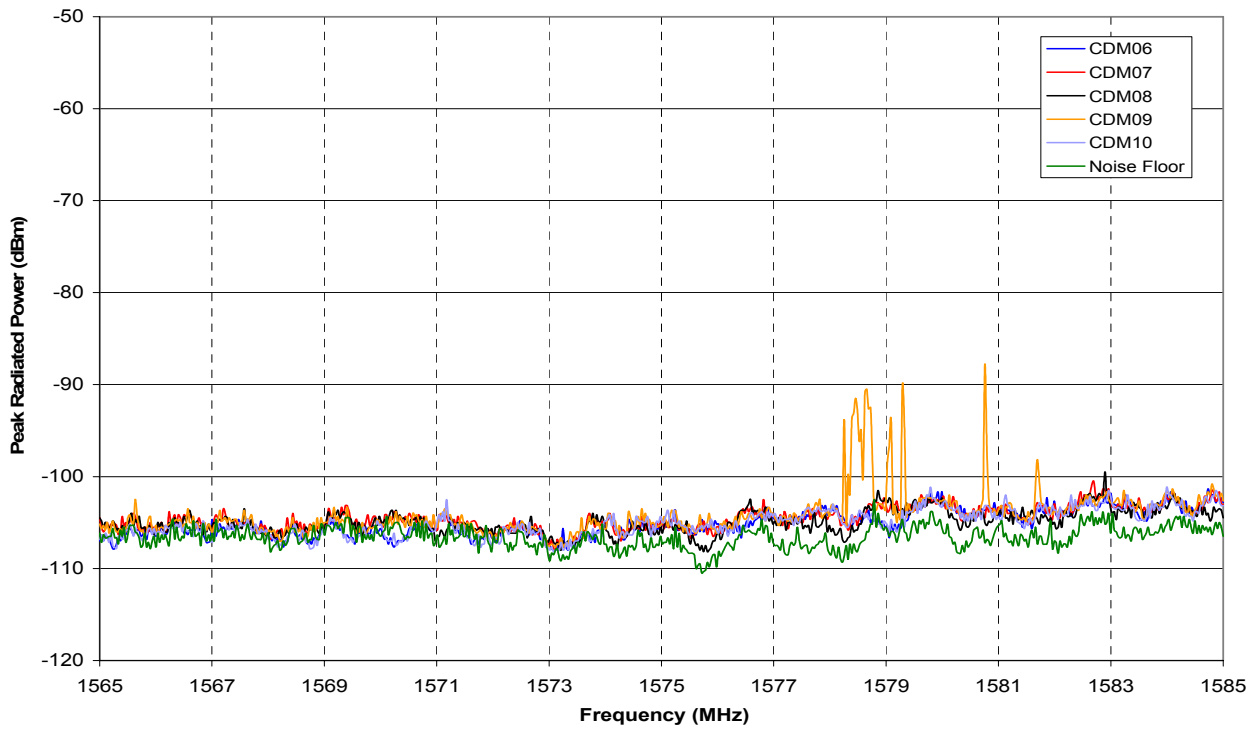


Figure 3.4-26: Individual phone emission envelopes. CDMA phones 6 through 10. Band 4.

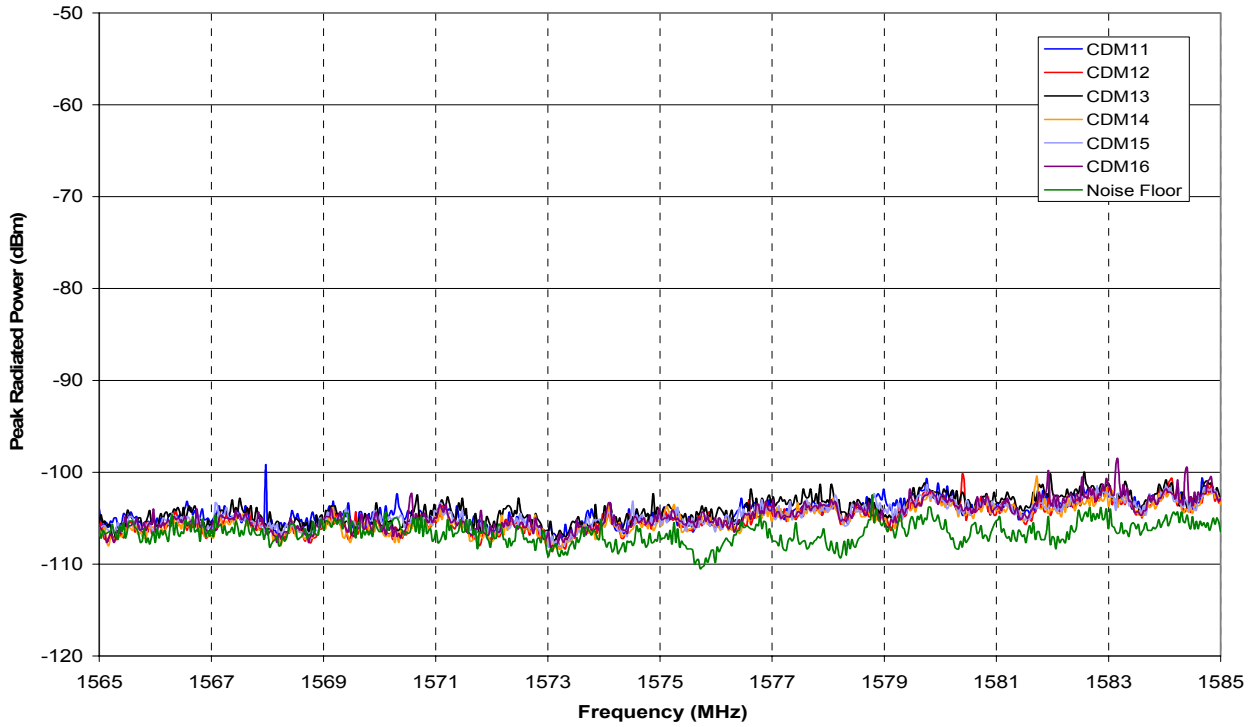


Figure 3.4-27: Individual phone emission envelopes. CDMA phones 11 through 16. Band 4.

Band 5

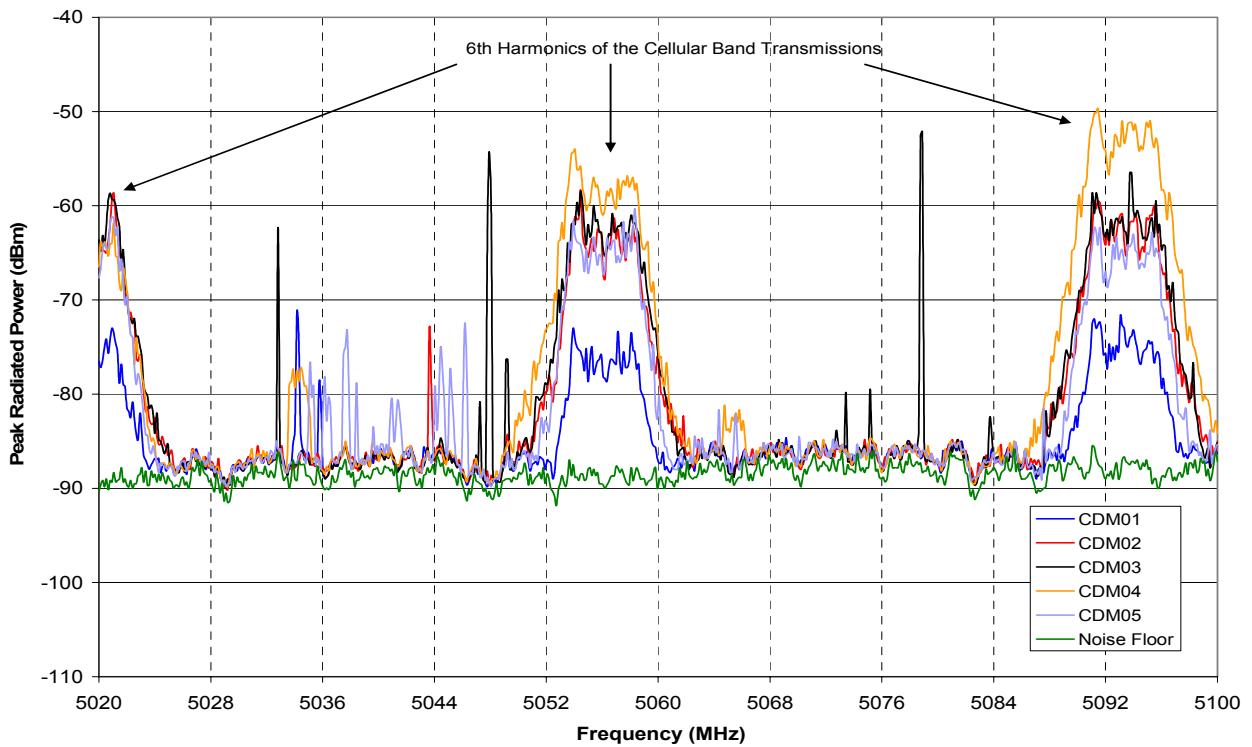


Figure 3.4-28: Individual phone emission envelopes. CDMA phones 1 through 5. Band 5.

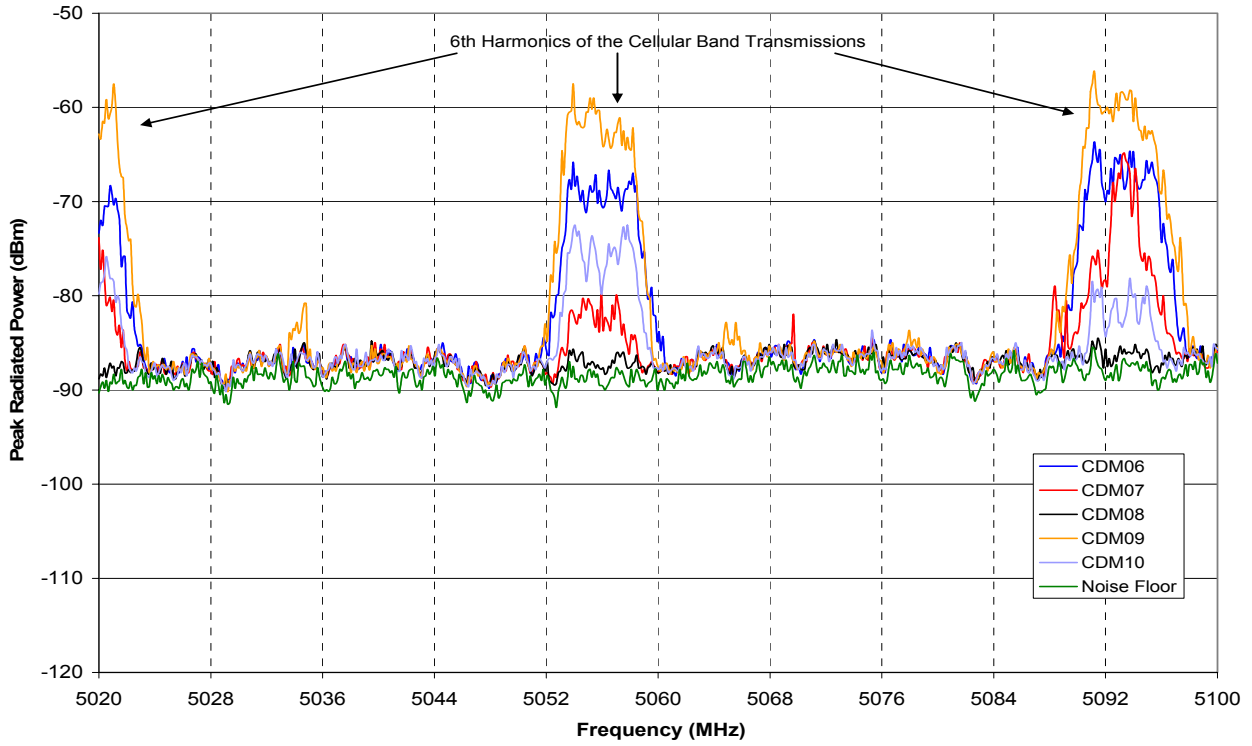


Figure 3.4-29: Individual phone emission envelopes. CDMA phones 6 through 7. Band 5.

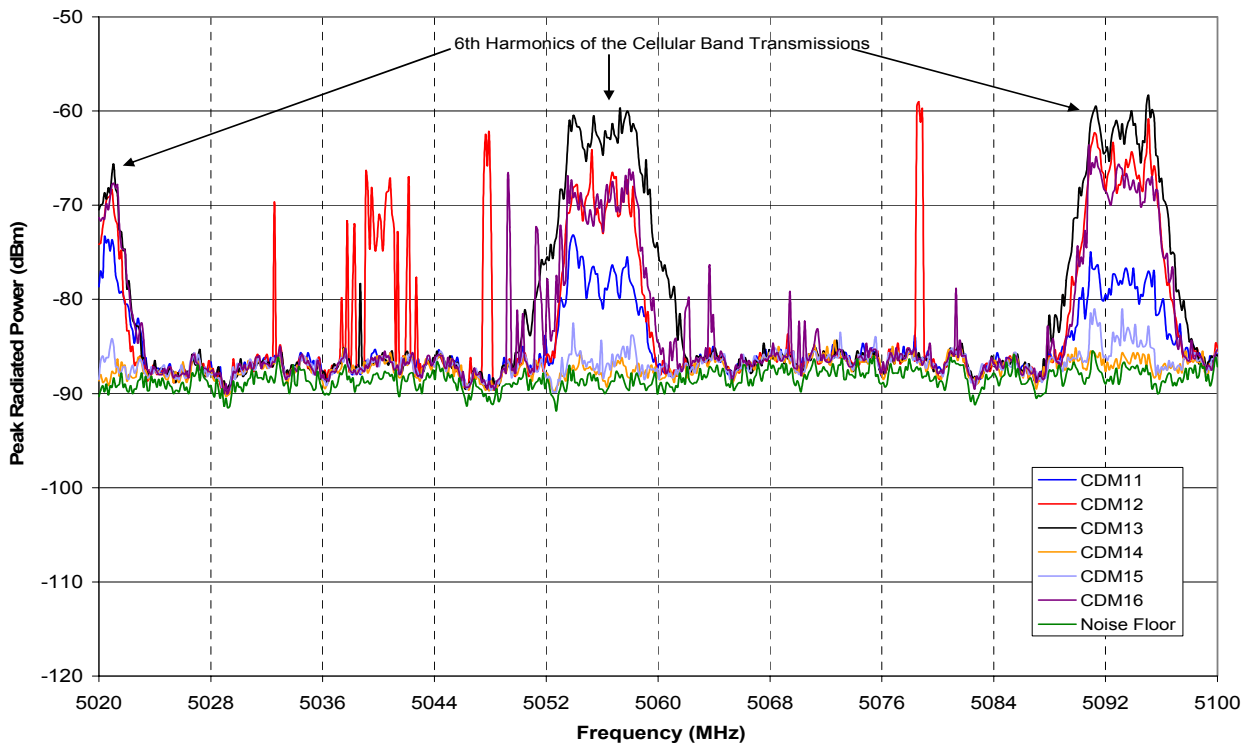


Figure 3.4-30: Individual phone emission envelopes. CDMA phones 11 through 16. Band 5.

3.4.3 Summary of Emission Data

This section summarizes all emission data from all phones and test modes into two charts for each measurement band. The maximum emissions in data and voice modes from each wireless phone are compared side-by-side within each of the GSM or CDMA groups. These charts show the different maximum emissions from each device operating in different spectrum and in voice versus data modes.

It is generally observed that in Band 1 and Band 2, each device's emissions are similar regardless whether it is operating in the cellular band or PCS band. This is not the case for Band 3, 4 or 5. In addition, in most cases the emissions in the voice and data modes are similar for any single device (within 2-5 dB). The exceptions include GSM01 in Band 2, CDM06 in Band 3, GSM09 in Band 4, and a few others.

The maximum emission values in the five bands are used in the safety margin calculations in a later section.

Band 1

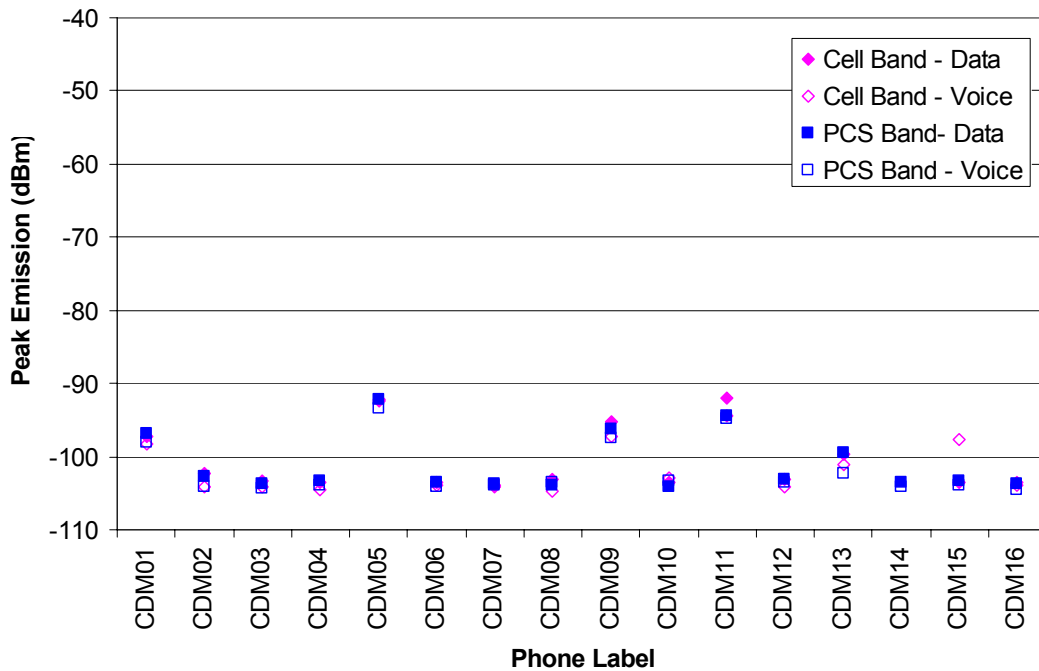


Figure 3.4-31: Band 1 CDMA wireless phone emission. Phone operating in cellular or PCS bands.

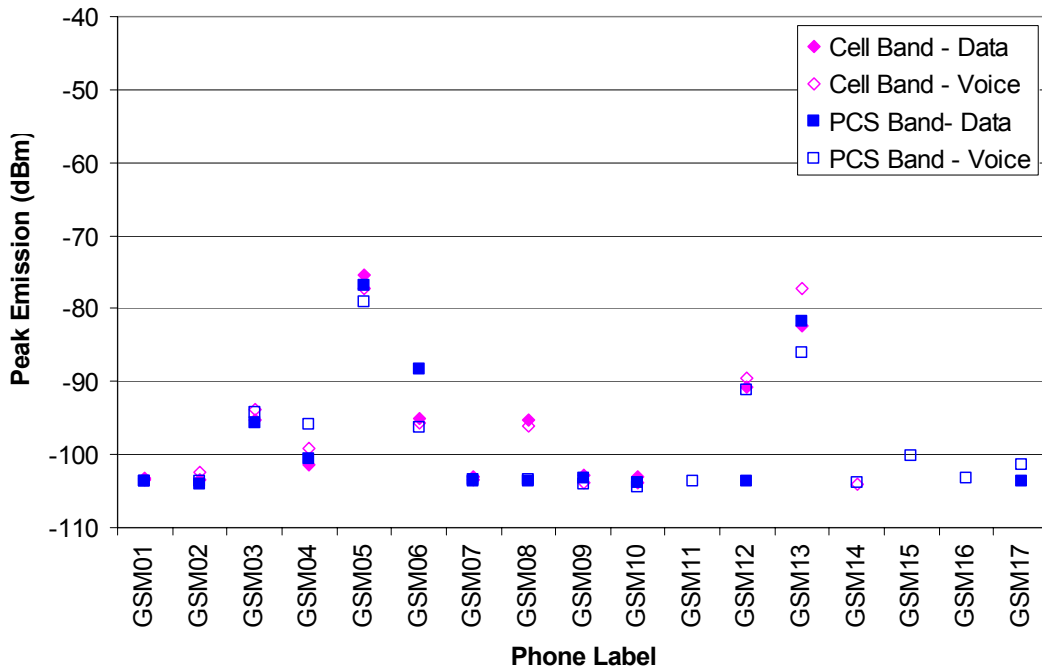


Figure 3.4-32: Band 1 GSM/GPRS wireless phone emissions. Phone operating in cellular or PCS bands.

Band 2:

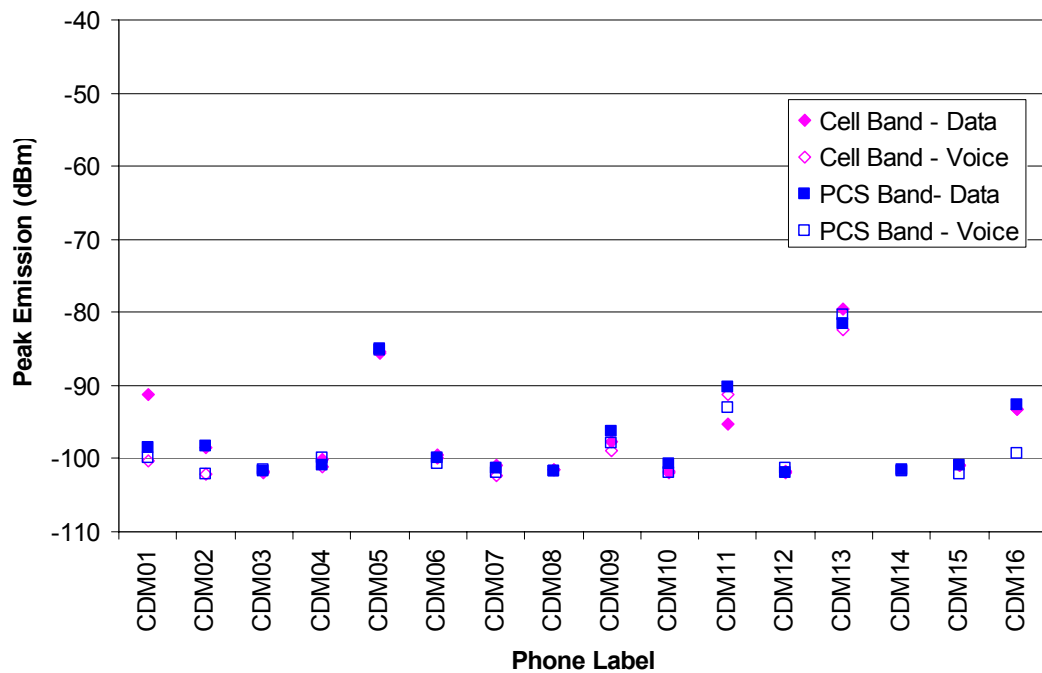


Figure 3.4-33: Band 2 CDMA wireless phone emissions. Phone operating in cellular or PCS bands.

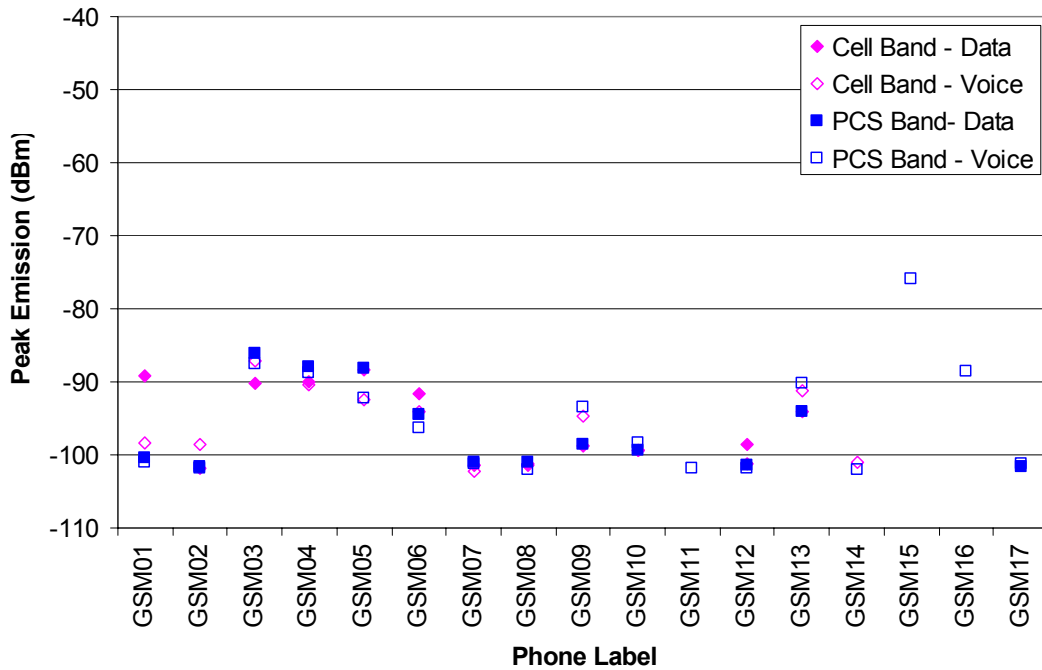


Figure 3.4-34: Band 2 GSM/GPRS wireless phone emissions. Phone operating in cellular or PCS bands.

Band 3

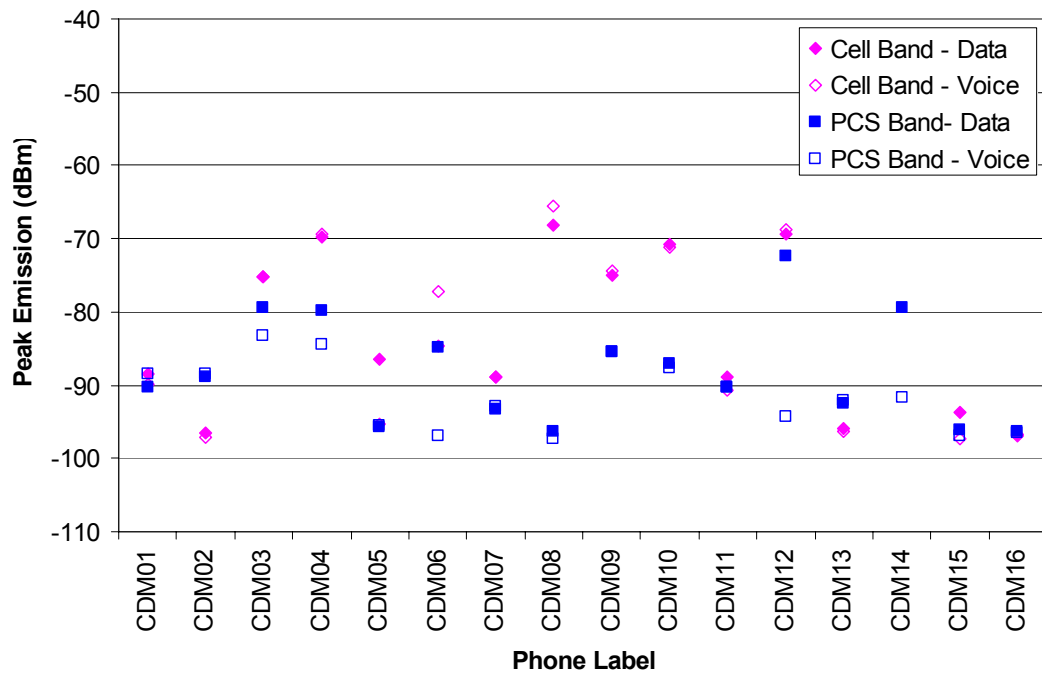


Figure 3.4-35: Band 3 CDMA wireless phone emissions. Phone operating in cellular or PCS bands.

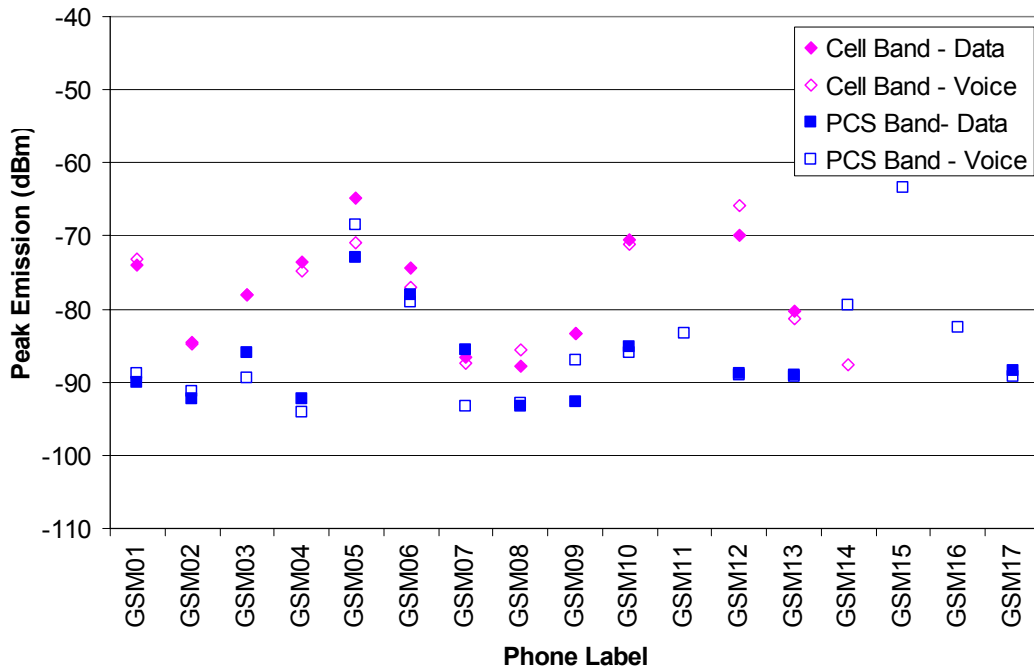


Figure 3.4-36: Band 3 GSM/GPRS wireless phone emissions. Phone operating in cellular or PCS bands.

Band 4

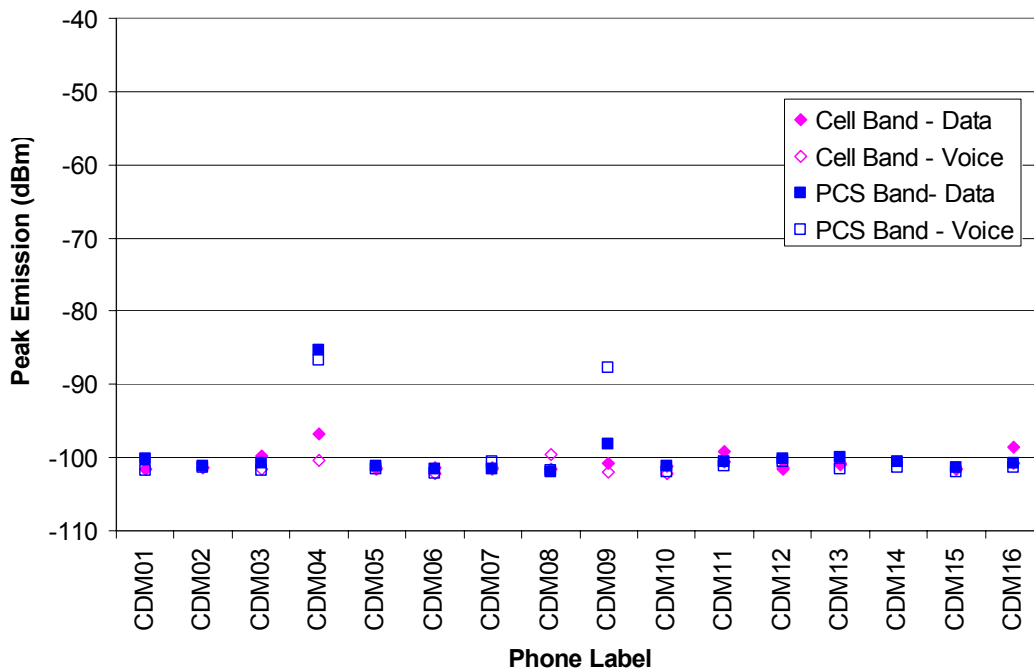


Figure 3.4-37: Band 4 CDMA wireless phone emissions. Phone operating in cellular or PCS bands.

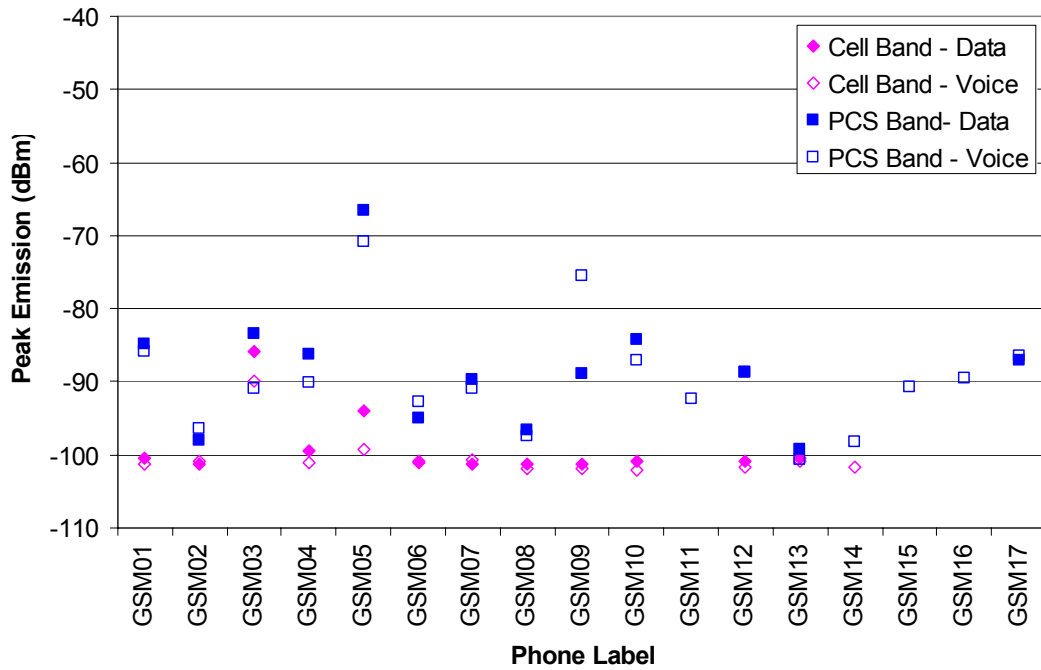


Figure 3.4-38: Band 4 GSM/GPRS wireless phone emissions. Phone operating in cellular or PCS bands.

Band 5:

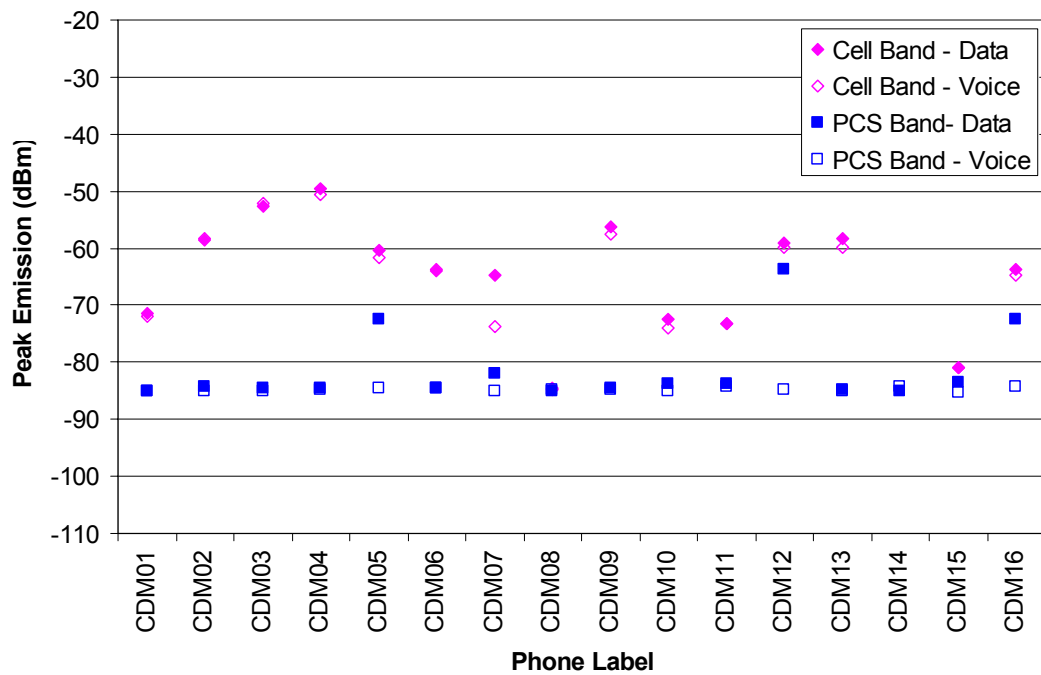


Figure 3.4-39: Band 5 CDMA wireless phone emissions. Phone operating in cellular or PCS bands.

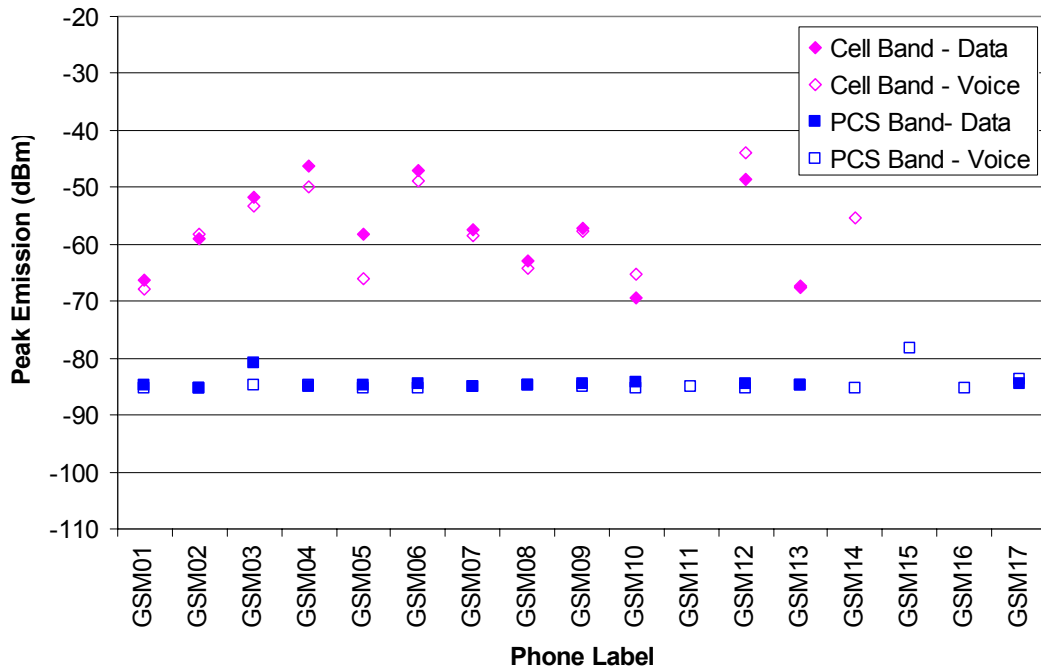


Figure 3.4-40: Band 5 GSM/GPRS wireless phone emissions. Phone operating in cellular or PCS bands.

3.5 Baseline Emissions from Standard Laptop Computers and PDA

Emission measurement results from several laptop computers, PDAs and a portable printer (PRN) are used as a baseline for devices currently allowed on an aircraft. The measurements were performed and reported in an earlier efforts [2]-[3], and the summary of the results are repeated here for comparison purposes. The comparison can be used to evaluate the risks to aircraft radio bands from wireless phones versus non-transmitting PEDs such as laptop computers and PDAs. These PEDs are currently allowed during certain phases of a flight.

Measurements of the PEDs emissions were performed in all five test bands similar to this effort. However, the 105-140 MHz band was divided into two separate bands, called Band 1 and Band 1a. Band 1 covers from 105 to 120 MHz, and the results were reported in [2]. Band 1a covers 116 to 140 MHz, with the results first reported in [2]-[3]. Since this current report combines the old Band 1 and Band 1a into a new band, named Band 1, the PEDs emission data in the new Band 1 are shown in two separate charts.

The PEDs tested are listed in Table 3.5-1

Table 3.5-1: Laptop Computers, PDA, and Mobile Printer Models

Host Designation	Manufacturer	Model
LAP1	Dell	Latitude C640
LAP2	Hewlett Packard	Pavilion n6395
LAP3	Sony Vaio & Dock	PCG-641R PCGA-DSM51
LAP4	Dell	Latitude C800
LAP5	Fujitsu	Lifebook
LAP6	Panasonic	Toughbook CF-47
LAP7	Fujitsu	Lifebook CP109733
LAP8	Gateway	450SX4
PDA1	Palm	m515
PDA2	Toshiba	e740
PRN	Hewlett Packard	DeskJet 350

Laptop Computers

Spurious radiated emissions were recorded for eight laptop computers, with each operating in five modes. Operating modes, or processing tasks that may be performed by a laptop, include: idle, screensaver, file transferring, CD playing, and DVD playing. Radiated emissions from the modes were measured separately. The overall maximum emission envelope across the band of all operating modes is termed as the radiated peak envelope of the laptop.

The PEDs devices were measured using the same facility and instruments. However, the PED emissions were measured with 1) a different pre-amplifier in the receive path, 2) an equipment operator in the chamber, and 3) without measurement path filters. These differences may affect the measurement noise floor, but should not affect the emission results since they are accounted for in the calibration. Different laptop computer operating modes are explained below:

- Idle: Idle mode testing is conducted as a normal desktop screen is displayed.
- Screensaver: The flowerbox screensaver was selected to be a large, smooth, checkerboard cube pattern that spins and blooms at maximum complexity. This selection is a simple way to simulate computationally intensive operations.
- File Transfer: This mode includes transferring files from the hard drive to the Personal Computer (PC) Card hard drive, which is well shielded with all metal casing.
- CD Playing: The computer plays music CD, exercising the audio circuitry.
- DVD Playing: The computer plays movie DVD, exercising the video system.

PDA and Printer

A PDA baseline consisted of the idle and file-transfer modes. File transfer in this case was performing a backup operation to a secure digital or compact flash card. The printer testing consisted of the idle mode with the unit powered on.

Results – PEDs Emission

The following charts in this section report the PED data envelopes, with each chart containing plots of all individual PED envelopes. Each individual PED envelope was generated from the measured emissions data, including idle mode and all other PED test modes discussed earlier. The charts also show composite maximum envelopes that represent the highest emission level of all devices at any given frequency.

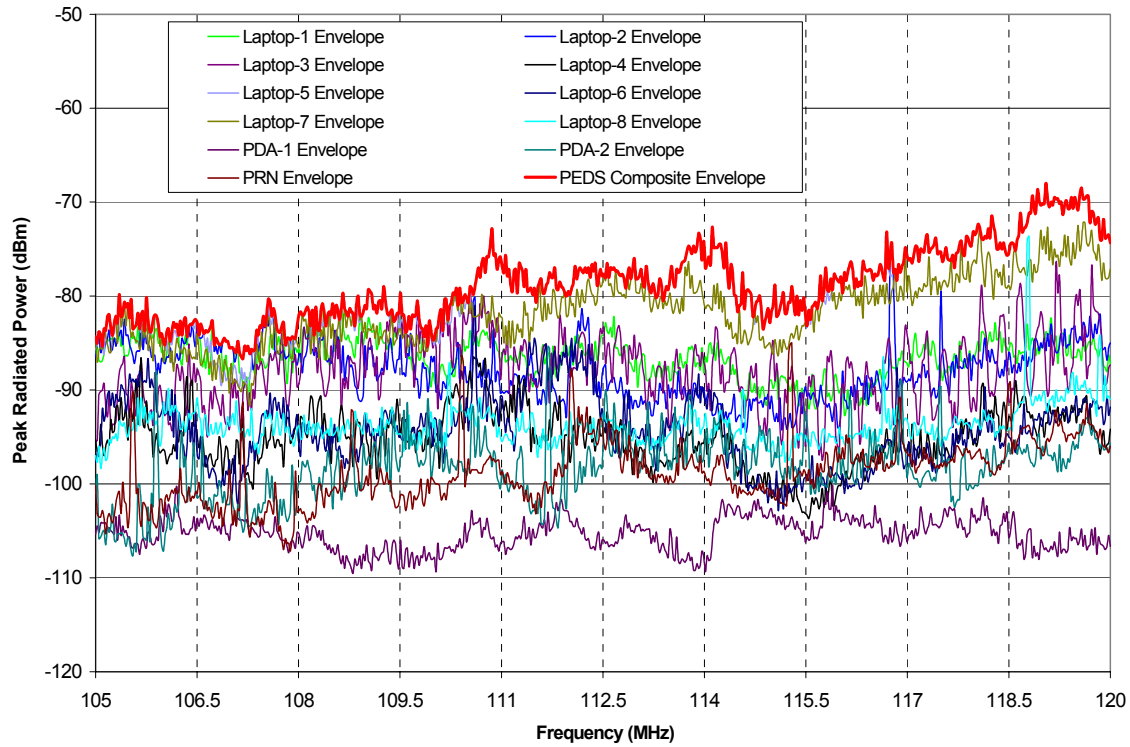


Figure 3.5-1: Individual PED Envelopes and PEDS Composite Envelope for Band 1a (105 MHz to 120 MHz).

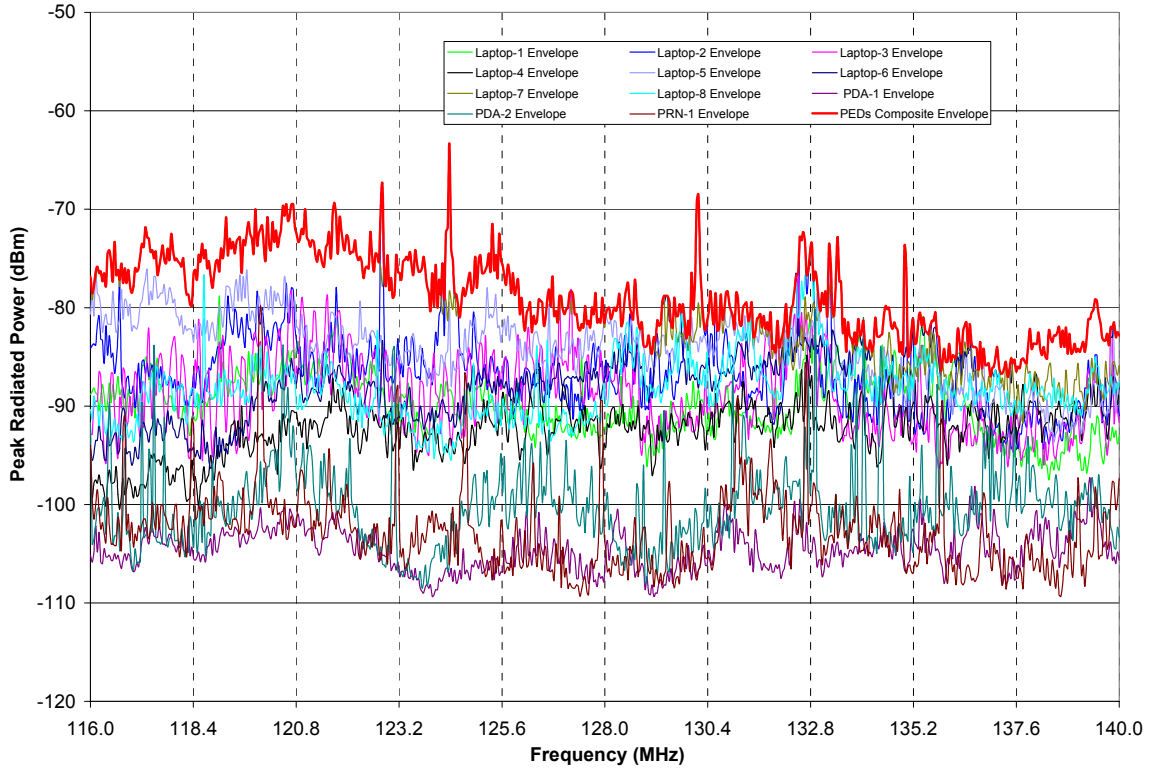


Figure 3.5-2: Individual PED Envelopes and PEDs Composite Envelope for Band 1b.

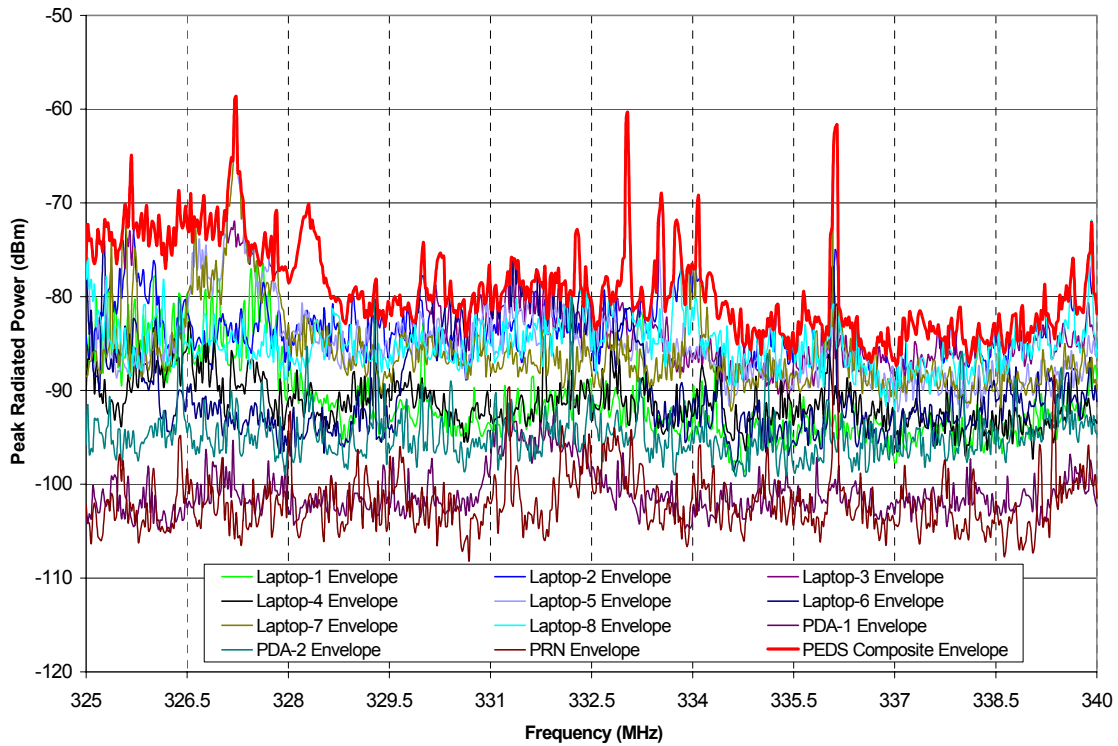


Figure 3.5-3: Individual PED Envelopes and PEDs Composite Envelope for Band 2.

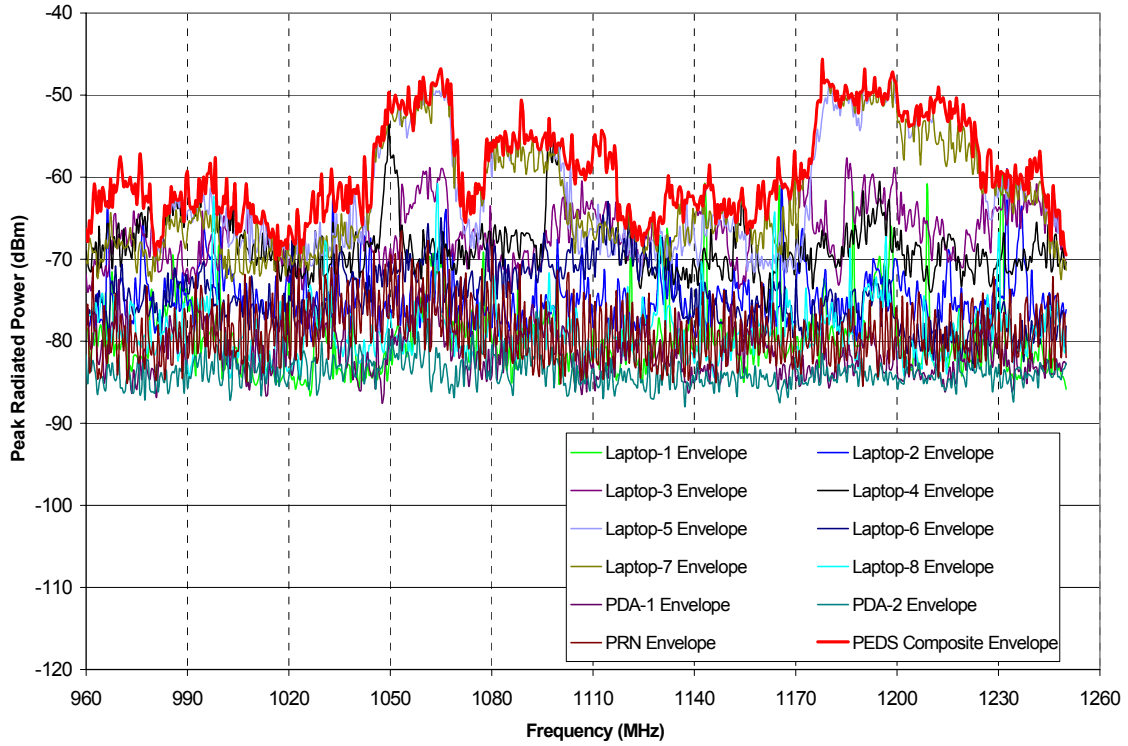


Figure 3.5-4: Individual PED Envelopes and PEDS Composite Envelope for Band 3.

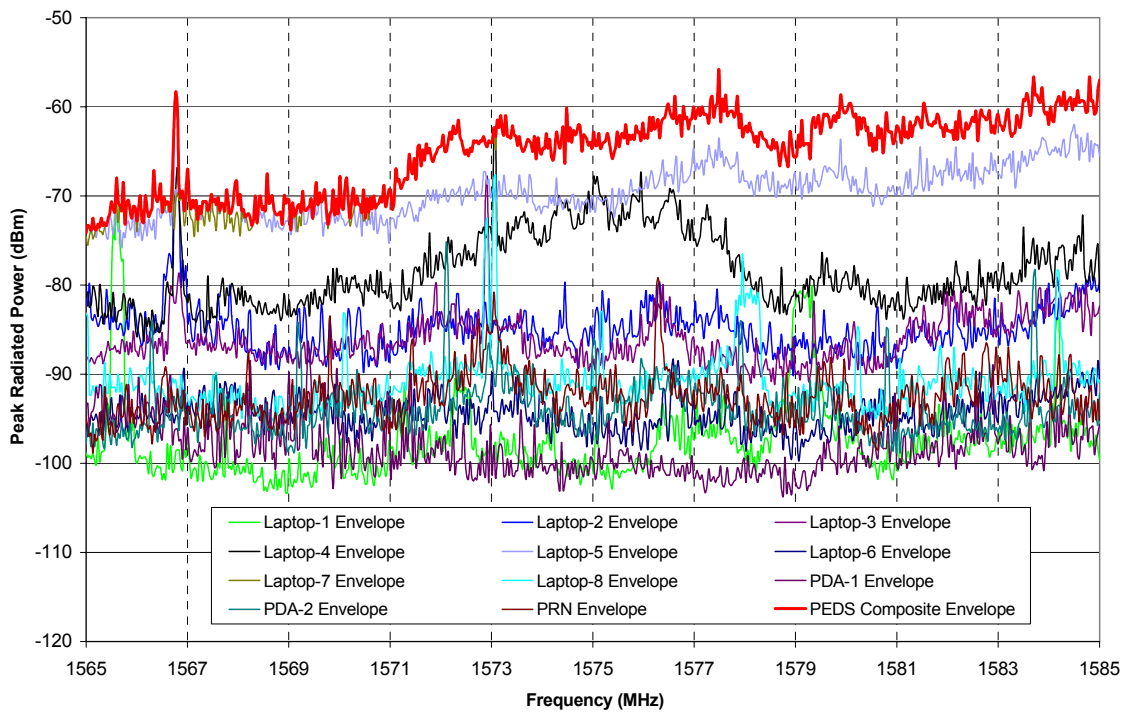


Figure 3.5-5: Individual PED Envelopes and PEDS Composite Envelope for Band 4.

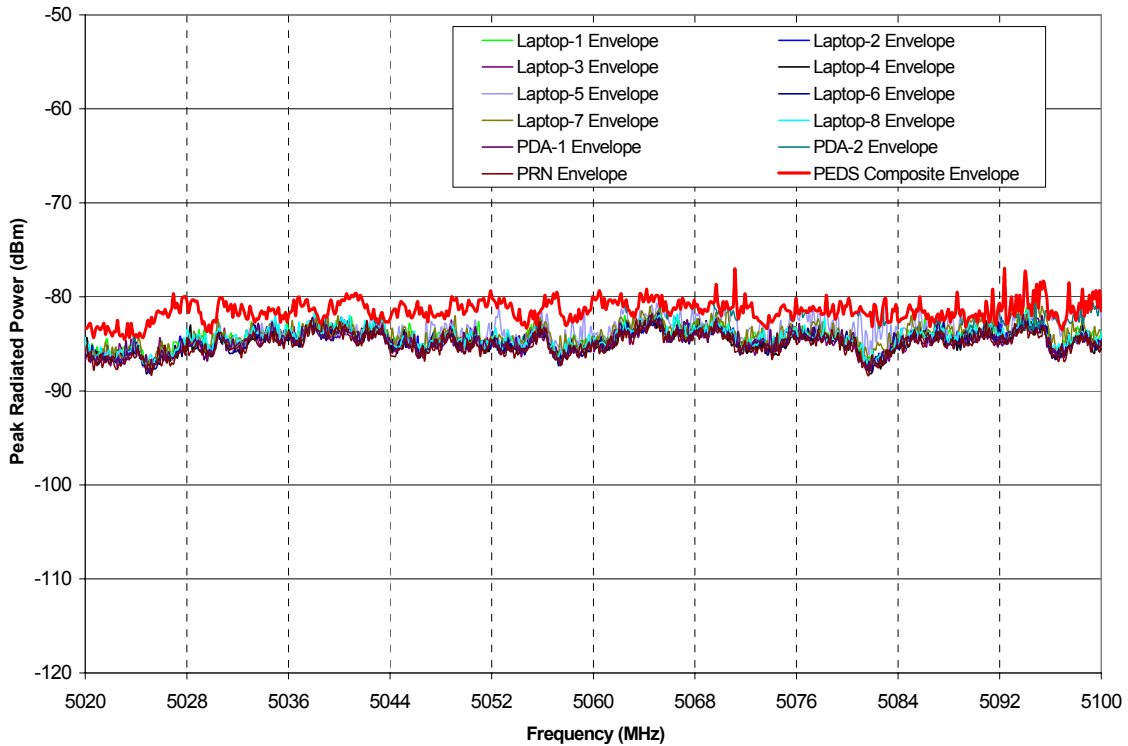


Figure 3.5-6: PEDs Individual and Composite Envelope for Band 5.

3.6 Summary of Maximum Emissions from Wireless Phones

This section summarizes maximum emission results reported in the earlier sections. In addition, comparisons with the corresponding FCC and RTCA/DO-160 emission limits are reported.

3.6.1 Summary of Maximum Emission Results

Table 3.6-1 summarizes emission data by reporting the maximum emission value of different device groups. The devices are grouped according to whether they operate in the cellular or PCS bands, or if they belong to the baseline laptop computers/PDA group.

The corresponding aircraft radio-navigation systems with frequency spectrum aligned within the measurement bands are grouped together as shown. These systems are potentially affected by any high emissions within their measurement bands. The data are also used in the safety margin calculations in a later section.

Figure 3.6-1 graphically illustrates the data in Table 3.6-1. The figure shows that the peak emissions from all 17 GSM and 16 CDMA phones are lower than the peak emissions from the eight laptop computers and PDAs. The exception is Band 5, where harmonics from the cellular band phones fall inside the band and their maximum levels exceed the laptop/PDA emissions. Fortunately, MLS is the only aircraft system operating in Band 5, and the system is not widely used in the US.

It is important to note that the lines in Figure 3.6-1 are only for linking the data points at the markers for visual effects. Their magnitudes between the markers have no data values.

Table 3.6-1: Maximum Emission from Wireless Phones in Aircraft Bands (in dBm)

Measurement Band	Frequency (MHz)	Cell-Band Phones (GSM & CDMA)	PCS-Band Phones (GSM & CDMA)	Baseline Laptops PDAs	Aircraft Bands
<u>Band 1</u>	105 - 140	-75.3	-76.8	-63.3	LOC, VOR, VHF-Com
<u>Band 2</u>	325 - 340	-79.5	-75.8	-58.7	GS
<u>Band 3</u>	960 - 1250	-64.7	-63.3	-45.7	TCAS, DME, GPS L2
<u>Band 4</u>	1565 - 1585	-85.8	-66.5	-55.8	GPS L1
<u>Band 5</u>	5020 - 5100	-43.8	-63.8	-77.0	MLS

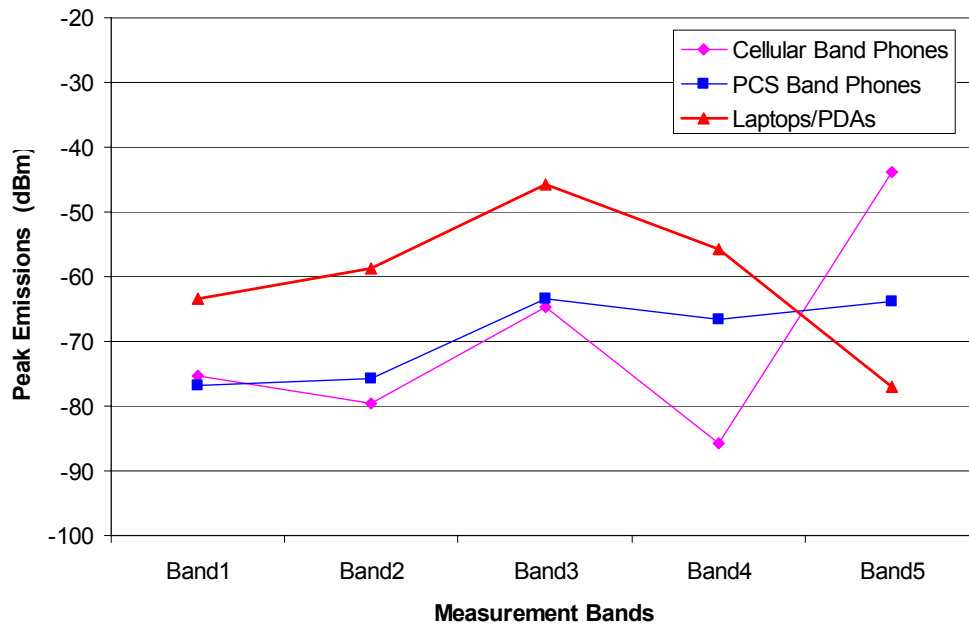


Figure 3.6-1: Maximum phone emissions and comparison with emissions from laptop computers and PDA.

3.6.2 Emission Limits

This section specifies the relevant limits used for comparison with the measurement results. The limits used include FCC limits for unintentional radiators (PEDs), FCC spurious emission limits for wireless phones, and the aircraft installed equipment limits. Table 3.6-2 summarizes the spurious emission limits used in the comparison in section 3.6.3.

FCC Emission Limits

Table 3.6-2 shows the FCC Part 15.109 [19] limits for unintentional radiators (PEDs), the RTCA/DO-160 Category M limits, and the FCC spurious emission limits for wireless phones in the cellular [20] and PCS bands [21].

For both cellular and PCS band operating phones, the out-of-band spurious and harmonic emissions must be attenuated below the intended output power, P , by at least $43 + 10 \log(P)$ dB. Calculation shows that the limit is simply -13 dBm ERP for cellular band devices and -13 dBm EIRP for PCS band devices.

RTCA/DO-160 Category M Limits

The RTCA/DO-160 Section 21 [22] Category M emission limit is selected for comparison with spurious emissions from passenger carry-on electronic devices since these devices can be located in the passenger cabin or in the cockpit of a transport aircraft, where apertures (such as windows) are electromagnetically significant. The quote below is the definition for the Category M radiated emissions limit specified in RTCA/DO-160 Section 21:

“Category M:

This category is defined for equipment and interconnected wiring located in areas where apertures are em significant and not directly in view of radio receiver’s antenna. This category may be suitable for equipment and associated interconnecting wiring located in the passenger cabin or in the cockpit of a transport aircraft.”

For the RTCA/DO-160 Category M limit listed in Table 3.6-2, the limit value for each *measurement band* is chosen to be the lowest limit of the *aircraft bands* within it. As an illustration, the emission measurement Band 3 covers TCAS, ATRBS, DME, GPS L2 and GPS L5. The emission limit for the whole measurement band is chosen to be the lowest limit of all the systems listed. In this case, the lowest value is 50 dBμV/m for TCAS, DME and ATRBS since the limits for GPS L2 and GPS L5 are higher. In addition, the emission limit for each aircraft radio band is chosen to be the lowest value between its lowest and highest frequency limits.

Power Conversion

To compare with measured emission data in dBm, the field limits in FCC Part 15 and the RTCA/DO-160 Category M are converted to the equivalent *EIRP* using Equation 3.6-1. In addition, *ERP* can be computed from *EIRP* using Equation 3.6-2.

$$EIRP = \frac{E^2 \cdot 4\pi R^2}{120\pi} \text{ (watts)} \quad \text{(Eq. 3.6-1)}$$

$$ERP \text{ (dBm)} = EIRP \text{ (dBm)} - 2.15 \text{ (dB)} \quad \text{(Eq. 3.6-2)}$$

where E = Electric Field Intensity at distance R (V/m)
 R = Distance (m)

Ideally, E field measurement is taken in the direction of maximum radiation from the test device. To convert power, $EIRP$, from watts to dBm, use the expression $10 * \log(1000 * EIRP)$. For the RTCA/DO-160 limit given in $dB\mu V/m$, the unit is converted to V/m before applying Equation 3.6-1.

Table 3.6-2: Estimated FCC and RTCA spurious radiated emission limits

	FCC Part 15 Limit ($\mu V/m @ 3m$)	RTCA/DO-160 Cat. M Limit ($dB\mu V/m @ 1m$)	FCC Part 15 Limit ($EIRP, dBm$)	RTCA/DO-160 Cat. M Limit ($EIRP, dBm$)	FCC Phone Limits ($EIRP, dBm$)	
					Cell-Band Device (= -13 dBm ERP)	PCS-Band Device
Band 1	150	34	-51.7	-70.8	-10.85	-13
Band 2	200	52.9	-49.2	-51.9	-10.85	-13
Band 3	500	50	-41.2	-54.8	-10.85	-13
Band 4	500	53	-41.2	-51.8	-10.85	-13
Band 5	500	71.8	-41.2	-33.0	-10.85	-13

3.6.3 Measurement Results and Spurious Emission Limit Comparison

Radiated emissions measured using a reverberation chamber provide results in “total radiated power” (TRP) within the measurement resolution bandwidth. TRP is different from $EIRP$ and ERP except for antennas or devices with an isotropic radiation pattern. Rather,

$$EIRP \text{ (dBm)} = TRP \text{ (dBm)} + D_G \text{ (dB)}, \text{ and} \quad (\text{Eq. 3.6-3})$$

where D_G is *directivity*, or maximum *directive gain* of the test device. Directive gain of any device is a measure of radiated power as a function of aspect angle referenced to the isotropic value. For spurious emissions, D_G is the directivity at the spurious emission frequency of interest. D_G is usually difficult to measure or calculate since maximum radiation angles and radiation mechanisms for *spurious* emissions are often not known. Maximum theoretical estimation of D_G based on device size tends to significantly over-estimate the real directivity, especially at high frequency, because the device geometry is typically not designed to radiate efficiently as an antenna as assumed in the theoretical estimation. However, there are recent theoretical statistical developments to estimate the “expected” directivity for non-intentional radiators [23]. Additional details on expected directivity are discussed in Section 3.6.4.

For simplicity, the tested devices (phones and computer laptops/PDAs) are assumed to have unity D_G for spurious emissions. Thus, TRP is assumed to be the same as $EIRP$ at all spurious frequencies of interest. This assumption introduces an uncertainty level equal to D_G , according to Equation 3.6-3. For a dipole antenna with small electrical length, D_G is close to 1.76 dBi (or dB relative to isotropic). For a half-wave dipole, D_G is close to 2.15 dBi. Thus, it is reasonable to assume for devices up to one-half a wavelength in size, the uncertainties should not be much more than 5 dB. This level of uncertainty is considered acceptable for a first order comparison.

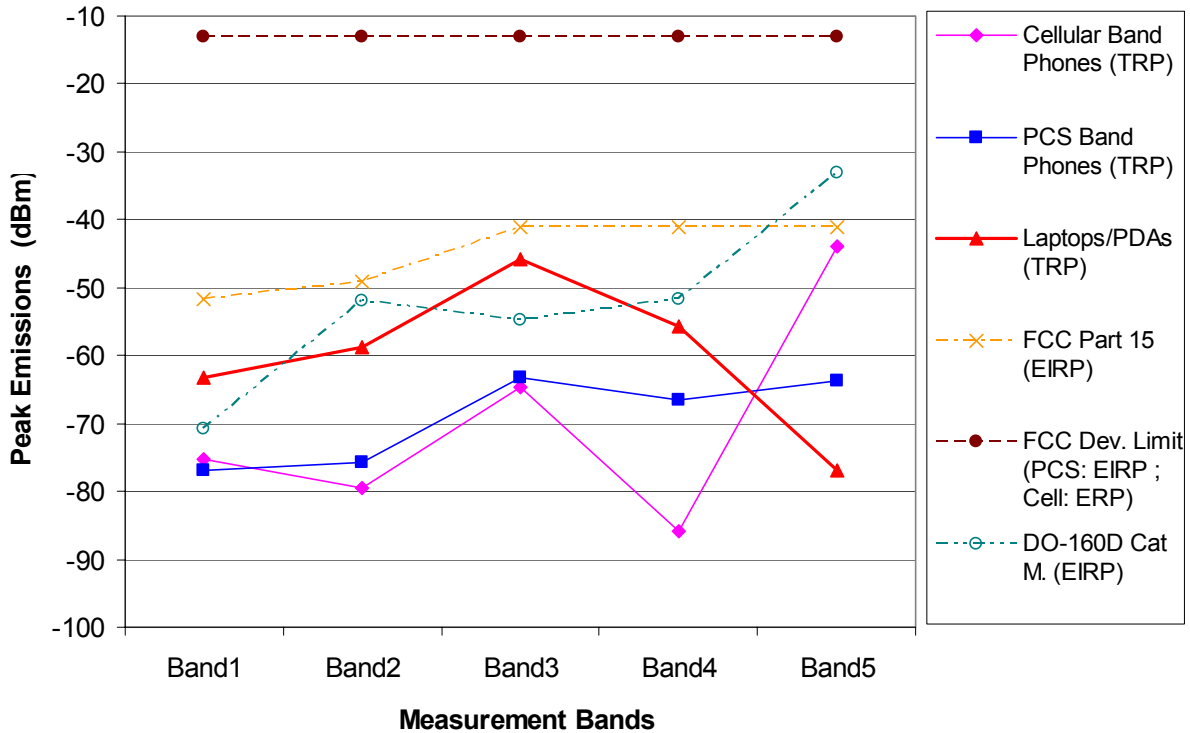


Figure 3.6-2: Emissions from wireless phones and comparison with emission limits.

Figure 3.6-2 shows that the spurious emissions from the wireless phones tested are below the aircraft installed equipment emission limits (RTCA/DO-160 Category M). They are also below the FCC Part 15 limits for unintentional transmitters such as laptop computers. The finding is still valid even after considering the uncertainty associated with devices' expected directivities. The expected directivity is between 5 and 8 dB for the wireless phones as shown in Section 3.6.4. The measured spurious emissions are also far below the -13 dBm FCC's wireless phone spurious limits (EIRP for PCS-band devices and ERP cellular-band devices).

3.6.4 Device Expected Directivity

The comparisons in the previous section were between the device's TRP and the FCC and RTCA/DO-160 equivalent EIRP limits, assuming unity directivity. For most devices, directivity is different than unity, and the limits must be adjusted downward by the amounts equal to the directivity of each individual device. This value can vary with frequency, device size and geometry. It is also difficult to estimate for spurious emissions since the specific radiation mechanisms are often not known.

Reference [23] provides a method to estimate the expected directivity from a statistical approach. This approach was intended for estimating the directivity of non-transmitting (intentionally) devices, or directivity at spurious frequencies. It is not intended for intentional transmitters such as antennas. In the approach, the expected directivity of a device can be estimated if its maximum dimension is known.

Wireless phones come in various sizes and configurations. Device sizes of the tested phones can vary from 8 cm (about 3 inches) to the maximum of 20 cm (about 8 inches) with the antennas extended and the phone in open configuration. Figure 3.6-3 shows the expected directivity for a device 20 cm in size,

using the equations given in [23]. This figure shows the results of three calculations: 1) the theoretical maximum directivity for a high gain antenna of the same size, 2) the expected directivity for a 1-planar cut measurement, and 3) expected directivity for a 3-planar cut measurement. The chart shows directivity is between 5 dB near 100 MHz to 8 dB near 5 GHz.

These expected directivity values are provided for information purposes only. The method is yet to be widely accepted.

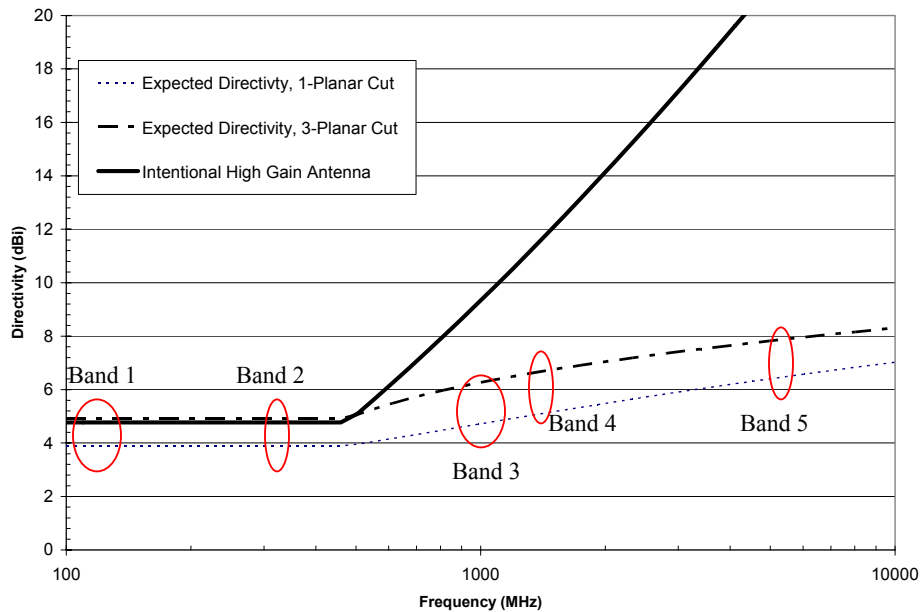


Figure 3.6-3: Expected directivity for a 20 cm (approximately 8 inches) unintentional transmitter

4 Aircraft Interference Path Loss

Aircraft IPL is the second of the three components needed for assessing the potential of interference from RF sources to aircraft receivers. Using World Jet Inventory [24] as a guide, there are about 35 different types of operational, commercial jet airplanes built in the US and Western Europe with a capacity of 30 seats or more as of 2002. Each aircraft type and series has a unique configuration of antenna placements and radio receiver installations. These variations may result in widely different IPL values. Reference [2] describes a recent effort to measure IPL for various radio receiver systems on six B737s and four B747s. The results were summarized and reported along with other previously available data for comparison. The summarized results are repeated here for risk assessment analysis.

This report defines IPL with respect to interference through aircraft radio receiver’s antenna port. This interference mechanism is often called “front-door” interference. “Back-door” mechanisms typically involve interference signals coupling onto wires connected to the equipment, and is not addressed in this report.

A possible approach and set-up to measure the IPL data is described in Section 4.1. This approach was used in measuring IPL on B737s and B747s reported in [2] and shown in Figure 4.1-1. The minimum IPL from these measurements are reported in Section 4.2 along with other existing IPL data. Section 4.3 summarizes the minimum IPL data that are then used in the interference risk assessment in a later section.

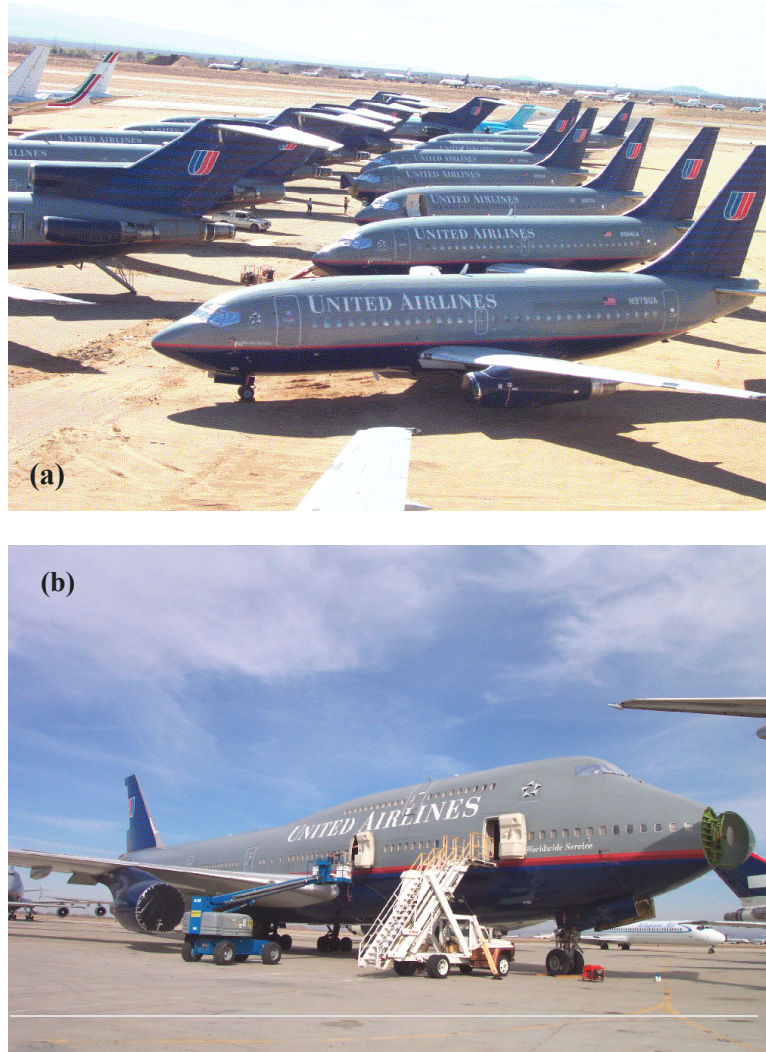


Figure 4.1-1: (a) B737-200 and (b) B747-400 aircraft at the measurement site. IPL data collected using the process described in this section.

4.1 IPL Measurement Method

It is assumed that for PEDs interference problems, the interference source is located within the passenger cabin, and the victims are aircraft radio receiver systems. A common path of PED interference is through the windows or door seams, along the aircraft body, and into the aircraft antennas. The interference signal picked up by the antennas is channeled back into the receivers to potentially cause interference if the signal is of sufficient strength.

Figures 4.1-2 and 4.1-3 illustrate typical radio receiver interference coupling paths and a possible setup for conducting IPL measurements. This setup was used in [2]. The setup shows a tracking source provides RF power to the transmit antenna, and a spectrum analyzer is utilized to measure the signal received by the aircraft antenna. The frequency-coupled spectrum analyzer and tracking source pair allows for frequency sweeps, resulting in more thorough measurements and reduced test time. Swept-CW setup is preferred over discrete frequency measurement, according to RTCA/DO-233. A pair of test cables connect the instruments to the aircraft antenna cable and to the transmit antenna. An amplifier may be needed to increase the signal strength delivered to the transmit antenna, and a pre-amplifier may be used in the receive path near the spectrum analyzer for increased dynamic range. This pre-amplifier (not shown in Figure 4.1-3) may be internal to the spectrum analyzer.

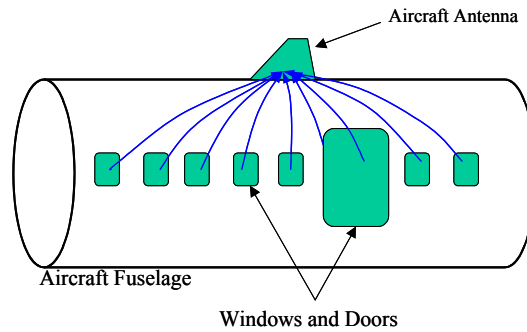


Figure 4.1-2: A typical radio receiver interference coupling path for a top mounted aircraft antenna.

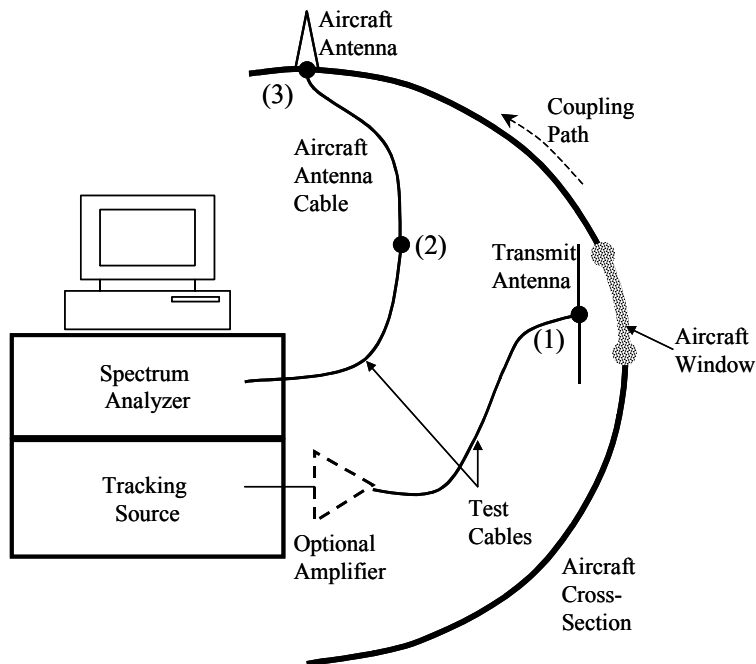


Figure 4.1-3: A typical setup for conducting an IPL measurement.

In Figure 4.1-3, IPL is defined to be the ratio, or the difference in dB, between the power radiated from the transmit antenna at location (1) to the power received at location (2). For GPS, IPL is defined to be the difference in power between location (1) and (3). Or,

$$IPL = P^T_{(1)} - P^R_{(2)} \text{ for most systems, and} \quad (\text{Eq. 4.1-1})$$

$$IPL = P^T_{(1)} - P^R_{(3)} \text{ for GPS,} \quad (\text{Eq. 4.1-2})$$

where $P^T_{(1)}$ is power transmitted at point (1), and $P^R_{(2)}$, and $P^R_{(3)}$ are power received at points (2) and (3), in dBm, respectively.

The transmit antennas used in the measurement typically include dipoles for frequencies in the GS band and below, and a dual-ridge horn antenna for the frequencies in the TCAS band and above. In this effort, no corrections are made to account for the transmit antenna gain. The close proximity between the transmit antenna and the surrounding (such as windows and passenger seats) could significantly alter the gain, and the free-space values may not be appropriate. Table 4.1-1 shows the relevant parameters for the measurement on the B747 and B737 IPL data reported in [2], Section 4.2 and Section 6. The free-space antenna gains for the source antenna used are also shown in the table.

Table 4.1-1: Transmit Antenna Free-Space Gain (dBi)

Aircraft Systems	Spectrum (MHz)	Measurement Frequency Range (MHz)	Transmit Antenna Type	Free-Space Antenna Gain (dBi)
VHF-Com	118 – 137	116-138	Dipole	2.1
LOC/VOR	LOC: 108.1 – 111.95 VOR: 108 – 117.95	108-118	Dipole	0.9
GS	328.6 – 335.4	325-340	Dipole	1.9
TCAS	1090	1080 – 1100	Dual-Ridge Horn	7.4
GPS (L1)	1575.42 ± 2	1565 – 1585	Dual-Ridge Horn	9.6
SatCom	1545-1559	1530 – 1561	Dual-Ridge Horn	9.6

For most systems, IPL included aircraft cable loss, since receiver susceptibility thresholds were specified at the receiver antenna port. For GPS, interference thresholds were specified at the output of a passive GPS antenna. Thus, IPL for GPS should not include the antenna cable loss. The test cable should connect directly to the GPS antenna output or very close to it, and the spectrum analyzer measured the power at the output of the antenna directly. If an aircraft active GPS antenna was powered with the help of a DC bias-tee, the bias-tee should be included in the total system loss measurement.

For GPS, interference threshold is specified at the output of a passive antenna, or at the output of an active GPS antenna, but before the pre-amplifier stage. Thus, the active GPS antenna pre-amplifier gain should be removed during post processing. This step was required in the GPS receiver's Minimum Operating Performance Standards (MOPS)

The measurement process for each system on each aircraft can involve the following steps:

1. Conduct 1-meter path loss measurement. IPL was measured with the transmit antenna positioned one meter from the aircraft antenna. This simple step established a baseline measurement and helped detect any excessive aircraft antenna cable loss. Excessive cable loss could indicate possible signs of connector corrosion in the path. These data were not needed to compute the IPL.
2. Configure the spectrum analyzer to the proper reference level, resolution bandwidth, attenuation level and desired measurement frequency band. Configure the tracking source to track the frequency sweep of the spectrum analyzer. Set the tracking source output to desired power level.
3. Measure test cable and aircraft cable “through” losses.
4. Position the transmit antenna at a desired location, typically near a window or door. Point the antenna to radiate toward a window or door seam.
5. Clear spectrum analyzer’s trace. Set spectrum analyzer to “Trace Max Hold” and sweep continuously across the desired measurement band.
6. Scan the transmit antenna slowly along the door seam, while the spectrum analyzer is still set at “Trace Max Hold”. No scanning was needed at the windows due to small window sizes.
7. Record trace and the peak marker value. For systems that experience narrowband peaks caused by strong local transmitters such as LOC, position the marker at the peak of the broadband envelope while avoiding the narrowband peaks. Record data at this marker location.
8. Change polarization and repeat from step 2 so that both vertical and horizontal polarizations of the transmit antenna are included.
9. Relocate the transmit antenna to another window/door and repeat from step 4.

Post processing helps remove the measured system “through” loss from the total path loss data. The system loss includes the effects of test cable losses, amplifier gains, and other types of losses/gains in the measurement path. Active GPS pre-amplifier gain is also removed in the final results.

Figure 4.1-4 shows a measurement being conducted with the transmit antenna at a window, and the computer and software used for data acquisition. Instruments and computers were located within the passenger cabin. Spurious emissions from the equipment were too low to be measurable or to affect the measurement. In contrast, the output signal from the tracking source was 10 dBm or higher depending upon whether an external amplifier was used.



Figure 4.1-4: IPL measurement at window locations. (a) A dipole was used as transmit antenna for LOC, VOR, GS and VHF-Com. (b) A dual ridge horn antenna was used for TCAS, GPS and SatCom. (c) A computer recorded data from the spectrum analyzer (located underneath the computer).

4.2 Interference Path Loss Results

Recent IPL results along with existing publicly available data are reported in this section. Section 4.2.1 reports the recent measured results using the described method. Section 4.2.2 discusses the results summarized from other efforts. The combined data are reported in Tables 4.2-1 to 4.2-7.

4.2.1 Recent Measured Results

Recent IPL data for several radio receivers on six B737-200 and four B747-400 aircraft are reported in Tables 4.2-1 to 4.2-7 [2]. In addition to the window and door locations, IPL measurements were also conducted at each of the seats, including one measurement between two adjacent seats on the left half of two B737 aircraft. As a result, each full-aircraft measurement provided approximately 160 locations (times two for two transmit antenna polarizations) rather than about 36 window and door locations. Statistics such as the minimum and the average IPL were also reported.

Comparing the window/door data against the full-aircraft data for these two B737s, it was recognized that the window/door measurements capture the *minimum* IPL for the systems on those aircraft. Also, the differences in *average* IPL values were not significant. The comparison validates the common understanding that the minimum IPL occurs at window and door locations, at which most measurements were made.

The same full-aircraft IPL data for the B737 aircraft were also used to provide a conservative estimate of the effects due to multiple PED devices. The approach computes the interference power at the receiver by first scaling each PED's emissions according to the IPL for its location. The total interference power

is the sum of all contributions, reasonably assuming the signals are incoherent. Multiple equipment factor (MEF) is defined as the ratio, in dB, of total interference power at the receiver to the interference power due to one PED located at the worst case location for the lowest IPL. Additional details on the computation and results of MEF for several radio systems are shown in Section 6.

4.2.2 Other Interference Path Loss Data

There are also other IPL data previously reported in various documents. These documents consist of RTCA/DO-199 [6], RTCA/DO-233 [25], a Veda report [26], and those from the cooperative agreement between NASA and Delta Airlines [27]. Most of these data were previously summarized in the report on interference effects of wireless phones to aircraft radio-navigation receivers [1]. For completeness, they are again reported in Tables 4.2-1 to 4.2-7.

The main difference between the path loss definition in this document and the definition used in parts of RTCA/DO-199 and RTCA/DO-233 is whether the transmit antenna's free-space antenna factors are included in the path loss data provided. In this document, it is assumed that the environment is far from free space and that free-space antenna factors are not valid correction factors. The true transmit antenna factors are not known, and are not included in the path loss calculations. However, free-space antenna factors for the antennas used are provided in Table 4.1-1 if corrections are desired.

In the Appendix A of RTCA/DO-199, most reported papers used the same definition for IPL as shown in Eq. 4.1-1, but with a correction for transmit antenna gain. However, there were also test papers in RTCA/DO-199 with path-loss-factors calculated *without* the correction applied (paper SC156-110). In these cases, the path loss definition is the same as in this report.

In RTCA/DO-233, path-loss-factor calculations “may” include T_x antenna gain. Antenna factors were given for a dipole antenna used but not for other transmit antennas.

In Tables 4.2-1 to 4.2-7, IPL was reported for LOC, GS, VHF Comm., SatCom, TCAS, and GPS. Data were grouped into large, medium, and small aircraft categories. For each aircraft measured, the minimum IPL (MIPL), the average IPL and the standard deviation (StDev) were reported.

The number of measurement points and measurement frequency range were also reported when available. The number of measurement points was often reported as a *number times 2*, i.e. “26x2”. This notation indicated that both transmit antenna polarizations, vertical and horizontal, were used at each measurement location, effectively doubling the number of data points. Thus, “26x2” indicated measurements were taken at 26 locations, with vertical and horizontal polarized source antenna, resulting in 52 data points.

The statistics of the MIPL for each large, medium and small aircraft category were also reported. In addition, statistics of the MIPL calculated using ALL available data were shown at the end of each table and again in Table 4.3-1. These statistics include the lowest MIPL and the average MIPL for the safety margin calculations in Section 5.

In the tables 4.2-1 to 4.2-7, the following symbols are used in identifying the sources for the measurement data:

- {1} United Airlines, Eagle Wings Inc., and NASA LaRC cooperative effort
- {2} Delta Airlines, Eagle Wings Inc., and NASA LaRC cooperative effort
- {3} United Airlines and Eagle Wings Inc.
- {4} RTCA/DO-233
- {5} RTCA/DO-199
- {6} RTCA/SC-177
- {7} Aerospatiale
- {8} Veda/FAA

Table 4.2-1: SatCom IPL

Recent Data	Aircraft & Model {Source}	Interference Path Loss (IPL) (dB)			No. of Meas.	Test Freq. Range (MHz)
		Min (MIPL)	Average	StDev		
	<u>Large Aircraft</u>					
✓	<u>B747 Nose No. 8173 {1}</u>	52.1	70.7	18.6	21x2	
✓	<u>B747 Nose No. 8174 {1}</u>	51.5	70.1	18.6	21x2	
✓	<u>B747 Nose No. 8188 {1}</u>	53.6	65.8	12.2	21x2	
✓	<u>B747 Nose No. 8186 {1}</u>	55.5	70.2	14.7	21x2	
	B747 {4}	87.0	96.8	5.0		
	<i>Column Minimum</i>	51.5	65.8			
	<i>Column Average</i>	59.9	74.7			
	<i>Column Maximum</i>	87.0	96.8			
	<i>Column Standard Deviation</i>	15.2	12.5			

Table 4.2-2: GPS IPL

Recent Data	Aircraft & Model {Source}	Interference Path Loss (IPL) (dB)			No. of Meas.	Test Freq. Range (MHz)
		Min (MIPL)	Average	StDev		
<u>Large Aircraft</u>						
✓	B747 Nose No. 8173 {1}	65.7	73.5	4.0	21x2	1565-1585
✓	B747 Nose No. 8174 {1}	66.3	72.9	3.3	21x2	1565-1585
✓	B747 Nose No. 8188 {1}	64.7	70.6	2.9	21x2	1565-1585
✓	B747 Nose No. 8186 {1}	66.3	74.0	3.5	21x2	1565-1585
	<i>Column Minimum</i>	64.7	70.6			
	<i>Column Average</i>	65.8	72.8			
	<i>Column Maximum</i>	66.3	74.0			
<u>Medium Aircraft</u>						
✓	B737 Nose No. 1989 {1}	64.9	75.0	4.0	36x2	1565-1585
✓	B737 Nose No. 1883 {1}	64.0	76.0	5.3	76x2	1565-1585
✓	B737 Nose No. 1879 {1}	71.2	77.1	3.9	33x2	1565-1585
✓	B737 Nose No. 1997 {1}	68.8	74.5	2.7	34x2	1565-1585
✓	B737 Nose No. 1994 {1}	67.4	74.4	3.9	34x2	1565-1585
✓	B737 Nose No. 1881 {1}	67.2	73.0	3.5	33x2	1565-1585
	CV-580 {8}	41.0				
	B727 N40 {5}	71.0	77.0		12	1575
	<i>Column Minimum</i>	41.0	73.0			
	<i>Column Average</i>	64.4	75.3			
	<i>Column Maximum</i>	71.2	77.1			
<u>Small Aircraft</u>						
	Gulf G4 {4}	82.4	91.4	5.7		
	CRJ {2}	43.2	53.5	6.1	14x2	
	<i>Column Minimum</i>	43.2	53.5			
	<i>Column Average</i>	62.8	72.5			
	<i>Column Maximum</i>	82.4	91.4			
	All Aircraft Column Minimum	41.0	53.5			
	All Aircraft Column Average	64.6	74.1			
	All Aircraft Column Maximum	82.4	91.4			
	All Aircraft Standard Deviation	10.6	8.0			

Table 4.2-3: TCAS IPL

Recent Data	Aircraft & Model {Source}	Interference Path Loss (IPL) (dB)			No. of Meas.	Test Freq. Range (MHz)
		Min (MIPL)	Average	StDev		
<u>Large Aircraft</u>						
✓	<u>B747 Nose No. 8173 {1}</u>	63.2	69.9	4.4	21x2	1080-1100
✓	<u>B747 Nose No. 8174 {1}</u>	61.7	67.3	3.3	21x2	1080-1100
✓	<u>B747 Nose No. 8188 {1}</u>	63.3	68.6	2.3	21x2	1080-1100
✓	<u>B747 Nose No. 8186 {1}</u>	64.2	71.0	3	21x2	1080-1100
	<i>Column Minimum</i>	61.7	67.3			
	<i>Column Average</i>	63.1	69.2			
	<i>Column Maximum</i>	64.2	71.0			
<u>Medium Aircraft</u>						
✓	<u>B737 Nose No. 1989 {1}</u>	53.0	66.1	4.4	36x2	1080-1100
✓	<u>B737 Nose No. 1883 {1}</u>	52.8	64.8	4.3	36x2	1080-1100
✓	<u>B737 Nose No. 1879 {1}</u>	55.8	67.6	4.4	36x2	1080-1100
✓	<u>B737 Nose No. 1997 Windows {1}</u>	<u>54.3</u>	68.3	4.4	36x2	1080-1100
✓	<u>B737 Nose No. 1997 Full Aircraft {1}</u>	<u>54.3</u>	70.9	3.8	179x2	1080-1100
✓	<u>B737 Nose No. 1994 {1}</u>	56.6	69.3	4.2	36x2	1080-1100
✓	<u>B737 Nose No. 1881 {1}</u>	56.3	69.0	4.5	36x2	1080-1100
	B757 {4}	69.1	83.3	7.3		
	B757-TCAS-Top {2}	58.6	71.5	6.9	55x2	
	B757-TCAS-Bottom {2}	57.6	75.0	7.7	53x2	
	A320 -TCAS-T {4}	54.8	74.6	11.3		
	A320 -TCAS-B {4}	63.0	78.5	7.1		
	A320 {7}					
	<i>Column Minimum</i>	52.8	64.8			
	<i>Column Average</i>	57.2	71.6			
	<i>Column Maximum</i>	69.1	83.3			
<u>Small Aircraft</u>						
	CRJ TCAS-Top {2}	53.1	59.2	4	14x2	
	CRJ TCAS-Bottom {2}	54.7	61.5	3.3	14x2	
	Emb 120 -TCAS-Top {2}	50.7	57.6	4.5	11x2	
	Emb 120 -TCAS-Bottom {2}	48.2	59.7	5.8	11x2	
	ATR72- TCAS-Top {2}					
	ATR72- TCAS-Bottom {2}					
	<i>Column Minimum</i>	48.2	57.6			
	<i>Column Average</i>	51.7	59.5			
	<i>Column Maximum</i>	54.7	61.5			
	All Aircraft Column Minimum	48.2	57.6			
	All Aircraft Column Average	57.3	68.7			
	All Aircraft Column Maximum	69.1	83.3			
	All Aircraft Standard Deviation	5.3	6.4			

Table 4.2-4: GS IPL

Recent Data	Aircraft & Model {Source}	Interference Path Loss (IPL) (dB)			No. of Meas.	Test Freq. Range (MHz)
		Min (MIPL)	Average	StDev		
	<u>Large Aircraft</u>					
✓	<u>B747 Nose No. 8173 {1}</u>	49.3	67.6	8.4	26x2	325-340
✓	<u>B747 Nose No. 8174 {1}</u>	51.0	69.6	9.3	26x2	325-340
✓	<u>B747 Nose No. 8188 {1}</u>	49.3	68.8	7.9	26x2	325-340
✓	<u>B747 Nose No. 8186 {1}</u>	48.9	66.1	8.5	26x2	325-340
	B747 {4}	54.6	86.2	14.1		
	B747 {3}	53.0	71.0	8.0	36	
	DC10 {5}	77.0	91.0		24	329-335
	L1011 {4}	64.4	82.6	8.1		
	<i>Column Minimum</i>	48.9	66.1			
	<i>Column Average</i>	55.9	75.4			
	<i>Column Maximum</i>	77.0	91.0			
	<u>Medium Aircraft</u>					
✓	<u>B737 Nose No. 1989 {1}</u>	58.9	70.1	5.0	36x2	325-340
✓	<u>B737 Nose No. 1883 {1}</u>	60.2	75.1	6.5	36x2	325-340
✓	<u>B737 Nose No. 1879 {1}</u>	59.7	75.4	5.5	36x2	325-340
✓	<u>B737 Nose No. 1997 Windows {1}</u>	<u>61.7</u>	72.2	5.2	36x2	325-340
✓	<u>B737 Nose No. 1997 Full Aircraft {1}</u>	<u>61.7</u>	73.3	4.3	<u>169</u> x2	325-340
✓	<u>B737 Nose No. 1994 {1}</u>	61.4	73.9	6.5	36x2	325-340
✓	<u>B737 Nose No. 1881 {1}</u>	59.5	72.2	5.7	36x2	325-340
	B737 {4}	68.8	83.1	4.9		
	B757 {4}	57.5	83.0	9.9		
	B757 {2}	58.9	72.1	6.0	53x2	
	B727 {6}	68.0	83.0			
	B727 {5}	68.0	76.0		12	328
	CV-580 {8}	64.0				
	MD80 {4}	63.5	85.4	11.0		
	A320 {4}	64.6	84.2	10.0		
	A320 {7}	56.0	70.0			
	<i>Column Minimum</i>	56.0	70.0			
	<i>Column Average</i>	62.0	76.6			
	<i>Column Maximum</i>	68.8	85.4			
	<u>Small Aircraft</u>					
	Canadair RJ {2}	51.6	59.7	3.2	14x2	
	Emb 120 {2}	46.2	51.5	2.3	10x2	
	ATR72	57.5	68.0	5.4	26x2	
	<i>Column Minimum</i>	46.2	51.5			
	<i>Column Average</i>	51.8	59.7			
	<i>Column Maximum</i>	57.5	68.0			

Table 4.2-4: Concluded

All Aircraft Column Minimum	46.2	51.5
All Aircraft Column Average	59.1	74.3
All Aircraft Column Maximum	77.0	91.0
All Aircraft Standard Deviation	7.2	8.8

Table 4.2-5: VOR IPL

Recent Data	Aircraft & Model {Source}	Interference Path Loss (IPL) (dB)			No. of Meas.	Test Freq. Range (MHz)
		Min (MIPL)	Average	StDev		
<u>Large Aircraft</u>						
✓	<u>B747 Nose No. 8173 {1}</u>	51.8	68.8	9.4	26x2	108-118
✓	<u>B747 Nose No. 8174 {1}</u>	62.7	82.3	10.9	26x2	108-118
✓	<u>B747 Nose No. 8188 {1}</u>	55.0	77.7	11.6	26x2	108-118
✓	<u>B747 Nose No. 8186 {1}</u>	58.9	77.0	10.6	26x2	108-118
	B747 {4}	84.7	105.0	5.1		
	B747 {3}	76.0	80.0	3.0	8	
	DC 10 {5}	80.0	89.0		20	113-117
	L1011 {4}	70.3	79.0	2.0		
	Column Minimum	51.8	68.8			
	Column Average	67.4	82.4			
	Column Maximum	84.7	105.0			
<u>Medium Aircraft</u>						
✓	<u>B737 Nose No. 1989 Windows {1}</u>	<u>65.0</u>	78.1	7.7	36x2	108-118
✓	<u>B737 Nose No. 1989 Full Aircraft {1}</u>	<u>65.0</u>	81.7	5.6	<u>156x2</u>	108-118
✓	<u>B737 Nose No. 1883 {1}</u>	56.5	73.0	9.8	36x2	108-118
✓	<u>B737 Nose No. 1879 {1}</u>	61.8	77.5	7.7	36x2	108-118
✓	<u>B737 Nose No. 1997 {1}</u>	74.2	87.3	6.2	36x2	108-118
✓	<u>B737 Nose No. 1994 {1}</u>	62.6	78.5	7.9	36x2	108-118
✓	<u>B737 Nose No. 1881 {1}</u>	67.0	78.6	6.0	36x2	108-118
	B737 {4}	76.0	90.0	5.0		
	B757 {4}	49.9	90.7	9.9		
	B757 {2}	46.7	65.8	6.8	56x2	
	B727-a {5}	70.0	74.0		6	112-117
	B727 -b {5}	30.0	56.0		86	112-117
	B727-c {5}	71.0	76.0		6	109-120
	B727 {6}	75.0	90.0			
	CV-580 {8}	45.0				
	MD80 {4}	66.2	87.8	9.4		
	A320 {4}	65.0	91.9	8.7		
	A320 {7}	59.0	84.0			
	Column Minimum	30.0	56.0			
	Column Average	61.4	80.1			
	Column Maximum	76.0	91.9			

Table 4.2-5: Concluded

Small Aircraft

Canadair RJ {2}	57.9	71.6	6.6	14x2
Emb 120 {2}	41.8	56.3	4.5	11x2
ATR72 {2}	63.9	72.1	4.2	25x2
<i>Column Minimum</i>	<i>41.8</i>	<i>56.3</i>		
<i>Column Average</i>	<i>54.5</i>	<i>66.7</i>		
<i>Column Maximum</i>	<i>63.9</i>	<i>72.1</i>		
All Aircraft Column Minimum	30.0	56.0		
All Aircraft Column Average	62.4	79.3		
All Aircraft Column Maximum	84.7	105.0		
All Aircraft Standard Deviation	12.2	10.6		

Table 4.2-6: LOC IPL

Recent Data	Aircraft & Model {Source}	Interference Path Loss (IPL) (dB)			No. of Meas.	Test Freq. Range (MHz)
		Min (MIPL)	Average	StDev		
<u>Large Aircraft</u>						
✓	B747 Nose No. 8173 {1}	51.8	68.8	9.4	26x2	108-118
✓	B747 Nose No. 8174 {1}	62.7	82.3	10.9	26x2	108-118
✓	B747 Nose No. 8188 {1}	55.0	77.7	11.6	26x2	108-118
✓	B747 Nose No. 8186 {1}	58.9	77.0	10.6	26x2	108-118
	B747 {4}	64.8	93.9	12.7		
	B747 {3}	55.0	61.0	2.0	38	
	DC10 {5}	82.0	91.0		10	108
	L1011 {4}	60.7	85.2	9.4		
	Column Minimum	51.8	61.0			
	Column Average	61.4	79.6			
	Column Maximum	82.0	93.9			
<u>Medium Aircraft</u>						
✓	B737 Nose No. 1989 Windows {1}	65.0	78.1	7.7	36x2	108-118
✓	B737 Nose No. 1989 Full Aircraft {1}	65.0	81.7	5.6	156x2	108-118
✓	B737 Nose No. 1883 {1}	56.5	73.0	9.8	36x2	108-118
✓	B737 Nose No. 1879 {1}	61.8	77.5	7.7	36x2	108-118
✓	B737 Nose No. 1997 {1}	74.2	87.3	6.2	36x2	108-118
✓	B737 Nose No. 1994 {1}	62.6	78.5	7.9	36x2	108-118
✓	B737 Nose No. 1881 {1}	67.0	78.6	6.0	36x2	108-118
	B737 {4}	72.7	90.7	8.8		
	B757 {4}	51.5	86.1	11.4		
	B757 {2}	56.1	75.3	10.2	52x2	
	B727 -a {5}	63.0	67.0		6	108-112
	B727 -b {5}	35.0	53.0		86	108-112
	B727 {6}	72.0	90.0			
	A320 {4}	48.8	85.7	14.8		
	A320 {7}	54.0	75.0			
	Column Minimum	35.0	53.0			
	Column Average	60.3	78.5			
	Column Maximum	74.2	90.7			
<u>Small Aircraft</u>						
	Canadair RJ {2}	57.9	71.6	6.6	14x2	
	Emb 120 {2}	41.8	56.3	4.5	11x2	
	ATR72 {2}	63.9	72.1	4.2	25x2	
	Column Minimum	41.8	56.3			
	Column Average	54.5	66.7			
	Column Maximum	63.9	72.1			

Table 4.2-6: Concluded

All Aircraft Column Minimum	35.0	53.0
All Aircraft Column Average	60.0	77.5
All Aircraft Column Maximum	82.0	93.9
All Aircraft Standard Deviation	10.0	10.4

Table 4.2-7: VHF Comm IPL

Recent Data	Aircraft & Model {Source}	Interference Path Loss (IPL) (dB)			No. of Meas.	Test Freq. Range (MHz)
		Min (MIPL)	Average	StDev		
Large Aircraft						
✓	B747 Nose No. 8173 {1}	31.5	53.9	7.7	21x2	116-138
✓	B747 Nose No. 8174 {1}	32.3	56.3	6.7	21x2	116-138
✓	B747 Nose No. 8188 {1}	35.3	58.9	6.6	21x2	116-138
✓	B747 Nose No. 8186 {1}	35.3	59.5	7.9	21x2	116-138
✓	B747 Nose No. 8188 {1}	43.2	61.5	5.9	21x2	116-138
	(AC Pressurized)					
	B747 -VHF1 {4}	40.5	79.2	12.0		
	B747 -VHF2 {4}	63.2	86.2	10.8		
	B747 -VHF3 {4}	71.5	92.9	7.4		
	DC 10 {5}	63.0	80.0		45	117-137
	L1011 -VHF1 {4}	56.2	72.9	6.1		
	L1011 -VHF2 {4}					
	L1011 -VHF3 {4}	62.2	77.2	4.2		
	Column Minimum	31.5	53.9			
	Column Average	48.6	70.8			
	Column Maximum	71.5	92.9			
Medium Aircraft						
✓	B737 Nose No. 1989 {1}	52.3	61.9	5.2	36x2	116-138
✓	B737 Nose No. 1883 {1}	46.8	59.3	5.2	36x2	116-138
✓	B737 Nose No. 1879 {1}	50.1	61.6	4.7	36x2	116-138
✓	B737 Nose No. 1997 Windows {1}	<u>51.5</u>	61.9	5.8	36x2	116-138
✓	B737 Nose No. 1997 Full Aircraft {1}	<u>51.5</u>	65.8	4.3	173x2	116-138
✓	B737 Nose No. 1994 {1}	48.6	63.5	5.1	36x2	116-138
✓	B737 Nose No. 1881 {1}	52.6	61.2	4.5	36x2	116-138
	B737 -VHF1 {4}	52.9	69.0	7.6		
	B737 -VHF2 {4}	58.4	74.2	9.3		
	B737 -VHF3 {4}	53.2	76.2	9.6		
	B757 -VHF1 {4}	49.7	72.9	9.8		
	B757 -VHF2 {4}	38.0	64.7	8.7		
	B757 -VHF3 {4}	53.0	79.3	8.7		
	B757-VHF-Left {2}	36.3	52.8	7.4	56x2	
	B757-VHF-Right {2}	49.3	60.6	6.2	38x2	
	B757-VHF-Center {2}	50.3	64.0	6.7	55x2	
	B727 N40 -a {5}	67.0	71.0		6	118-135
	B727 N40 -b {5}	44.0	53.0		49	118-135
	B727 N40 -c {5}	76.0	<u>80.0</u>		6	109

Table 4.2-7: Concluded

MD80-VHF1 {4}	57.2	74.5	9.2
MD80-VHF2 {4}	64.9	81.7	10.0
MD80-VHF3 {4}	55.2	81.7	13.3
A320 -VHF1 {4}	51.5	70.0	8.4
A320 -VHF2 {4}	62.1	77.6	6.7
A320 -VHF3 {4}	55.6	76.2	7.4
<i>Column Minimum</i>	36.3	52.8	
<i>Column Average</i>	53.1	68.6	
<i>Column Maximum</i>	76.0	81.7	

Small Aircraft

CRJ VHF-L {2}	36.7	53.7	7.6	14x2
CRJ VHF-R {2}	50.9	62.3	6.0	14x2
Emb 120 -VHF-L {2}	28.7	47.0	7.3	12x2
Emb 120 -VHF-R {2}	45.0	53.5	3.7	11x2
ATR72- VHF-L {2}	48.4	61.3	8.2	13x2
ATR72- VHF-R {2}	43.5	60.0	6.3	26x2
<i>Column Minimum</i>	28.7	47.0		
<i>Column Average</i>	42.2	56.3		
<i>Column Maximum</i>	50.9	62.3		

All Aircraft Column Minimum	28.7	47.0
All Aircraft Column Average	50.4	67.4
All Aircraft Column Maximum	76.0	92.9
All Aircraft Standard Deviation	10.9	10.6

4.3 Summary of Minimum Interference Path Loss Data

Table 4.3-1 summarizes the MIPL shown in Section 4.2. Data in this table were taken from the “All Aircraft” summary rows at the end of each table. In this table, the *minimum MIPL* values displayed are the *lowest* MIPL of all aircraft. Likewise, the *average MIPL* values displayed are the *average* of the MIPL of all aircraft. The minimum MIPL and the average MIPL are used in the later calculations for interference safety margins. The maximum MIPL and the StDev of the MIPL of all aircraft are also shown. The standard deviations were calculated without assigning additional weight to any specific aircraft model or number of measurement points.

Table 4.3-1 shows there can be a large difference in dB between the maximum MIPL and the minimum MIPL. MIPL can vary between 35 dB to 82 dB for LOC and between 30 dB to 84.7 dB for VOR. TCAS system has the smallest MIPL range, 48.2 dB to 69.1 dB, and the lowest MIPL standard deviation value of 5.3 dB.

Table 4.3-1: Summary of Aircraft Minimum IPL (MIPL)

	Min MIPL (dB)	All Aircraft Ave MIPL (dB)	Max MIPL (dB)	StDev (dB)
LOC	35.0	60.0	82.0	10.0
VOR	30.0	62.4	84.7	12.2
VHF	28.7	50.4	76.0	10.9
GS	46.2	59.1	77.0	7.2
TCAS	48.2	57.3	69.1	5.3
SatCom	51.5	59.9	87.0	15.2
GPS	41.0	64.6	82.4	10.6
MLS*	78			

* From DO-199; Note: Average IPL in DO-199 are defined differently than the average MIPL and therefore are not used.

5 Interference Analysis

In this section, receiver susceptibility thresholds are discussed, and the measured interference thresholds are summarized from RTCA/DO-199. In addition, safety margins are calculated from the interference susceptibility thresholds, the path loss data in Section 4, and the emissions from the wireless phones.

5.1 Published Receiver Susceptibility

Of the three elements required for risk assessment (wireless phone emission; aircraft IPL; and receiver interference threshold), receiver interference threshold (to PED interfering signal) is the one element with the least amount of available data. RTCA/DO-199 and RTCA/DO-233 provide the most information on the subject. However, the amount of data available is far from being sufficient to provide a high level of confidence in the figures provided. Except for GPS, the ICAO Annex 10, Vol.1 [24] and receiver MOPS did not properly address the in-band, on-channel interference. Also, spurious signals were too low to cause other types of interference, such as desensitization, addressed in these documents.

5.1.1 RTCA/DO-233

For LOC, RTCA/DO-233 sets four different interference thresholds for in-band, on-channel interference. Signal-to-Interference (S/I) ratio for the four interference types can vary between 7 dB to as much as 46 dB depending upon the frequency spacing between the CW interference signal from the 90 Hz or 150 Hz ILS sidebands of the LOC carrier. In addition, a modulated interference signal may result in a different interference threshold than CW interference. Additional information is documented in [1].

RTCA/DO-233 did not provide similar guidance for other systems such as VOR or GS. And unlike RTCA/DO-199, RTCA/DO-233 did not provide data to support their findings and recommendations concerning receiver interference thresholds.

5.1.2 RTCA/DO-199

RTCA/DO-199 is the only publicly available document that provided results from testing of receiver interference thresholds. In RTCA/DO-199, receiver interference levels along with test signal strengths were documented in the form of tables and charts, from which relevant threshold data for LOC, GS, VOR, TCAS, VHF-Com and SatCom were extracted. For a CW interference signal, the official S/I ratios were chosen from the typical values, which were valid across most of the channel bandwidth. However, when the interfering signal was such that it mixed with the local carrier to produce a frequency close to the receiver's side band, susceptibility notches could occur. Test results show the S/I ratio can be as high as 38 dB for LOC, 35 dB for GS and 46 dB for VOR. Theoretical analysis was also conducted and presented for LOC and VOR.

For CW interference, the disruption threshold tends to vary along with the signal level in such a way that the S/I ratio stays constant. As a result, the disruption threshold can only be determined if the test signal is known. In the document, the test signals were set equal to the minimum desired signals at the receivers. These signals were calculated from the minimum desired external field environments within the coverage airspace assuming an isotropic, lossless antenna, and fixed values of cable losses. The minimum desired external field environments were taken from several sources, including the ICAO Annex 10, Vol.1, and FAA National Orders, and others. Additional details on the desired signal strength calculations and the interference criteria unique to each system can be found in RTCA/DO-199.

According to the document, it was very difficult to maintain signal lock at the susceptibility notches to cause undetected interference even if it was intended. The official thresholds were selected, therefore, by ignoring narrowband notches. Table 5.1-1 summarizes the test signal level used, the official disruption threshold, along with the unofficial disruption threshold at the susceptibility notches. The underlined data in this table were used in the safety margin calculations in Section 5.2.

Table 5.1-1: RTCA/DO-199 Interference Thresholds

	LOC	VOR	GS	VHF	GPS	MLS
Desired Signal at Receiver (dBm)	-88	-97	-78	-89		
Typical Interference Level (dBm)	<u>-104</u>	<u>-110</u>	<u>-93</u>	<u>-107</u>	<u>-126.5*</u>	<u>-62</u>
Signal/Inteference (S/I) Ratio (dB)	16	13	15	18		
Minimum Interference Level (dBm) (at notches)	<u>-127</u>	<u>-143</u>	<u>-113</u>	<u>-107</u>		
Signal/Interference ratio (dB)	39	46	35	18		
Theoretical Thresholds (dBm)	-130	-148	-120			
Theoretical S/I Ratio (dB)	42	51	42			

* For GPS, -126.5 dBm minimum interference level is required in GPS receiver MOPS such as DO-208 and DO-229B. DO-199 provides -130 dBm interference level for GPS.

For GPS, the interference threshold was very well defined and was consistent across various standards, Technical Standard Orders (TSOs) and receiver MOPS for airborne navigation equipment. These documents provided the minimum performance standards for stand-alone, satellite-based and ground-based GPS systems and sensors. A few of these documents include: ITU-R M.1477 [28], RTCA/DO-235A [7], RTCA/DO-229B [29], RTCA/DO-253A [30], RTCA/DO-228 [31], and RTCA/DO-208 [32].

These documents show that the lowest interference threshold is **-126.5 dBm** for a GPS system in acquisition mode with CW interference or signals with bandwidth up to 700 Hz. This threshold was specified at the output of a passive antenna, or at the output of an active antenna, but before the pre-amplifier stage. Thus, the active GPS antenna pre-amplification gain must be accounted for in the path loss value in order to use the -126.5 dBm threshold value.

The values provided assume that there is only one interference signal. In the presence of additional interference sources and noise, the threshold values may have to be re-evaluated.

5.2 Safety Margin Calculations

Knowing device emission “A”, aircraft minimum path loss “-B”, and receiver susceptibility threshold “C”, safety margins can be computed using

$$\text{Safety Margin} = C - (A + B)$$

This section first calculates the interference signal strength at the receiver’s antenna port (A +B). Safety margin can then be computed with the knowledge of “C”.

Applying the minimum and the average values of MIPL (“-B”) in Table 4.3-1 to the emission data (“A”) in Table 3.6-1, the resulting interference signals at the receiver (“A+B”) are shown in Table 5.2-1. Due to the large range of IPL “-B” values, the results of the calculation (A+B) are presented with only the maximum and the average values that are calculated from the minimum and the average path loss “-B” values.

Table 5.2-1: Interference Signal Strength at Receiver’s Antenna Port (A+B). Maximum and Average values in dBm

	Maximum and Average Interference Signal at Receiver (A+B)					
	Cellular-Band Phones		PCS-Band Phones		Laptops/PDA	
	Max (Min IPL)	Ave (Ave IPL)	Max (Min IPL)	Ave (Ave IPL)	Max (Min IPL)	Ave (Ave IPL)
LOC	-110.3	-135.3	-111.8	-136.8	-98.3	-123.3
VOR	-105.3	-137.7	-106.8	-139.2	-93.3	-125.7
VHF	-104.0	-125.7	-105.5	-127.2	-92.0	-113.7
GS	-125.7	-138.6	-122.0	-134.9	-104.9	-117.8
TCAS	-112.9	-122.0	-111.5	-120.6	-93.9	-103.0
GPS	-126.8	-150.4	-107.5	-131.1	-96.8	-120.4
SatCom(*)	-137.3	-145.7	-118.0	-126.4	-107.3	-115.7
MLS(**)	-121.8		-141.8		-155.0	

(*) SatCom Band device’s emission are assumed to be the same as for the GPS band

(**) from RTCA/DO-199

Comparing the maximum and the average signal strength at the receivers, (A+B), in Table 5.2-1 to the typical and the minimum susceptibility thresholds in Table 5.1-1, safety margins can be calculated. The result for each system is a 2x2 matrix. Deciding which element of the safety margin matrix to use depends upon whether the maximum or the average value for (A+B) was used, and on whether the typical or the minimum interference threshold was used. In the cases where there was only one value for interference threshold, such as GPS, the safety margin results are 2x1 matrices.

Tables 5.2-2 to 5.2-7 report the results of the calculation with the safety margin results highlighted in **bold** for each combination of wireless phone’s emissions, MIPL, and interference threshold values. The calculations were conducted for LOC, VOR, VHF Comm, GS, GPS and MLS. To determine safety margins, one simply locates the right combinations of devices (cellular or PCS-band phones), the MIPL values, and interference thresholds on the tables. Thus, the combination of cellular-band phone, minimum MIPL (resulting in the interference signal at receiver of -110.3 dBm), and the minimum LOC interference threshold (-127 dBm) results in -16.7 dB safety margin. A large positive safety margin is desirable, whereas a large negative safety margin indicates a possibility of interference.

Safety margin calculations for TCAS and SatCom were not possible due to the lack of interference threshold data. However, the remaining IPL and spurious emissions data can be used in future calculations once the interference threshold is defined.

Table 5.2-2: LOC Safety Margin (in dB) for Different Combinations of Wireless Phones, MIPL and Interference Thresholds

Interference Signal at Receiver (dBm) =	Cellular-Band Phones &		PCS-Band Phones &		Laptops/PDAs &	
	Min	Ave	Min	Ave	Min	Ave
	MIPL	MIPL	MIPL	MIPL	MIPL	MIPL
	-110.3	-135.3	-111.8	-136.8	-98.3	-123.3
<u>LOC Interference Threshold</u>						
Minimum (dBm) -127	-16.7	8.3	-15.2	9.8	-28.7	-3.7
Typical (dBm) -104	6.3	31.3	7.8	32.8	-5.7	19.3

Table 5.2-3: VOR Safety Margin (in dB) for Different Combinations of Wireless Phones, MIPL and Interference Thresholds

Interference Signal at Receiver (dBm) =	Cellular-Band Phones &		PCS-Band Phones &		Laptops/PDAs &	
	Min	Ave	Min	Ave	Min	Ave
	MIPL	MIPL	MIPL	MIPL	MIPL	MIPL
	-105.3	-137.7	-106.8	-139.2	-93.3	-125.7
<u>VOR Interference Threshold</u>						
Minimum (dBm) -143	-37.7	-5.3	-36.2	-3.8	-49.7	-17.3
Typical (dBm) -110	-4.7	27.7	-3.2	29.2	-16.7	15.7

Table 5.2-4: VHF Safety Margin (in dB) for Different Combinations of Wireless Phone, MIPL and Interference Thresholds

Interference Signal at Receiver (dBm) =	Cellular-Band Phones &		PCS-Band Phones &		Laptops/PDAs &	
	Min	Ave	Min	Ave	Min	Ave
	MIPL	MIPL	MIPL	MIPL	MIPL	MIPL
	-104	-125.7	-105.5	-127.2	-92	-113.7
<u>VHF Interference Threshold (dBm)</u>						
-107	-3.0	18.7	-1.5	20.2	-15	6.7

Table 5.2-5: GS Safety Margin (in dB) for Different Combinations of WLAN/Radio Devices, MIPL and Interference Thresholds

Interference Signal at Receiver (dBm) =	Cellular-Band Phones &		PCS-Band Phones &		Laptops/PDAs &	
	Min MIPL	Ave MIPL	Min MIPL	Ave MIPL	Min MIPL	Ave MIPL
		-125.7	-138.6	-122.0	-134.9	-104.9
<u>GS Interference Threshold</u>						
Minimum (dBm) -113	12.7	25.6	9.0	21.9	-8.1	4.8
Typical (dBm) -93	32.7	45.6	29.0	41.9	11.9	24.8

Table 5.2-6: GPS Safety Margin (in dB) for Different Combinations of WLAN/Radio Devices, MIPL and Interference Thresholds

Interference Signal at Passive Antenna Output (dBm) =	Cellular-Band Phones &		PCS-Band Phones &		Laptops/PDAs &	
	Min MIPL	Ave MIPL	Min MIPL	Ave MIPL	Min MIPL	Ave MIPL
		-126.8	-150.4	-107.5	-131.1	-96.8
<u>GPS Interference Threshold (dBm)</u>						
-126.5	0.3	23.9	-19.0	4.6	-29.7	-6.1

Table 5.2-7: MLS Safety Margin (in dB) for Different Combinations of WLAN/Radio Devices, MIPL and Interference Thresholds

Interference Signal at Receiver (dBm) =	Cellular-Band Phones &		PCS-Band Phones &		Laptops/PDAs &	
	Min MIPL	Ave MIPL	Min MIPL	Ave MIPL	Min MIPL	Ave MIPL
		-121.8		-141.8		-155.0
<u>MLS Interference Threshold (dBm)</u>						
-62	59.8		79.8		93.0	

* For MLS both path loss and receiver susceptibility thresholds came from DO-199.

Note that the emissions and safety margins for systems operating in Band 1 (LOC, GS, VHF-Com) are different than in [2], even though the same data are used in both reports. Band 1 in this report covers 105 – 140 MHz, whereas Band 1 in [2] was defined to cover 105 – 120 MHz.

From the tables, interference safety margins can be positive or negative depending upon the combinations of MIPL and receiver interference thresholds used. The wireless phones considered generally have better safety margin than standard laptops and PDAs based on test data in this effort.

The exception is the MLS band. In this band, emissions from the wireless devices are higher than emissions from the laptop computers by at least 13 to 33 dB (emission from the laptop computers were below the measurement noise floor). There appears no cause for concern due to the large positive safety margins. However, the safety margin for MLS seems unusually large. In addition, there was lack of additional data to validate the interference threshold and the IPL data provided in RTCA/DO-199 and used in this analysis. Additional measurement data in the MLS band is needed.

In general, there is a need for better understanding and characterization of receiver's susceptibility thresholds. Additional data on all receiver systems based on measurement and theoretical analysis are highly desirable.

6 Multiple Equipment Cumulative Effects

In dealing with PED interference with aircraft systems, multiple equipment cumulative effects must be addressed. This issue is a concern for both back-door interference (where interference signals couple into system wiring) and front-door interference (where unintended transmissions couple into aircraft exterior antennas to the victim aircraft receiver).

This paper provides a conservative bound on the cumulative effects for several aircraft systems. Similar to the previous sections, this effort only addresses the effects associated with front-door interference. However, the approach can be similarly applied to other types of interference coupling.

6.1 Approach

In simplest form, front-door cumulative effects of multiple PEDs are the ratio of cumulative PED interference powers to the interference power from just one device, all measured at receivers' antenna ports.

For non-coherence sources with equal signal strength, it is often assumed that $P'_N = N * P'_I$, where P'_N and P'_I is interference signal power at the receiver for N devices and for one device, respectively. This assumption is often valid for sources that are physically co-located (ideally), or for sources located in such a way that the interference contributions from all sources are nearly equal. For sources not co-located, or if the assumption above is not valid, an individual device's contribution should be adjusted for its path-loss value before being summed. Thus, to study the cumulative effects of multiple PEDs on "front-door" interference, IPL should be factored in the calculations.

This paper utilizes existing IPL data to derive a Multiple Equipment Factor (MEF). The following subsections describe the formulations for calculating MEF.

6.1.1 MEF Formulation

To compute the cumulative effects from multiple devices, the spurious emission value for each device is first weighted proportional to its linear (not dB) interference coupling value, C_i . The results for all devices are summed, and normalized to the single-PED worst-case contribution to arrive at the cumulative effects.

The C_i is computed from the IPL at the same source location using:

$$C_i = 10^{-IPL/10} \quad (\text{Eq. 6.1-1})$$

Thus, the maximum power, in watts, coupled from seat n to the receiver is simply:

$$P_{rec}^n = P_{xmit}^n * C_i^n \quad (\text{Eq. 6.1-2})$$

Summing all P_{rec}^n and normalizing to the maximum value, P_{rec}^{\max} , MEF for N devices is defined as

$$\begin{aligned} MEF &= \left(\sum_N P_{rec}^n \right) / \left(P_{rec}^n \right)^{\max} \\ &= \left(\sum_N P_{xmit}^n * C_i^n \right) / \left(P_{xmit} * C_i \right)^{\max} . \end{aligned} \quad (\text{Eq. 6.1-3})$$

Note that $\left(P_{xmit} * C_i \right)^{\max}$ is the maximum $\left(P_{xmit}^n * C_i^n \right)$ for all N values. For the devices with maximum emission located at the minimum path loss location, $\left(P_{xmit}^n * C_i^n \right)$ becomes $\left(P_{xmit}^{\max} * C_i^{\max} \right)$

If P_{xmit} is the same for all transmitting sources, it can be normalized, and (3) become:

$$MEF = \sum_N \left(C_i^n / C_i^{\max} \right) ; \text{ for } n=1, \dots, N \quad (\text{Eq. 6.1-4})$$

with $C_i^{\max} = \max \left(C_i^n \right)$ for all n values (or simply C_i at the minimum IPL location).

Alternatively, defining the normalized coupling factor $\langle C_i^n \rangle$ and the normalized IPL $\langle IPL^n \rangle$ as

$$\langle C_i^n \rangle = C_i^n / C_i^{\max}, \text{ and} \quad (\text{Eq. 6.1-5})$$

$$\langle IPL^n \rangle = IPL^n - IPL^{\min}, \quad (\text{Eq. 6.1-6})$$

it can be shown that

$$\langle C_i^n \rangle = 10^{-\langle IPL^n \rangle / 10}, \quad (\text{Eq. 6.1-7})$$

$$MEF = \sum_N \langle C_i^n \rangle. \quad (\text{Eq. 6.1-8})$$

The MEF result is a power ratio. To convert to decibels,

$$MEF_{dB} = 10 \log_{10} (MEF) \quad (\text{Eq. 6.1-9})$$

6.1.2 Assumptions

This effort provides a reasonable upper bound for the MEF. The following simplifying assumptions are made concerning interference signals and their summing effects to establish the upperbound:

1. There are as many devices as there are passenger seats, and there is one device located at each seat.
2. All interference signals are of the same form, i.e. continuous-wave (CW), or similarly modulated.
3. All devices transmit on the same frequency.
4. Signals are non-coherent, and their summing effects at the victim receivers are additive in power, not in voltage (a reasonable assumption as the devices are operating independently).
5. Interference signals are polarized either vertically or horizontally. The worse case coupling of the two polarizations is used in the calculation. These two polarizations are typically used in IPL measurement.
6. All devices have the same emission level in the aircraft radio bands. As a result, the absolute signal strength is calibrated out. However, the formulation can be easily modified to include devices having different emissions levels.

6.2 Aircraft Path Loss Measurement

Aircraft minimum IPL data are insufficient for MEF calculations since they are usually reported as a single value for each system. Full-aircraft IPL data are much more desirable as they include many possible PED locations within the cabin. The full-aircraft IPL data are usually measured with the transmitting source located at all the windows and the seat locations. Full-aircraft IPL data should also capture the minimum IPL value.

Under a recent effort between United Airlines, Eagle Wings Inc., and NASA LaRC, full-aircraft IPL were collected on two B737 airplanes. For each of the four receiver system considered, measurements were conducted with approximately 160 transmit antenna locations covering the left or right halves of the airplanes. In addition, the transmit antennas were in vertical and horizontal polarizations. As stated in [2], these measurements confirmed that the window measurements indeed captured the minimum IPL for that aircraft.

Due to the large number of transmit antenna locations considered, aircraft resonance and local effects are automatically accounted for in the summation. A mechanical stirrer, typically used to help in collecting the statistics of the reverberating field environment, is not necessary.

Additional details for window measurements are reported in [2]. Full-aircraft measurements are reported in this section. However, only relevant details pertaining to the full-aircraft measurement method, analysis, and results applicable to MEF analysis are reported. Subsections 6.2.1 and 6.2.2 briefly touch on the measurement method and the IPL results for the four systems for which full-aircraft data are available. While full-aircraft IPL are not simple to present graphically, window IPL are shown to provide additional insight into the strength of coupling at different aircraft locations.

6.2.1 Method

Section 4.1 discussed in further details about the measurement methods for conducting IPL measurements on the six B737 aircraft. As discussed, the source antennas used include dipoles for frequencies in the GS band and below, and a dual-ridge horn antenna for the frequencies in the TCAS band and above. No corrections were made to account for (to remove the effects of) the transmit antenna gain. For the MEF calculation, antenna-gain correction is not necessary since the same factor exist in all measurements. These antenna-gains are removed in the normalization as shown in Equation 6.1-3.

As stated, full-aircraft data were collected with the transmit antenna:

1. Positioned at all window locations
2. Scanned along door seams
3. Positioned in all seat locations, at window level
4. Positioned in armrest locations, at window level
5. Positioned in the aisle, one per row of seats, at window level
6. In both vertical and horizontal polarizations

Full-aircraft measurements were performed on four systems. Details concerning spectrum and measurement range are shown in Table 6.2-1.

Table 6.2-1: B737 Full-Aircraft IPL - System Measured and Frequency Bands

Aircraft Systems	Aircraft Antenna Location	Measurement Frequency Range (MHz)	Spectrum (MHz)
VHF-Comm 1	Top	116-138	118 – 137
LOC/VOR	Tail	108-118	LOC: 108.1 – 111.95 VOR: 108 – 117.95
GS	Nose	325-340	328.6 – 335.4
TCAS	Top	1080 – 1100	1090

6.2.2 Measurement Results

Two-dimensional graphical presentations of some of the available full-aircraft data have been previously reported [33]. In addition, window IPL data for the six B737s are repeated here, Figures 6.2-1 to 6.2-4, for the VHF, LOC, GS and TCAS systems.

On these plots, IPL data for each receiver system on each aircraft are represented by two traces for the two vertical and horizontal polarizations of the transmit antennas. The window locations are simply labeled as the n^{th} side window starting from the cockpit. The door locations are labeled as “L1” and “L2”

for left side doors; and “EE” for emergency exits. At the doors, a sweep was typically conducted with the transmit antenna scanning along the door seam. A door sweep at L1 is labeled as “L1 Dr Swp”.

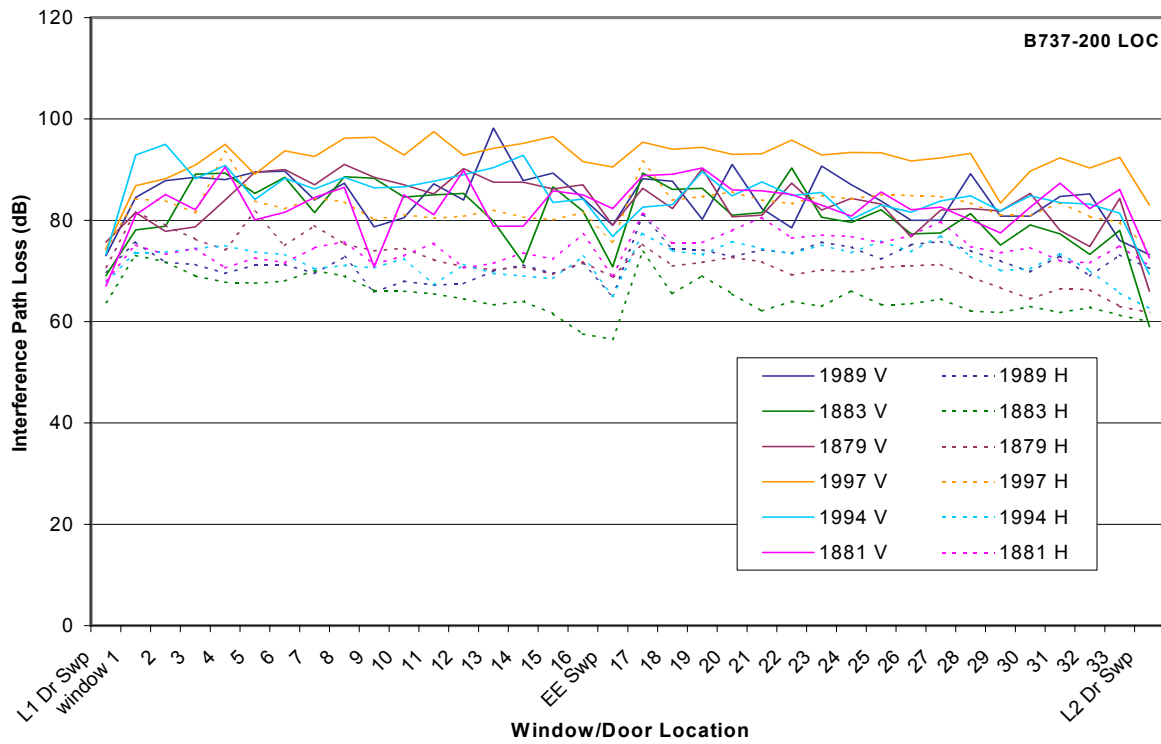


Figure 6.2-1: B737-200 LOC/VOR (Tail) interference path loss. Left windows/doors excitation.

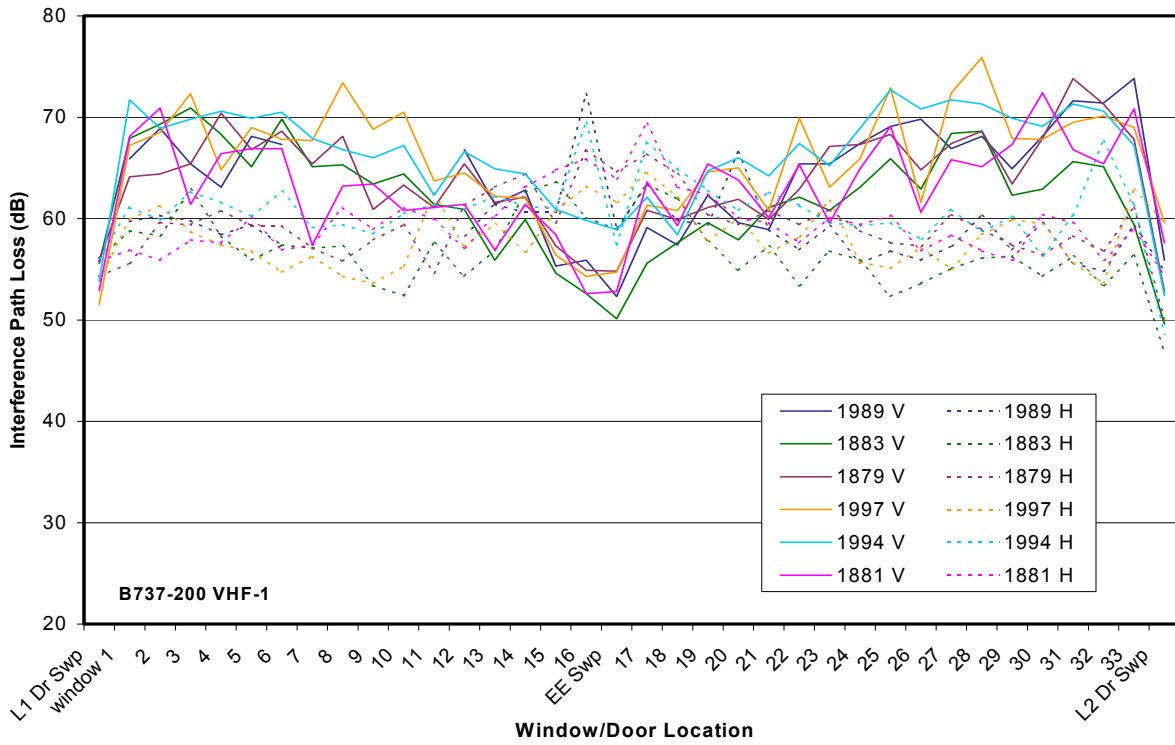


Figure 6.2-2: B737-200 VHF-1 Comm. (Top) interference path loss. Left windows/doors excitation.

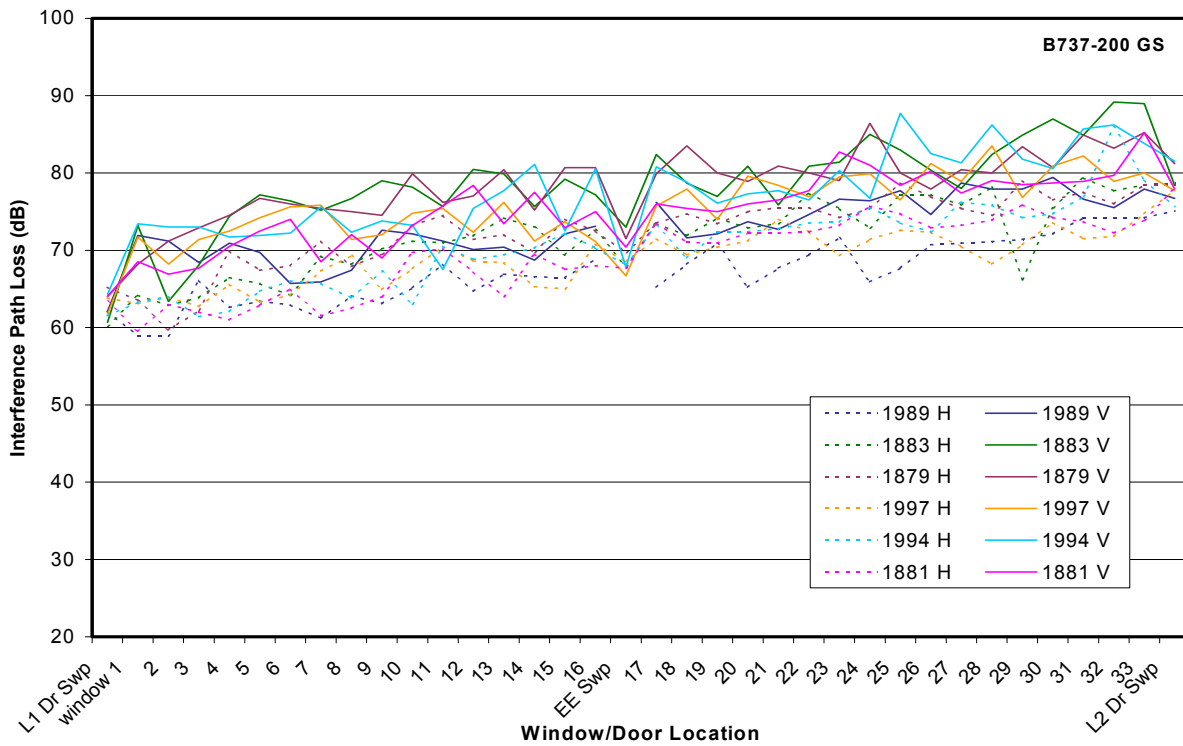


Figure 6.2-3: B737-200 GS (Nose) interference path loss. Left windows/doors excitation. Cockpit windows taped.

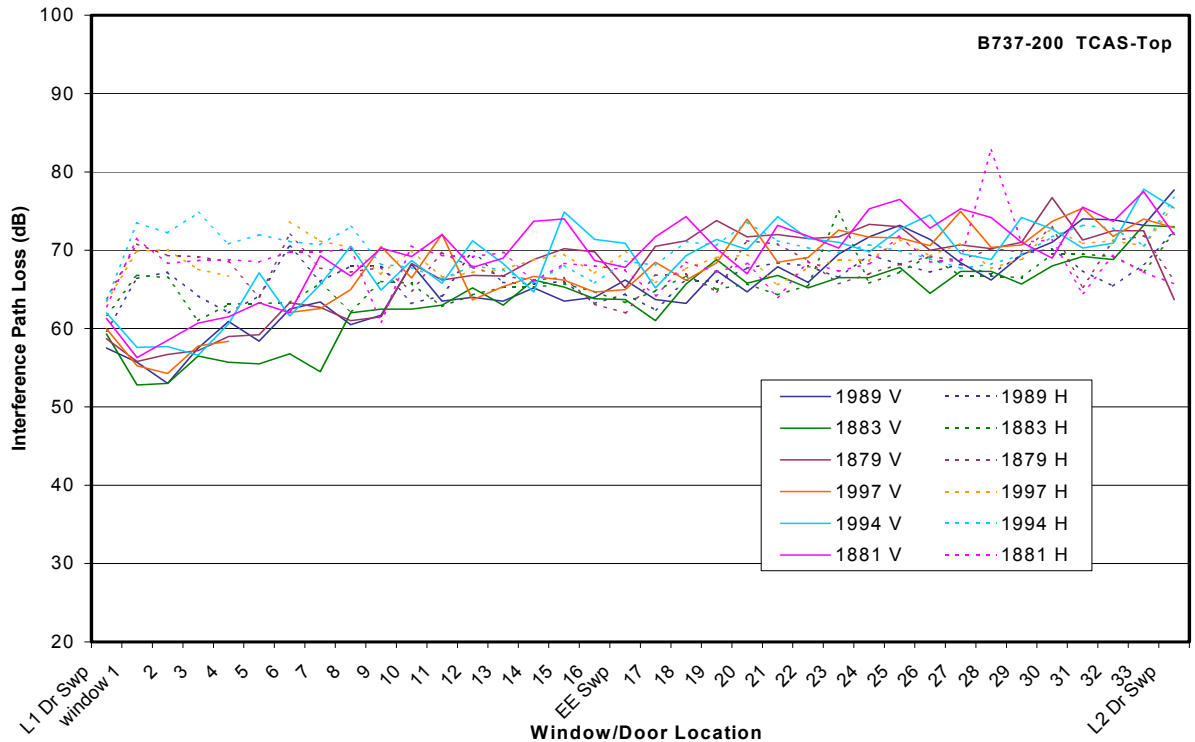


Figure 6.2-4: B737-200 TCAS (Top) interference path loss. Left windows/doors excitation.

6.3 MEF Based on IPL Measurements

As a result of the full-aircraft IPL measurements, there were more data points collected than there were seats. This happened since data were taken at every window (there are more windows than there are number of rows), at every seat, at every armrest position, and also in the aisle. For MEF calculations, the number of data points needs to be reduced to the number of seats or the number of PEDs. To achieve that goal, each seat's IPL is chosen to be the lowest IPL value (maximum coupling) for the vicinity locations. Referring to Figure 6.3-1, the specifics on the data reduction approach are listed below:

1. Seat-A Data: the IPL value is chosen to be the lowest among the Location Set A (LS-A). LS-A includes locations: 1) seat A; and 2) nearest windows and doors. There may be more than one window considered.
2. Seat-B Data: the lowest IPL among the Location Set B (LS-B). LS-B includes locations: 1) in middle of seat B; and 2) arm-rest between seats A and B (Location Set B).
3. Seat-C Data: the lowest IPL among the Location Set C (LS-C). LS-C includes locations: 1) armrest between seats B and C; 2) in the middle of seat C; and 3) the armrest next to the aisle.
4. Aisle Data: the IPL measured in the center of the aisle
5. No First Class: While data were collected on an airplane with first class seating (2 seats per row), this section assumes there are three seats per row for ease of data arrangement in the table format. This is reasonable since many configurations do not include first class seats.

6. All measurement points are considered only once. If a window data point was considered in an earlier row, the same data point cannot be considered in any other row.

Data points near a seat are compared and the minimum IPL (maximum coupling) is chosen for that seat. Table 6.3-1 shows the relationship between seat location and its measurement locations.

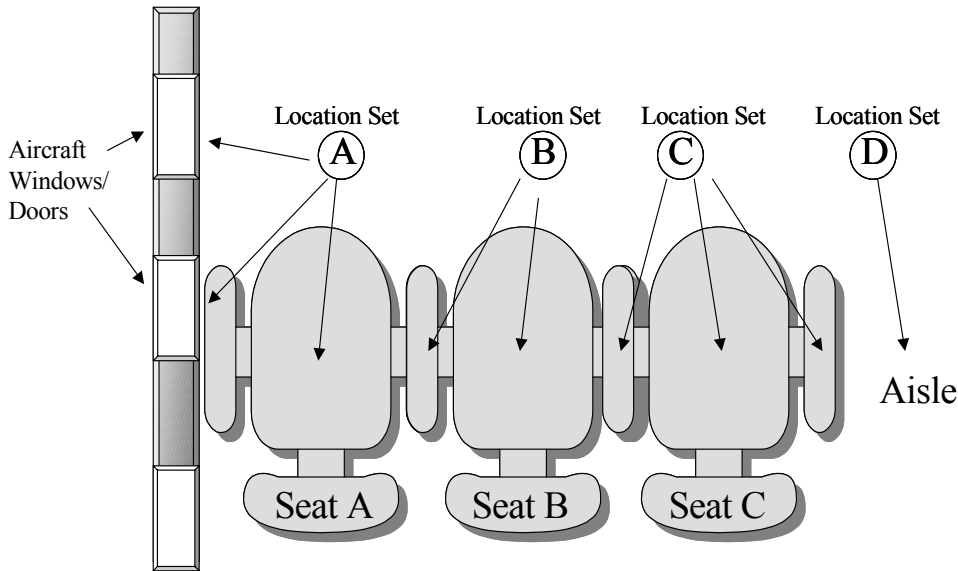


Figure 6.3-1: Seat Locations and Relationship with Measurement Locations.

Table 6.3-1: Explanation of Figure 6.3-1

Seat Location	Data Set
Seat-A	Location Set A (LS-A)
Seat-B	Location Set B (LS-B)
Seat-C	Location Set C (LS-C)
Aisle	Location Set D (LS-D)

6.4 Results of MEF Calculations

The minimum IPLs for the four aircraft systems are reported in Table 6.4-1, The same data is also shown for an isotropic transmit test antenna by removing the transmit antenna gain from the minimum IPL, thereby resulting in higher IPL values. Determination of MEF in this section does not require the minimum IPL, however, since it is normalized out in the process. They are provided so that the true IPL can be determined.

As a result of the data reduction process, normalized IPL for different systems are shown in Tables 6.4-2 to 6.4-5. In these tables, the number of IPL data points is approximately equal to the number of aircraft seats. The use of normalized IPL also helps to overcome the problem of having different definitions of IPL, or whether it includes antenna gain. The normalized IPL values in the table remain the same, while the minimum IPL may be scaled to conform to different definitions. The data in the table can

also be used to apply to interference sources having different emission levels according to their locations. In this report, however, only sources having the same emissions level are assumed.

Figures 6.4-1 to 6.4-4 show the statistical cumulative distribution as the number of locations (seats) is increased. This process involves sorting and incrementally summing the normalized IPL, starting from the worst case IPL. Equations 6.1-8 and 6.1-9 are used on the incremental sums. Note that the numbers of seats/windows are for **both** sides of the aircraft for the purpose of calculating MEF. Actual number of data points measured is only half if performed on only one side.

In addition, Figures 6.4-1 to 6.4-4 also show the MEF computed using only the window IPLs. It is suspected that there are possible relationships between the MEF using the seats data and the MEF using only the window data. After all, interference signals are assumed to pass through window/door-seams as they propagate to aircraft receiver antennas.

The comparisons show that the MEF calculated using seat-IPL data and window-IPL data are within one dB of one another.

While there are significantly more number of seats than windows, the similar MEF values can be explained in that: 1) There are more windows than number of rows of seats; and 2) Coupling data at the windows are significantly higher than the same data for the inside seats.

Table 6.4-1: Aircraft Systems Minimum IPL

Aircraft Systems	B737-200 UAL Nose No.	Transmit Antenna Type	Free Space Transmit Ant. Gain (dBi)	Minimum IPL (dB)	Minimum IPL (Isotropic Source) (dB)
LOC/VOR	1989	Dipole	0.9	65	65.9
VHF-1 Com (top)	1997	Dipole	2.1	51.5	53.6
TCAS	1997	Dual-Ridge Horn	7.4	54.3	61.7
GS	1997	Dipole	1.9	61.7	63.6

Table 6.4-2: LOC-Tail Normalized IPL- B737 (Nose No. 1989)

Row	Seat-A Data	Seat-B Data	Seat-C Data	Aisle Data	Windows/Doors considered in Seat-A Data
1	4.8	16	14.2	15.5	L1, W1
2	4.5	17.7	16.5	17.5	w1,s2,w3
3	6.2	19.2	18.3	17.7	w5,w6
4	4.5	17.2	15.3	16.7	w7
5	0.8	11.8	13.5	13.2	w8,w9,w10
6	2.2	8	13.5	17.5	w11,w12
7	5	13.7	14.3	16	w13
8	6.2	12.2	14	14.8	w14
9	4.5	9.8	13.5	13	w15
10	6.3	11.5	15	14.2	w16
11	0	17.8	17	16	EE,w17
12	9.3	15.7	15.7	15.7	w18
13	7.8	20.7	17.2	17	w19,w20
14	9.2	17.2	16.8	18.8	w21
15	8.5	18.3	14	16.7	w22,w23,w24
16	7.3	15.5	15.2	15.5	w25,w26,w27
17	4.8	10	11	15.5	w28,w29,w30,w31
18	4	11.5	12.8	11.1	w32,w33,L2

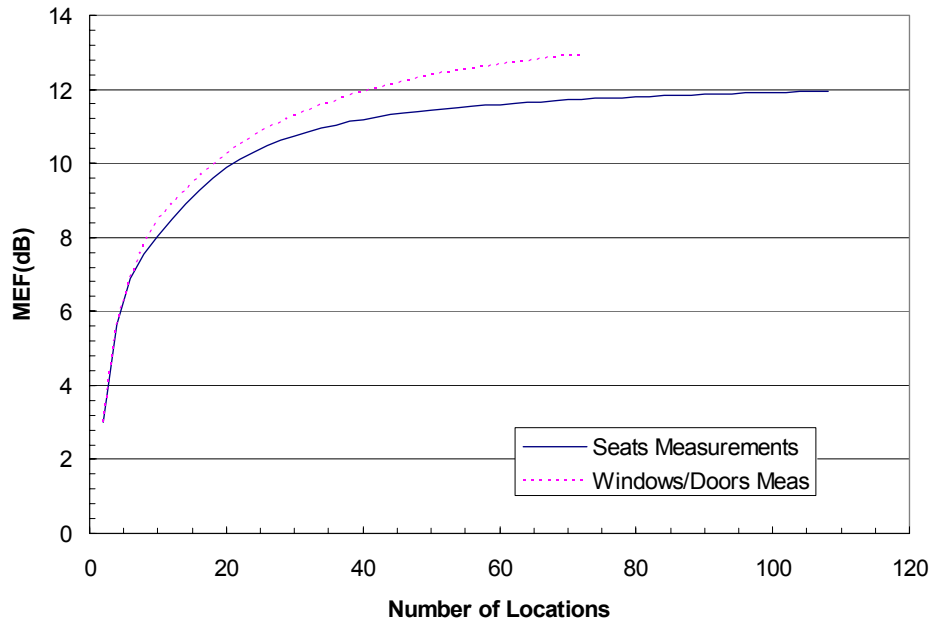


Figure 6.4-1: MEF versus number of locations. B737-Loc-Tail.

Table 6.4-3: VHF-Comm 1 Normalized IPL. B737 (Nose No. 1997)

Seat Row	Seat-A	Seat-B	Seat-C	Aisle	Windows/Doors included in Seat-A Measurements
1	0	13.2	11.8	10	L1, w1
2	5.9	15.7	13.6	16.7	w2,w3,w4
3	3.2	16.3	13.3	12.2	w5,w6
4	2.8	16.8	13.9	15.4	w7,w8
5	2.1	15.9	12.8	12.1	w9,w10
6	5.7	13.7	11.9	13	w11,w12
7	8	14.4	12	11.1	w13
8	4.9	10.8	13	15.4	w14,w15
9	2.8	9.5	9.8	13.8	w16
10	3.2	14.9	10.7	12.5	EE(w16),w17
11	9.3	13.5	10.8	11.2	w18
12	6.2	14	14	12.4	w19,w20
13	5.1	12.9	11.7	15.9	w21
14	6.7	15.3	13.1	17.7	w22,w23
15	3.6	13.2	9.9	14.3	w24,w25
16	5.7	15.1	14.1	15.7	w26
17	3.5	16.6	13.8	16.8	w27,w28
18	8.4	15.2	13.6	13.5	w29
19	4.2	12.1	12.7	16.7	w30,w31
20	2.1	10.3	6.2	13.3	w32
21	8.1	9.9	6.1	9.6	w33,L2

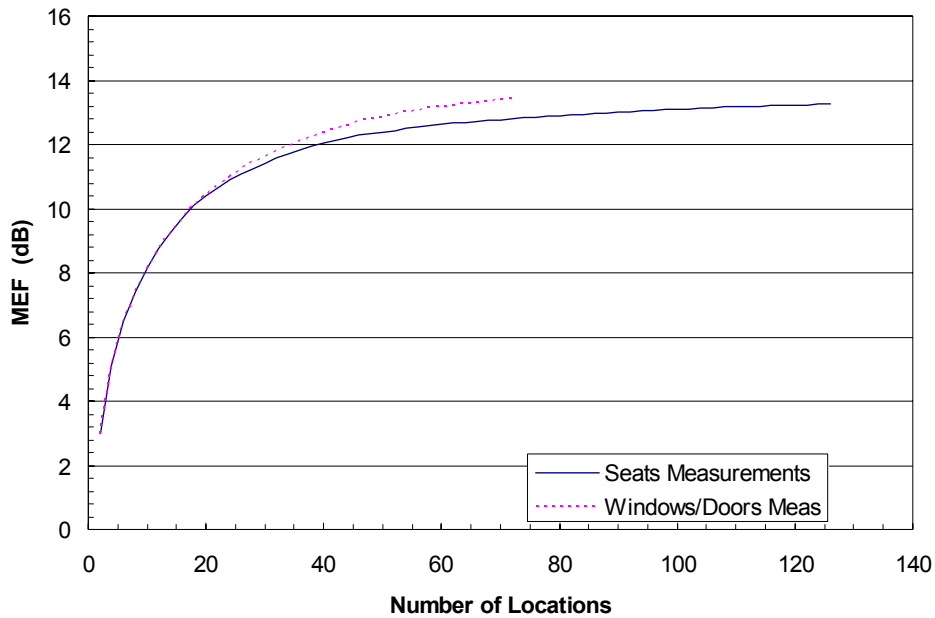


Figure 6.4-2: MEF versus number of locations. B737-VHF-Top.

Table 6.4-4: TCAS-Top- Normalized IPL. B737-1997

Seat Row	Seat-A	Seat-B	Seat-C	Aisle	Windows/Doors included in Seat-A Measurements
1	1	11	13.2	15.4	L1, w1
2	0	9	9.7	12.8	w2,w3,w4
3	7.8	10.3	8.8	14.6	w6
4	8.3	13.1	13.9	13.8	w7,w8
5	12.2	12.9	11.4	19.2	w9,w10
6	9.4	13.6	11.8	17	w11,w12
7	11.1	14.7	13.6	14.9	w13
8	12.4	14.3	13.4	16.1	w14
9	9.5	13.6	13	16.3	w15
10	10.4	13.6	16.2	15.8	w16
11	10.7	13.3	14.8	19.4	EE,w17
12	11.9	14.8	15.7	18	w18
13	12.7	16.3	16.3	13.8	w19,w20
14	11.3	16.3	15.1	17.7	w21
15	13.5	11.3	17.2	18.8	w22,w23
16	14.4	17.3	16.9	19.9	w24,w25
17	15	16.3	19.2	23	w26
18	13.4	16.5	18	16.1	w27,w28
19	14.6	16.4	17	17.5	w29
20	16.6	19.4	20.2	21.1	w30,w31
21	16.9	16.3	19.7	21.2	w32
22	14.8	18.6	17.1	20.3	w33,L2

*Note: Window 5 data not available. Antenna used would not fit due to seat blockage.

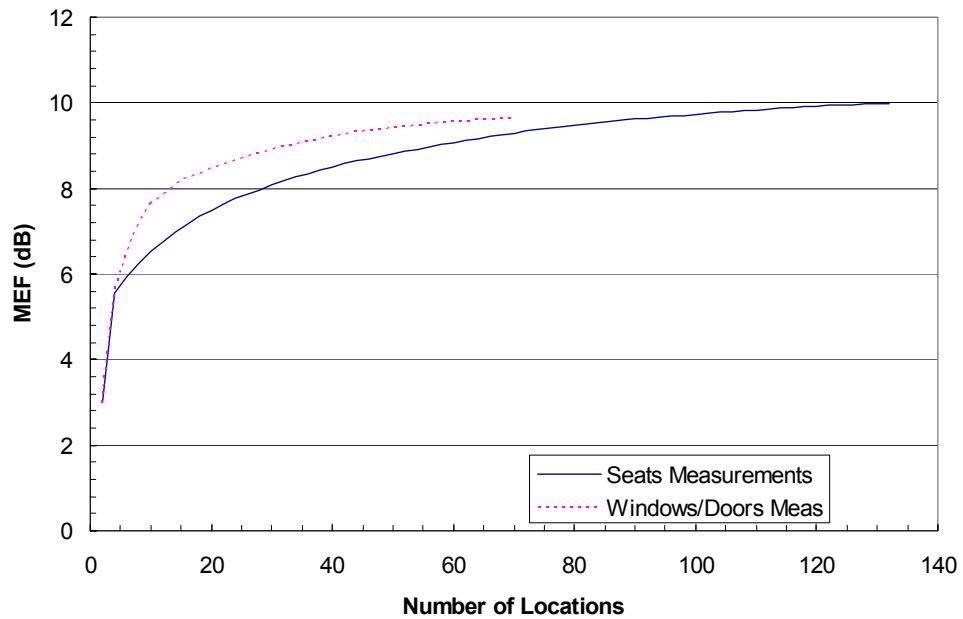


Figure 6.4-3: MEF versus number of locations. B737-TCAS-Top.

Table 6.4-5: Glideslope. B737-1997. Cockpit windows taped

Seat Row	Seat-A	Seat-B	Seat-C	Aisle	Windows/Doors included in Seat-A Measurements
1	0	4	8.7	4.1	L1, w1
2	1	3.1	4.3	6.6	w2,w3,w4
3	1.6	6.8	6	6.3	(w5),w6
4	5.6	7.2	5	5.9	w7,w8
5	3.2	5.3	5.8	7.2	w9,w10
6	6.9	6.6	8.1	8.9	w11,w12
7	5.3	7.4	6.7		w13
8	3.3	7	9.2	14.5	w14,15
9	5	10.7	9	6.8	w16, EE
10	9.8	7.2	7.6	8.4	w17
11	6.3	9.3	6.3	10.3	w18
12	8.6	11.2	6.9	9.7	w19,w20
13	12.3	11.1	11	12.2	w21
14	6.2	9.9	11.5	15.7	w22,w23
15	9.7	11.9	13.5	14.3	w24,w25
16	9.9	11.3	12.1	12.9	w26
17	6.5	15.8	12	14.3	w27,w28
18	9	12.1	13.2	16.8	w29
19	9.8	12	15.2	13.9	w30,w31
20	10.1	15.3	14.9	14.5	w32
21	13	14.9	14.7	15.3	w33

* Note: IPL for window 5 was interpolated from data for the nearby readings.

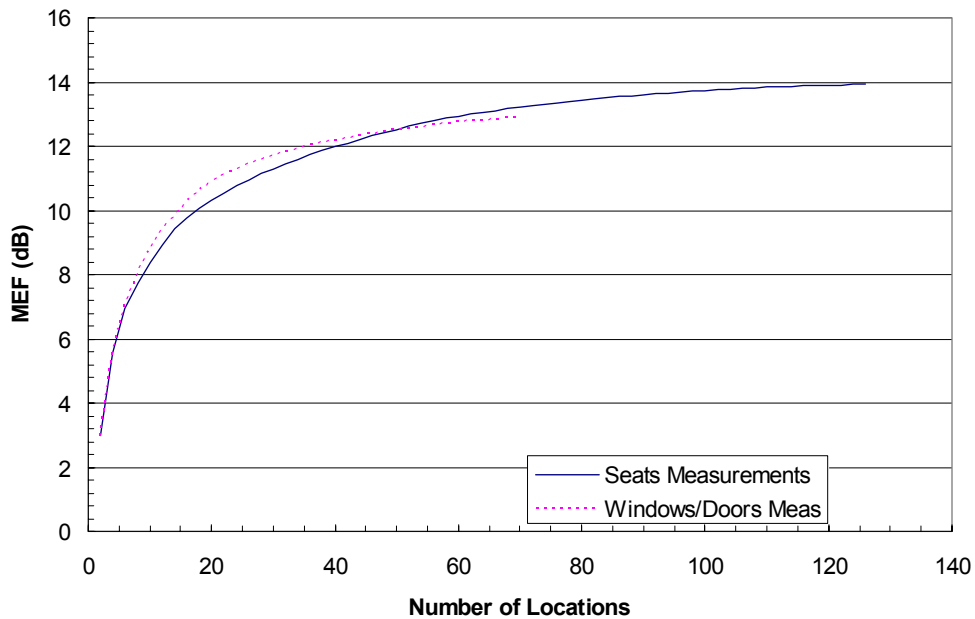


Figure 6.4-4: MEF versus number of locations. B737-GS- Nose. (Cockpit windows taped).

In addition, it is of interest to determine the incremental effects of the seat locations. Using seat-A as the base line, Tables 6.4-6 to 6.4-9 compute the incremental effects as all seat-B data and all seat-C data are added. With the aisle data, incremental effects are also shown as one adds additional inside seats. In this case aisle data are counted only once per row of seat, rather than doubled as the seat data.

As expected, the effects on MEF decrease as the seats are further inward from the windows. The addition of aisle data implies that each additional seat column only adds no more than 0.4 dB to the total MEF, with decreasing effects further inside. For large airplane, this implies that only outside seats should be considered, and that further inside seats contribute little to the overall MEF.

Table 6.4-6: Incremental Effects of Including Additional Seat Locations – LOC/VOR-Tail

Combination	Seat Locations Included	MEF (dB)	Incremental Effects (dB)	No. of Locations
1	Seat-A	10.87	0	42
2	Seat-A and Seat-B	12.72	1.85	84
3	Seat-A, Seat-B and Seat-C	<u>13.93</u>	1.21	105
4	Seat-A, Seat-B, Seat-C and Aisle	14.33	0.4	126
5	Windows/ Doors Only (All)	<u>12.90</u>		70

Table 6.4-7: Incremental Effects of Including Additional Seat Locations – VHF-1-Top

Combination	Seat Locations Included	MEF (dB)	Incremental Effects (dB)	No. of Locations
1	Seat-A	12.02	0	42
2	Seat-A and Seat-B	12.54	0.52	84
3	Seat-A and Seat-B and Seat-C	<u>13.26</u>	0.72	126
4	Seat-A and Seat-B and Seat-C and Aisle	13.46	0.2	147
5	Windows/ Doors Only (All)	<u>13.41</u>		72

Table 6.4-8: Incremental Effects of Including Additional Seat Locations – TCAS-Top

Combinations	Seat Locations Included	MEF (dB)	Incremental Effects (dB)	No. of Locations
1	Seat-A	8.02	0	44
2	Seat-A and Seat-B	9.15	1.13	88
3	Seat-A and Seat-B and Seat-C	<u>9.98</u>	0.83	132
4	Seat-A and Seat-B and Seat-C and Ailse	10.19	0.21	154
5	Windows/ Doors Only (All)	<u>9.64</u>		70

Table 6.4-9: Incremental Effects of Additional Seat Locations – GS-Nose

Combinations	Seat Locations Included	MEF (dB)	Incremental Effects (dB)	No. of Locations
1	Seat-A	10.87	0	42
2	Seat-A and Seat-B	12.72	1.85	84
3	Seat-A and Seat-B and Seat-C	<u>13.93</u>	1.21	126
4	Seat-A and Seat-B and Seat-C and Ailse	14.33	0.4	146
5	Windows/ Doors Only (All)	<u>12.9</u>		70

Due to airplane symmetry and that IPL measurements were conducted only on one side of the airplane, contributions from Seats, Windows and Doors to the total cumulative effects are doubled to simulate full configuration. The Aisle measurements are counted only once, however.

6.5 Observations

A few observations can be made from the previous tables and charts:

1. MEF determined using the windows-only IPL data are within one dB of the MEF determined using full-aircraft seat data. This is significant in that only window IPLs are needed if this observation can be further proven for other systems and aircraft. Window IPL data are readily available, while full-aircraft data are more difficult and expensive to collect, especially for large aircraft.

2. The cumulative distribution curves can help to determine the minimum number of measurements to make for the purpose of MEF calculations.
3. The conservative estimates of the bounds for MEF for the systems measured are between 10 dB and 14 dB, depending on systems.
4. The additional seat effects on the MEF diminish rapidly as the seat locations moved away from windows/doors. At the worst case, the addition of seat-B contributes only 2 dB to the MEF. Seat-C and aisle (simulating another column of seats) contribute even less.

A MEF comparison between different aircraft would be of interest. However, that would be difficult since full-aircraft IPLs are time consuming to collect. Alternatively, Appendix C provides an indirect comparison by comparing MEF computed from window IPL data for different airplanes. The validity of this comparison hinges upon further validations of the observation that MEF computed using window IPL and using full-aircraft IPL are similar.

7 Summary and Conclusions

Emission measurements were conducted on 33 wireless phones of various design configurations by different manufacturers. Seventeen of the phones were GSM phones, and most devices were dual-band (a few were tri-band or even quad-band) and had GPRS data capabilities. Likewise, the remaining 16 CDMA phones were mostly dual-band devices and 1xRTT capable. These mobile phones were more representative of those available in today's market place than the mobile phones tested previously by NASA [1]. The following observations were made:

- The 33 wireless phones tested did not generate higher emissions in most aircraft radio bands than standard laptop computers. An exception is the MLS band, where the emissions from the phone exceeded the emissions from the laptop computers. However, the safety margins in this band were positive for all devices. It is noted that operation of non-intentionally transmitting laptop computers is currently allowed during certain parts of flight.
- Spurious emissions from the wireless phones tested were below the aircraft installed equipment emission limits (RTCA/DO-160 Category M). They were also below the FCC Part 15 limits for unintentional transmitters such as laptop computers.
- The calculated safety margins can be negative or positive depending upon the interference thresholds (minimum or typical) and the minimum IPL data (the lowest or the average) used. The safety margins are based on the measured emission data, the existing IPL and interference threshold data.
- It is generally observed that in lower frequency bands (VHF-Com, LOC, VOR and GS), each mobile phone's maximum emissions are similar regardless whether it is operating in the cellular or PCS bands. This is not the case for higher frequency bands (TCAS, DME, GPS or MLS).
- The measured emissions in the voice and data modes are generally similar for any single device (within 2-5 dB) in most cases.

An approach was developed to provide an estimate of the upper bound on the front-door interference effects of multiple PEDs. This approach sums the interference powers at the receivers after scaling each

device's emission by the IPL corresponding to its location. Using full-aircraft B737 IPL data, conservative upper bounds were derived for LOC, VHF and TCAS on a B737 airplane. The following observations were made:

- MEF determined using the windows-only IPL data were within one dB of the MEF determined using full-aircraft seat data.
- Conservative bounds for MEF for the systems measured were between 10 dB and 14 dB for LOC, VHF-Com, VOR and GS.
- The effects of additional seats on the MEF calculation diminished rapidly with the increased distance between the seat locations and the windows/doors.

8 Recommended Future Work

- Additional receiver interference threshold data are needed for greater confidence level. Tests on multiple receivers from different manufacturers are recommended. Signal modulation and types should be considered.
- Assessment should be performed for software-defined-radios, active and passive RFID (radio-frequency-identification) tags, and the latest portable music playing devices (non-intentional transmitters).
- Assessment of the potential for emerging radio technologies that overlay existing spectrum (such as Ultra Wideband) to cause interference to aircraft systems.
- Conduct additional IPL measurements on different types of aircraft where minimal data currently exists. Cargo-bay IPL data are also desirable.
- Conduct additional assessment of multiple equipment effects.

9 References

- [1] Ely, J. J.; Nguyen T. X.; Koppen, S. V.; Salud, M. T.; and Beggs J. H.: *Wireless Phone Threat Assessment and New Wireless Technology Concerns for Aircraft Navigation Radios*, NASA/TP-2003-212446, July 2003.
- [2] Nguyen, T. X.; Koppen, S. V.; Ely, J. J.; Williams R. A.; Smith, L. J., and Salud, M. T.: *Portable Wireless LAN Device and Two-Way Radio Threat Assessment for Aircraft Navigation Radios*, NASA/TP-2003-212438, July 2003.
- [3] Nguyen, T. X.; Koppen, S. V.; Ely, J. J.; Williams R. A.; Smith, L. J., and Salud, M. T.: *Portable Wireless LAN Device and Two-Way Radio Threat Assessment for Aircraft VHF Communication Radio Band*, NASA/TM-2004-213010, March 2004.
- [4] Nguyen, Truong X.: *Evaluation of a Mobile Phone for Aircraft GPS Interference*, NASA/TM-2004-213001, March 2004.
- [5] Hill, David A.: *Electromagnetic Theory of Reverberation Chambers*, Chapter 4, Technical Note 1506, National Institute of Standards and Technology, December 1998.
- [6] RTCA/DO-199, *Potential Interference to Aircraft Electronic Equipment from Devices Carried Aboard*, September 16, 1988.
- [7] RTCA/DO-235A, *Assessment of Radio Frequency Interference Relevant to the GNSS*, Dec. 5, 2002.
- [8] *3rd Generation Partnership Project 2*; www.3gpp2.org.
- [9] Willtek Communications GmbH CDMA/P0851/0303/EN, 2003.
- [10] ANSI/TIA/EIA-98-D-2001 *Recommended Minimum Performance Standard for cdma2000 Spread Spectrum Mobile Stations*, June 2001.
- [11] (CDMA Intro) *Introduction to CDMA2000 Standards for Spread Spectrum Systems, Version July 1999; 3GPP2 C.S0001-0 Version 1.0*.
- [12] *Agilent E1991B Mobile Test Application Suite for the 8960 Series 10 Wireless Communications Test Set*. Agilent Technologies, Inc., April 2004; 5988-9798EN.
- [13] (ITU) *Mobile Network Code (MNC) for the international identification plan for mobile terminals and mobile users* (According to ITU-T Rec. E.212 (11/98)), Annex to ITU OB No. 801 – 1.XII.2003.
- [14] *Agilent E1968A GSM/GPRS/EGPRS Test Application Data Sheet*; October 2003; 5988-9684EN.
- [15] Ladbury, J.; Koepke, G.; and Camell, D.: *Evaluation of the NASA Langley Research Center Mode-Stirred Chamber Facility*, NIST Technical Note 1508, January 1998.
- [16] Crawford, M. L.; and Koepke, G. H.: *Design, Evaluation, and Use of a Reverberation Chamber for Performing Electromagnetic Susceptibility/Vulnerability Measurements*, NBS Technical Note 1092, U. S. Department of Commerce/National Bureau of Standards, April 1986.
- [17] RTCA DO-160D, Change No. 1, Section 20, “Radio Frequency Susceptibility (Radiated and Conducted)”, *Environmental Conditions and Test Procedures for Airborne Equipment*”, Prepared by SC-135, December 14, 2000.

- [18] International Electrotechnical Commission (IEC) 61000-4-21, 2003 (Draft).
- [19] 47CFR Ch. 1, Part 15.109, “Radiated Emission Limits”, *US Code of Federal Regulations*, Federal Register dated December 19, 2001.
- [20] FCC 22.917: 47 CFR, Chapter I – Federal Communication Commission, Part 22.917 “Cellular Radiotelephone Service - Emission Limits for Cellular Equipment”, 1 October 2003 Edition.
- [21] FCC 24.238: 47 CFR, Chapter I – Federal Communication Commission, Part 24.138 “Personal Communication Services – Broadband PCS – Emission Limits”, 1 October 2003 Edition.
- [22] RTCA DO-160D, Change No. 1, Section 21, “Emission of Radio Frequency Energy”, *Environmental Conditions and Test Procedures for Airborne Equipment*, Prepared by SC-135, July 29, 1997.
- [23] Koepke, G.; Hill, D.; and Ladbury, J.: “Directivity of the Test Device in EMC Measurements”, *2000 IEEE International Symposium on Electromagnetic Compatibility*, Aug. 21-25, 2000.
- [24] *World Jet Inventory Report Year-End 2002*, Jet Information Service, Inc.
- [25] RTCA DO-233, *Portable Electronic Devices Carried On Board Aircraft*, Prepared by SC-177, August 20, 1996.
- [26] Veda Inc., *CV-580 RF Coupling Validation Experiment Report*, Report #79689-96U/P30041, 11/15/1996.
- [27] Delta Airlines Engineering, *ENGINEERING REPORT Delta/NASA Cooperative Agreement NCC-1-381 Deliverable Reports*, Report No. 10-76052-20, December 8, 2000.
- [28] International Telecommunication Union (ITU), Recommendations ITU-R M.1477 (2000).
- [29] RTCA/DO-229B, *Min. Operational Perf. Standards for Global Positioning System (GPS)/ Wide Area Augmentation System*, Oct. 6, 1999.
- [30] RTCA/DO-253A, *Min. Operational Perf. Standards for GPS Local Area Augmentation System Airborne Equipment*, Nov. 28, 2001.
- [31] RTCA/DO-228, *Min. Operational Perf. Standards for Global Navigation Satellite Systems (GNSS) Airborne Antenna Equipment*, Oct. 10, 1995.
- [32] RTCA/DO-208, *Min. Operational Perf. Standards for GPS Airborne Supplemental Navigation Equipment using Global Positioning System (GPS)*, July 12, 199, Change 1, Sept. 21, 1993
- [33] Jafri, M.; Ely, J. and Vahala, L.: *Graphical and Statistical Analysis of Airplane Passenger Cabin RF Coupling Paths to Avionics*, 22nd Digital Avionics Systems Conference, Indianapolis, Indiana, October 12-16, 2003.

Appendix A: CDMA Phone Test Results

The following charts illustrate each wireless phone's cell data, cell voice, PCS data, and PCS voice mode envelopes. An equivalent measurement noise floor is included in each chart for each band to represent the instrument noise floor. The data in these charts were further reduced to produce the data plotted in charts found in Sections 3.4.1 to 3.4.3.

A.1 Band 1

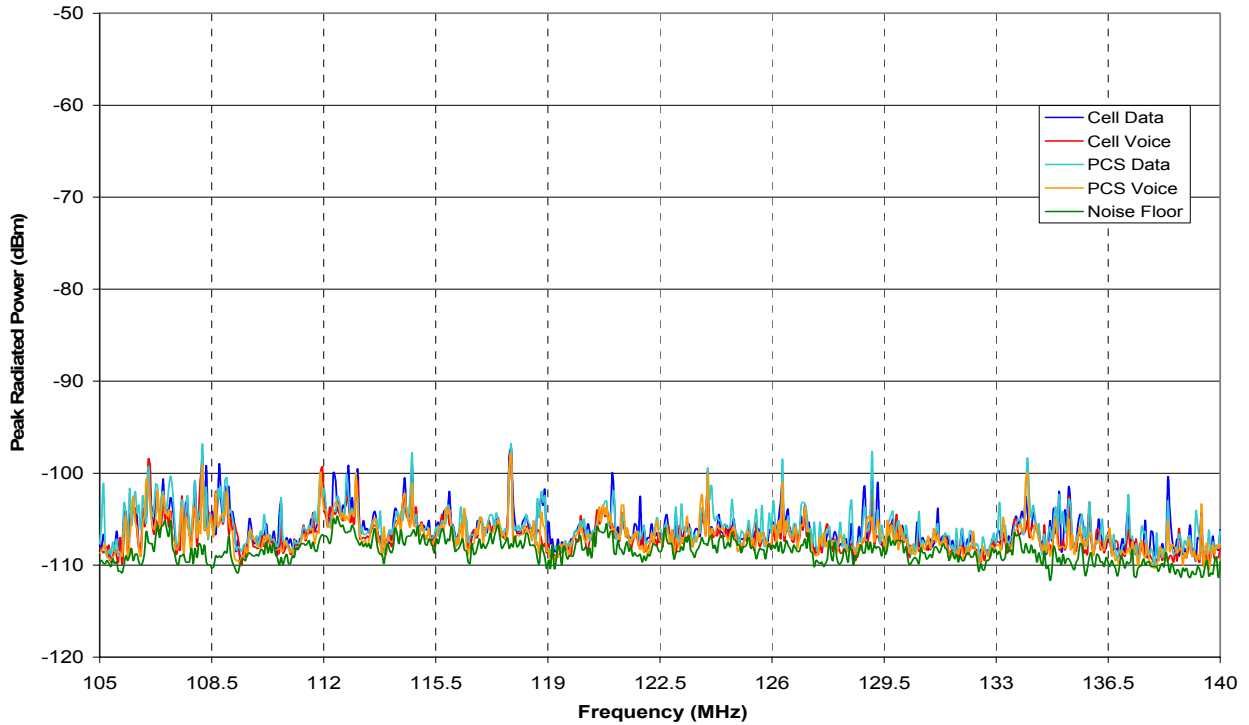


Figure A1: CDM01 four mode envelopes, Band 1.

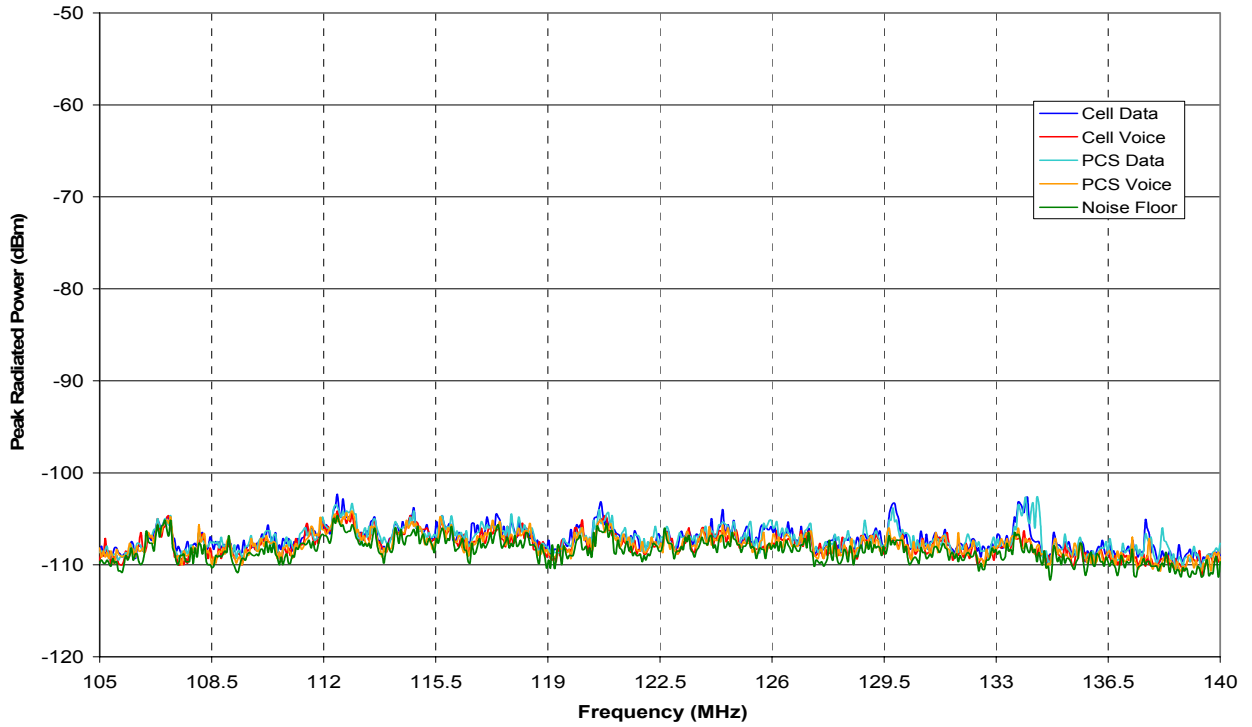


Figure A2: CDM02 four mode envelopes, Band 1.

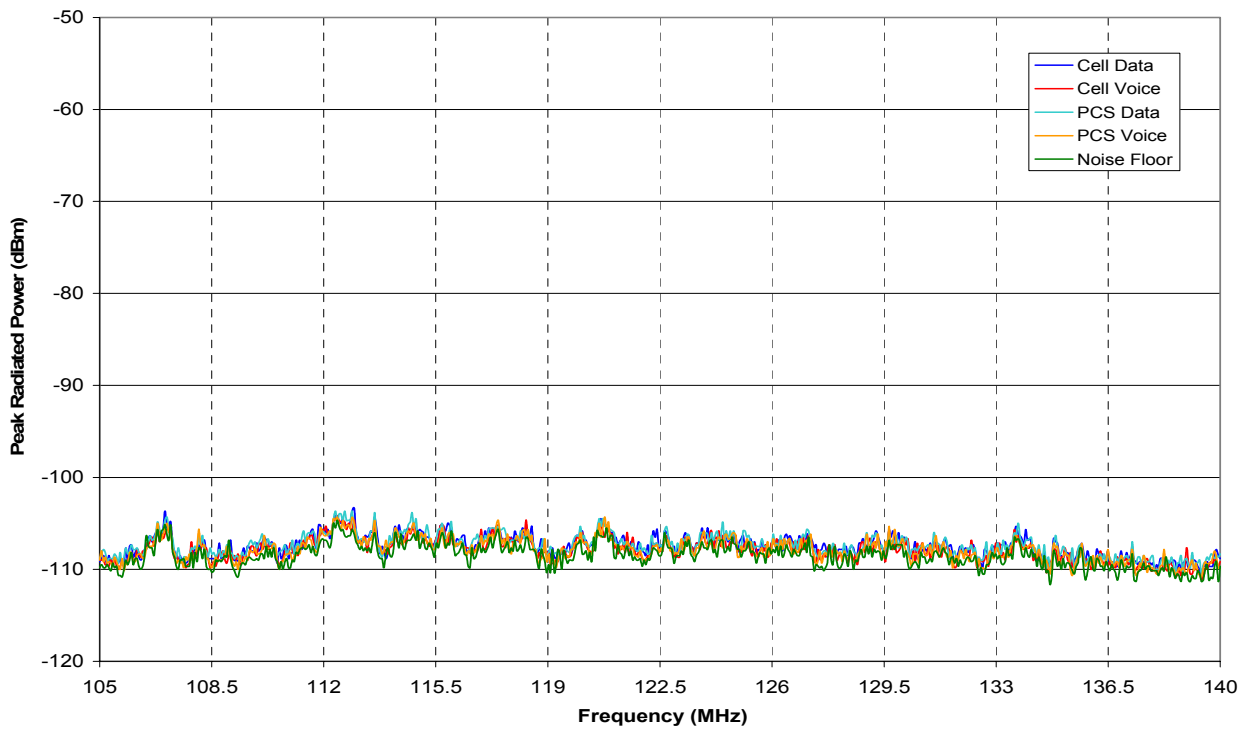


Figure A3: CDM03 four mode envelopes, Band 1.

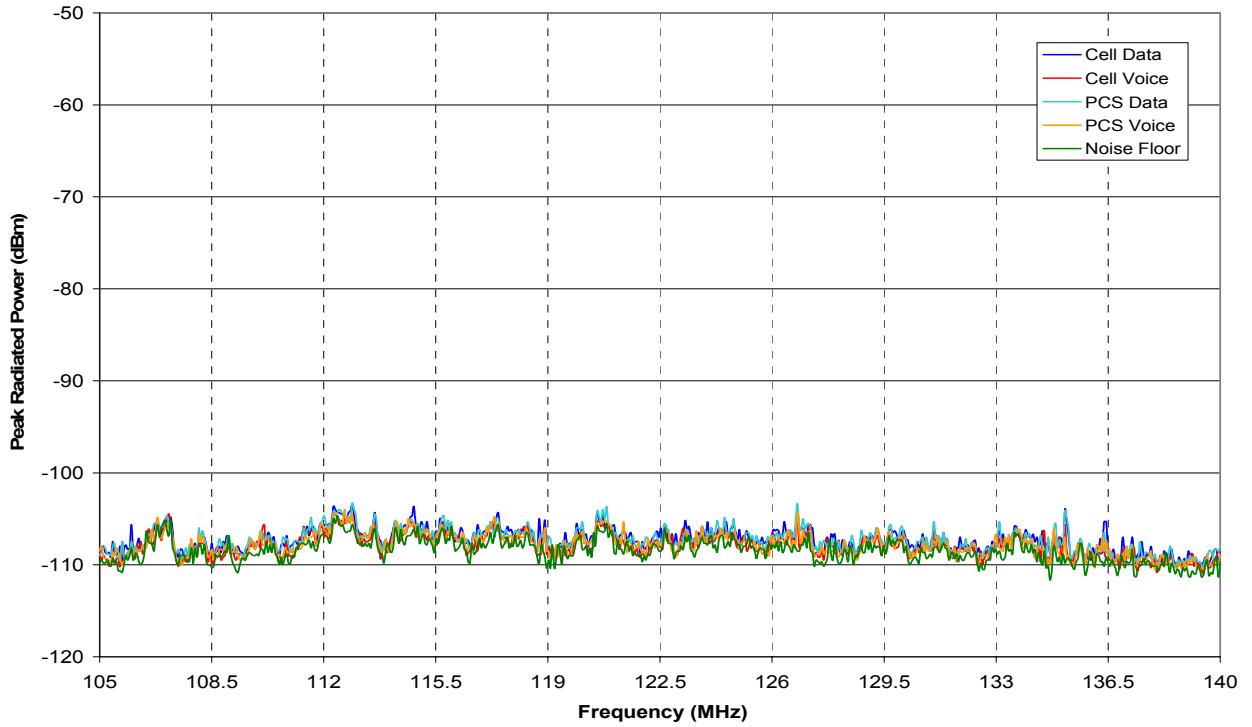


Figure A4: CDM04 four mode envelopes, Band 1.

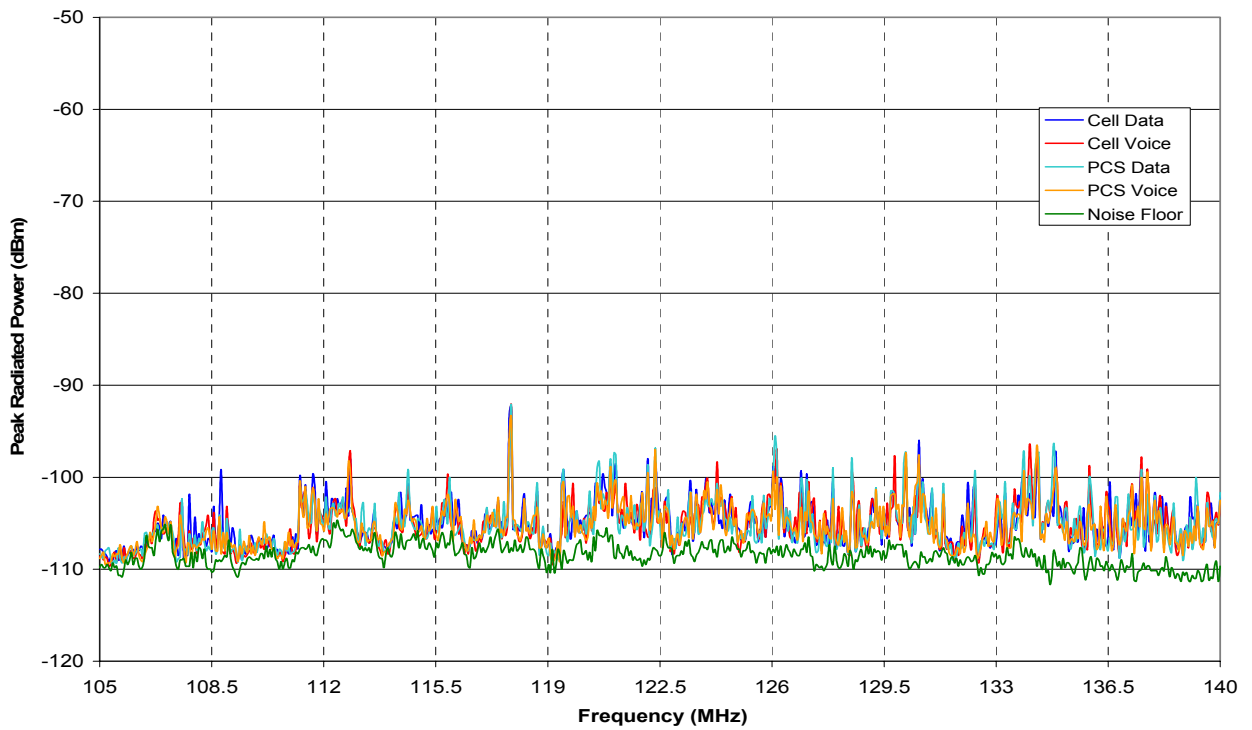


Figure A5: CDM05 four mode envelopes, Band 1.

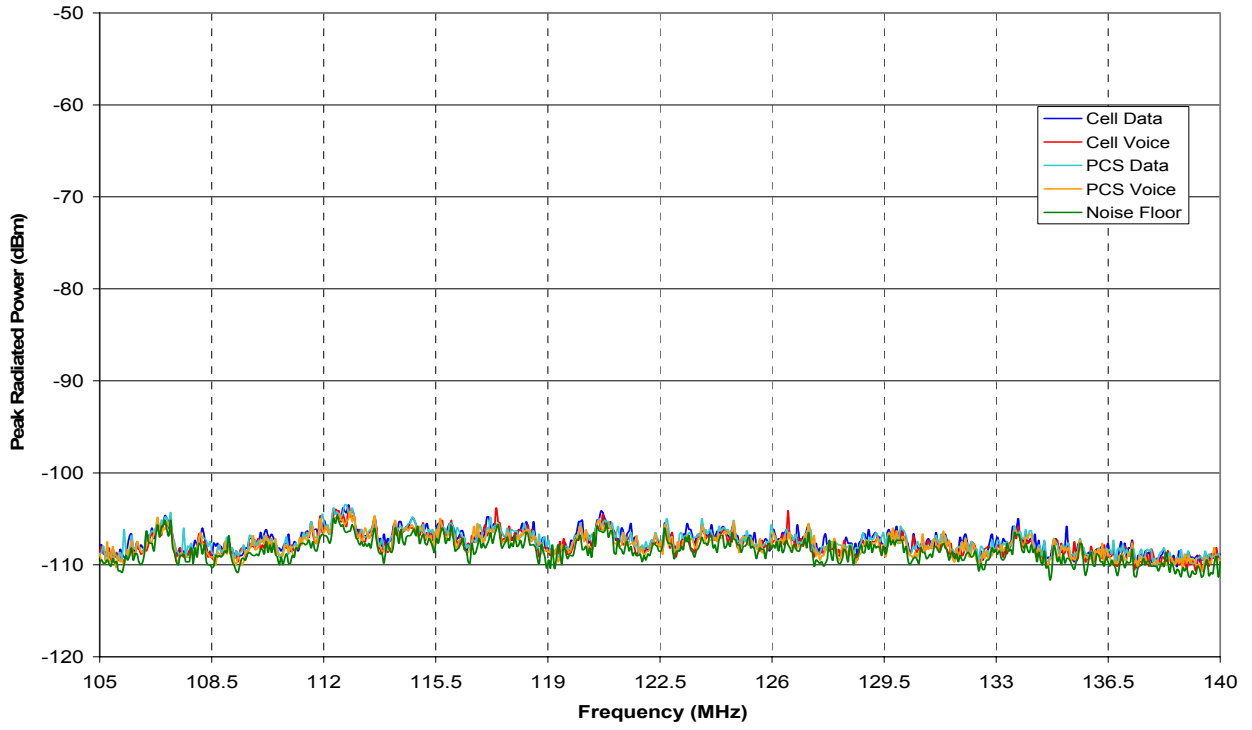


Figure A6: CDM06 four mode envelopes, Band 1.

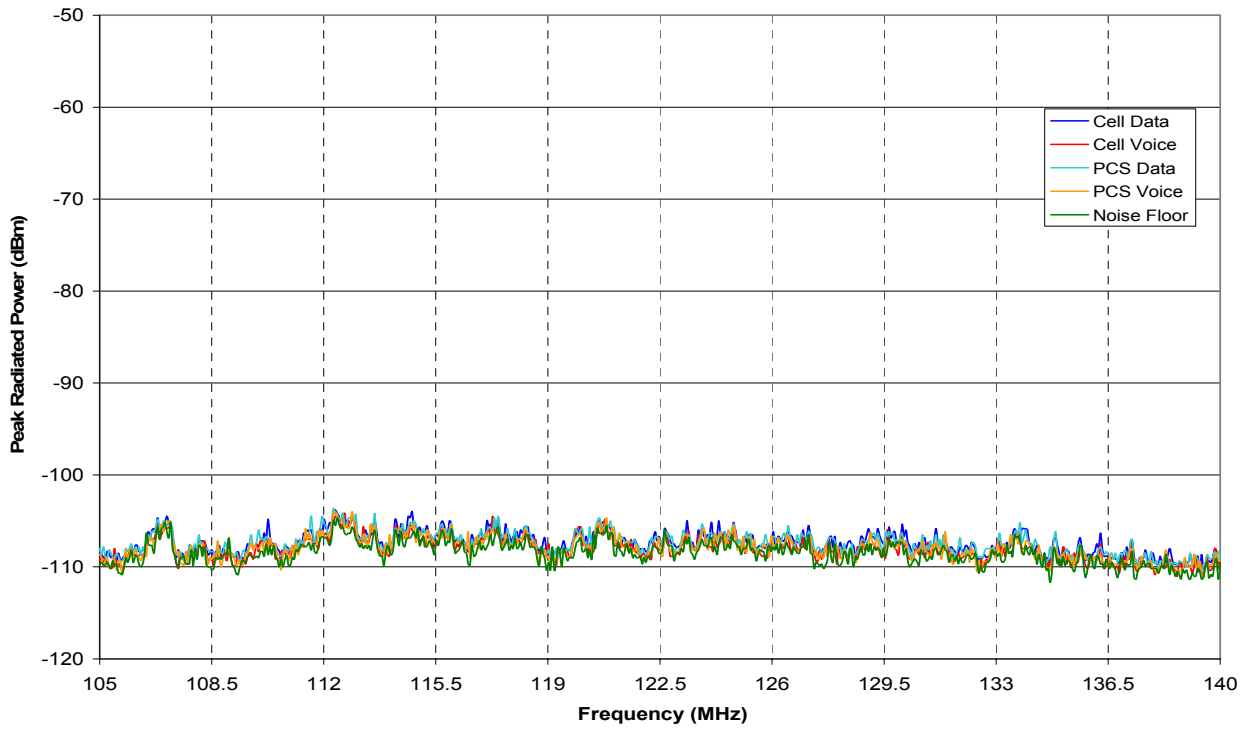


Figure A7: CDM07 four mode envelopes, Band 1.

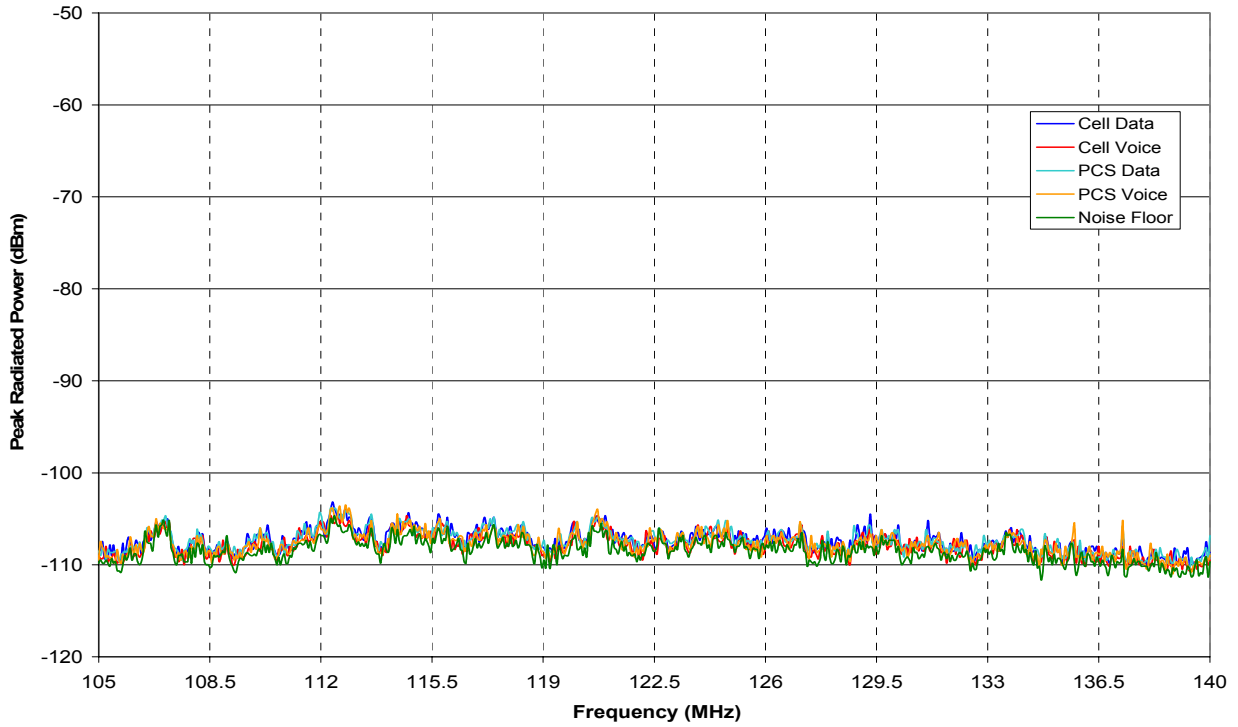


Figure A8: CDM08 four mode envelopes, Band 1.

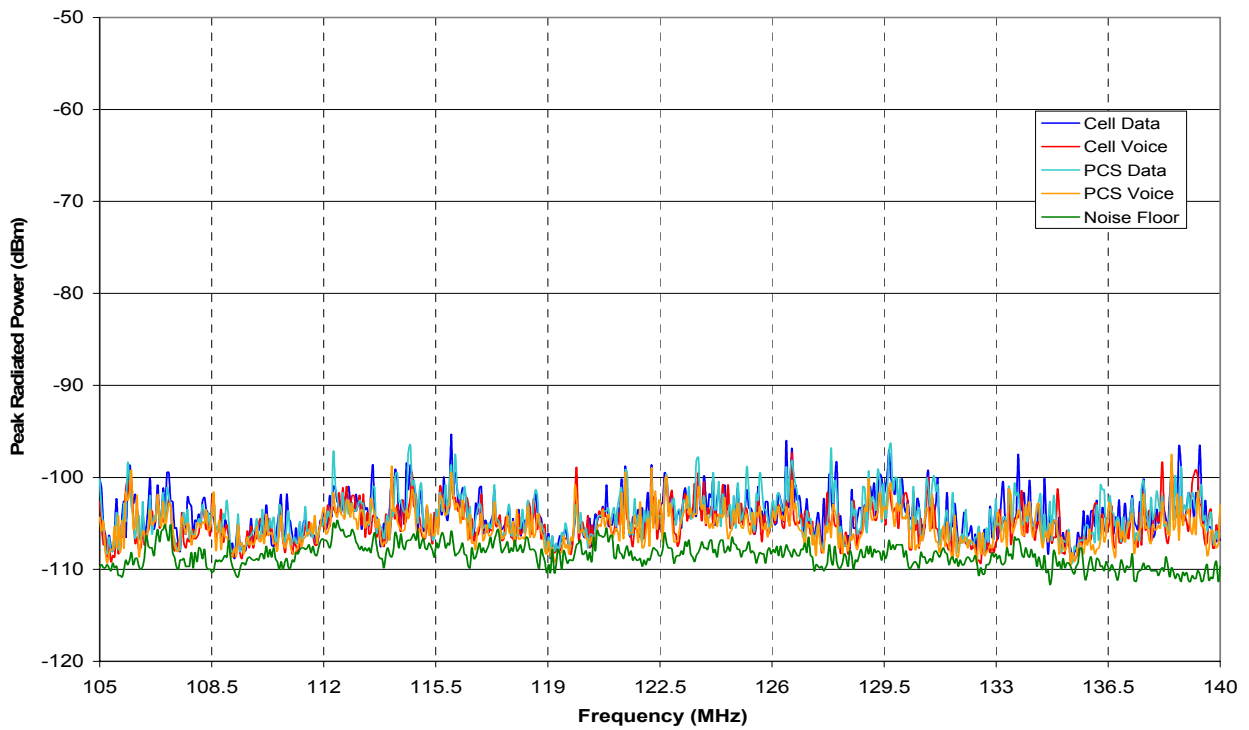


Figure A9: CDM09 four mode envelopes, Band 1.

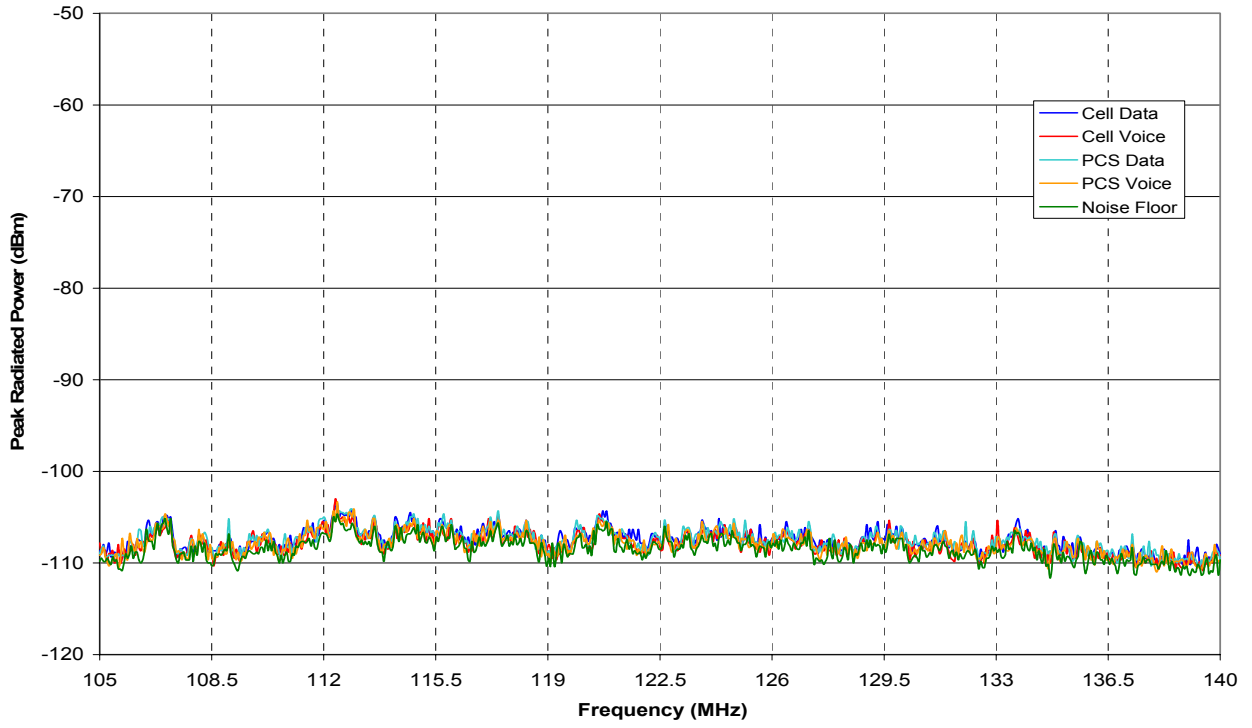


Figure A10: CDM10 four mode envelopes, Band 1.

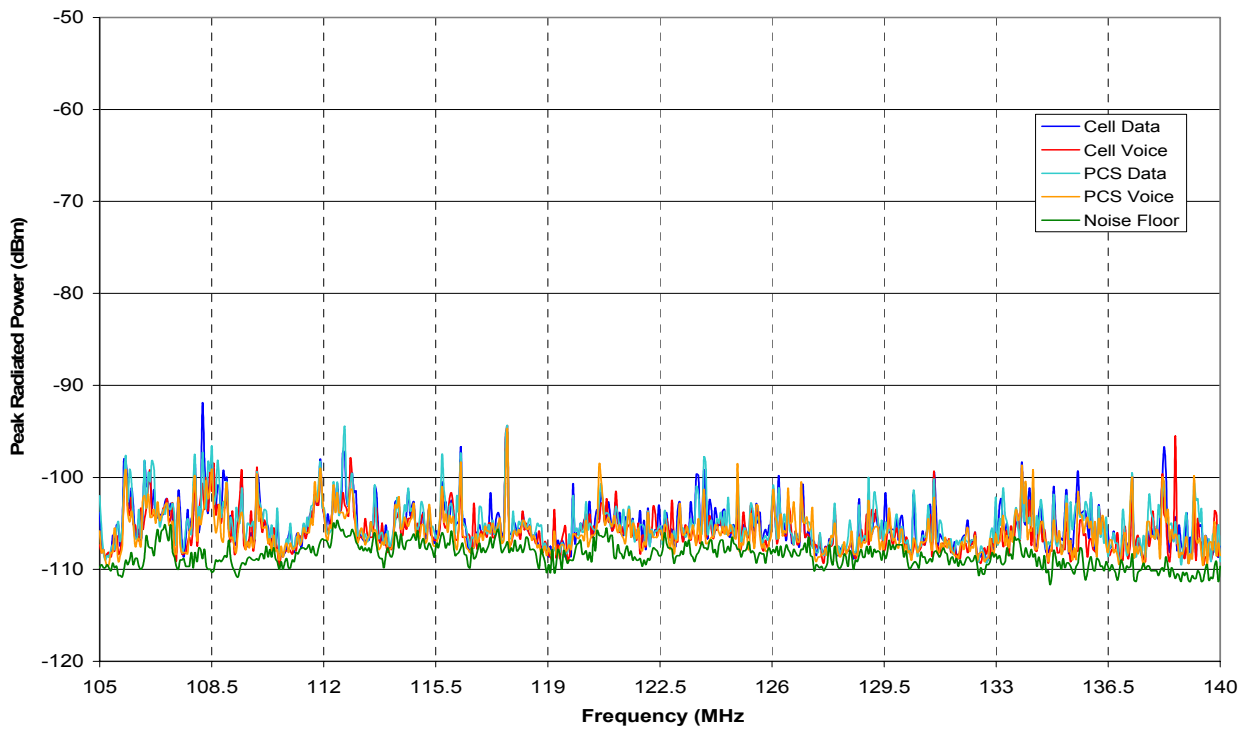


Figure A11: CDM11 four mode envelopes, Band 1.

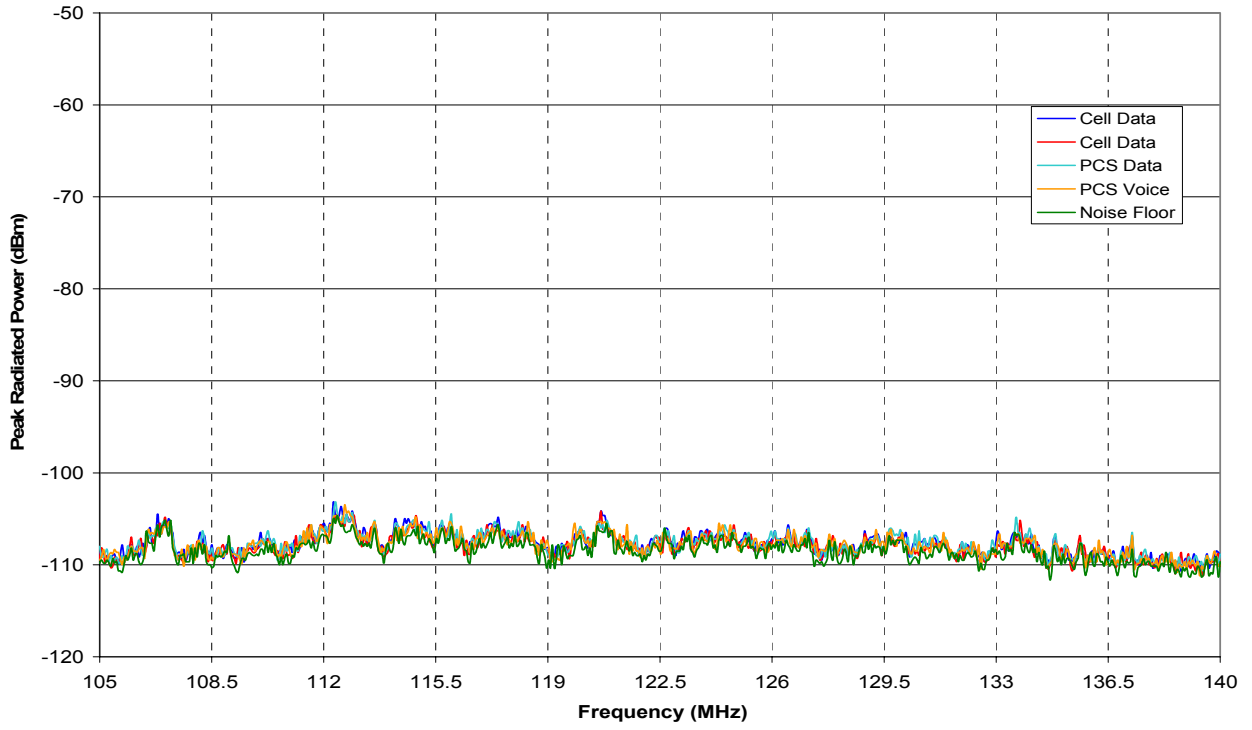


Figure A12: CDM12 four mode envelopes, Band 1.

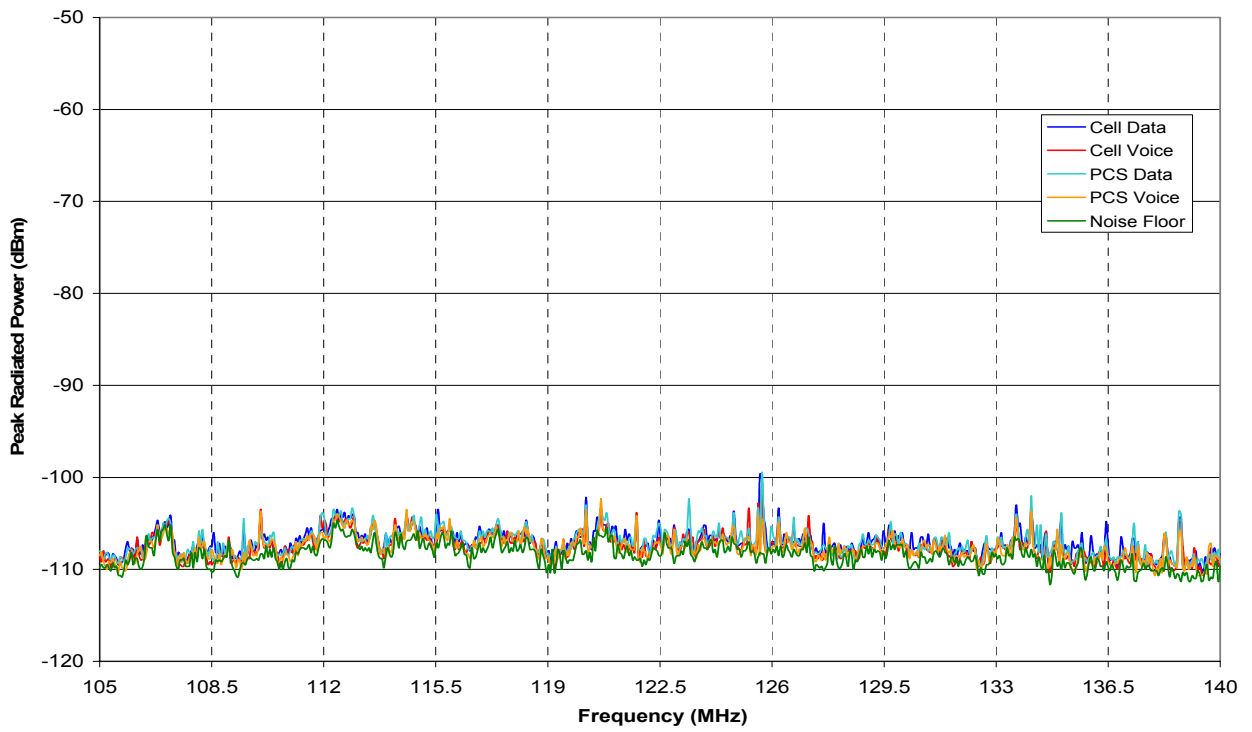


Figure A13: CDM13 four mode envelopes, Band 1.

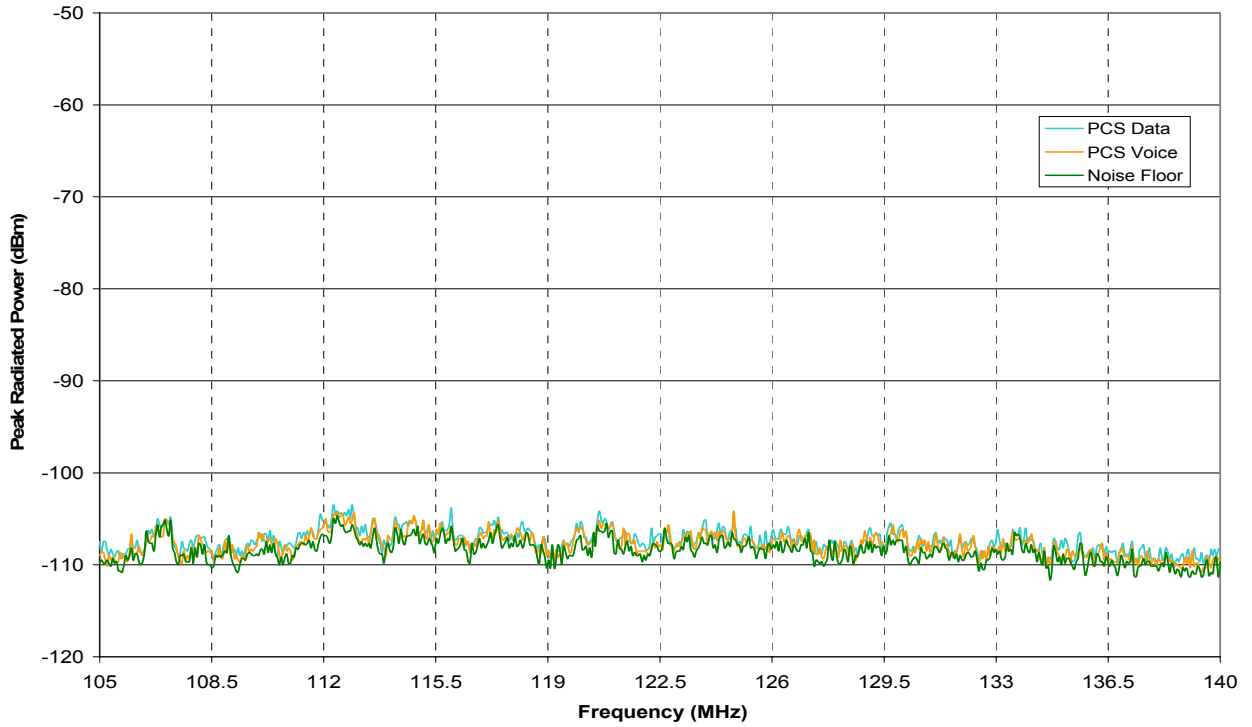


Figure A14: CDM14 two mode envelopes, Band 1.

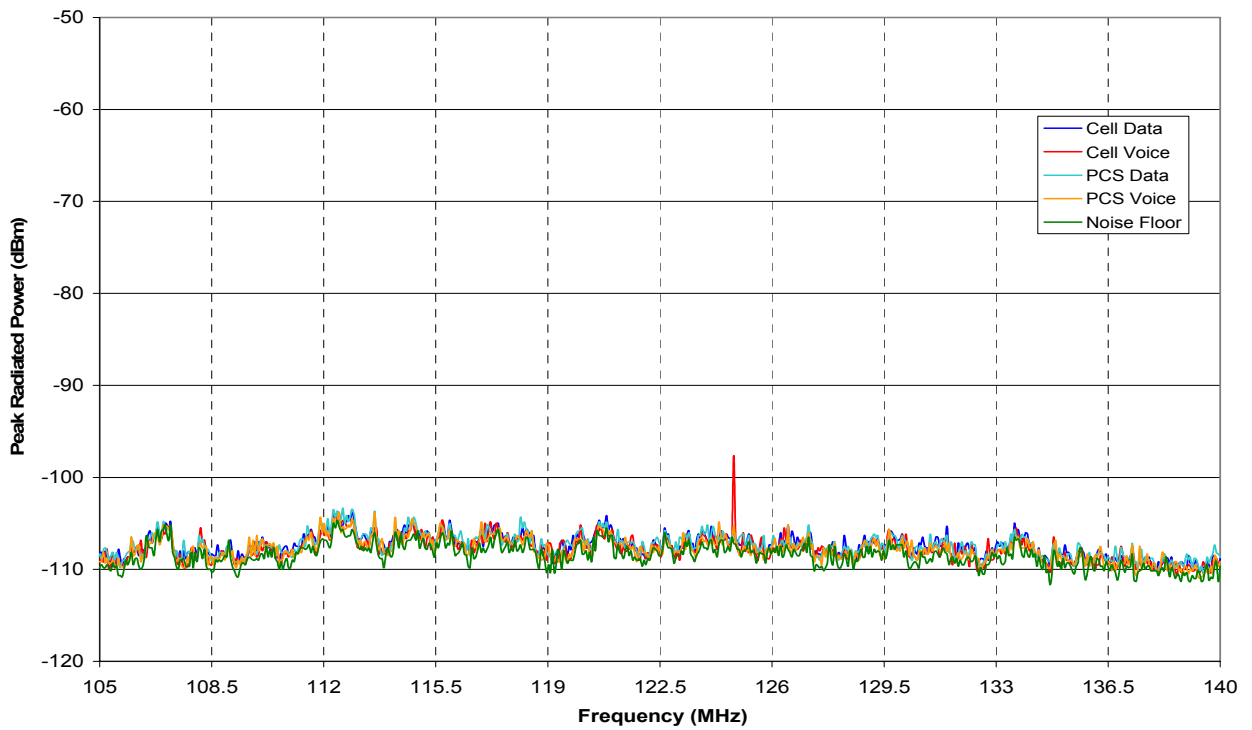


Figure A15: CDM15 four mode envelopes, Band 1.

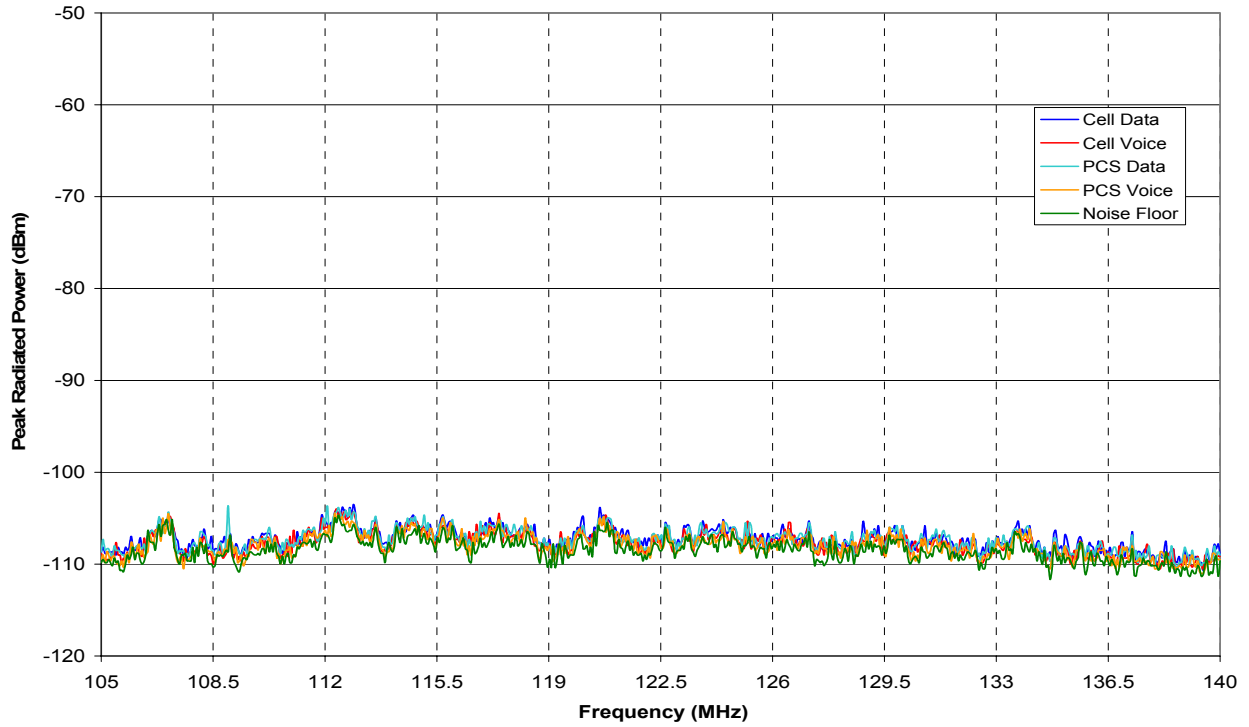


Figure A16: CDM16 four mode envelopes, Band 1.

A.2 Band 2

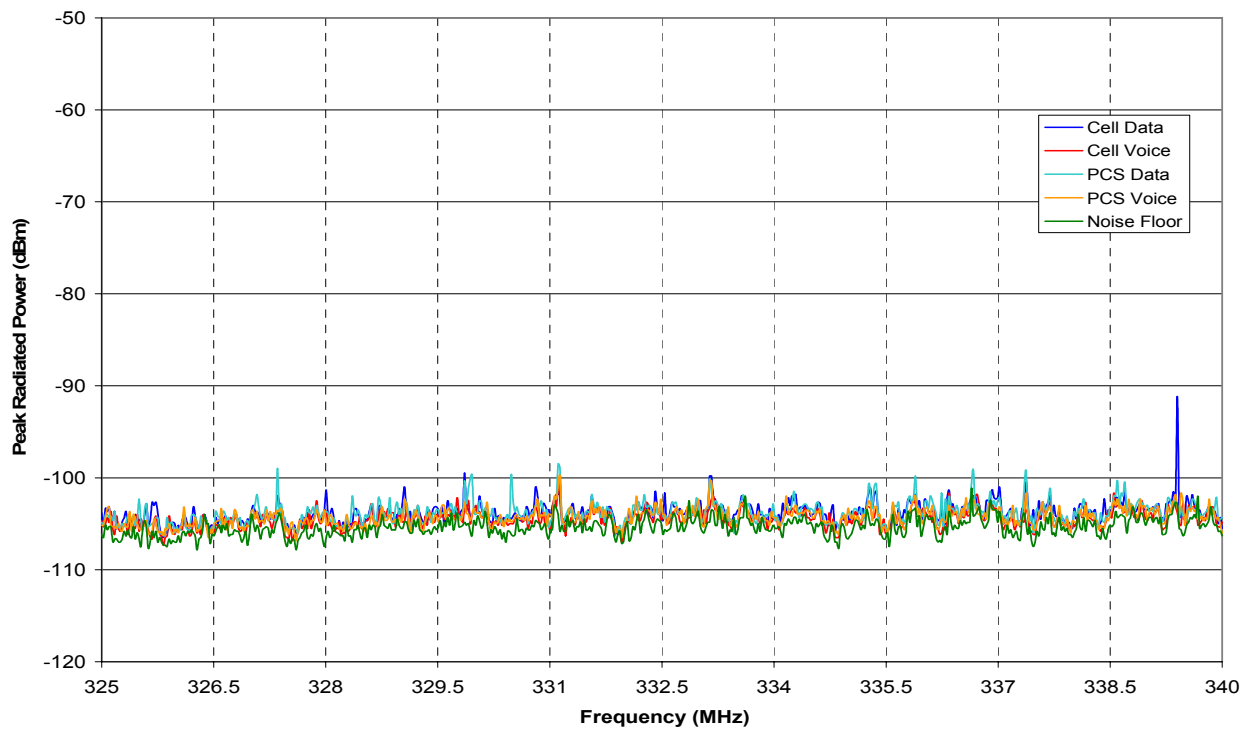


Figure A17: CDM01 four mode envelopes, Band 2.

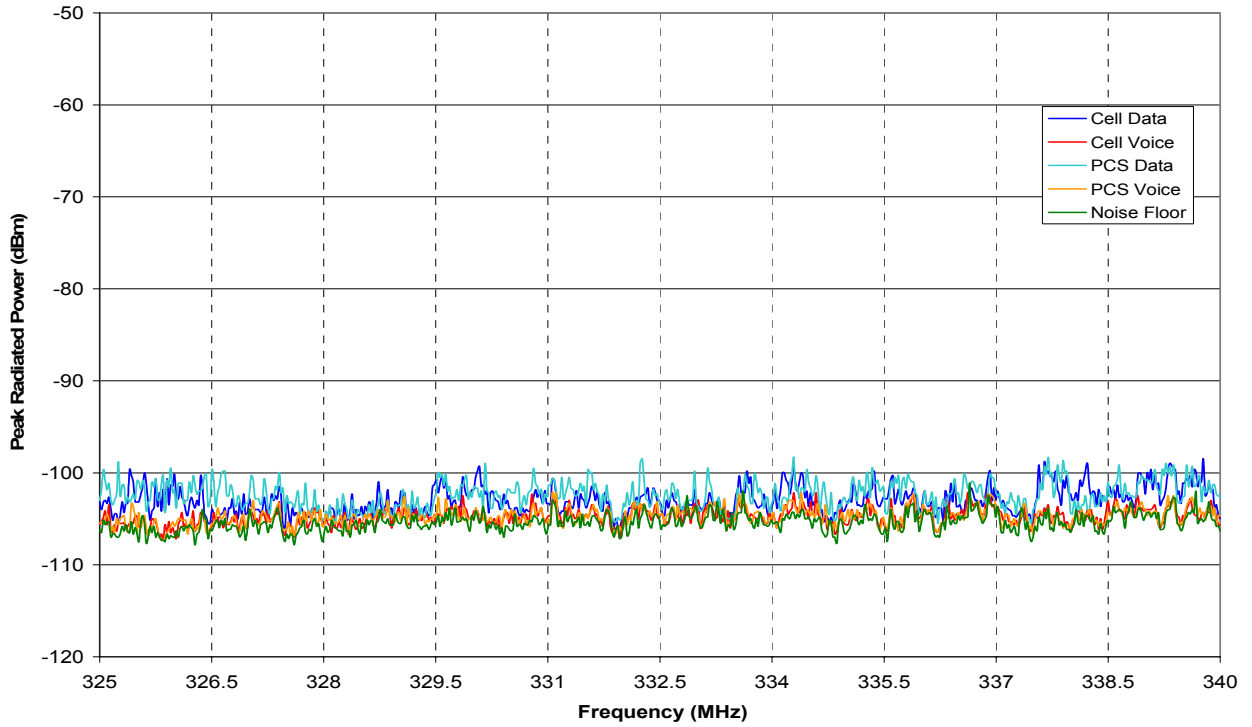


Figure A18: CDM02 four mode envelopes, Band 2.

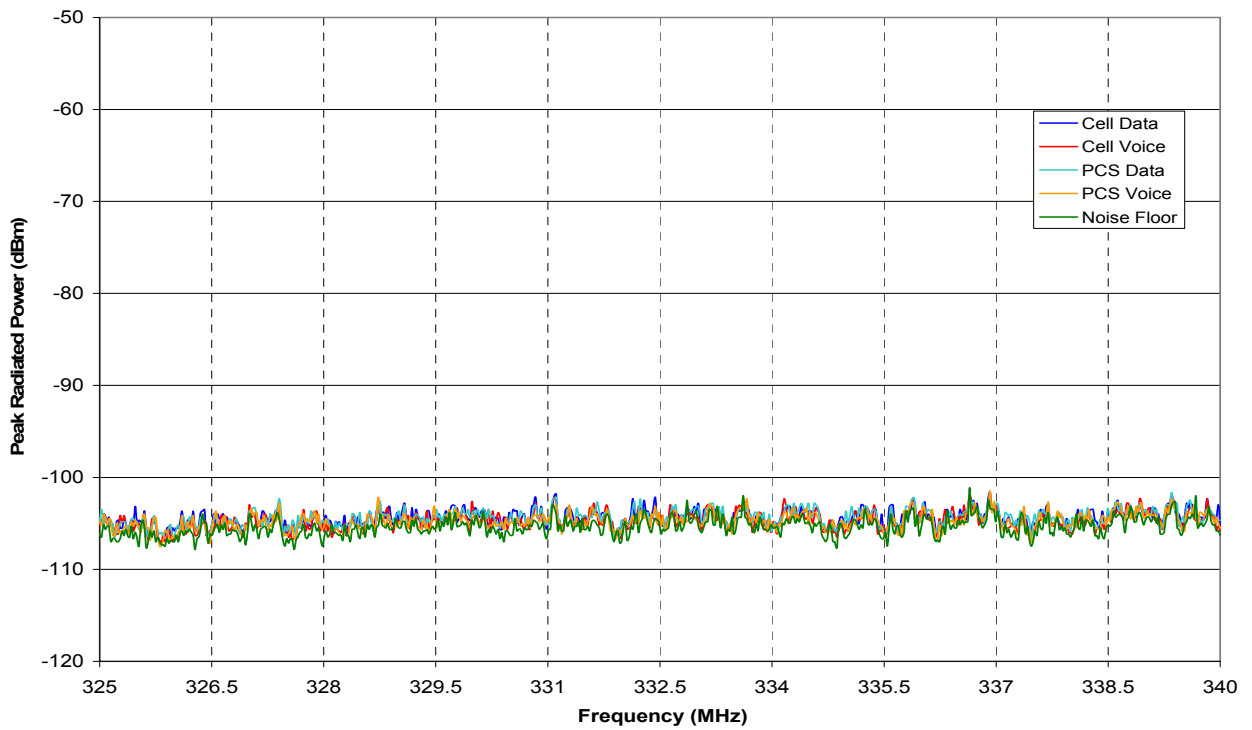


Figure A19: CDM03 four mode envelopes, Band 2.

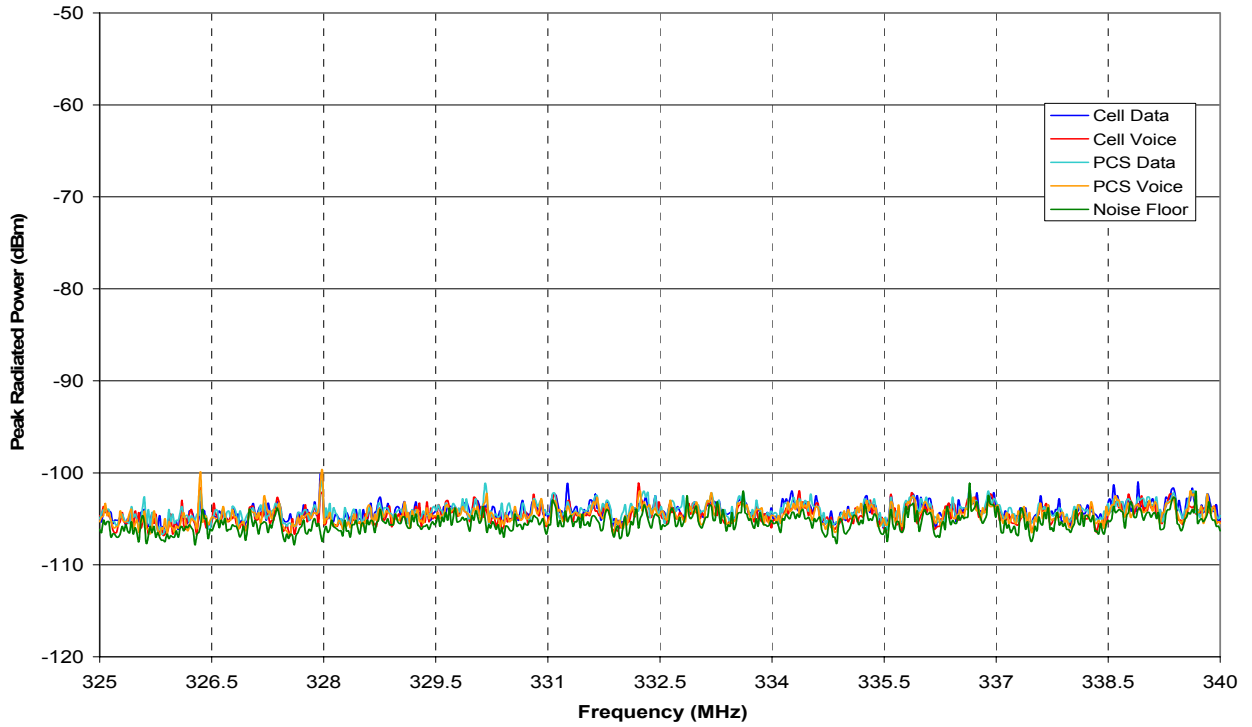


Figure A20: CDM04 four mode envelopes, Band 2.

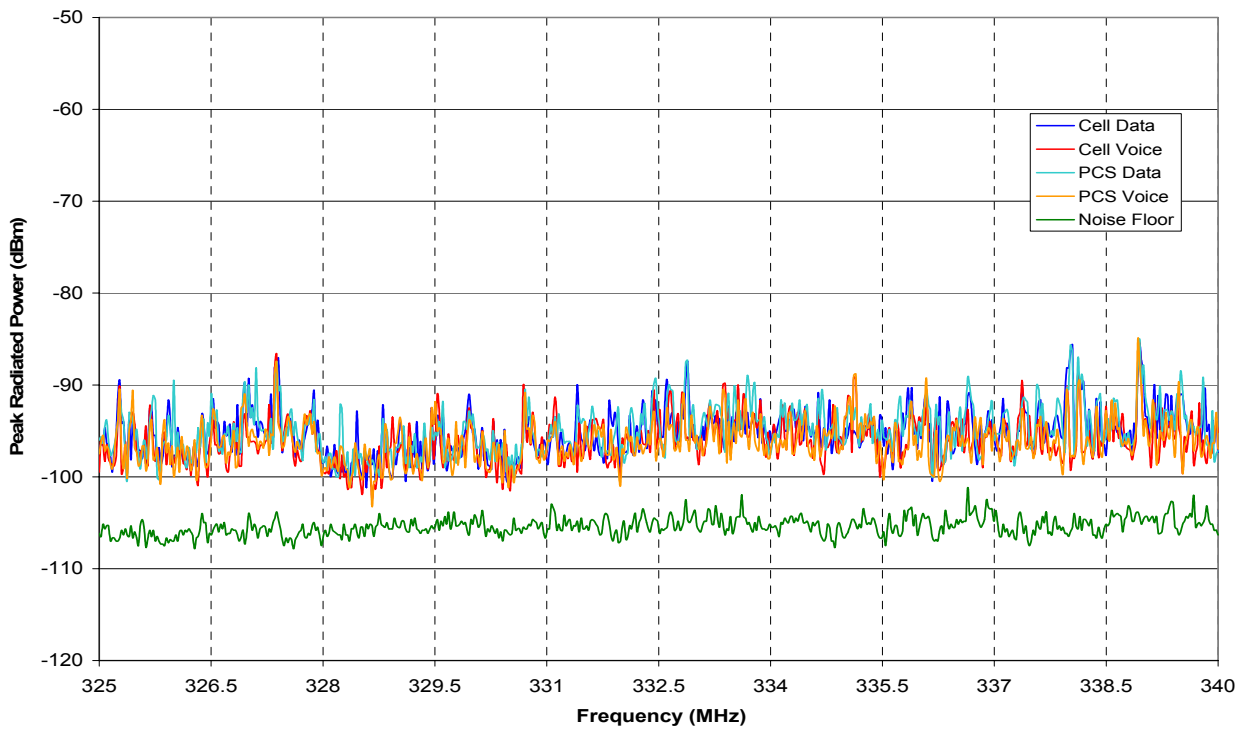


Figure A21: CDM05 four mode envelopes, Band 2.

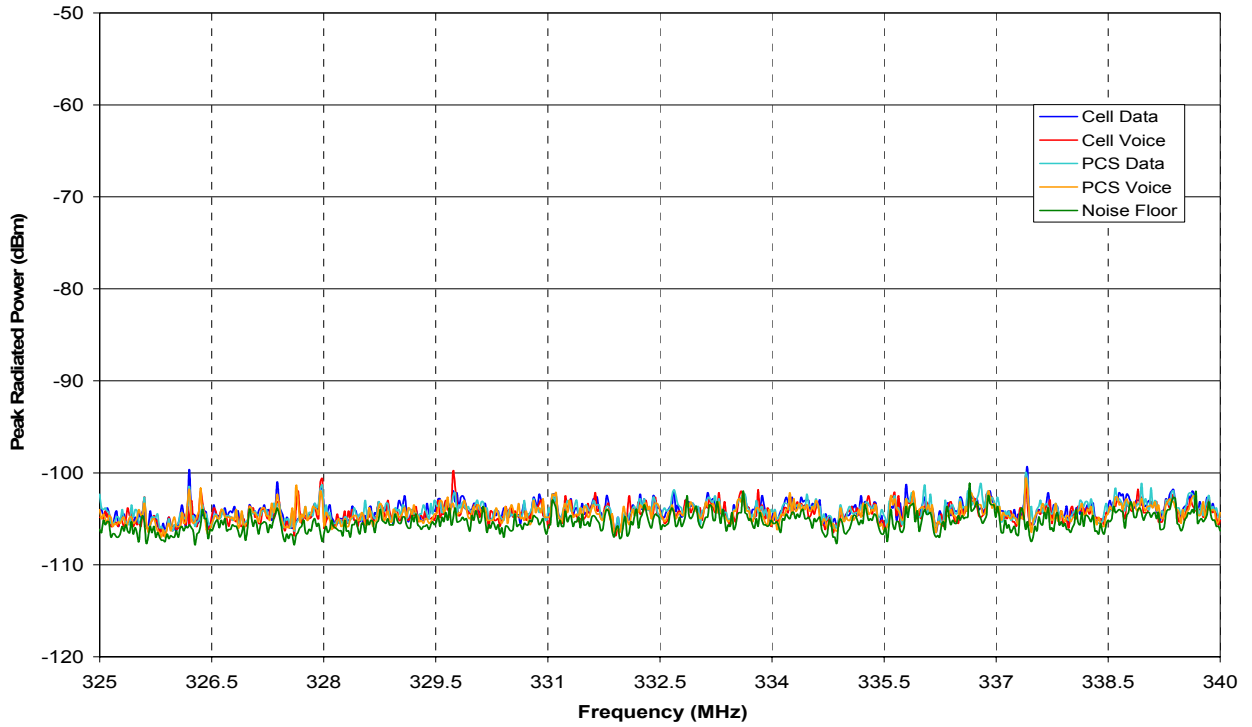


Figure A22: CDM06 four mode envelopes, Band 2.

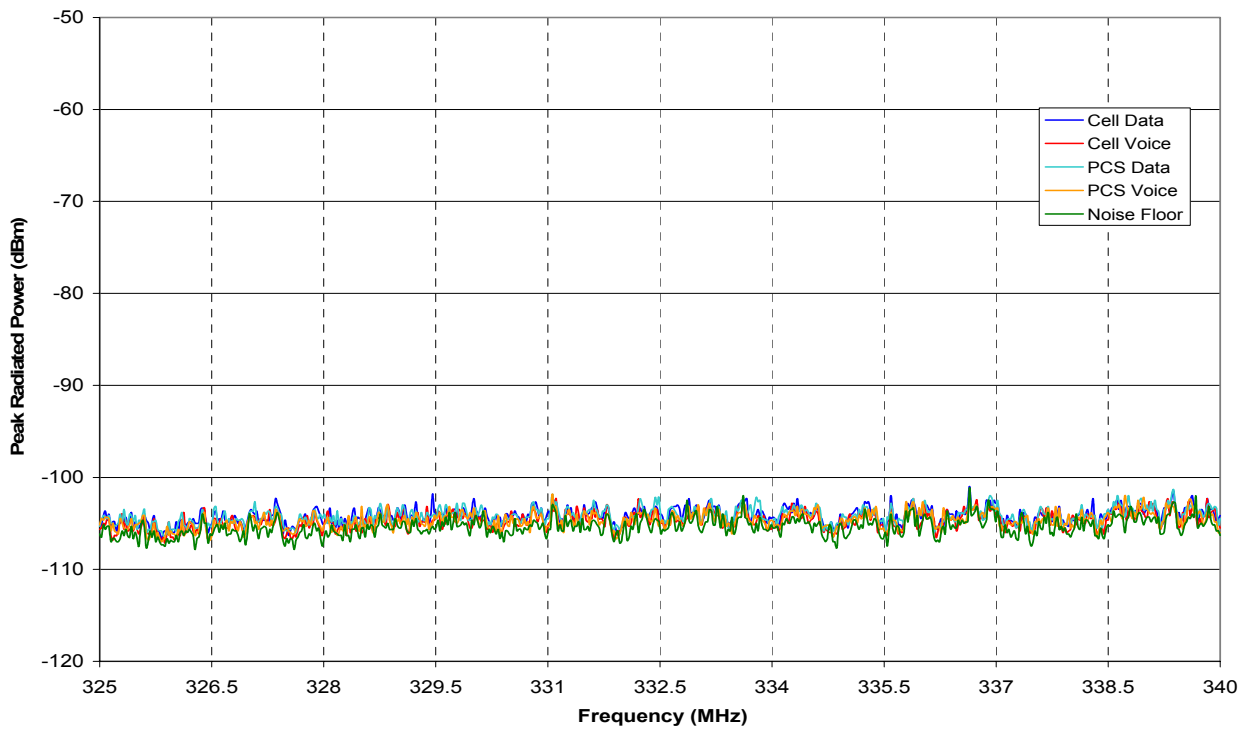


Figure A23: CDM07 four mode envelopes, Band 2.

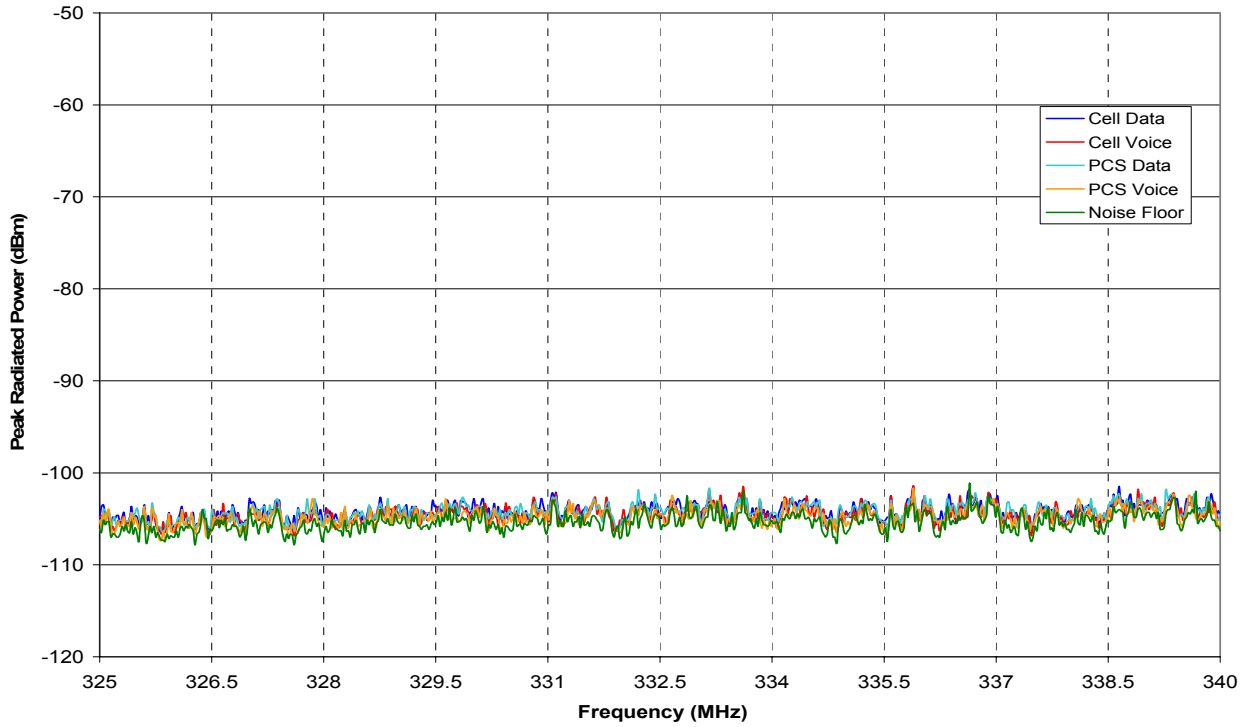
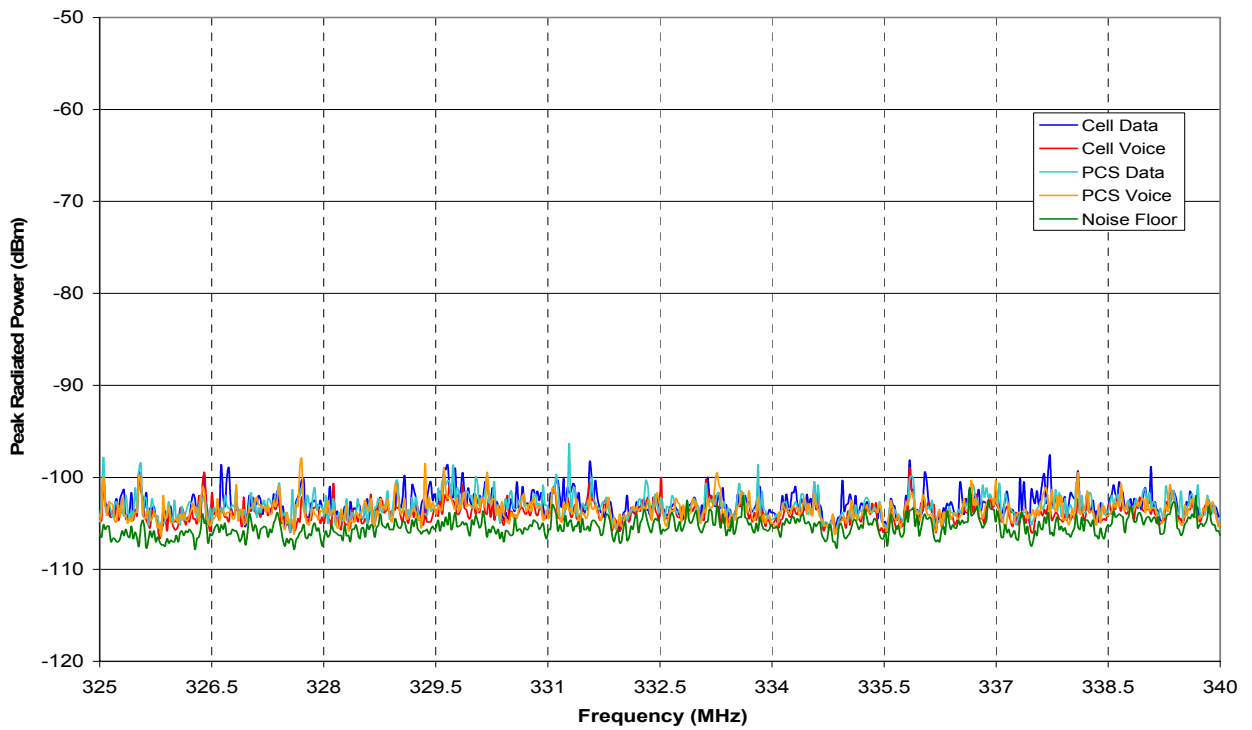


Figure A24: CDM08 four mode envelopes, Band 2.



FigureA25: CDM09 four mode envelopes, Band 2.

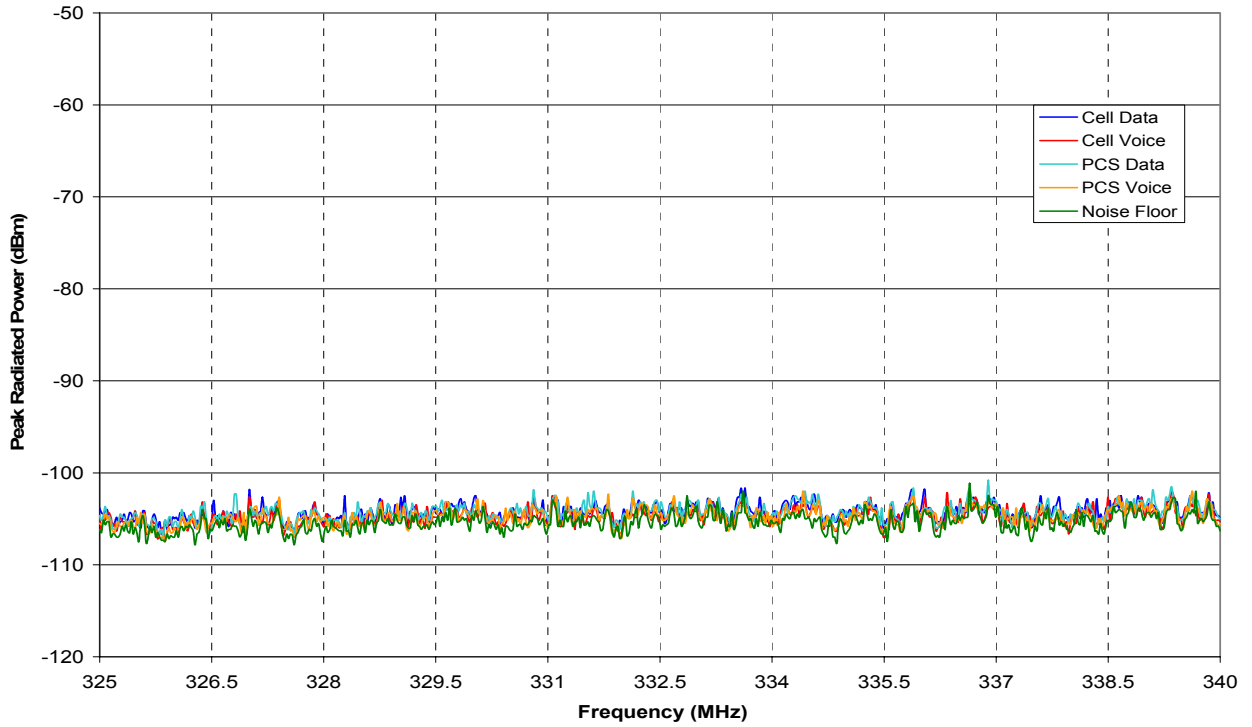


Figure A26: CDM10 four mode envelopes, Band 2.

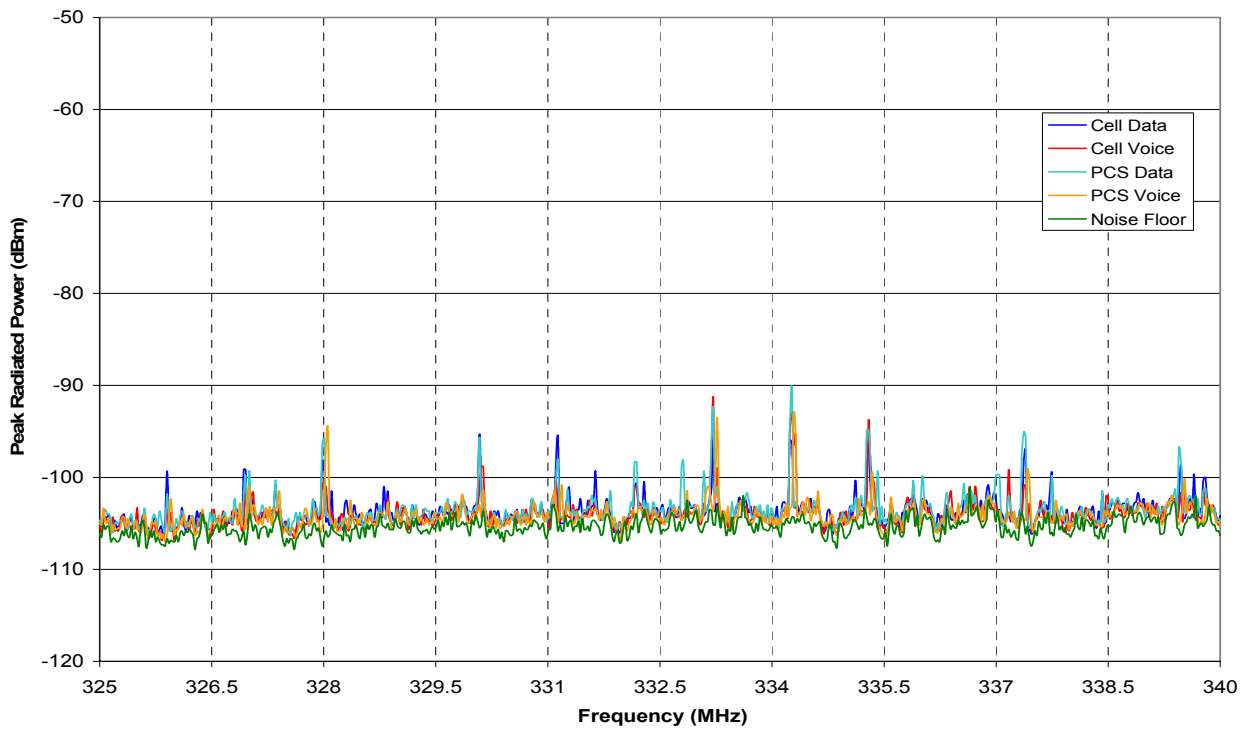


Figure A27: CDM11 four mode envelopes, Band 2.

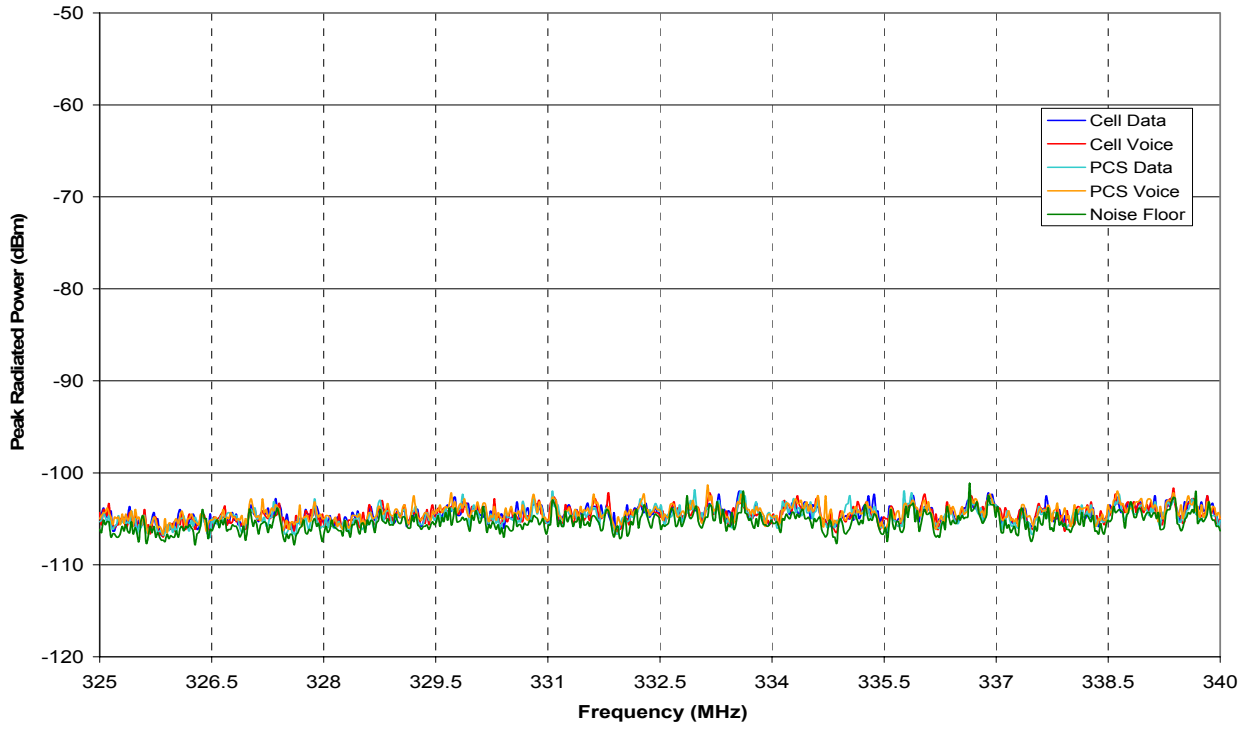


Figure A28: CDM12 four mode envelopes, Band 2.

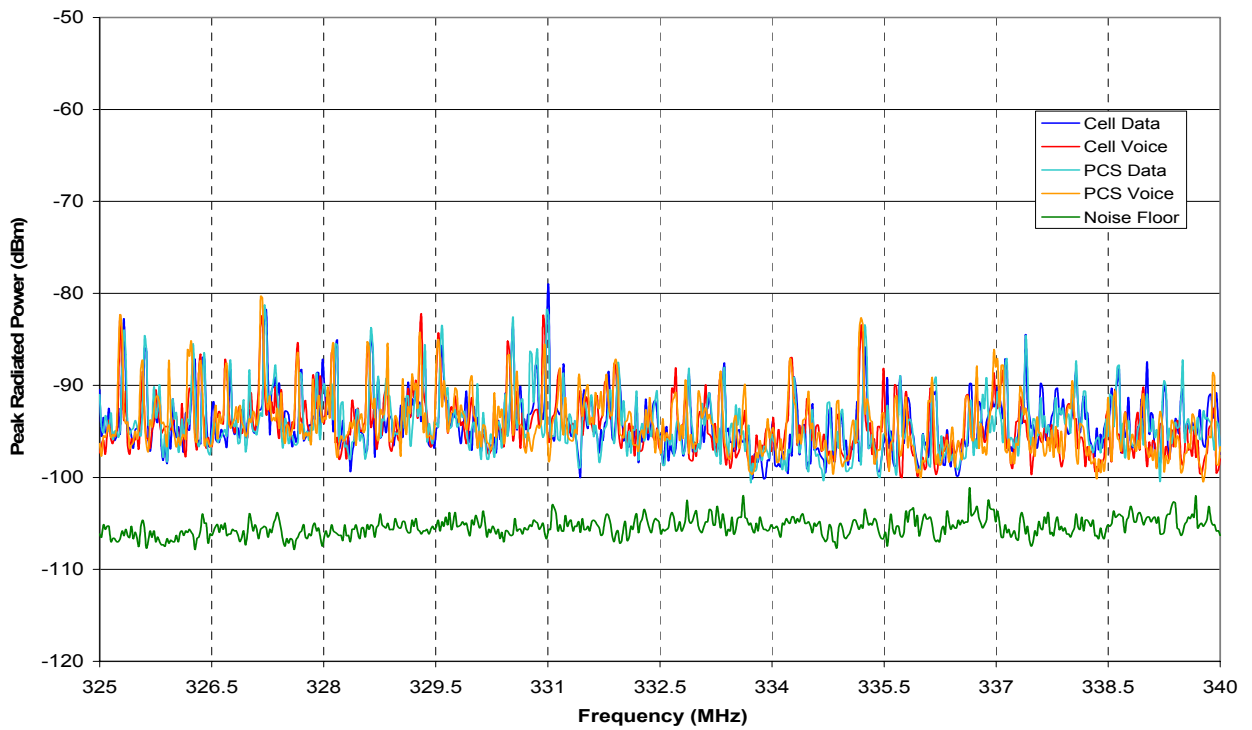


Figure A29: CDM13 four mode envelopes, Band 2.

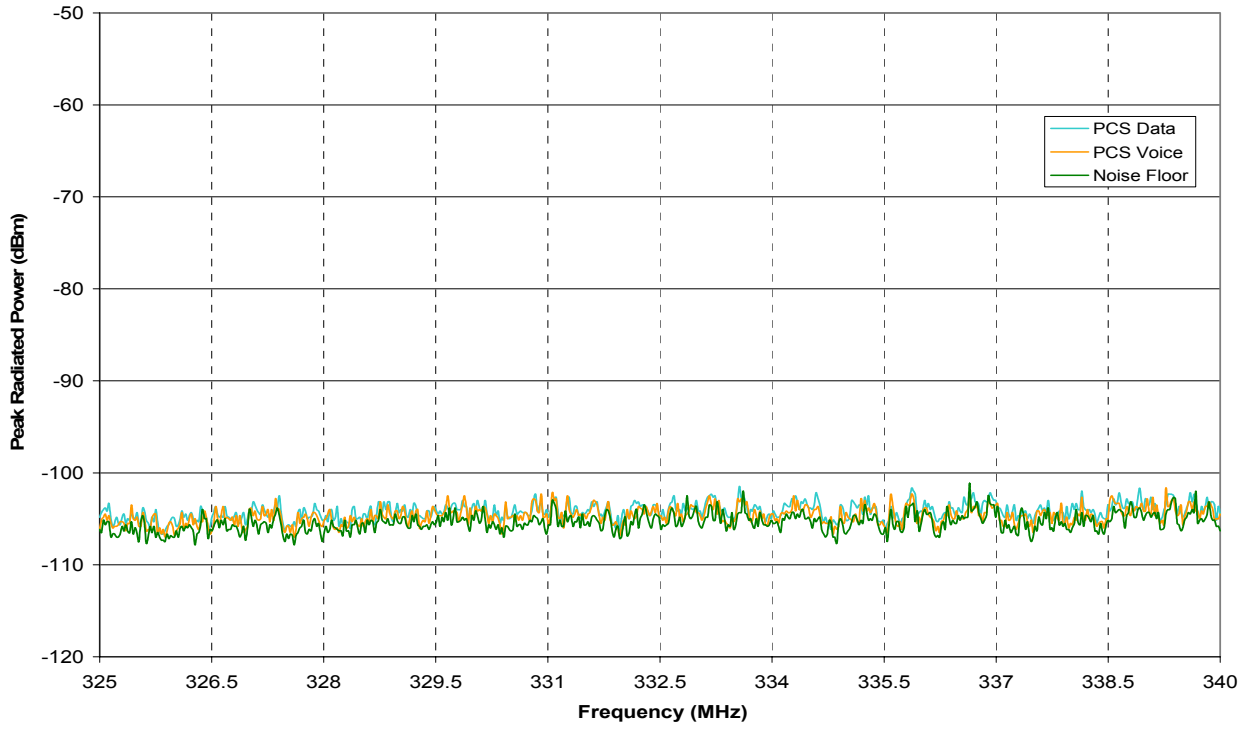


Figure A30: CDM14 two mode envelopes, Band 2.

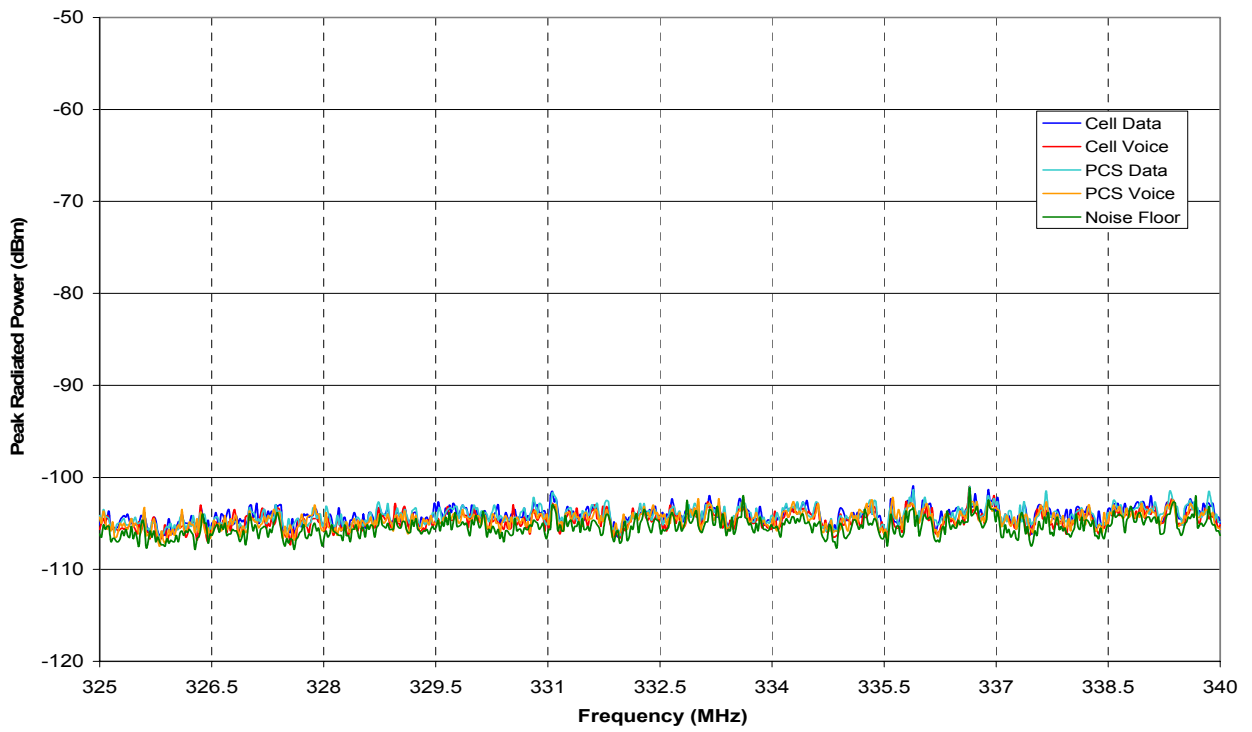


Figure A31: CDM15 four mode envelopes, Band 2.

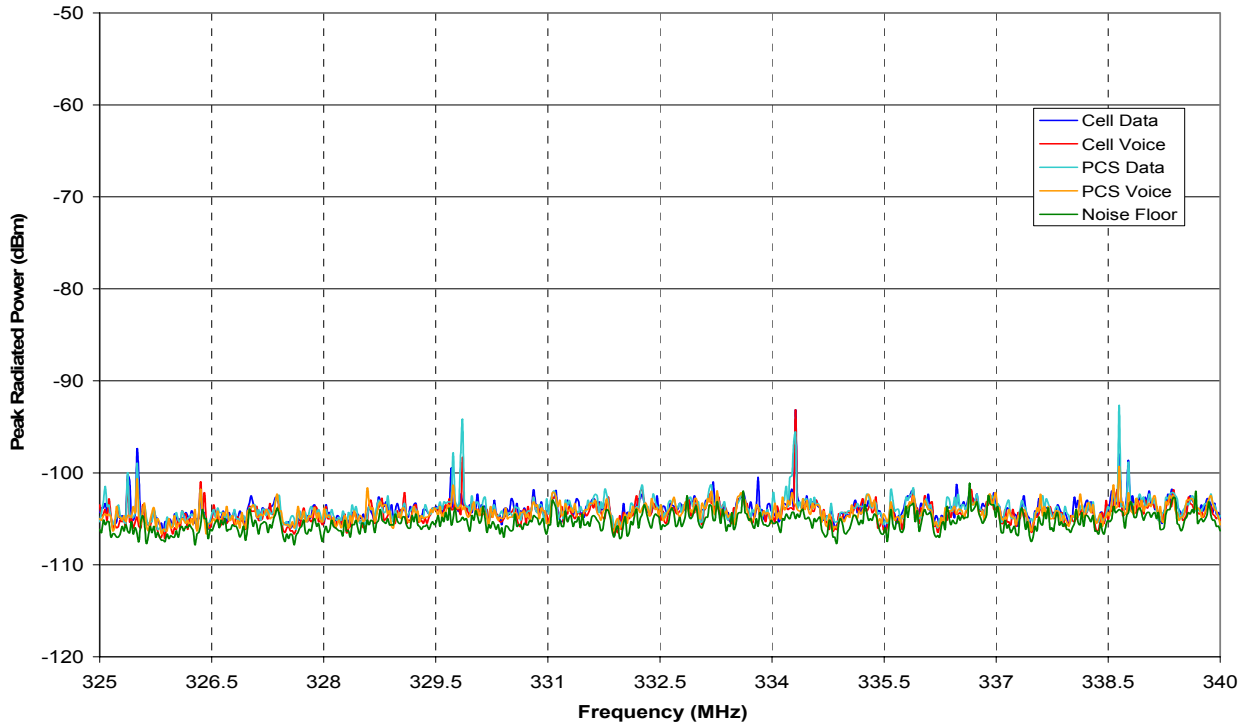


Figure A32: CDM16 four mode envelopes, Band 2.

A.3 Band 3

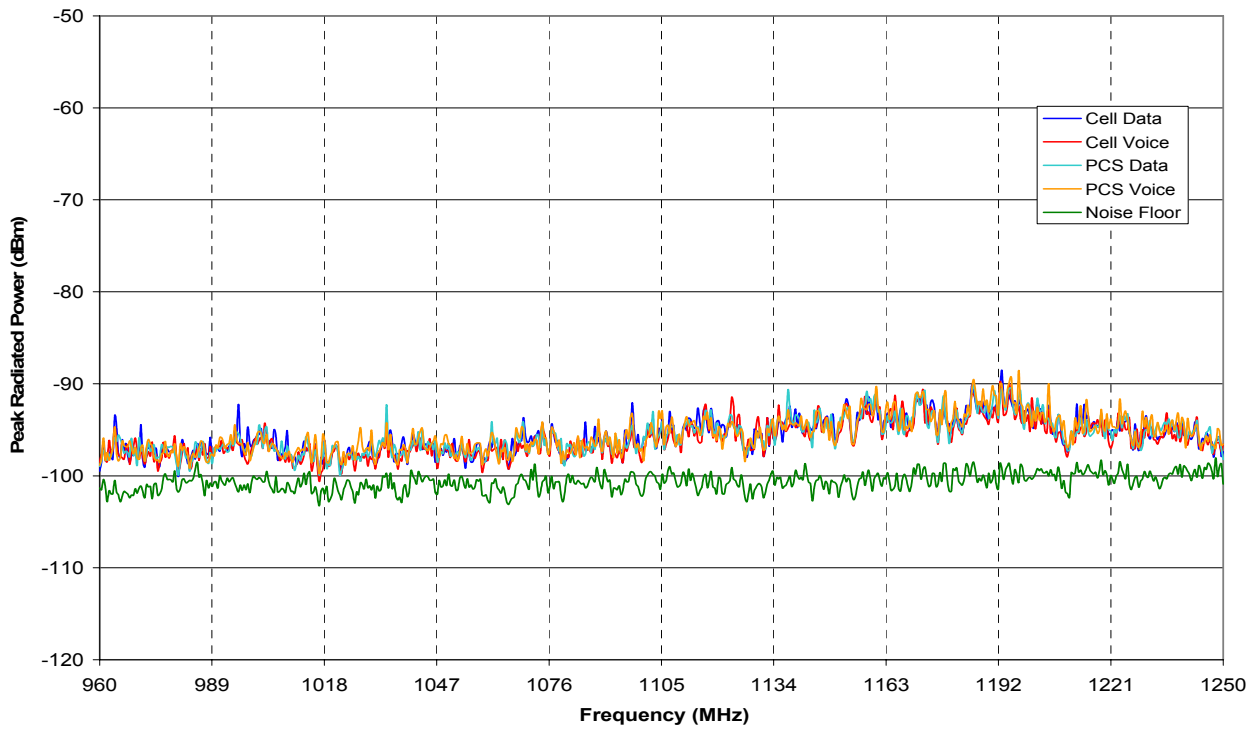


Figure A33: CDM01 four mode envelopes, Band 3.

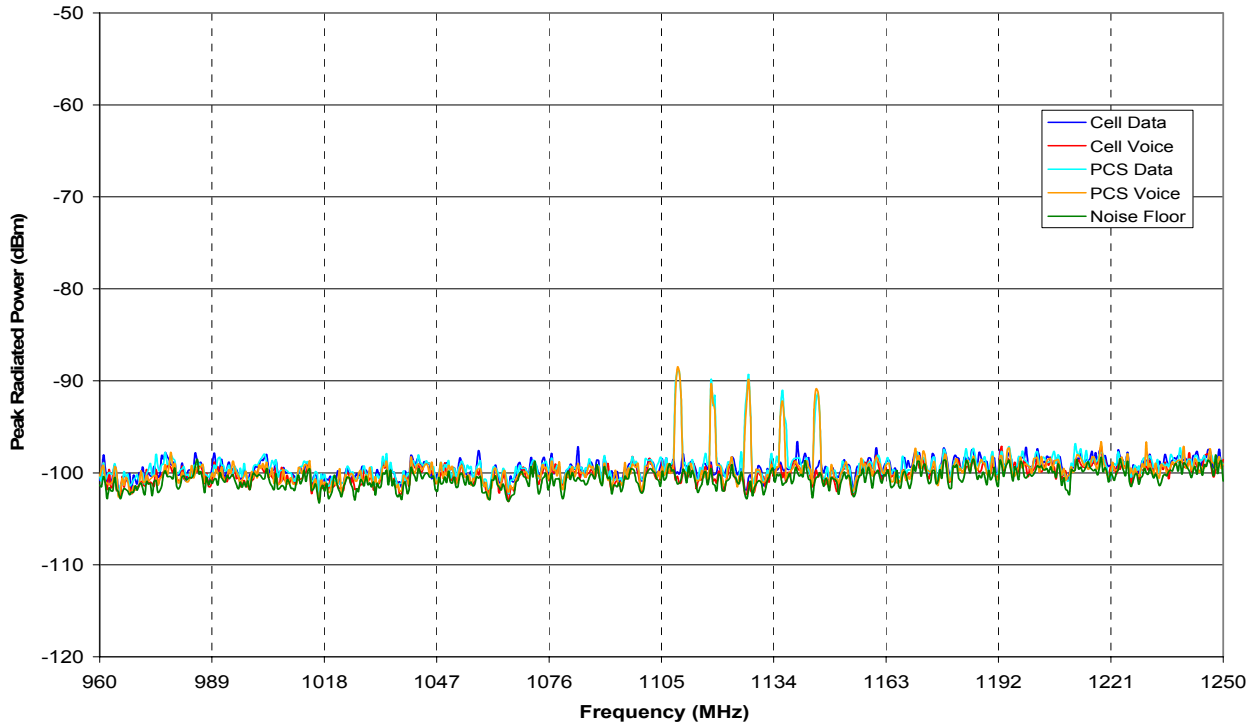


Figure A34: CDM02 four mode envelopes, Band 3.

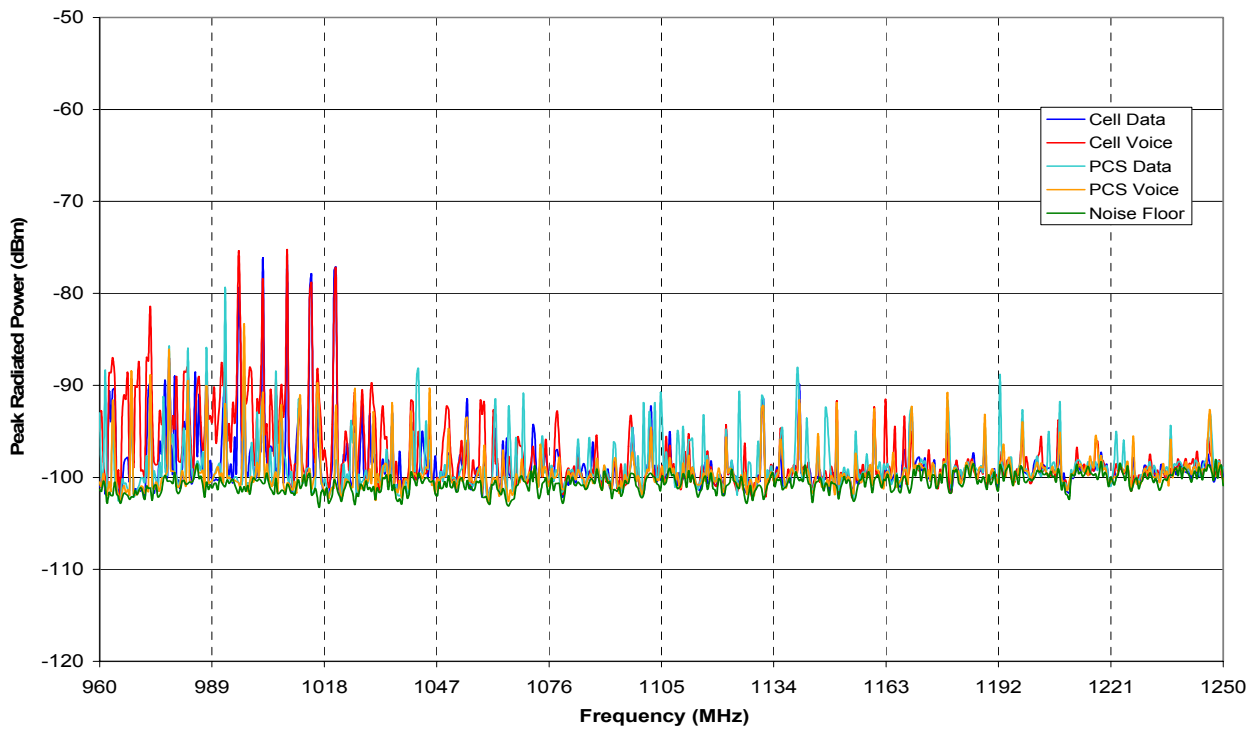


Figure A35: CDM03 four mode envelopes, Band 3.

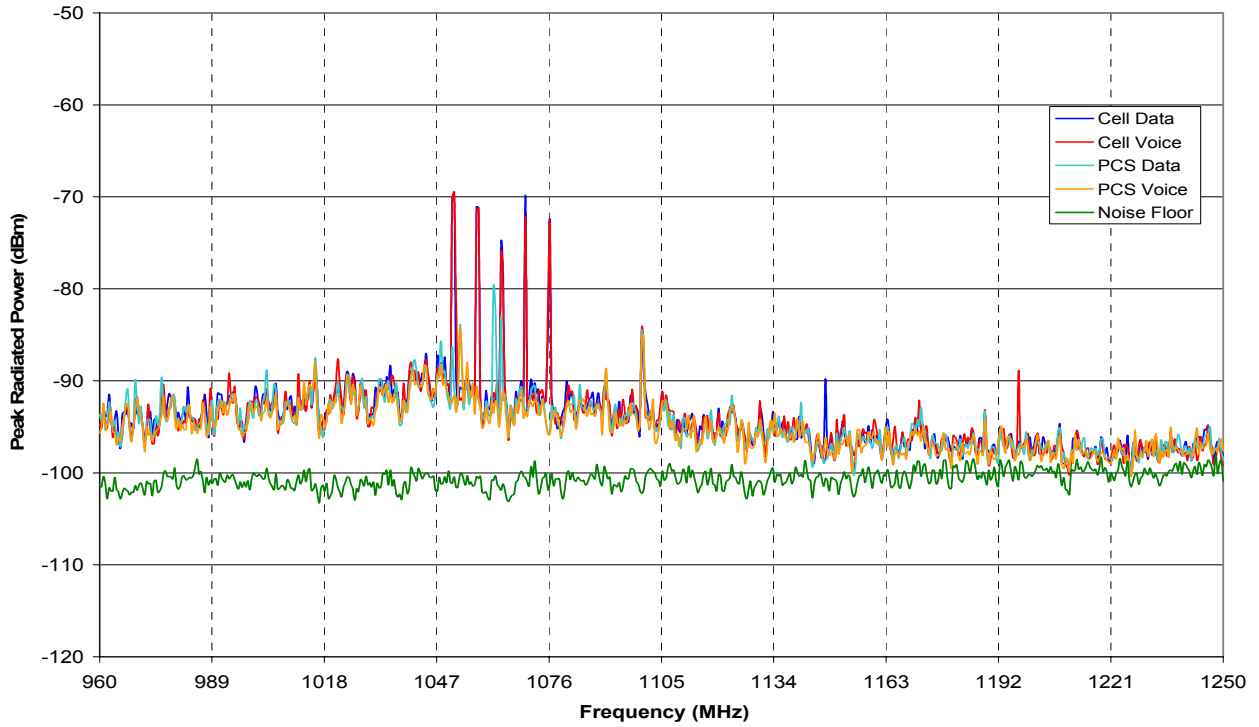


Figure A36: CDM04 four mode envelopes, Band 3.

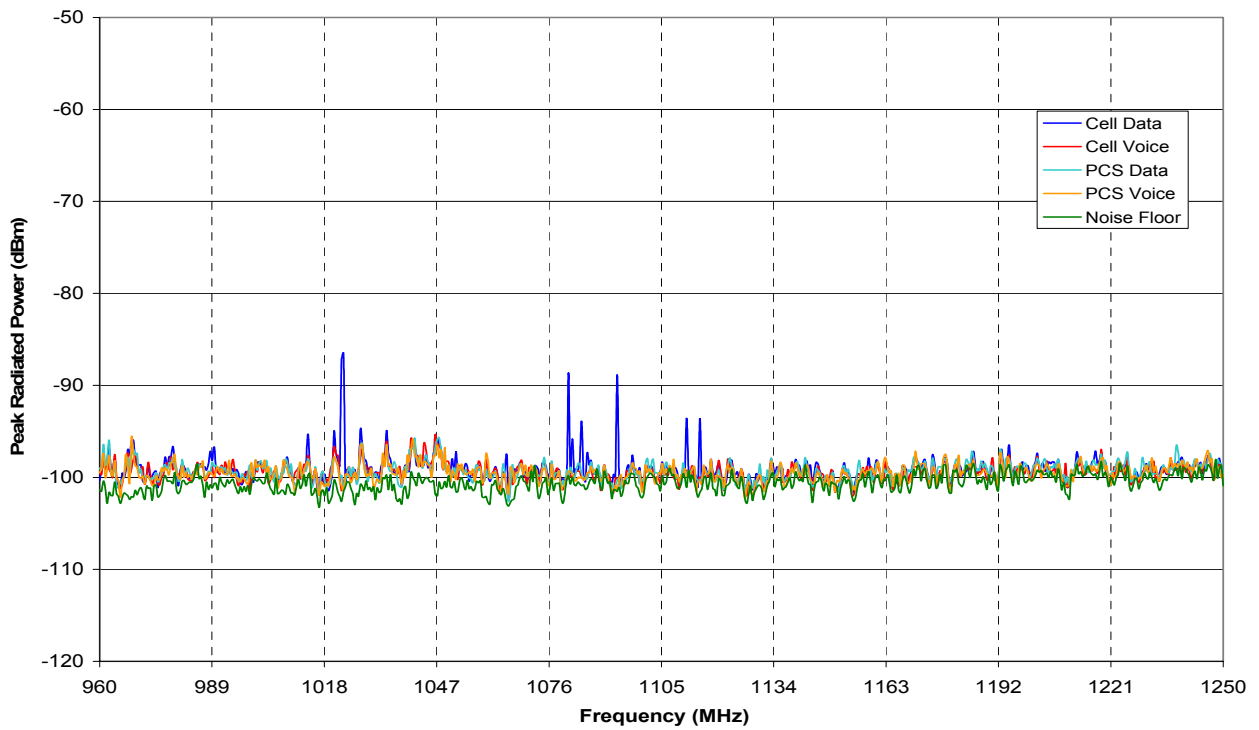


Figure A37: CDM05 four mode envelopes, Band 3.

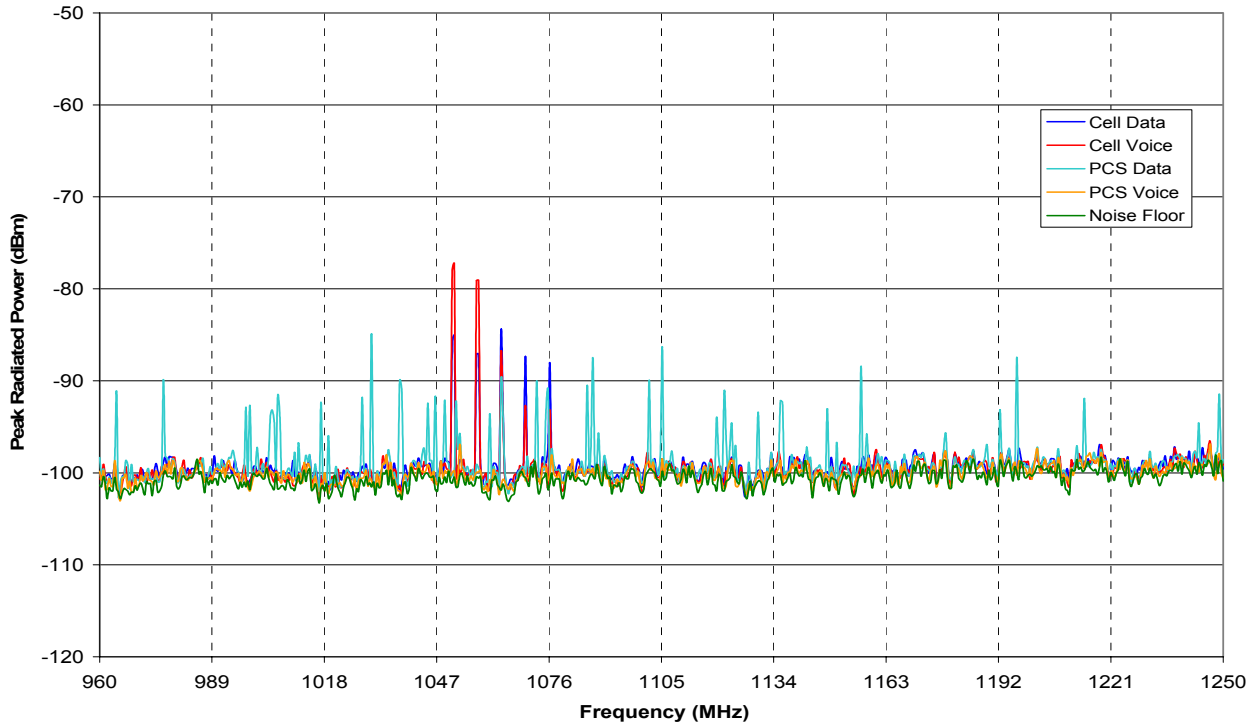


Figure A38: CDM06 four mode envelopes, Band 3.

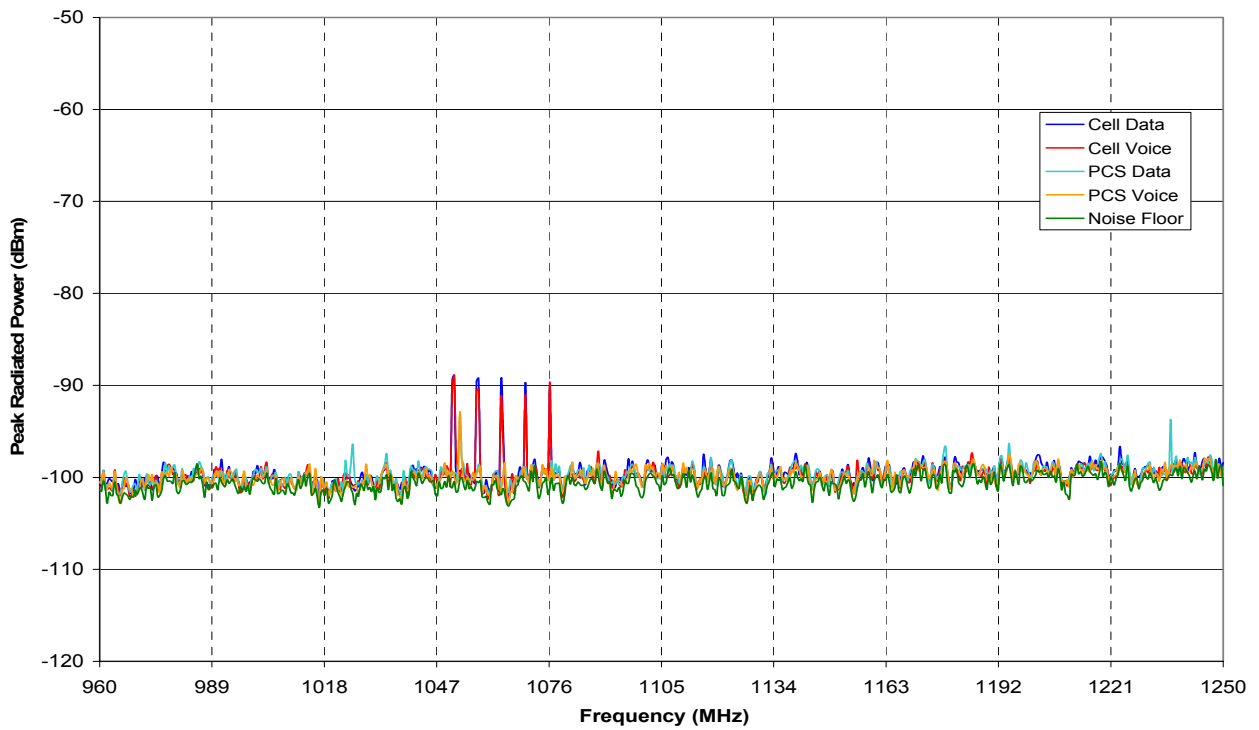


Figure A39: CDM07 four mode envelopes, Band 3.

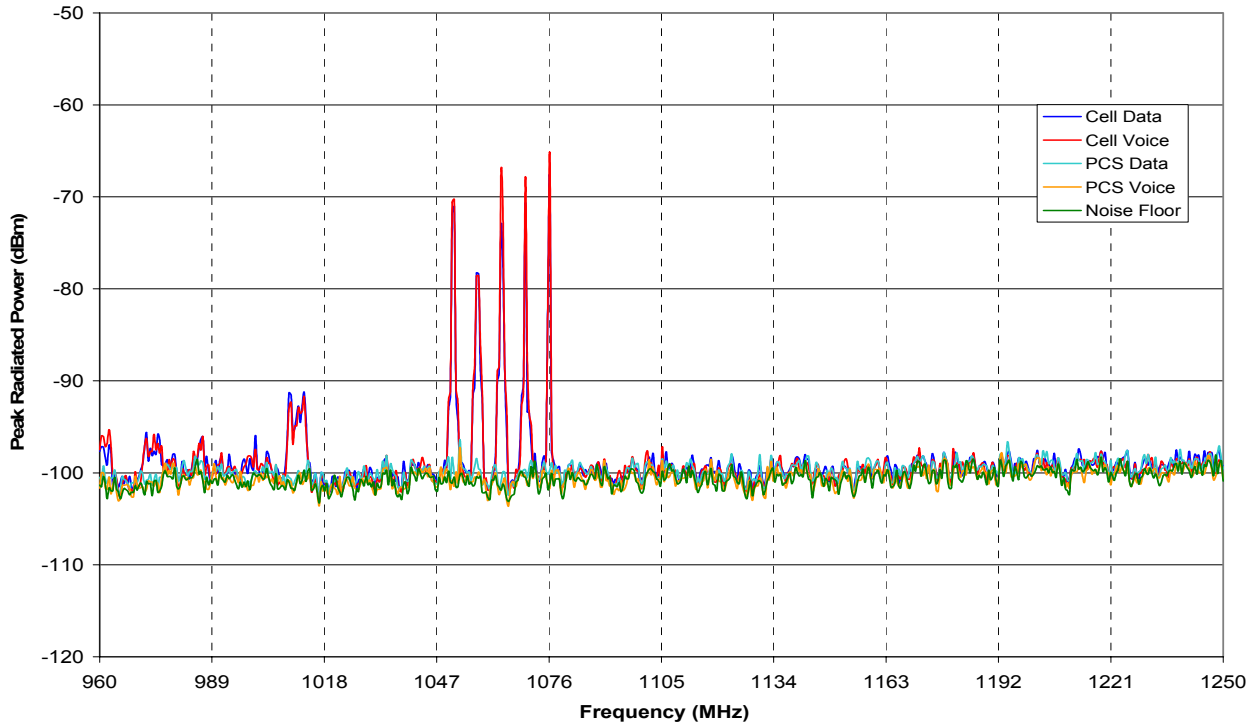


Figure A40: CDM08 four mode envelopes, Band 3.

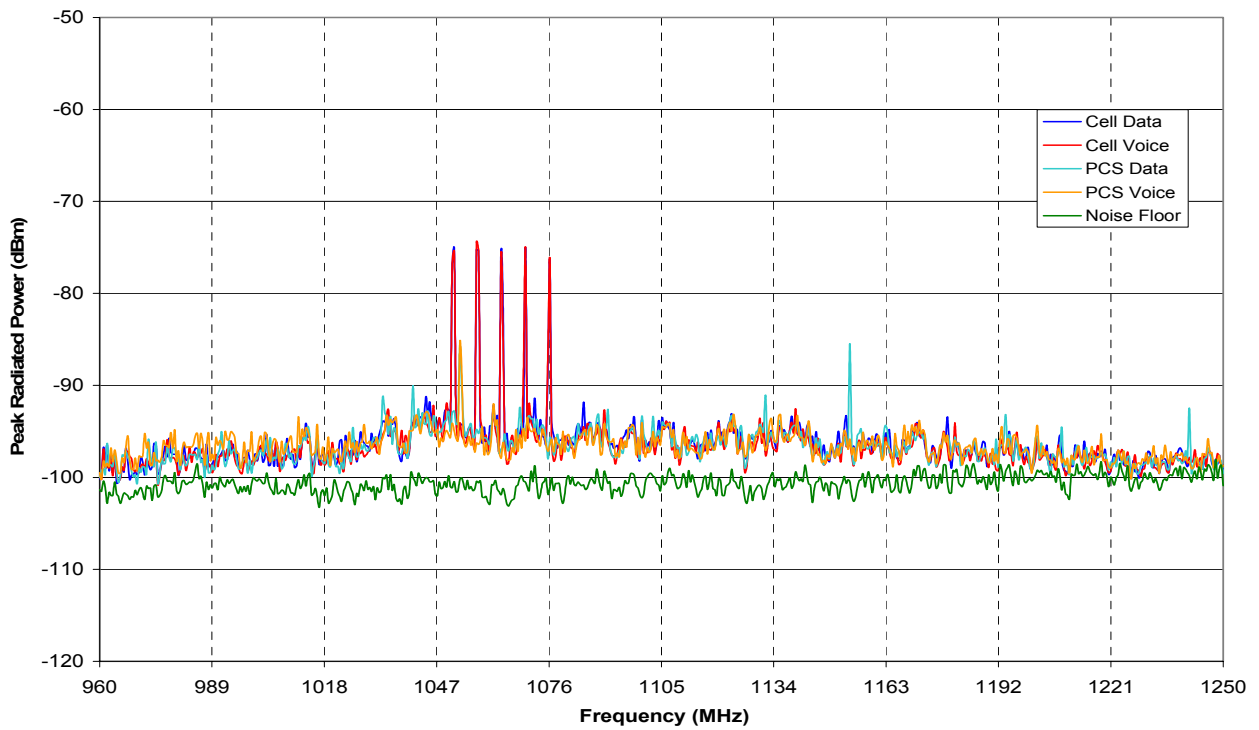


Figure A41: CDM09 four mode envelopes, Band 3.

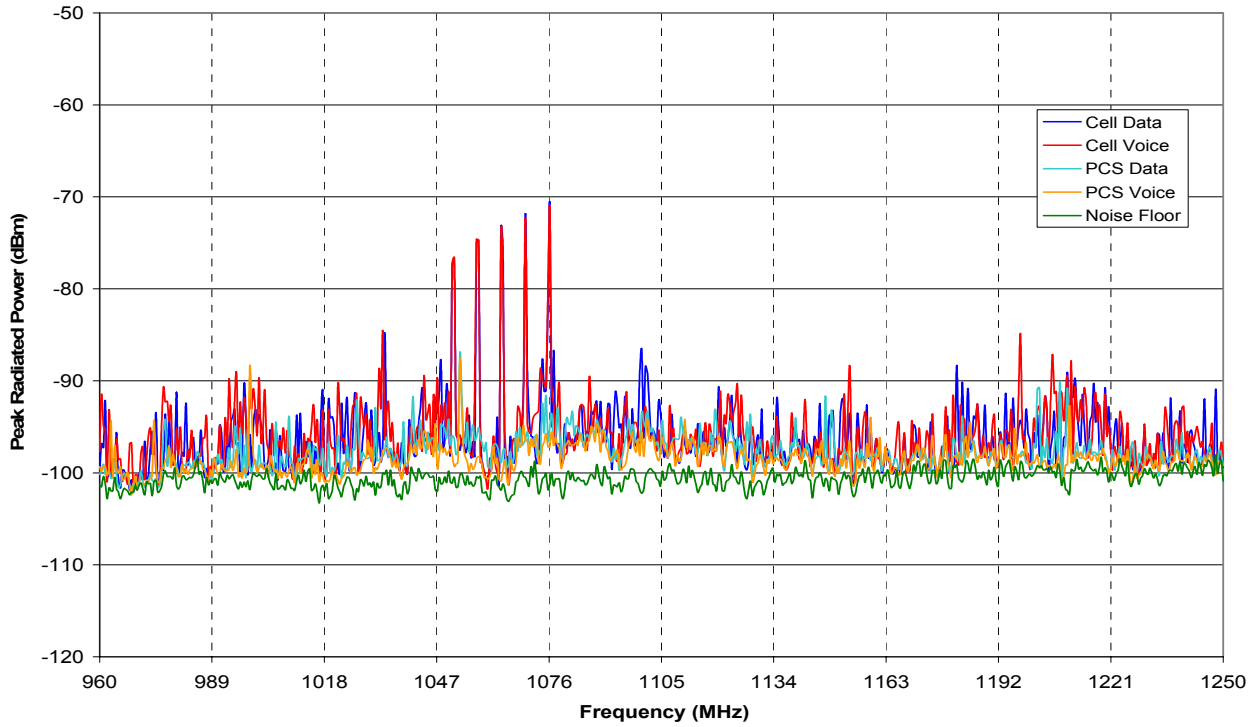


Figure A42: CDM10 four mode envelopes, Band 3.

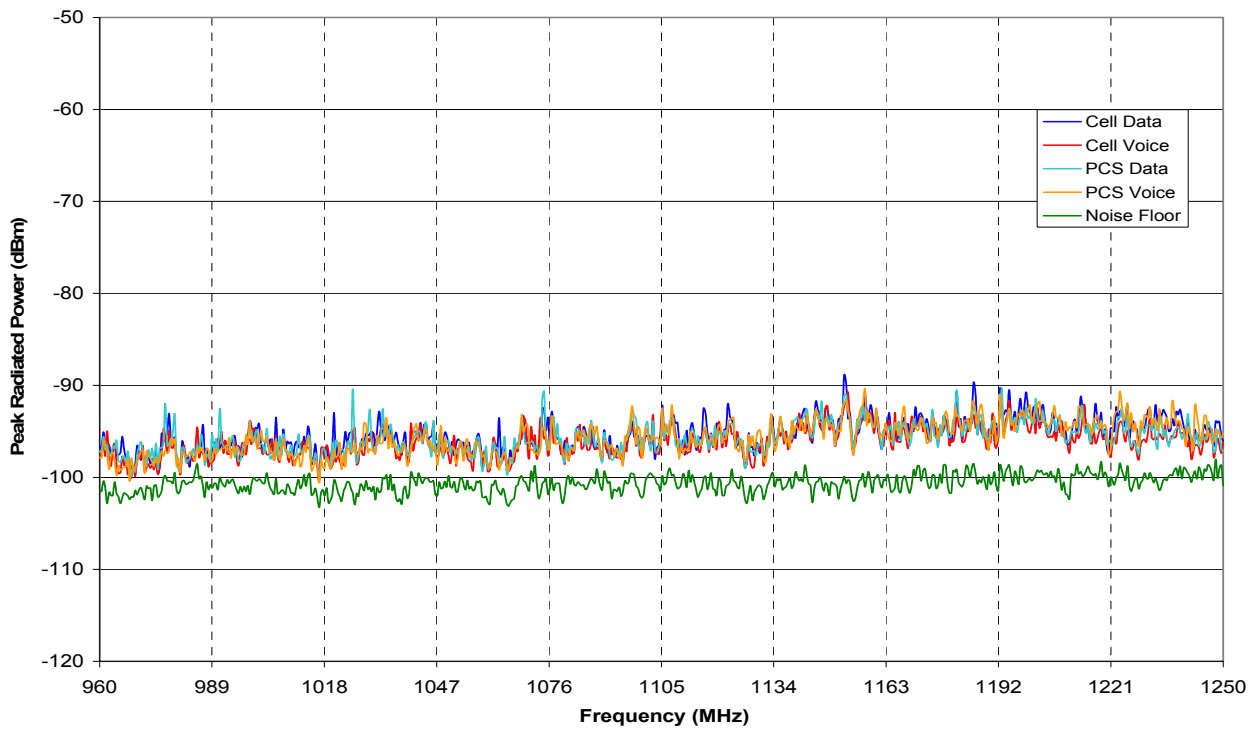


Figure A43: CDM11 four mode envelopes, Band 3.

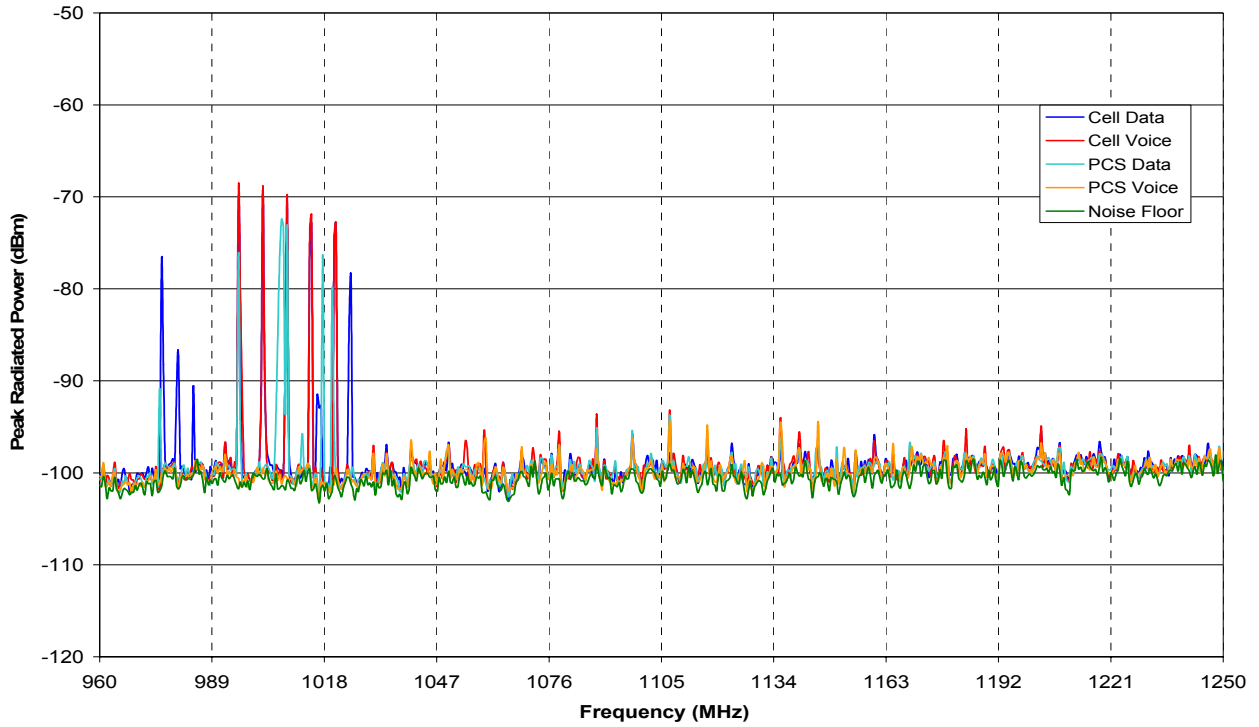


Figure A44: CDM12 four mode envelopes, Band 3.

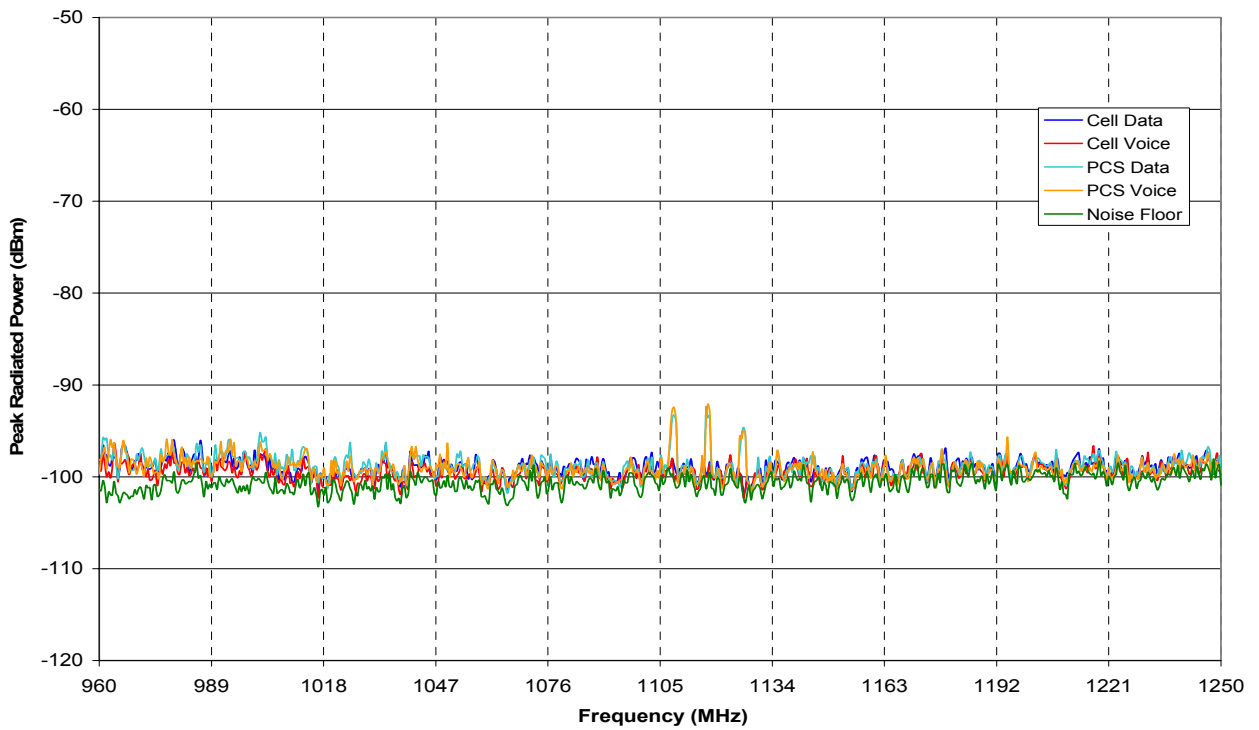


Figure A45: CDM13 four mode envelopes, Band 3.

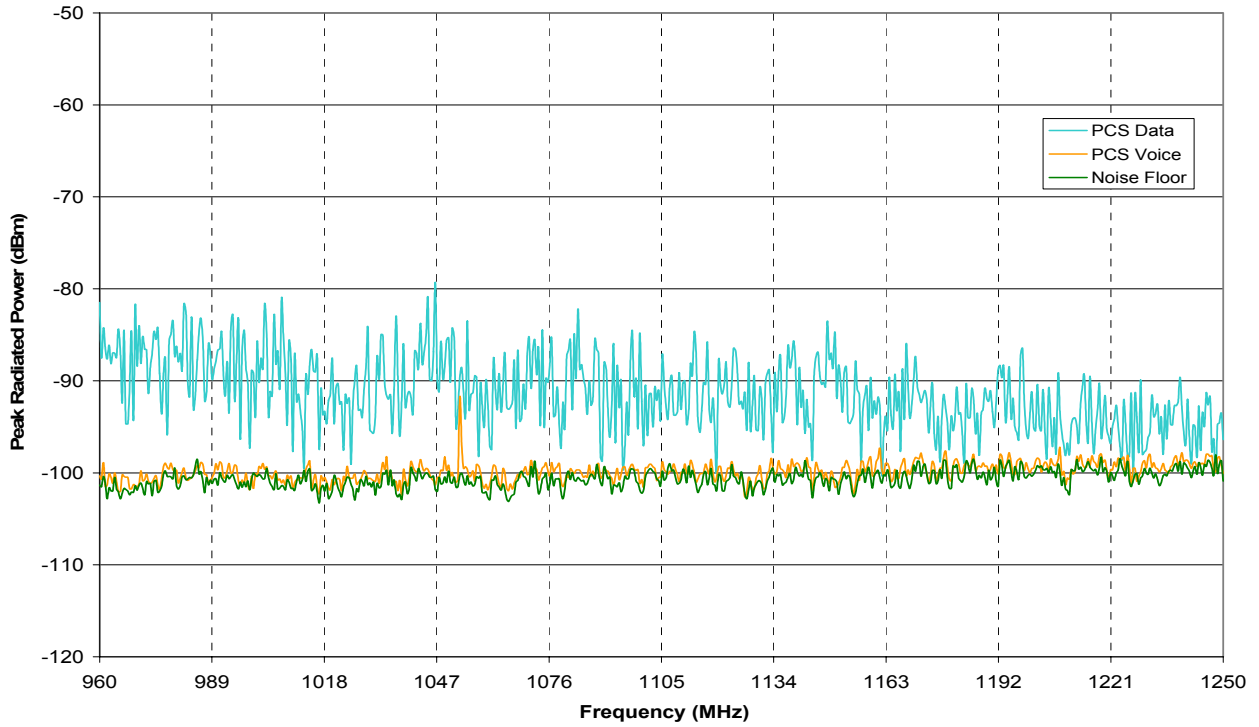


Figure A46: CDM14 two mode envelopes, Band 3.

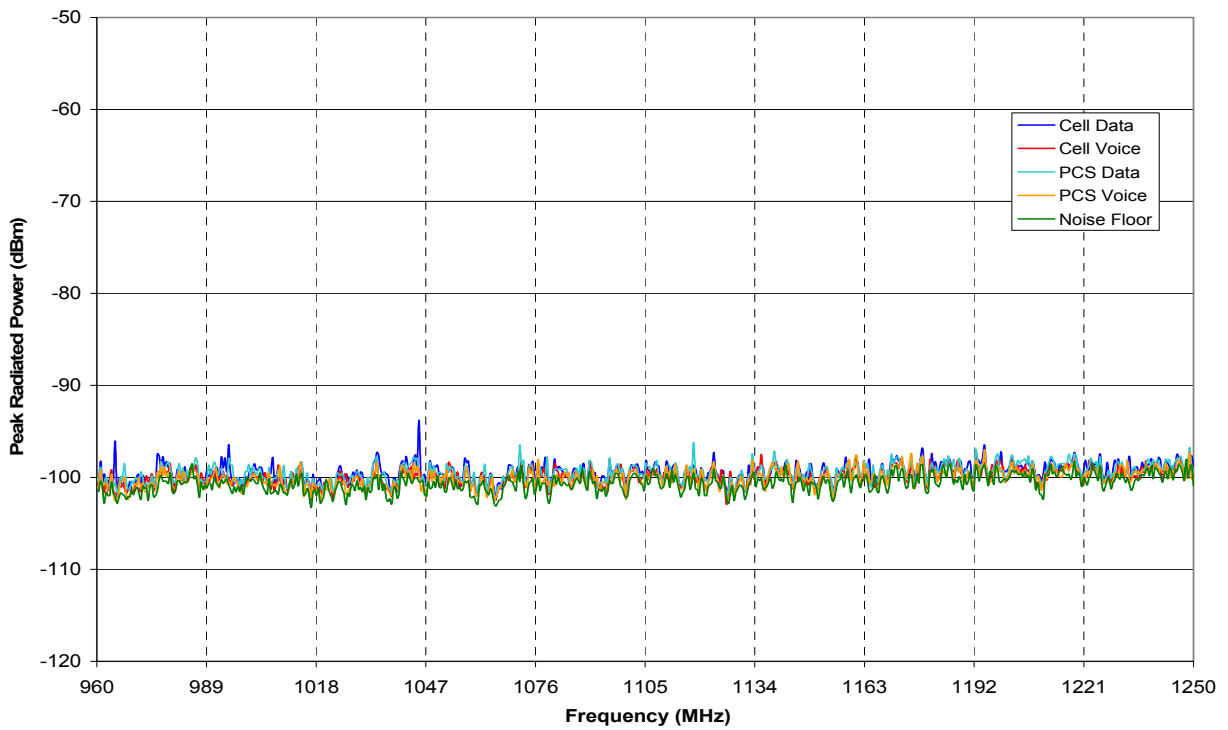


Figure A47: CDM15 four mode envelopes, Band 3.

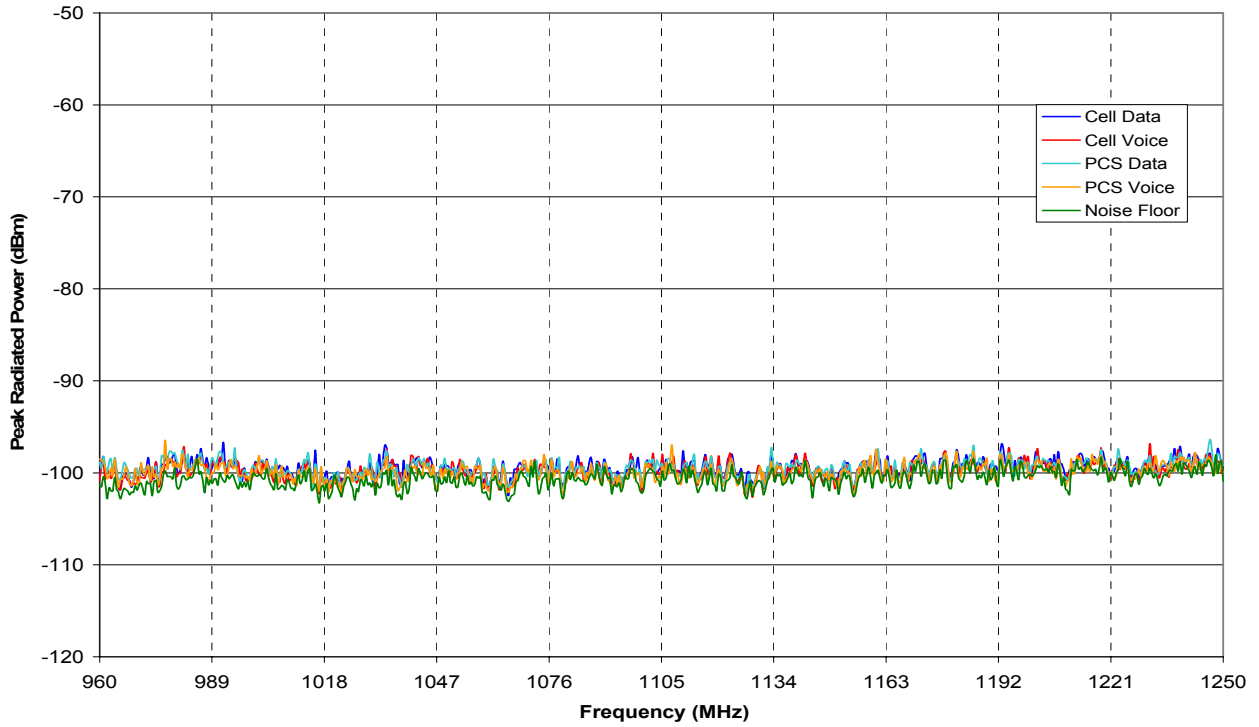


Figure A48: CDM16 four mode envelopes, Band 3.

A.4 Band 4

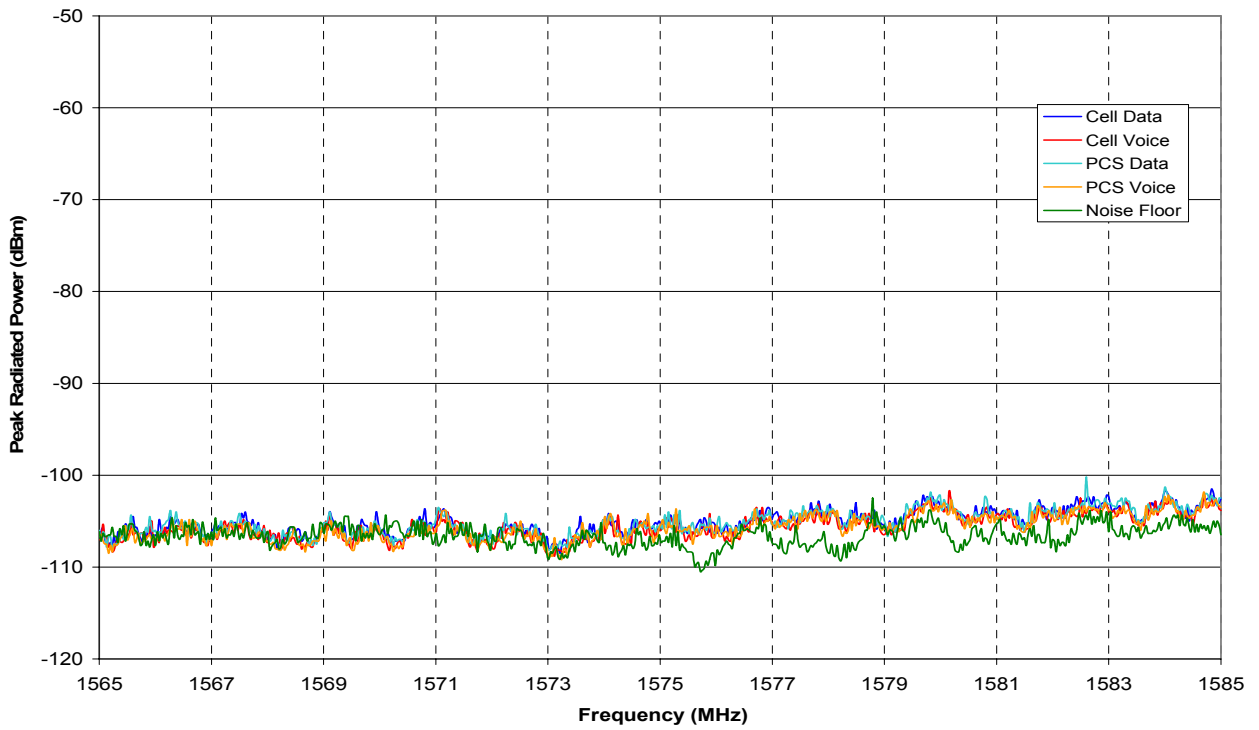


Figure A49: CDM01 four mode envelopes, Band 4.

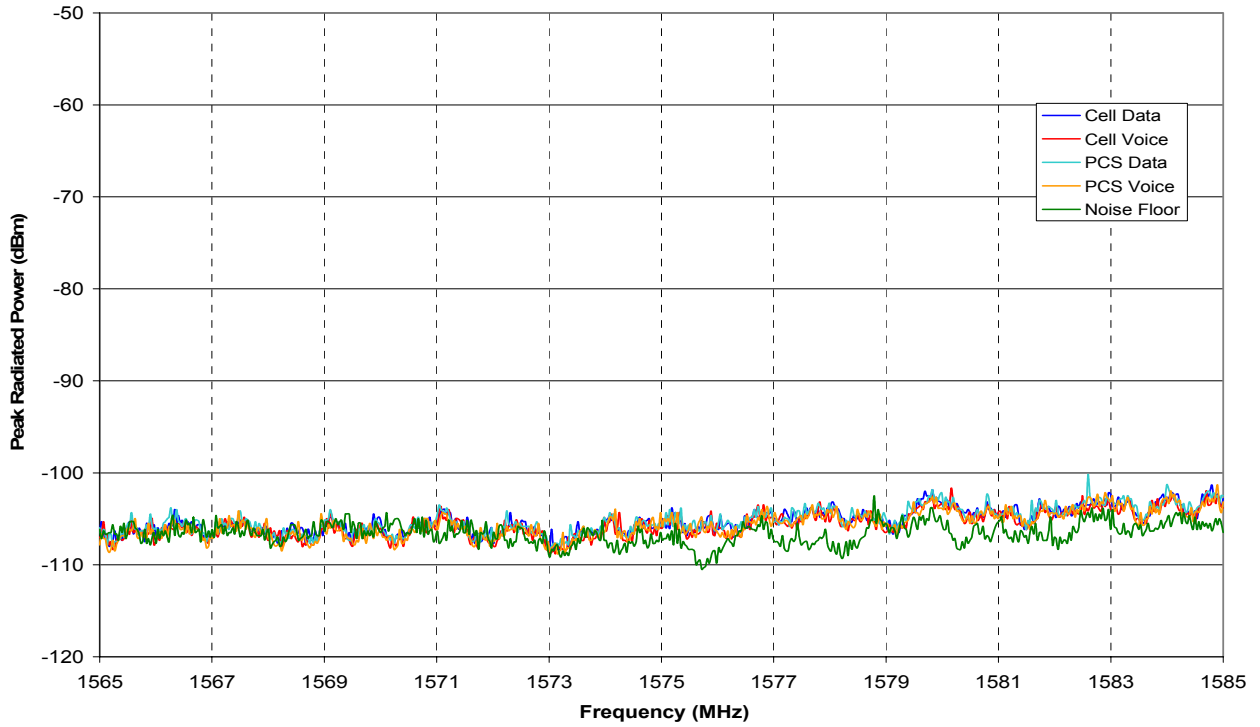


Figure A50: CDM02 four mode envelopes, Band 4.

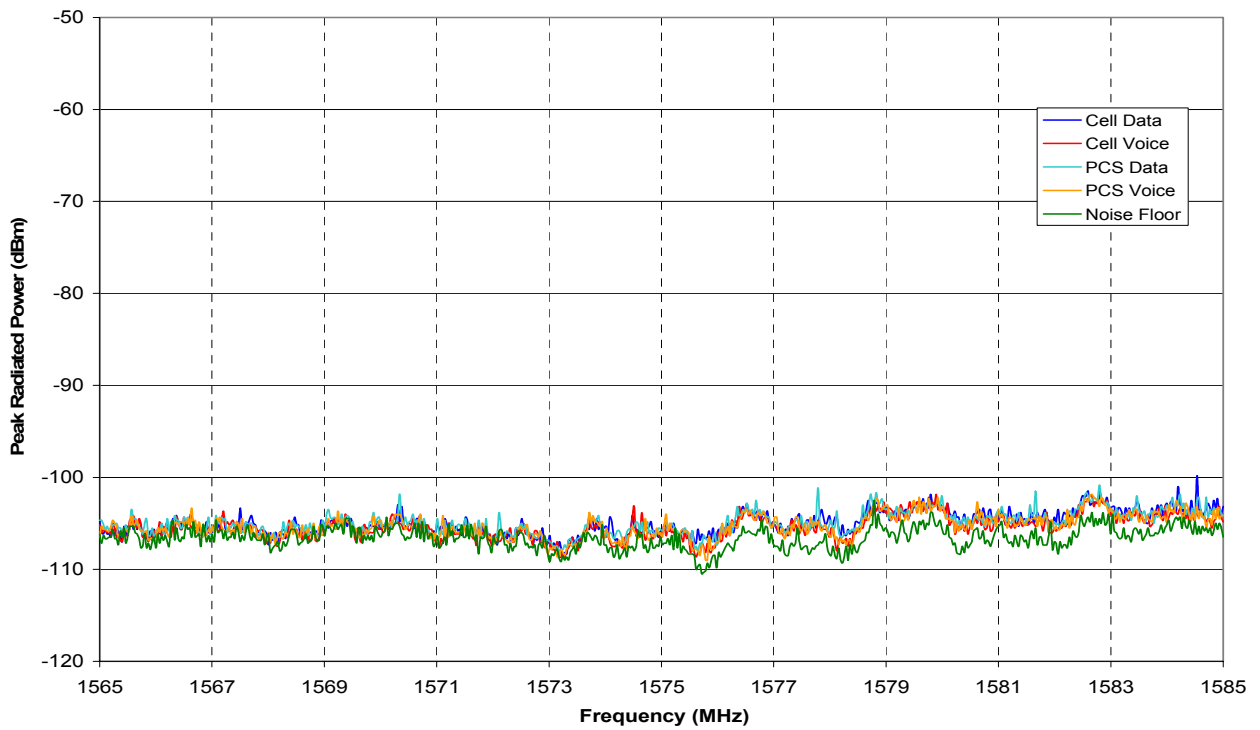


Figure A51: CDM03 four mode envelopes, Band 4.

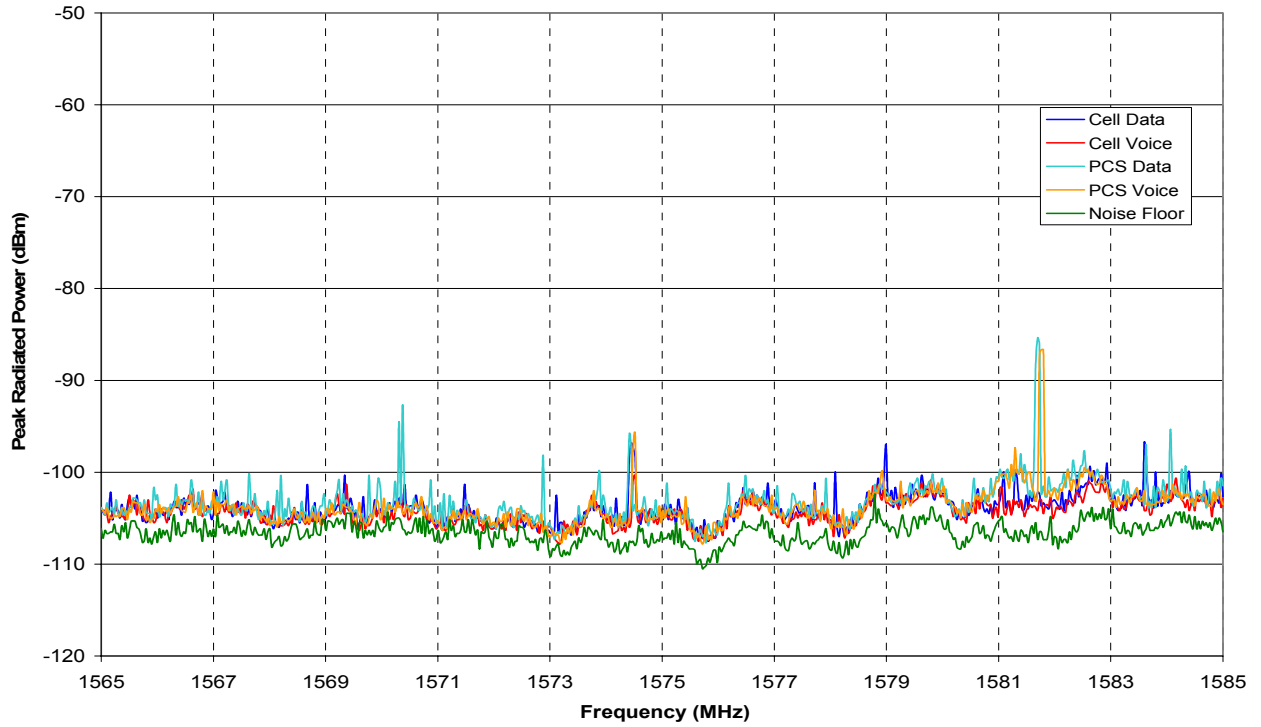


Figure A52: CDM04 four mode envelopes, Band 4.

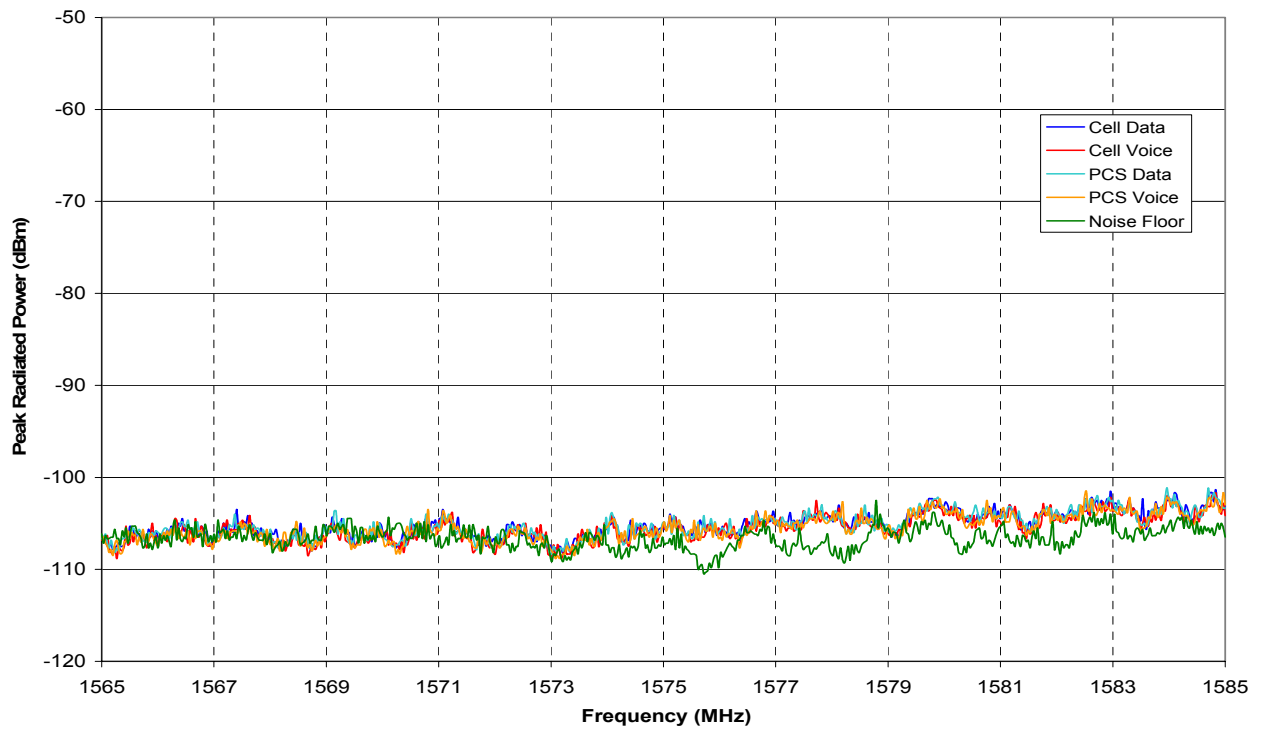


Figure A53: CDM05 four mode envelopes, Band 4.

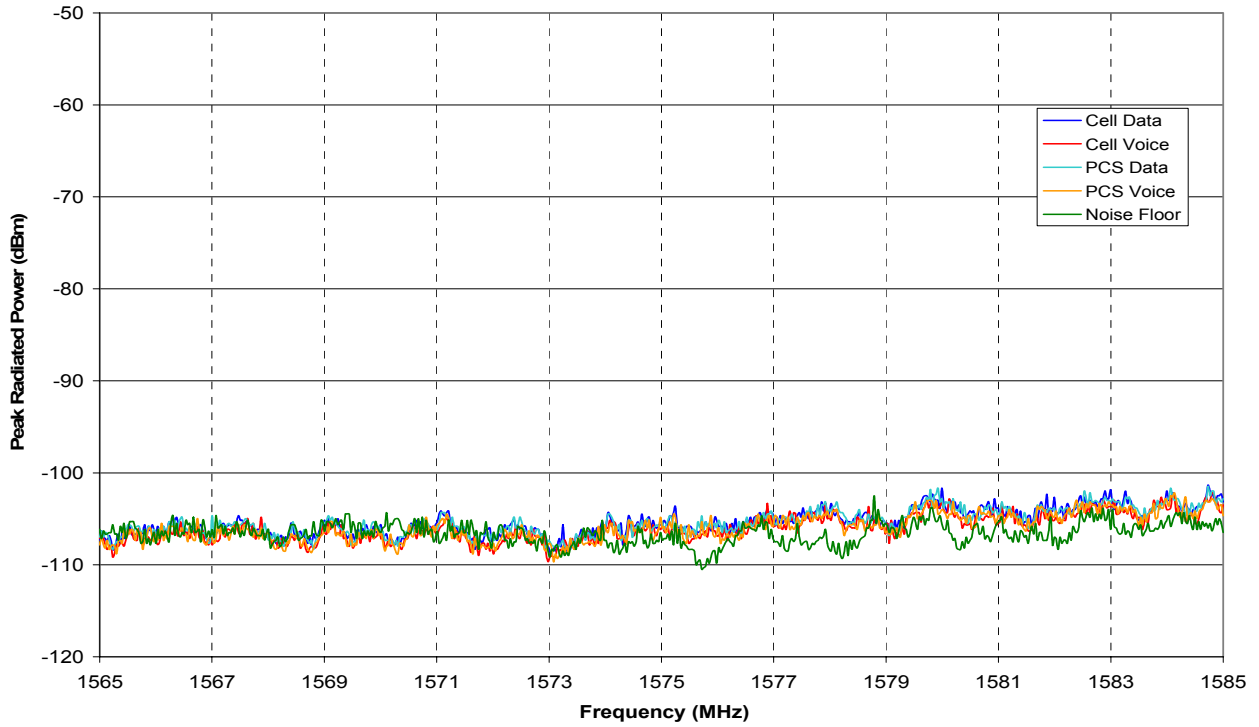


Figure A54: CDM06 four mode envelopes, Band 4.

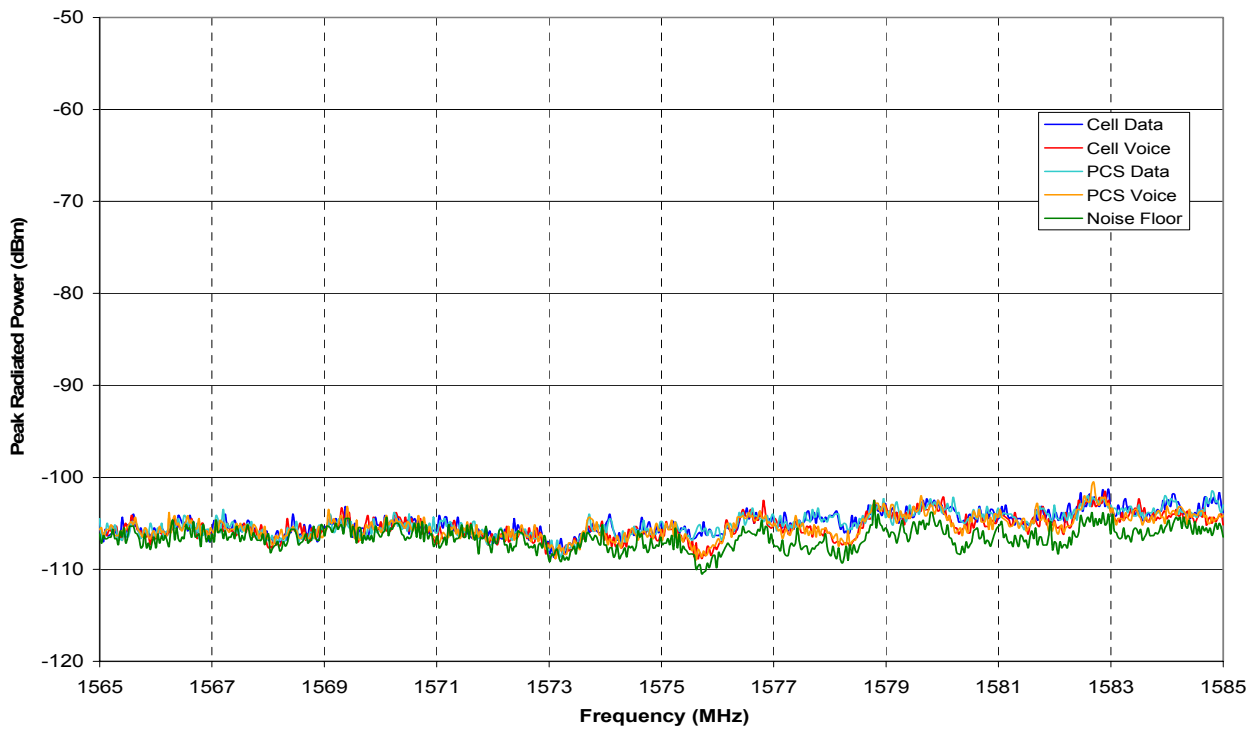


Figure A55: CDM07 four mode envelopes, Band 4.

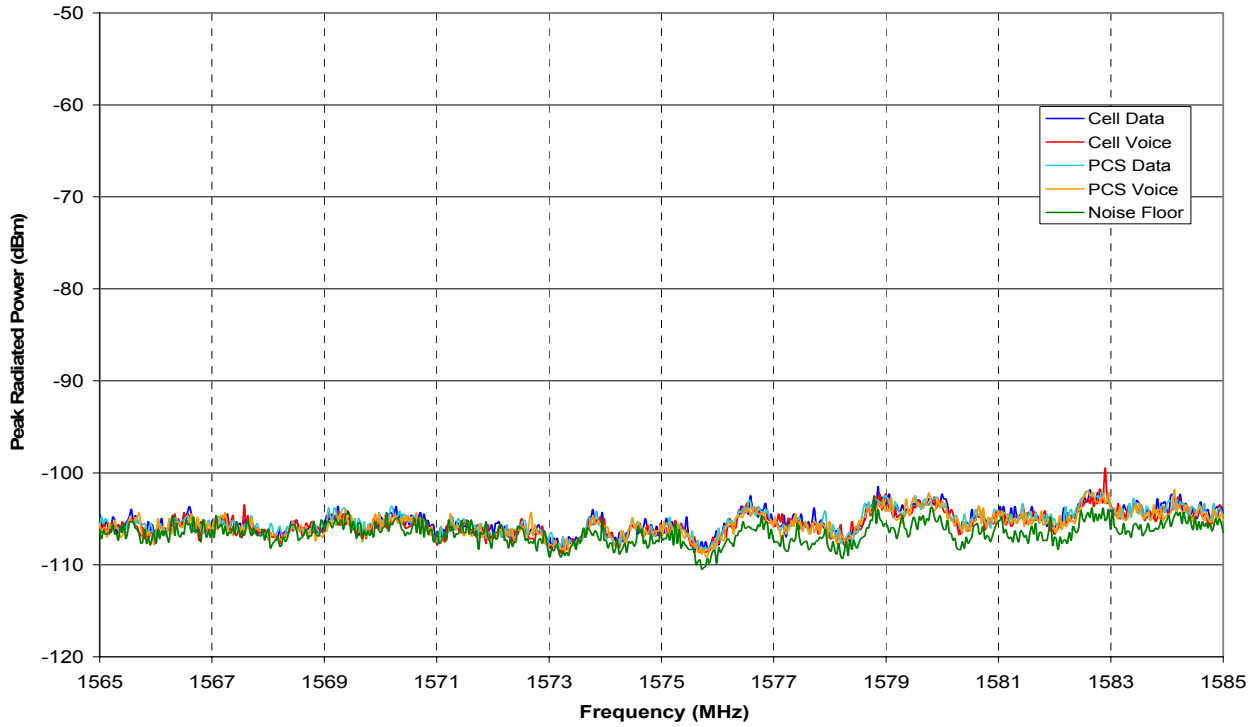


Figure A56: CDM08 four mode envelopes, Band 4.

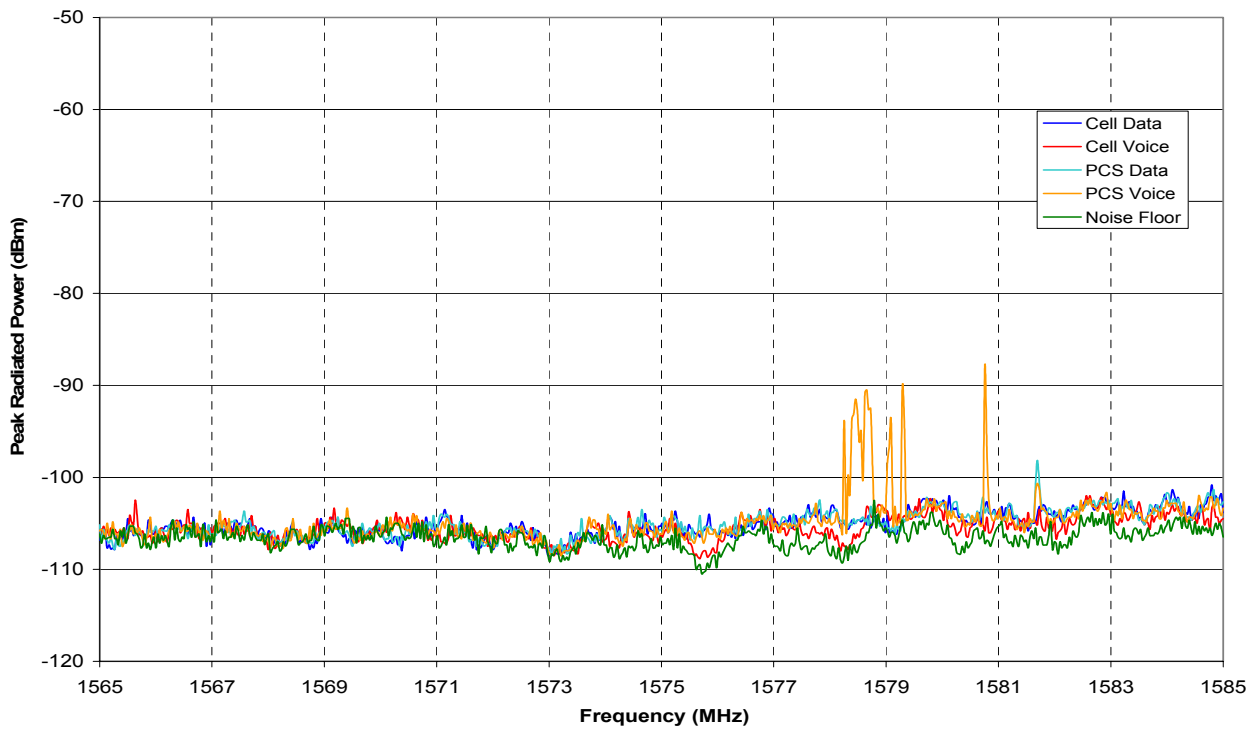


Figure A57: CDM09 four mode envelopes, Band 4.

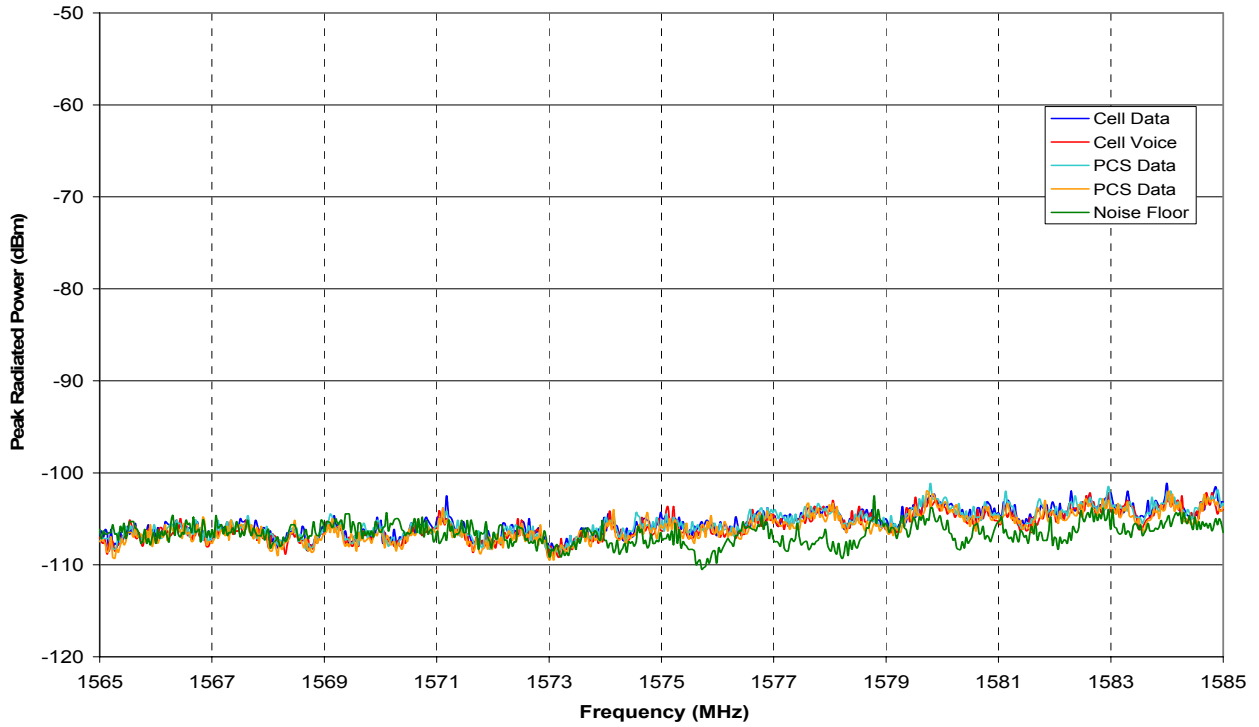


Figure A58: CDM10 four mode envelopes, Band 4.

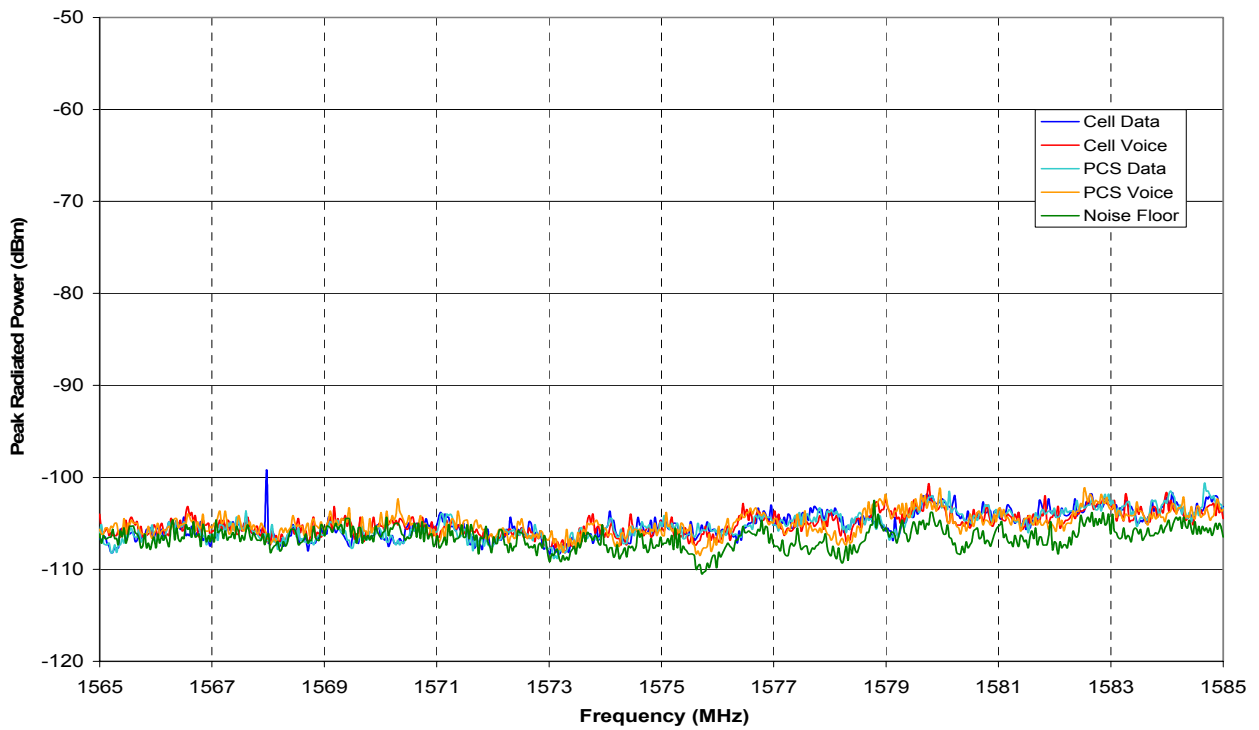


Figure A59: CDM11 four mode envelopes, Band 4.

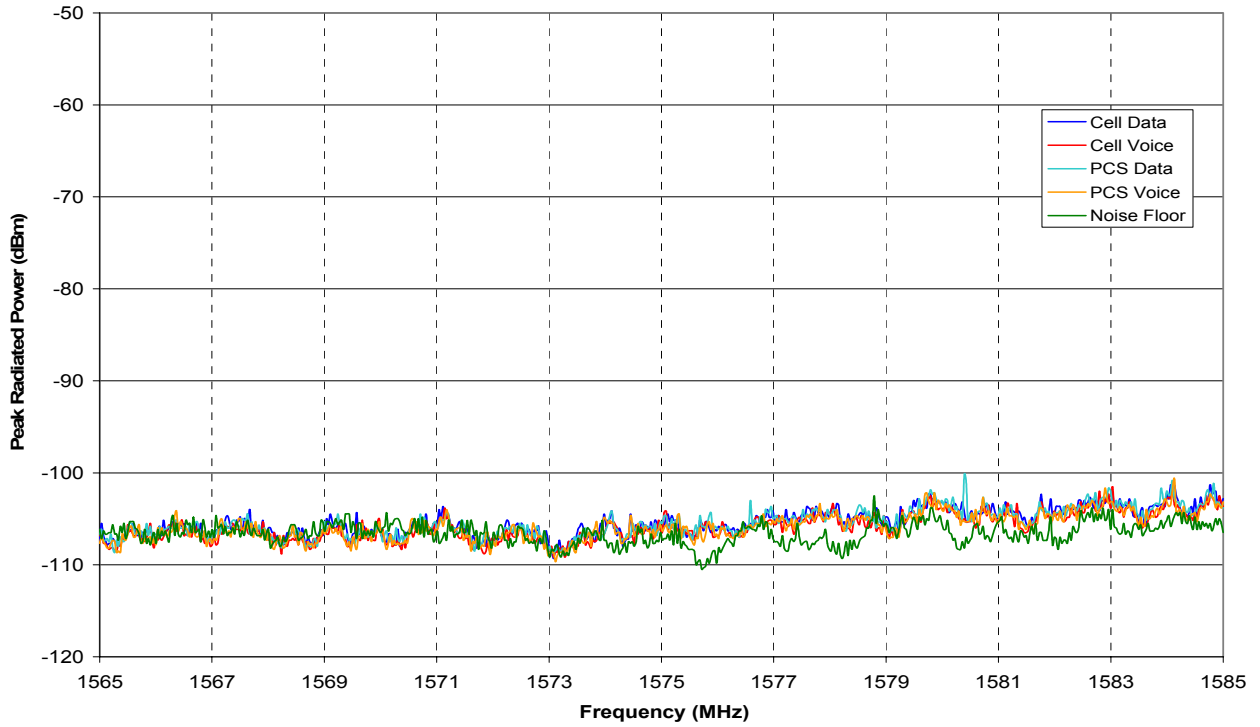


Figure A60: CDM12 four mode envelopes, Band 4.

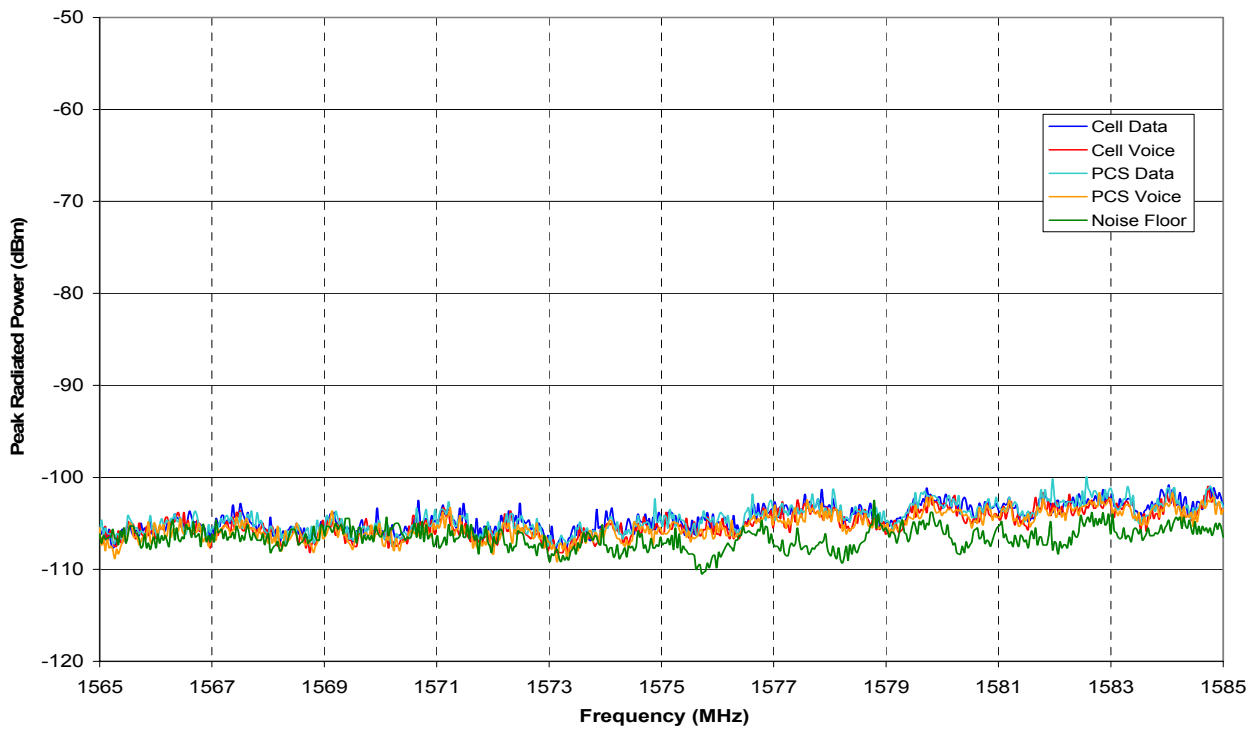


Figure A61: CDM13 four mode envelopes, Band 4.

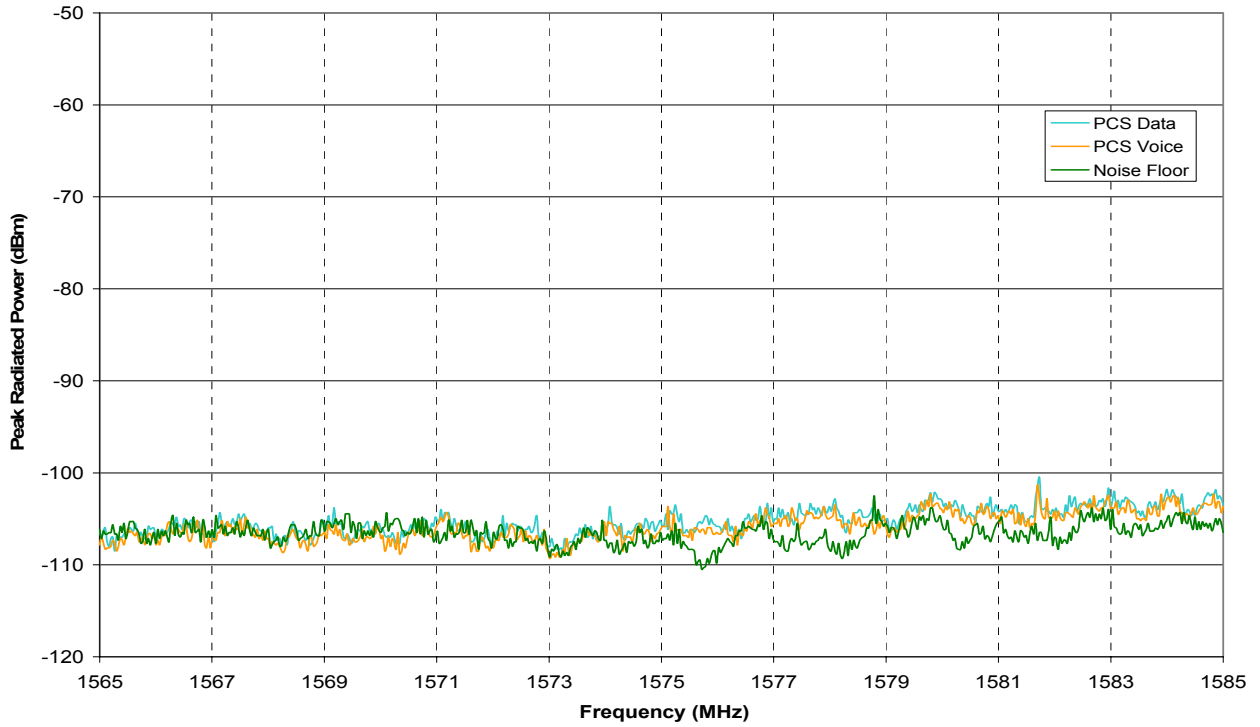


Figure A62: CDM14 four mode envelopes, Band 4.

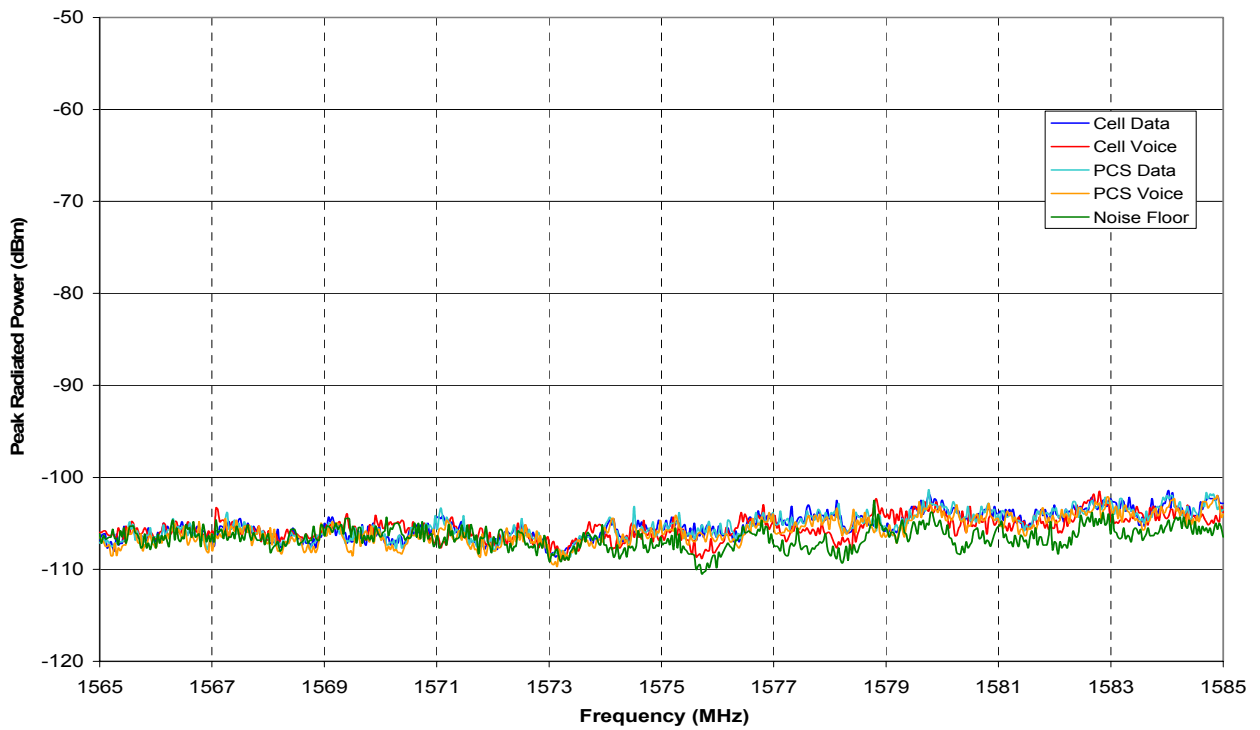


Figure A63: CDM15 four mode envelopes, Band 4.

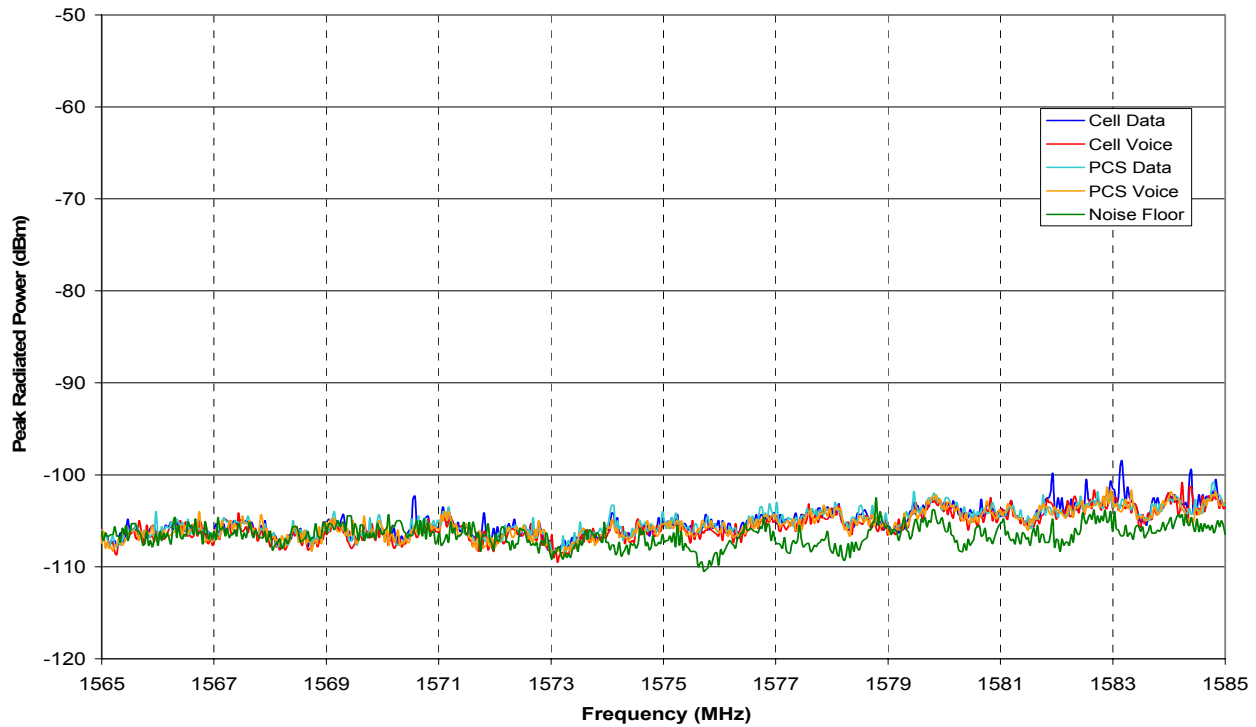


Figure A64: CDM16 four mode envelopes, Band 4.

A.5 Band 5

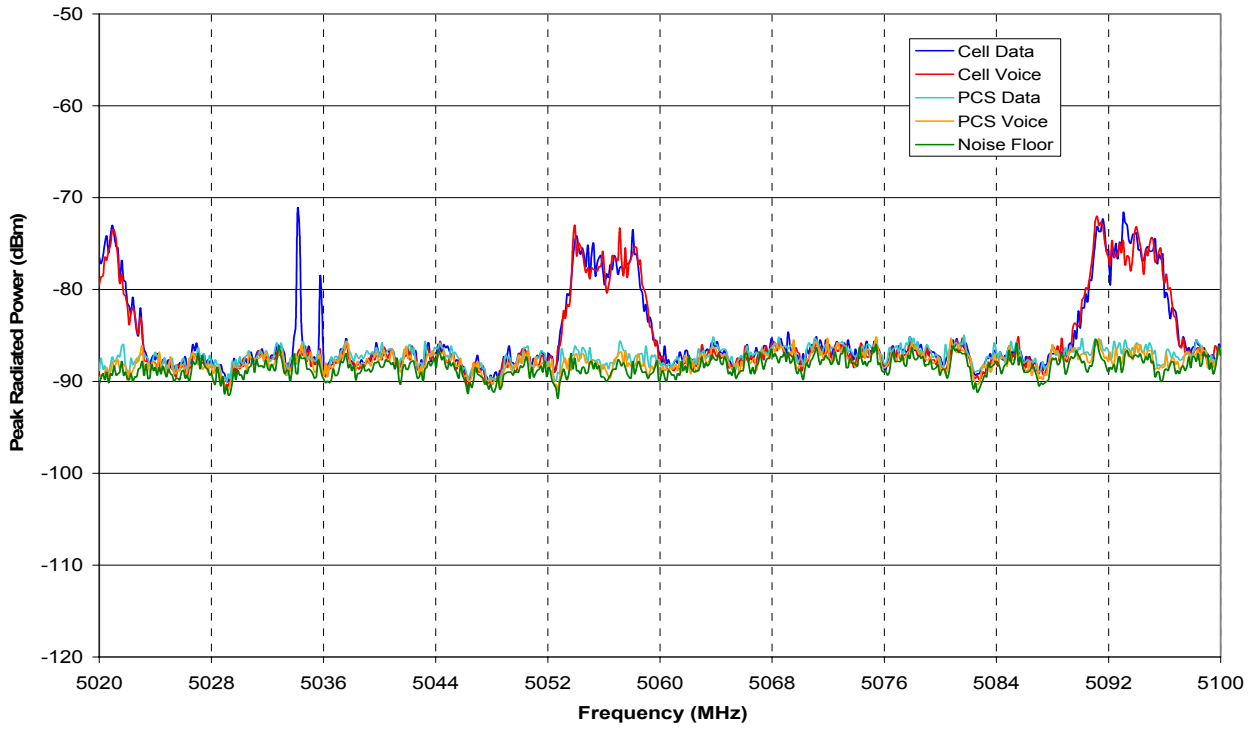


Figure A65: CDM01 four mode envelopes, Band 5.

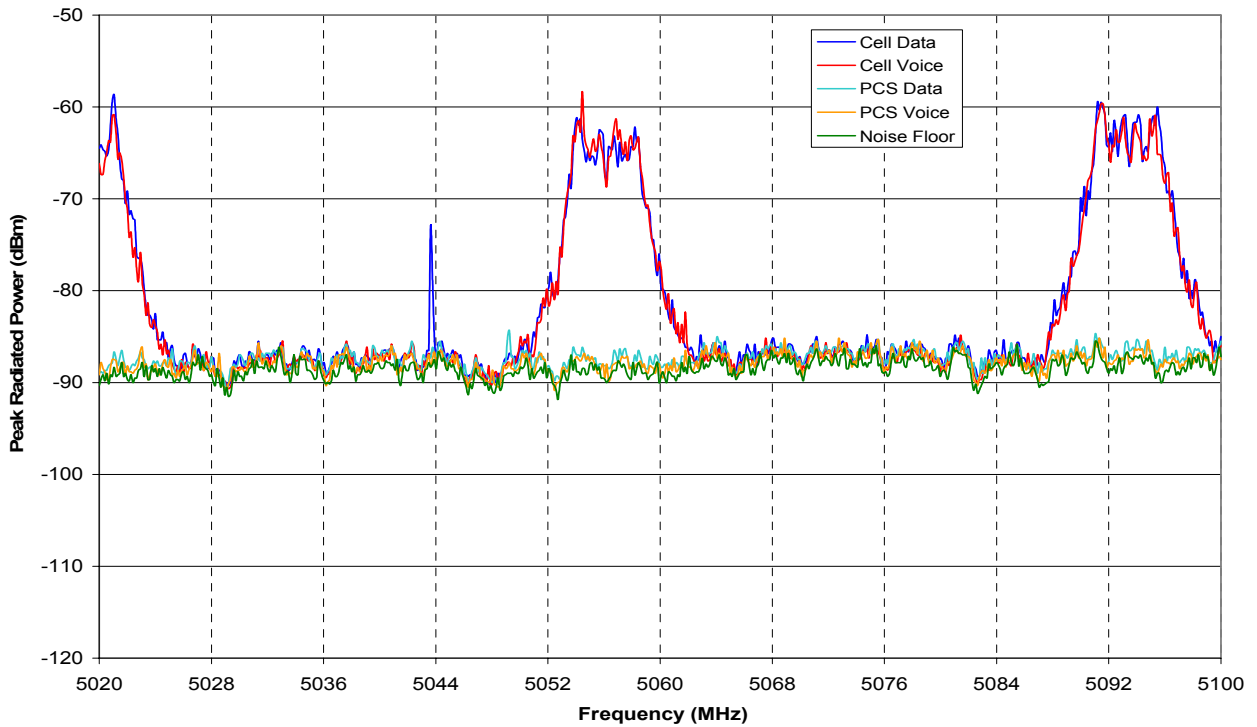


Figure A66: CDM02 four mode envelopes, Band 5.

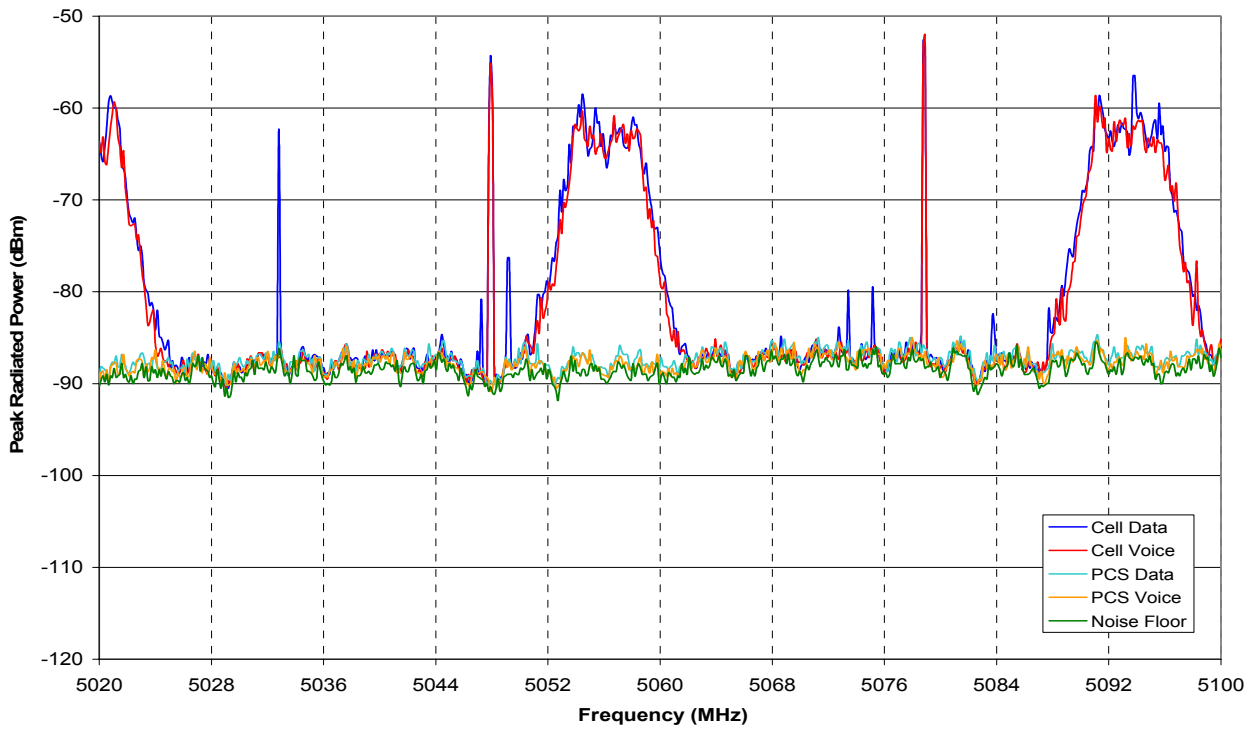


Figure A67: CDM03 four mode envelopes, Band 5.

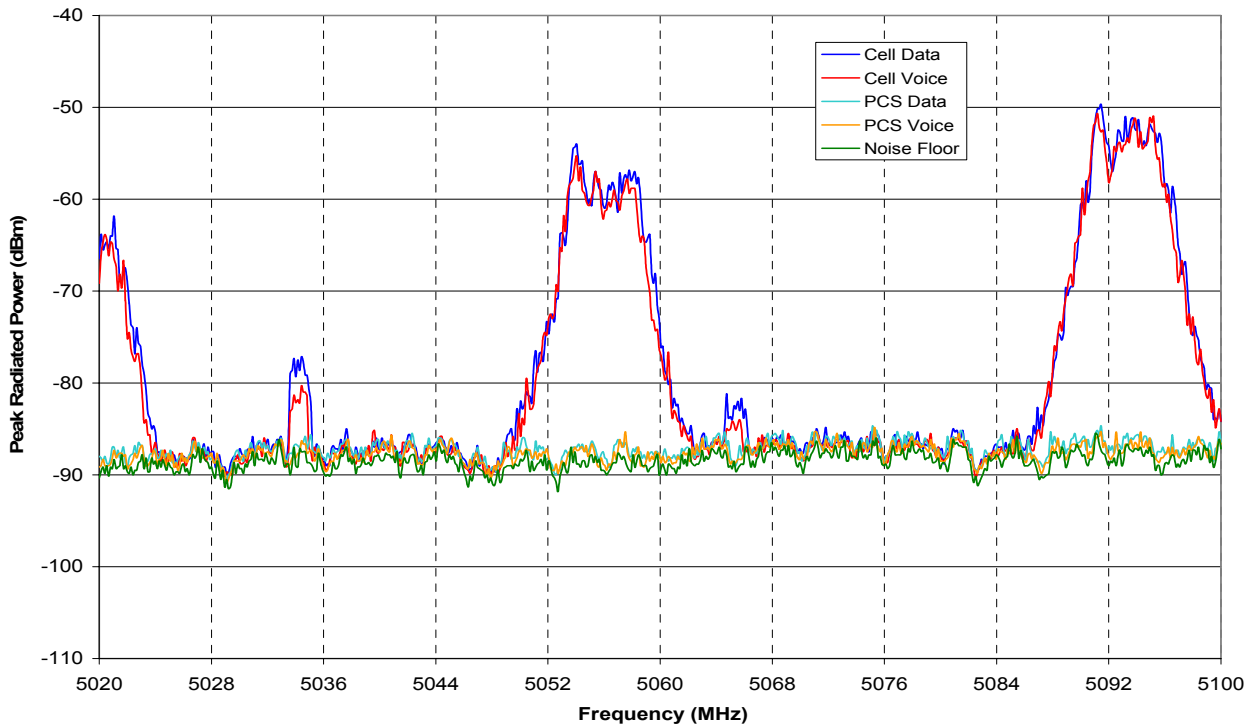


Figure A68: CDM04 four mode envelopes, Band 5.

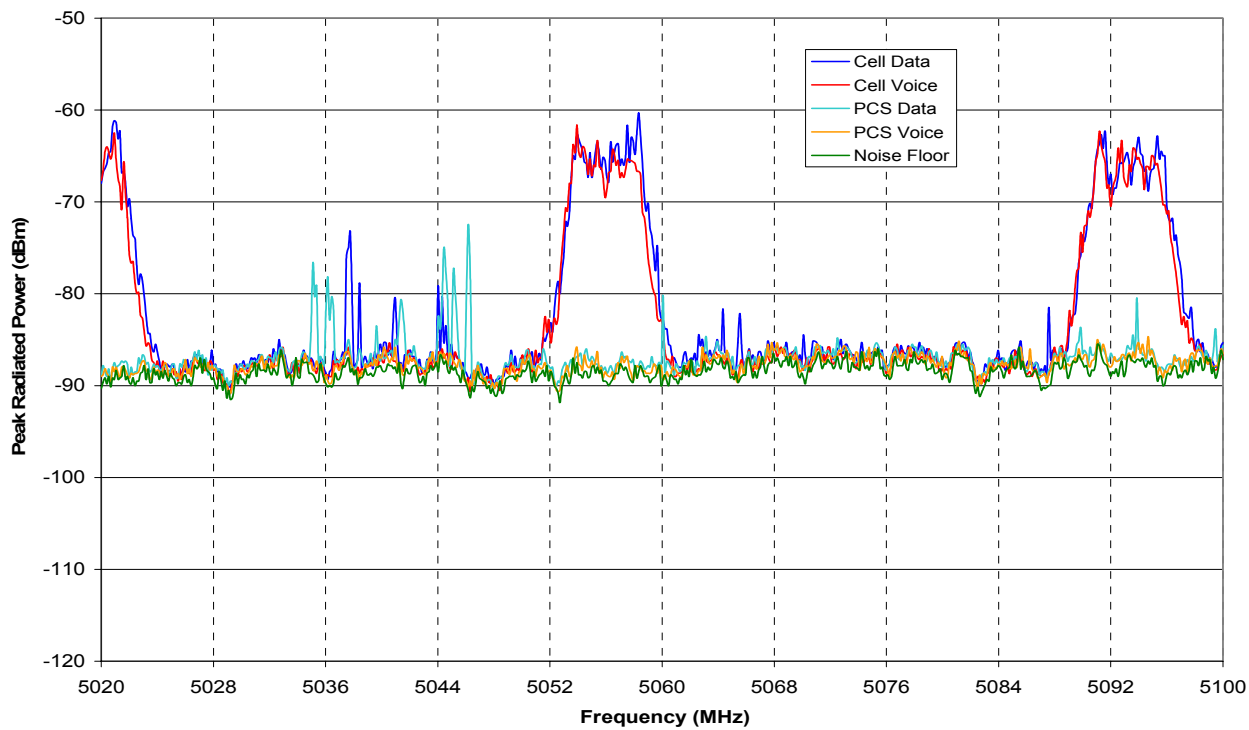


Figure A69: CDM05 four mode envelopes, Band 5.

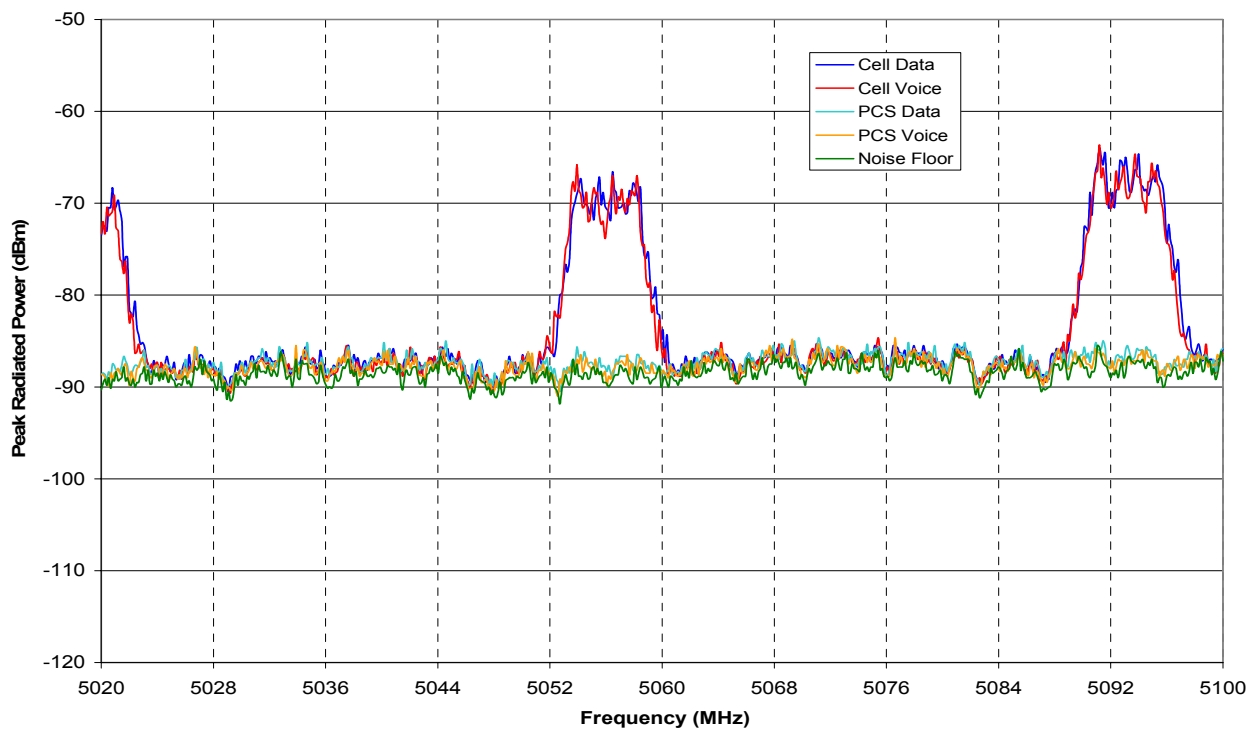


Figure A70: CDM06 four mode envelopes, Band 5.

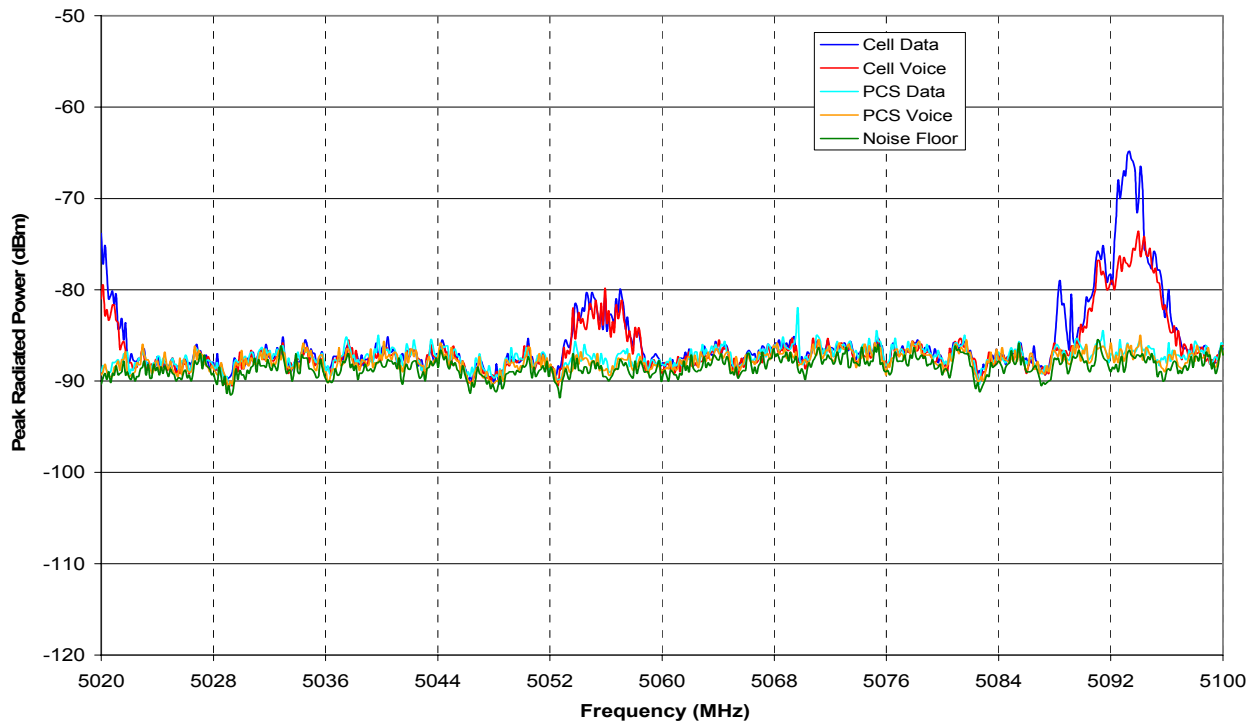


Figure A71: CDM07 four mode envelopes, Band 5.

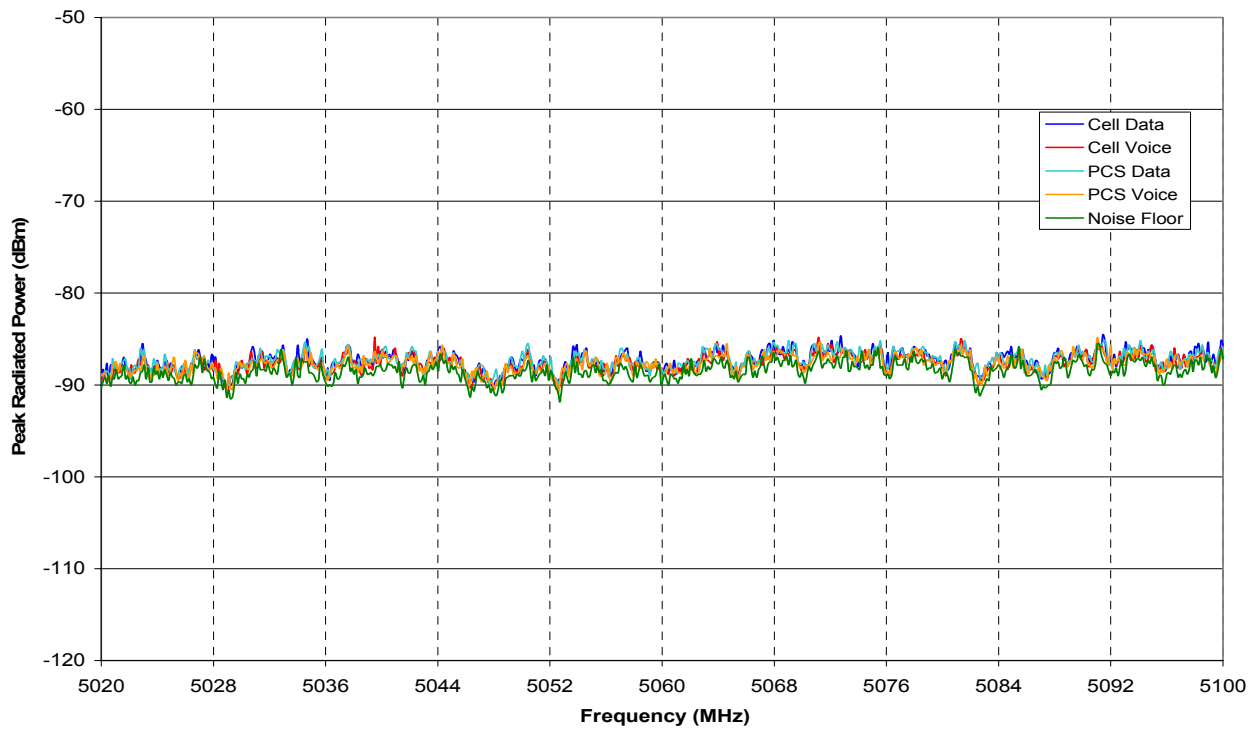


Figure A72: CDM08 four mode envelopes, Band 5.

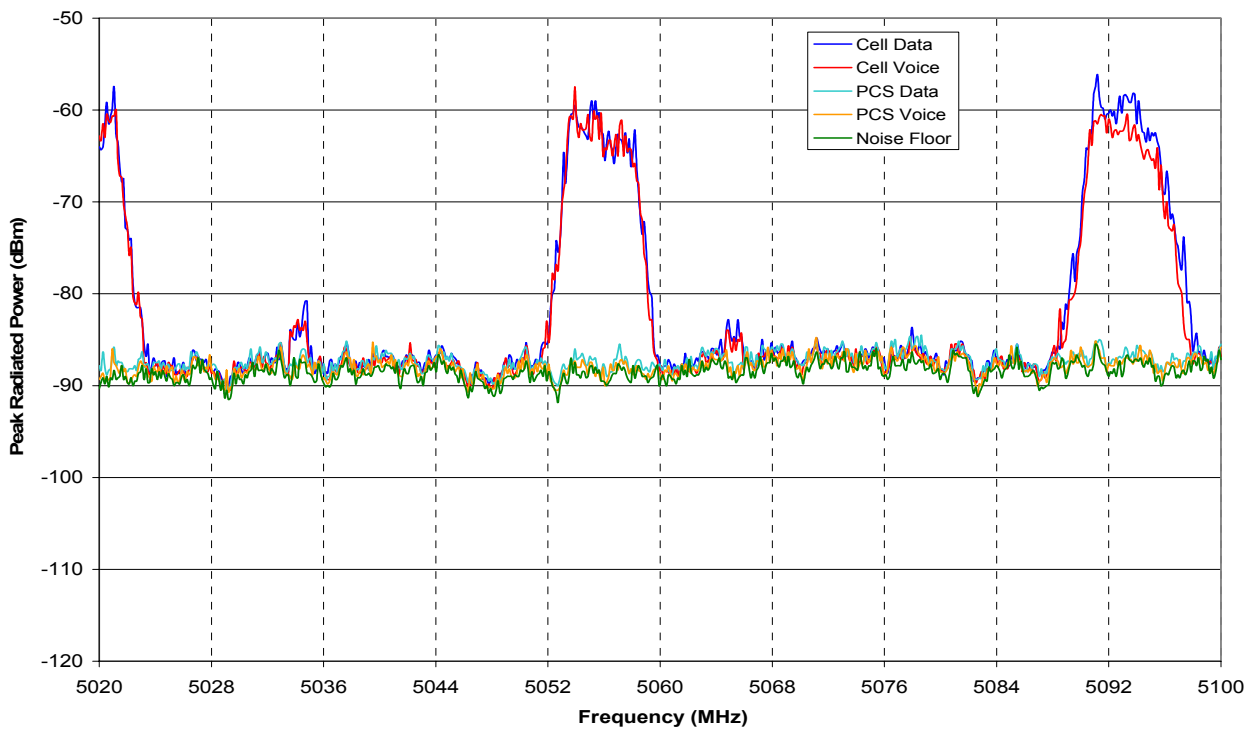


Figure A73: CDM09 four mode envelopes, Band 5.

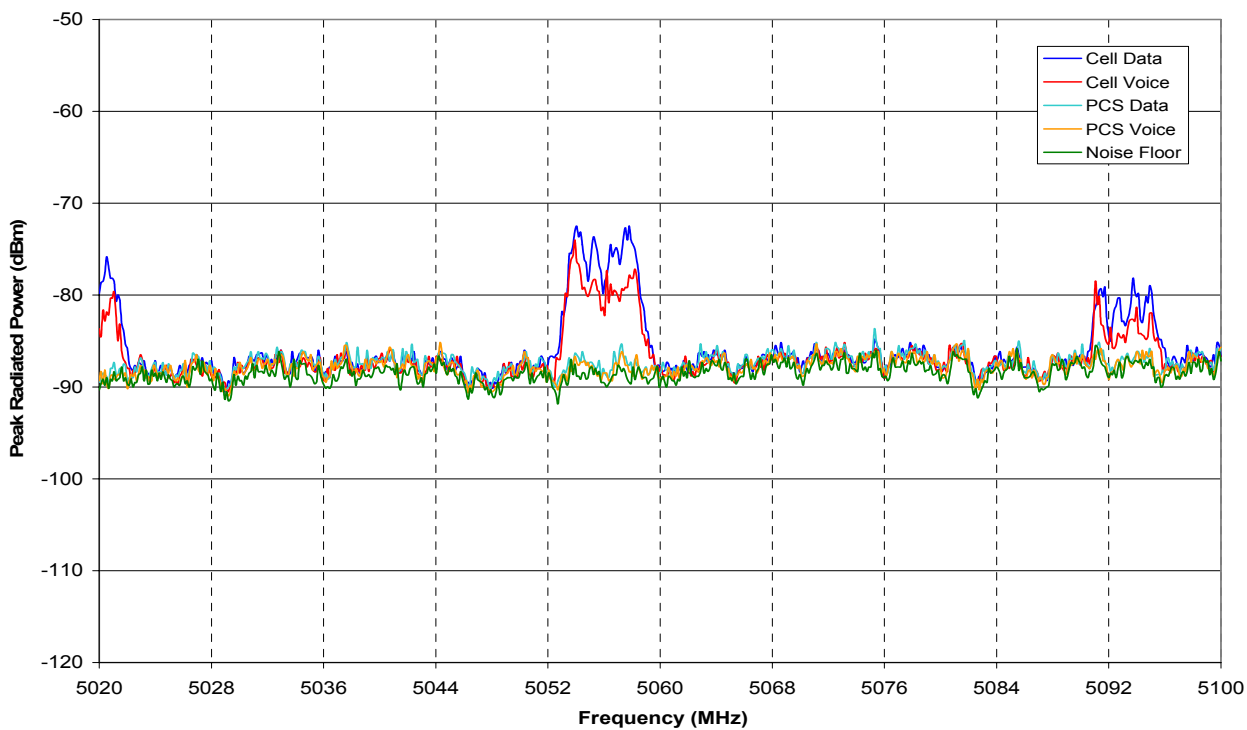


Figure A74: CDM10 four mode envelopes, Band 5.

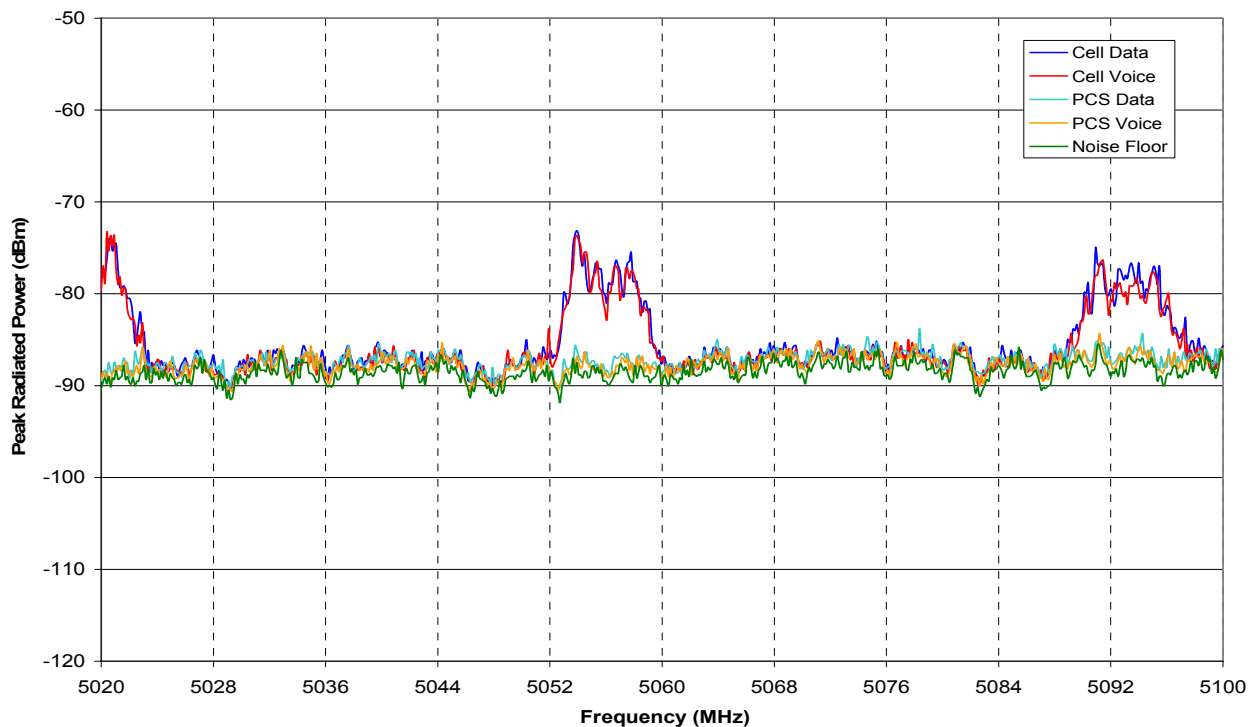


Figure A75: CDM11 four mode envelopes, Band 5.

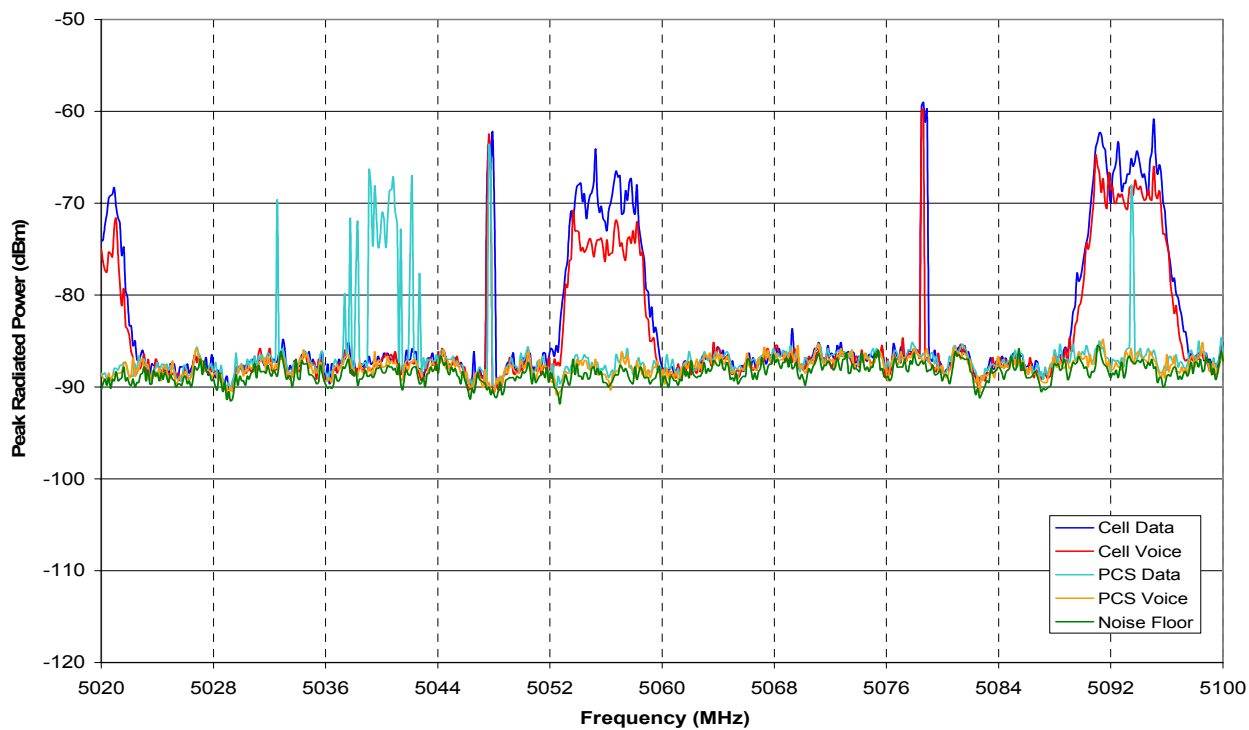


Figure A76: CDM12 four mode envelopes, Band 5.

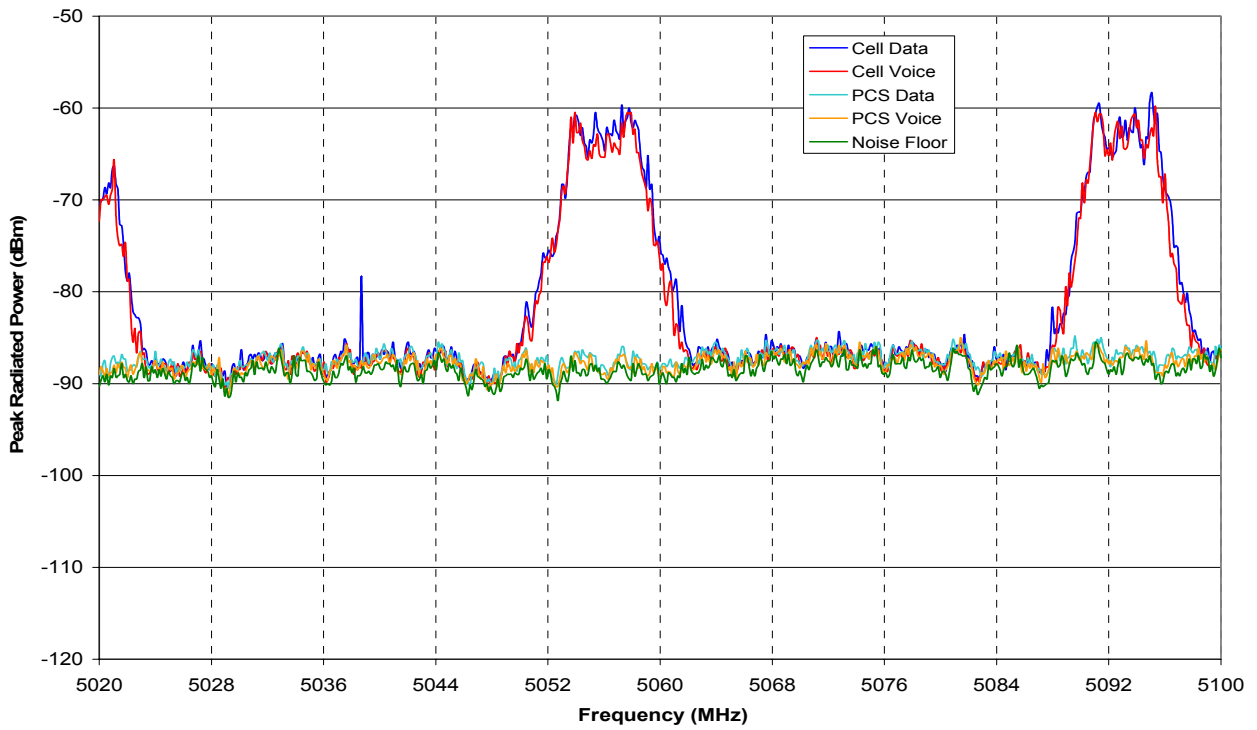


Figure A77: CDM13 four mode envelopes, Band 5.

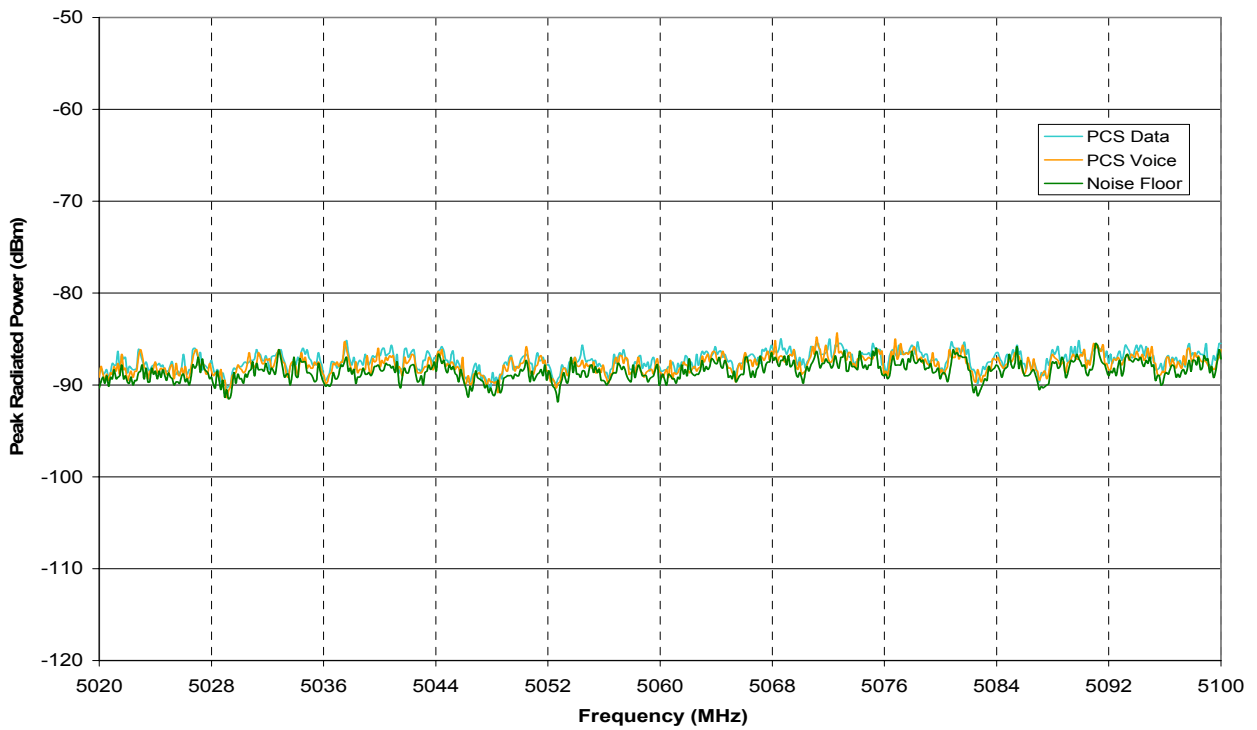


Figure A78: CDM14 two mode envelopes, Band 5.

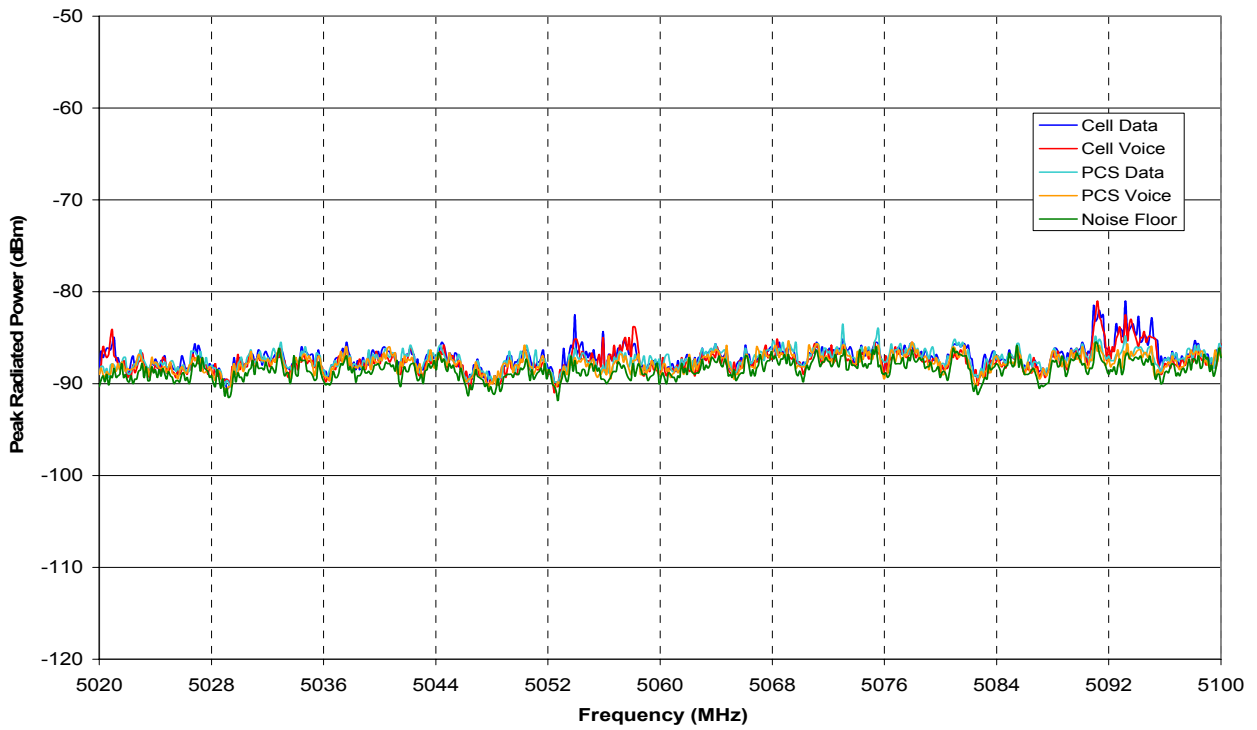


Figure A79: CDM15 four mode envelopes, Band 5.

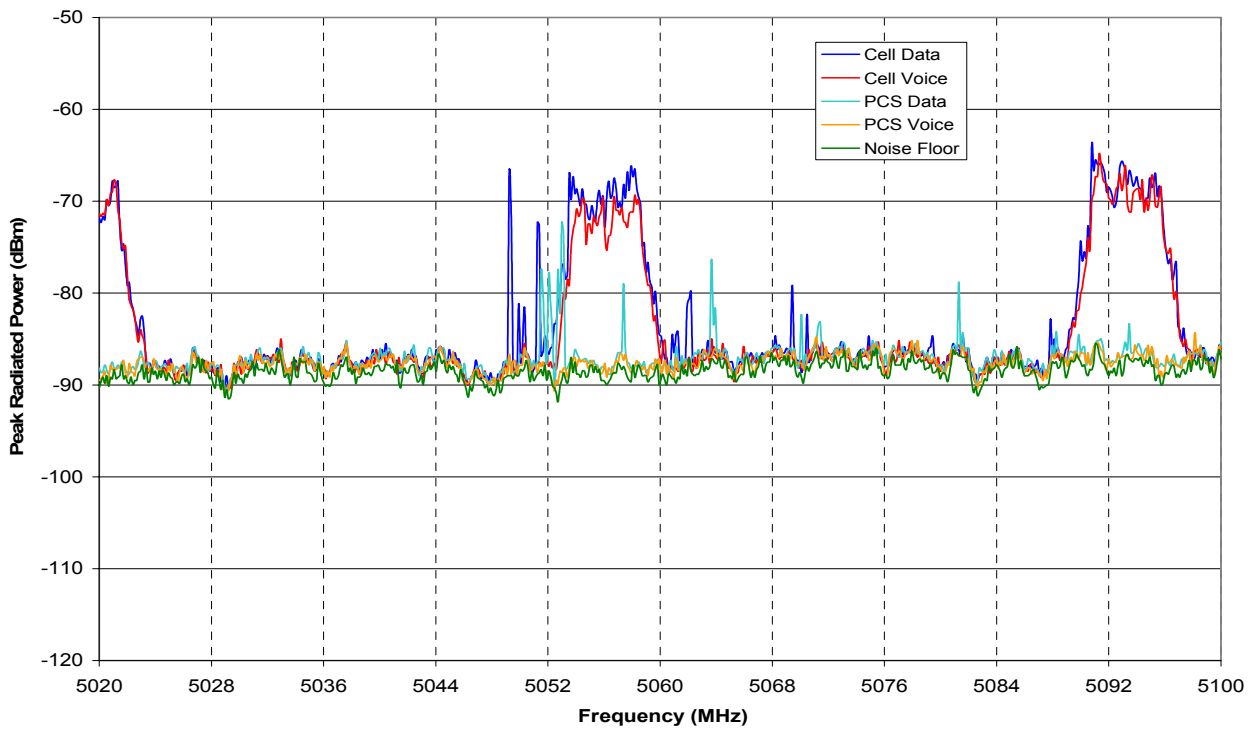


Figure A80: CDM16 four mode envelopes, Band 5.

(This page intentionally left blank)

Appendix B: GSM Phone Test Results

The following charts illustrate each wireless phone's cell data, cell voice, PCS data, and PCS voice mode envelopes. An equivalent measurement noise floor is included in each chart for each band to represent the instrument noise floor. The data in these charts were further reduced to produce the data plotted in charts found in Sections 3.4.1 to 3.4.3.

B.1 Band 1

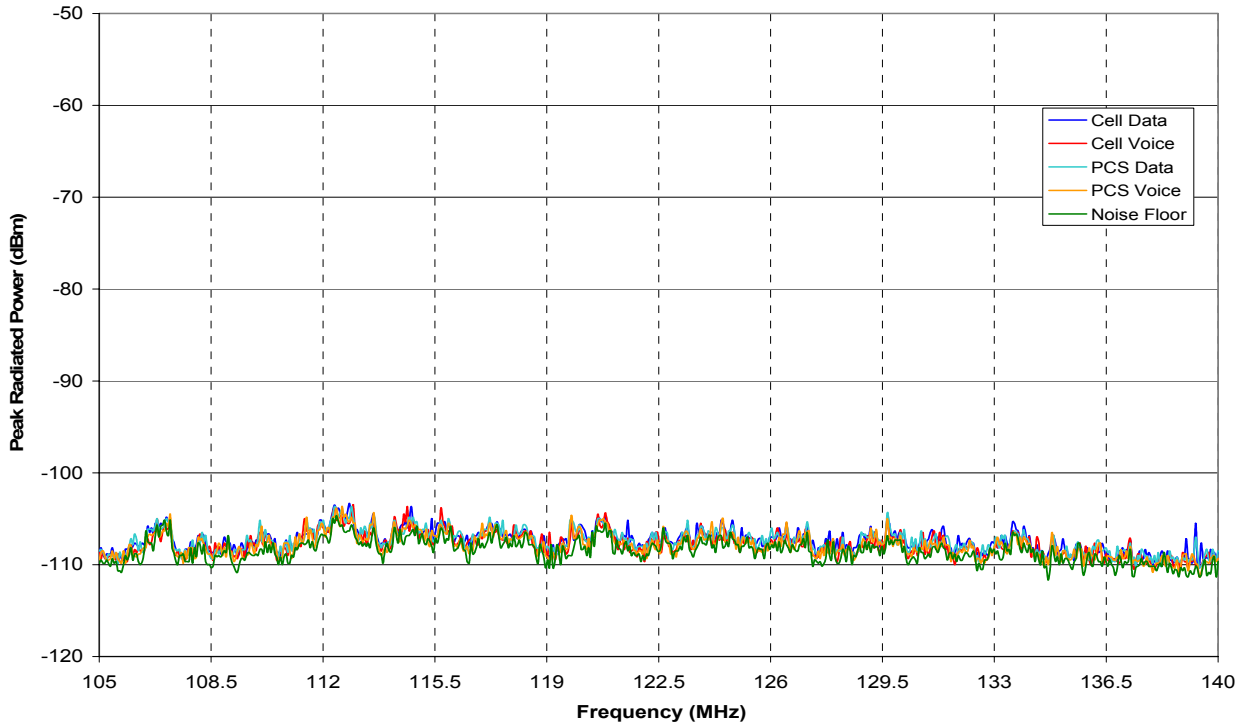


Figure B1: GSM01 four mode envelopes, Band 1.

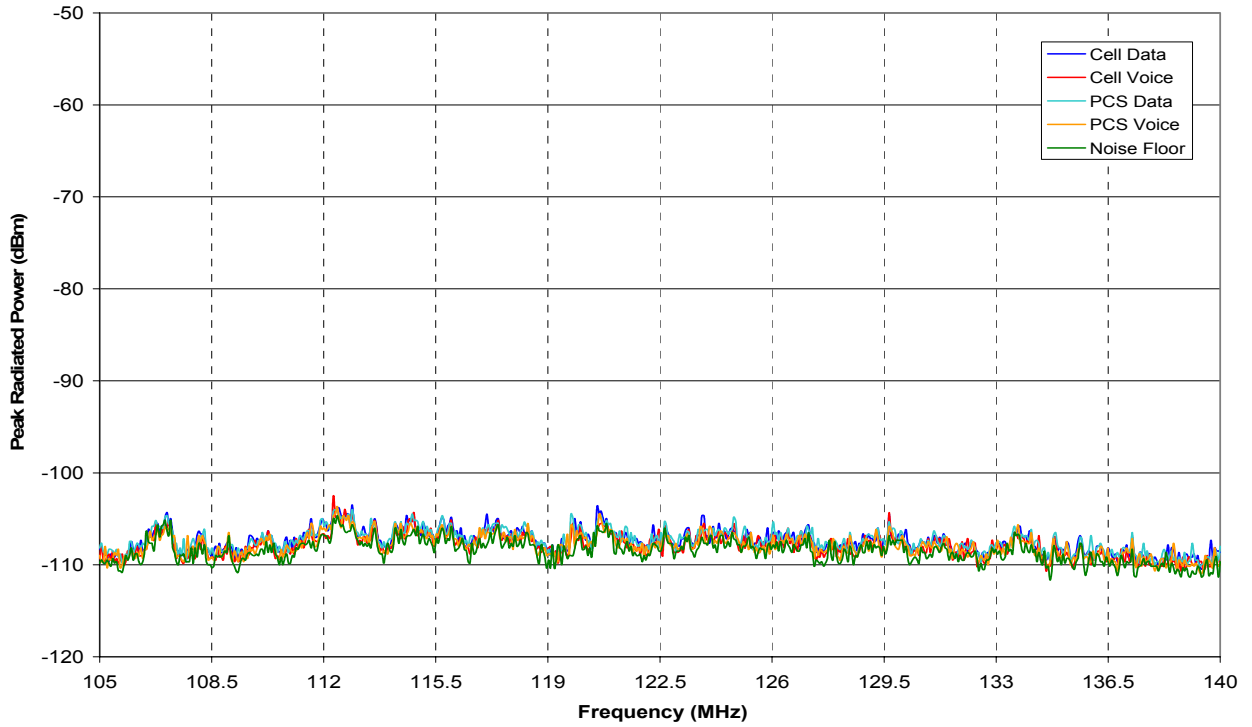


Figure B2: GSM02 four mode envelopes, Band 1.

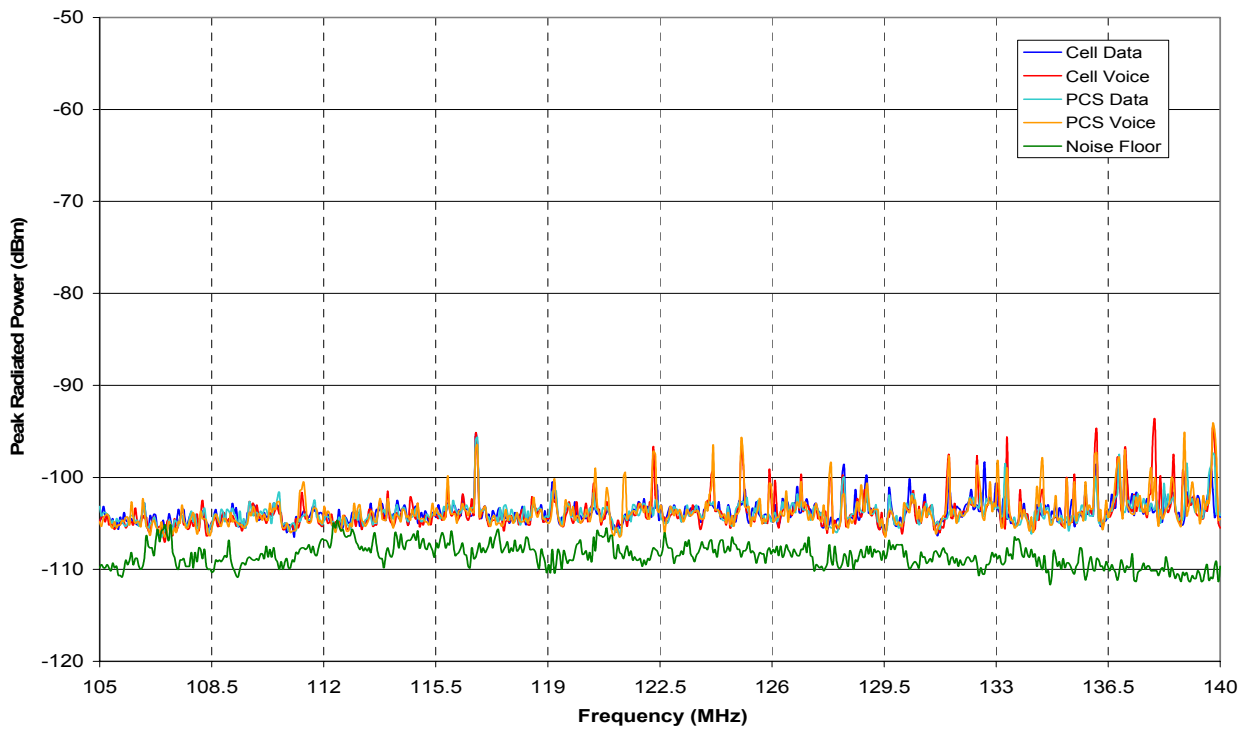


Figure B3: GSM03 four mode envelopes, Band 1.

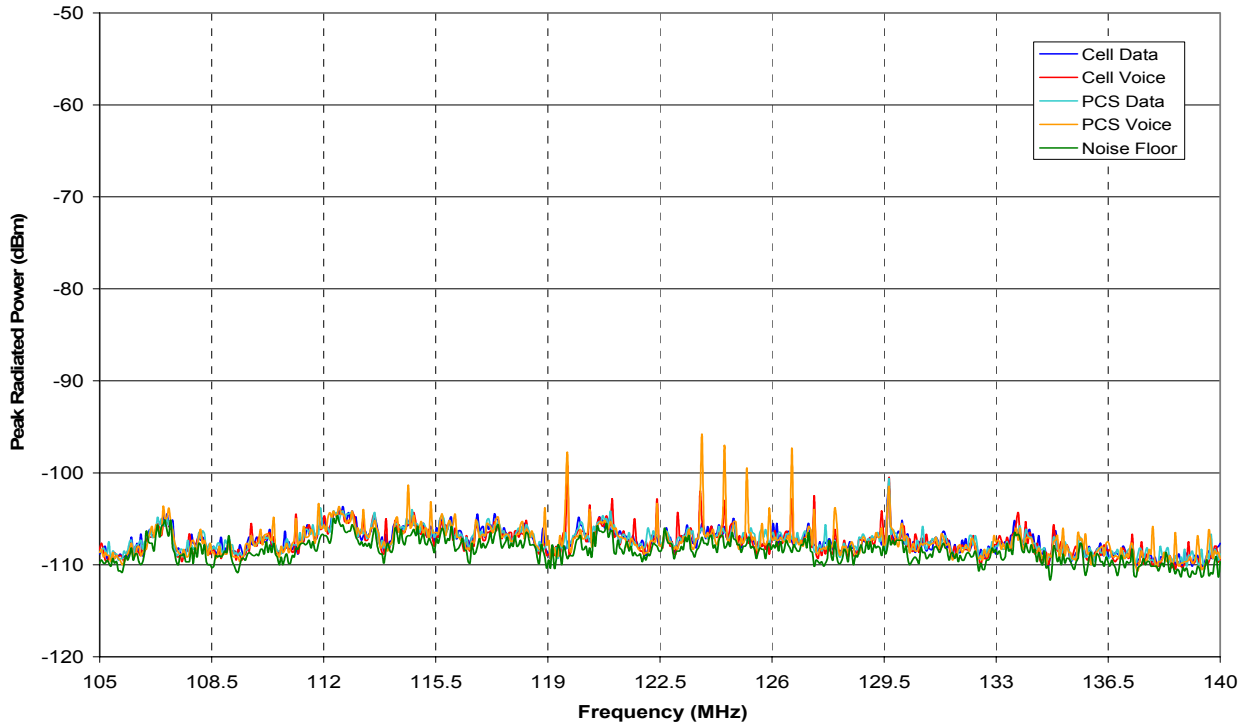


Figure B4: GSM04 four mode envelopes, Band 1.

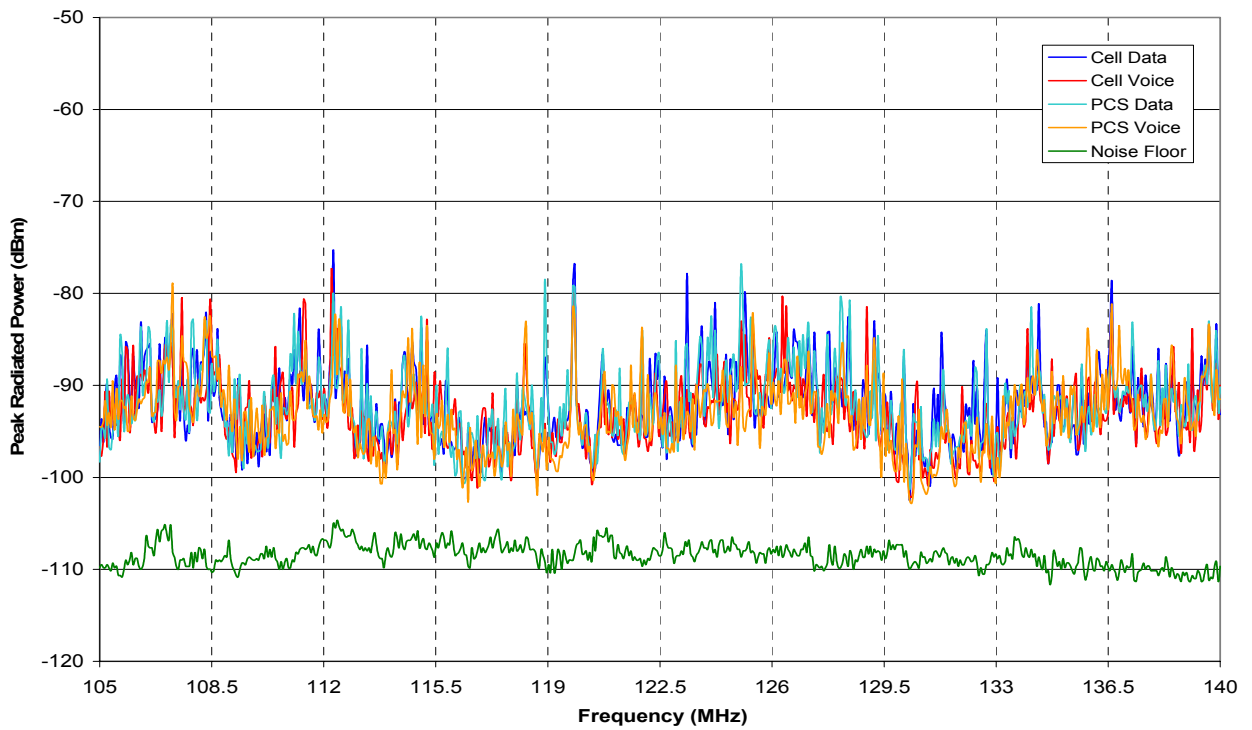


Figure B5: GSM05 Four mode envelopes, Band 1.

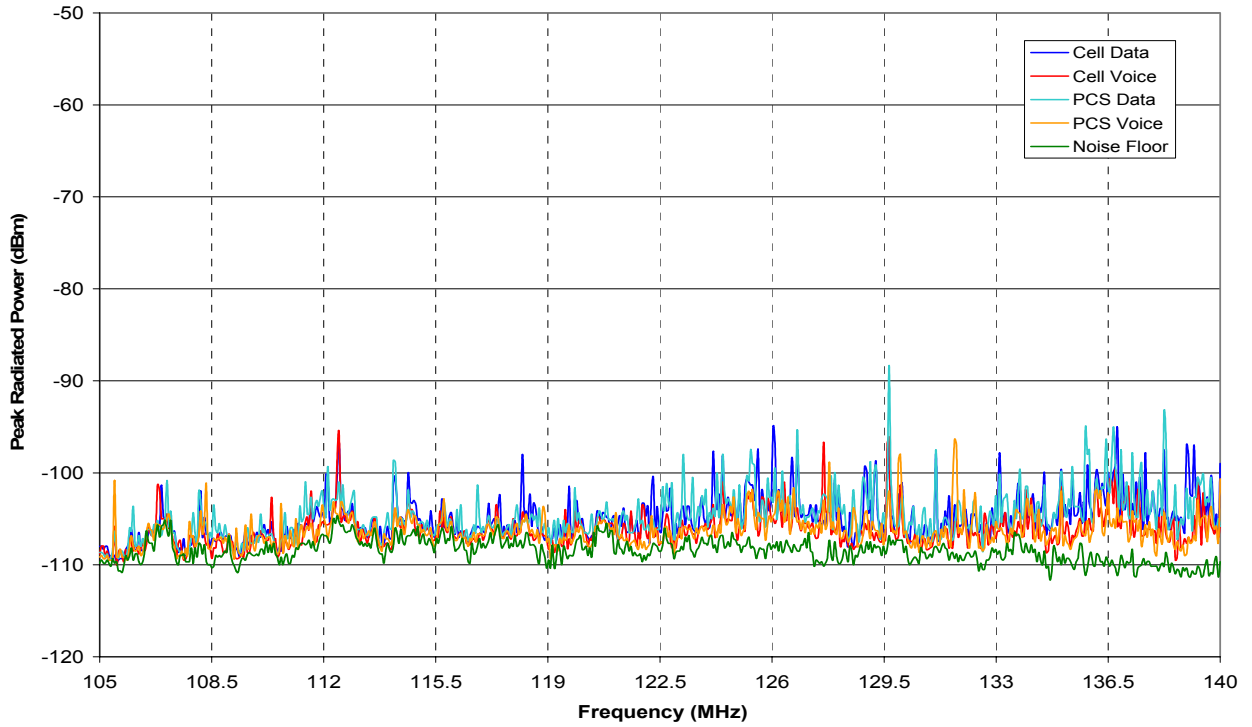


Figure B6: GSM06 four mode envelopes, Band 1.

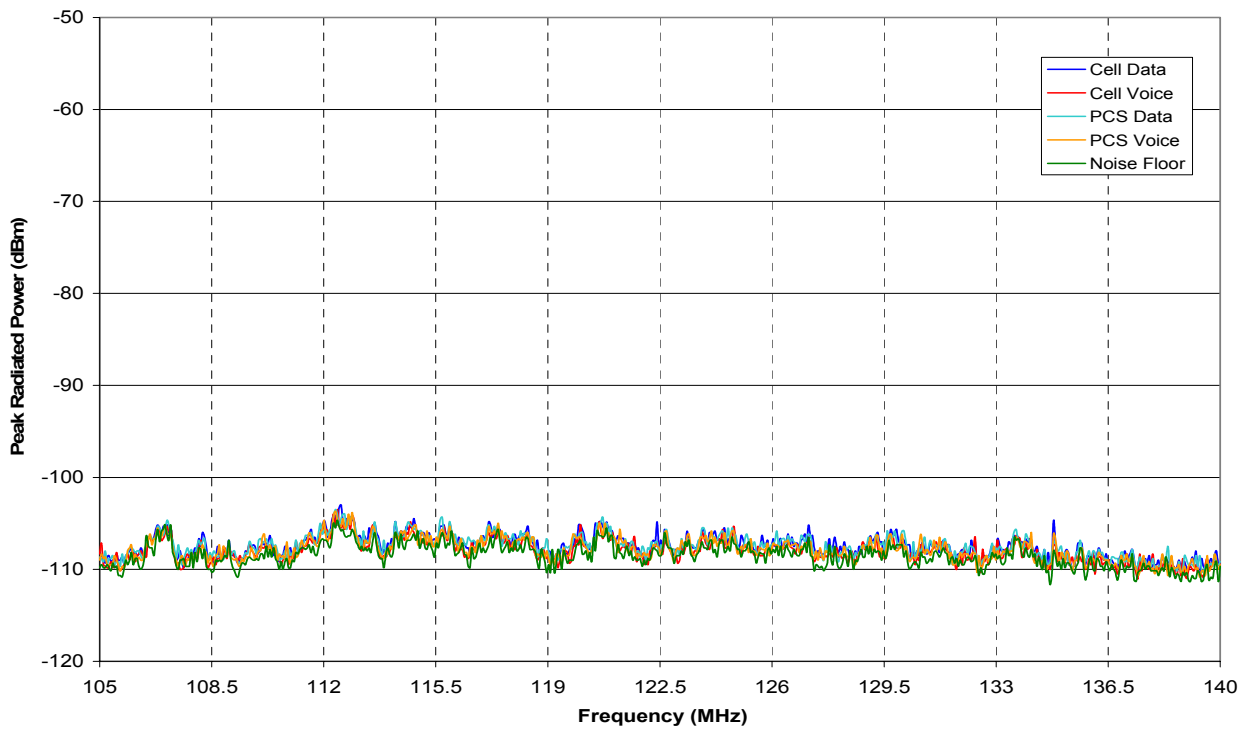


Figure B7: GSM four mode envelopes, Band 1.

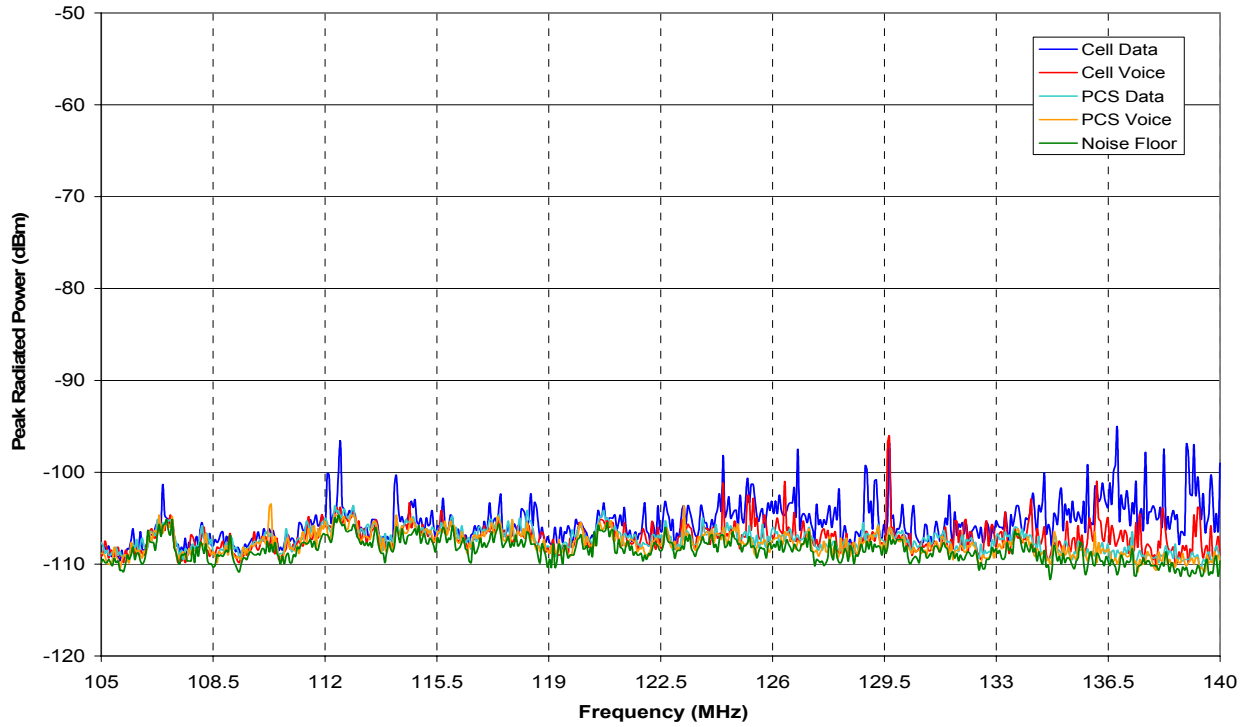


Figure B8: GSM08 four mode envelopes, Band 1.

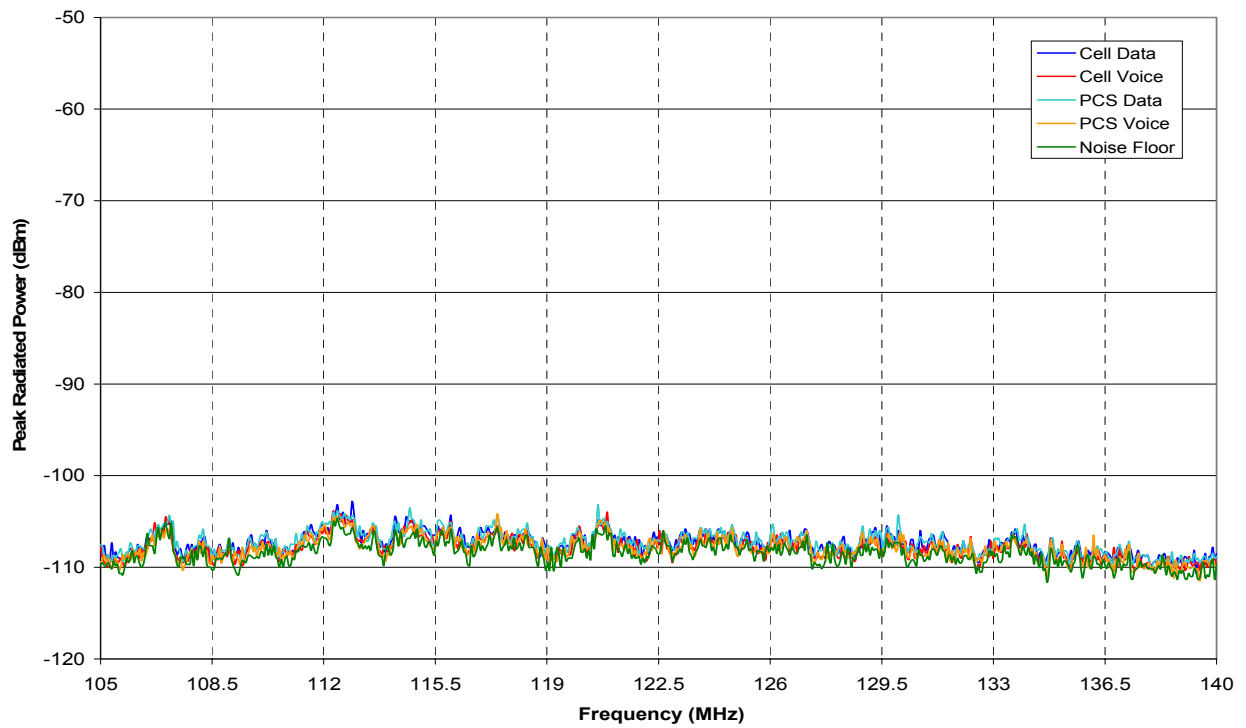


Figure B9: GSM09 four mode envelopes, Band 1.

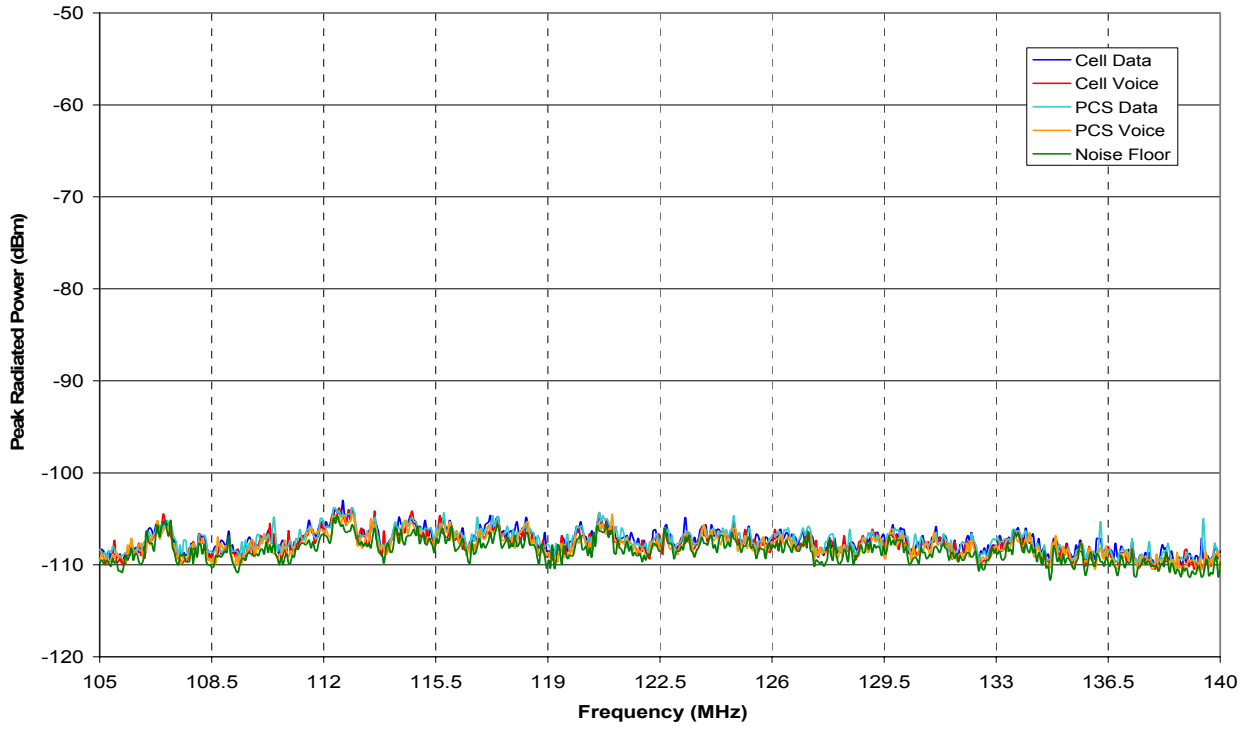


Figure B10: GSM10 four mode envelopes, Band 1.

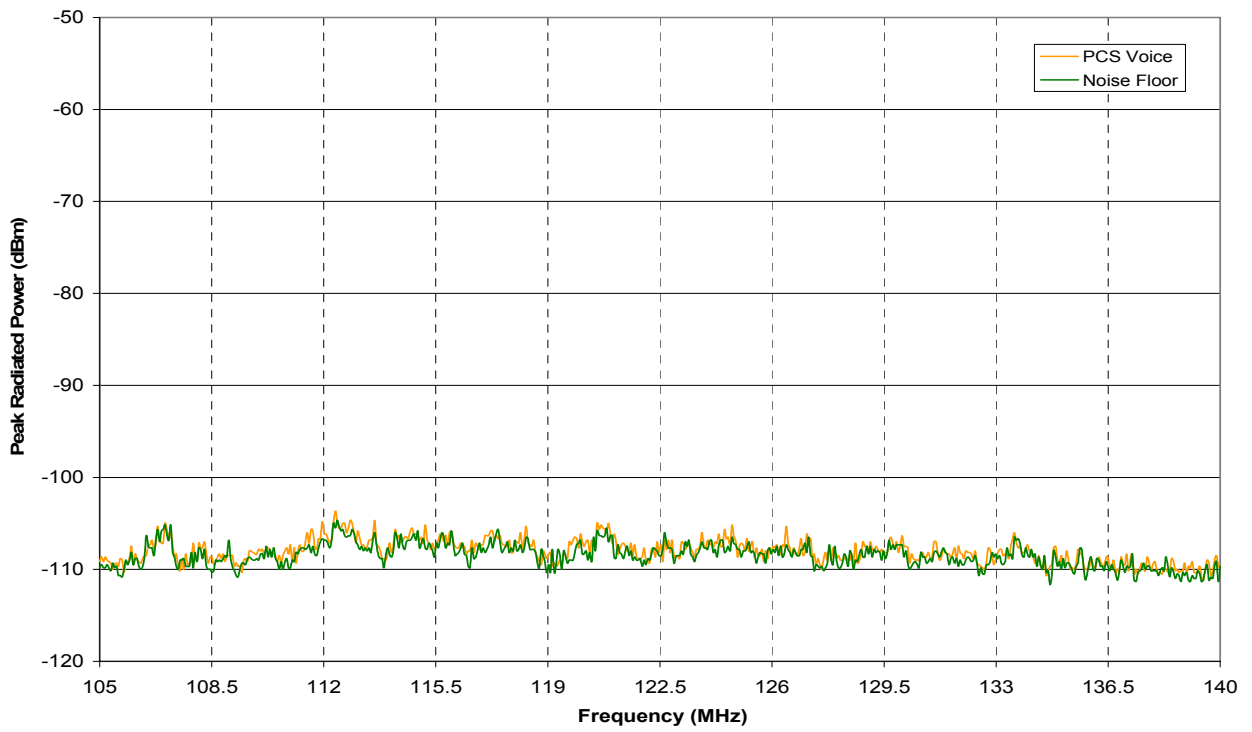


Figure B11: GSM11 four mode envelopes, Band 1.

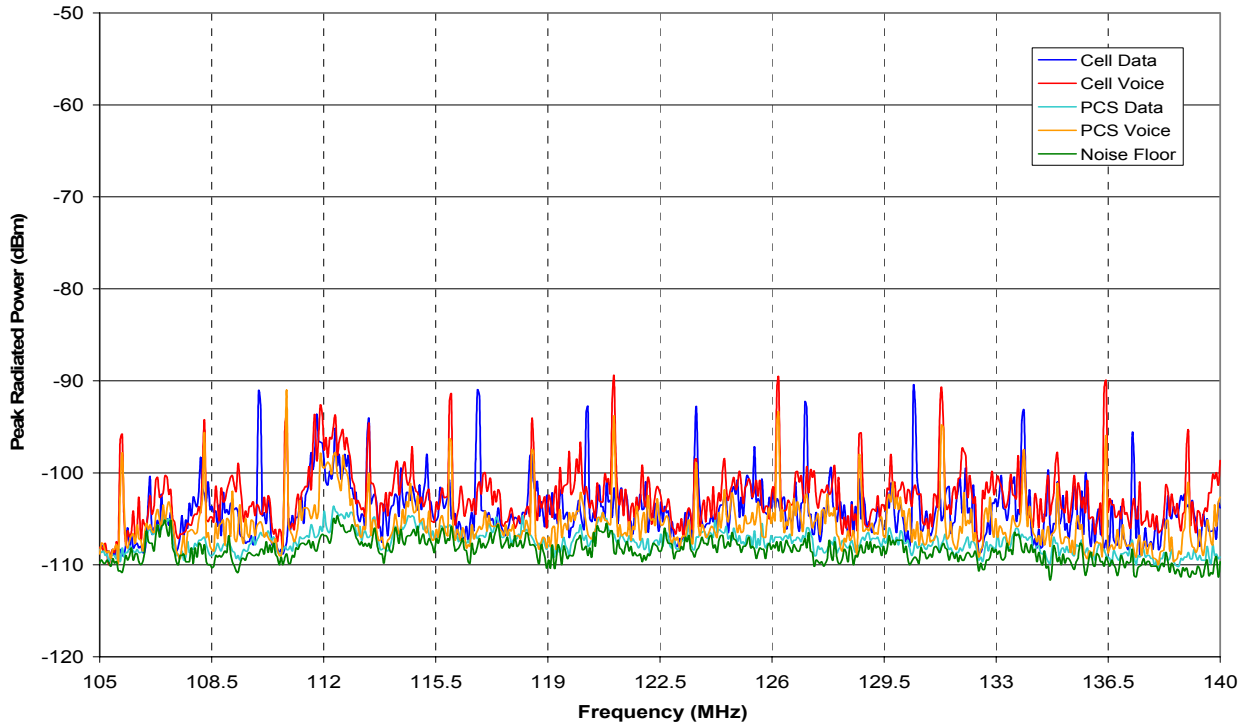


Figure B12: GSM12 four mode envelopes, Band 1.

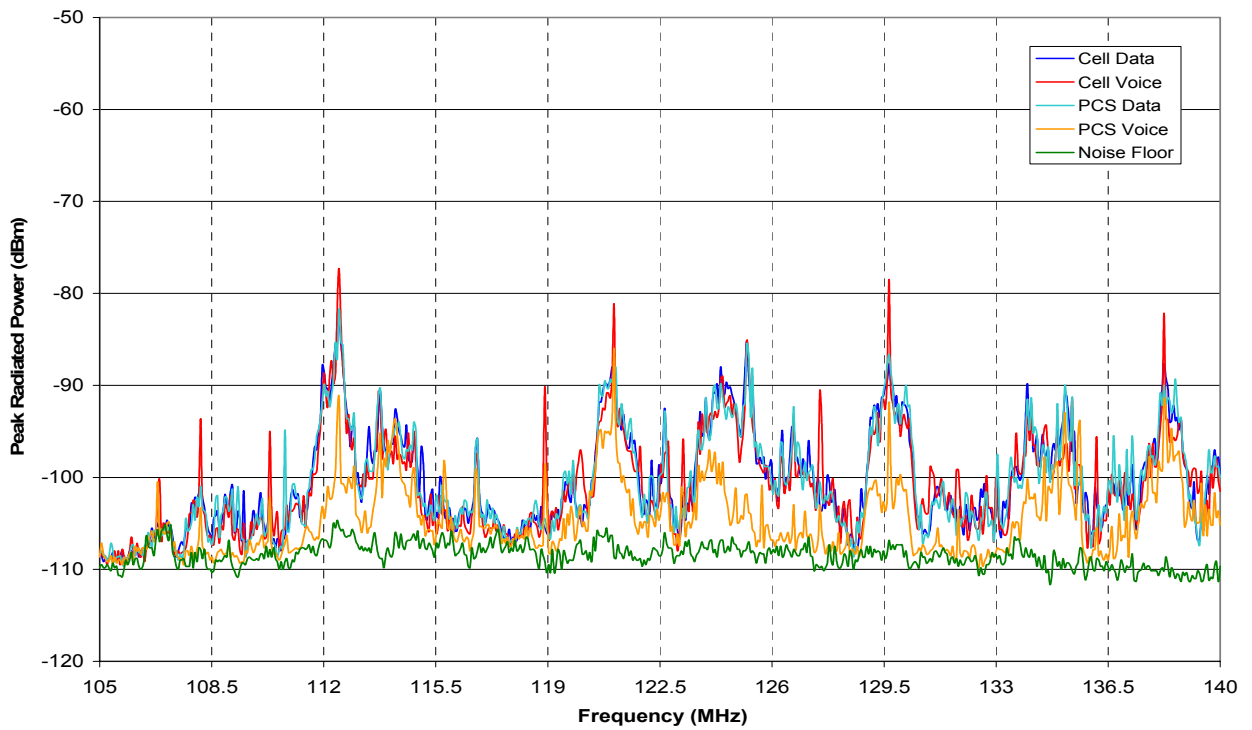


Figure B13: GSM13 four mode envelopes, Band 1.

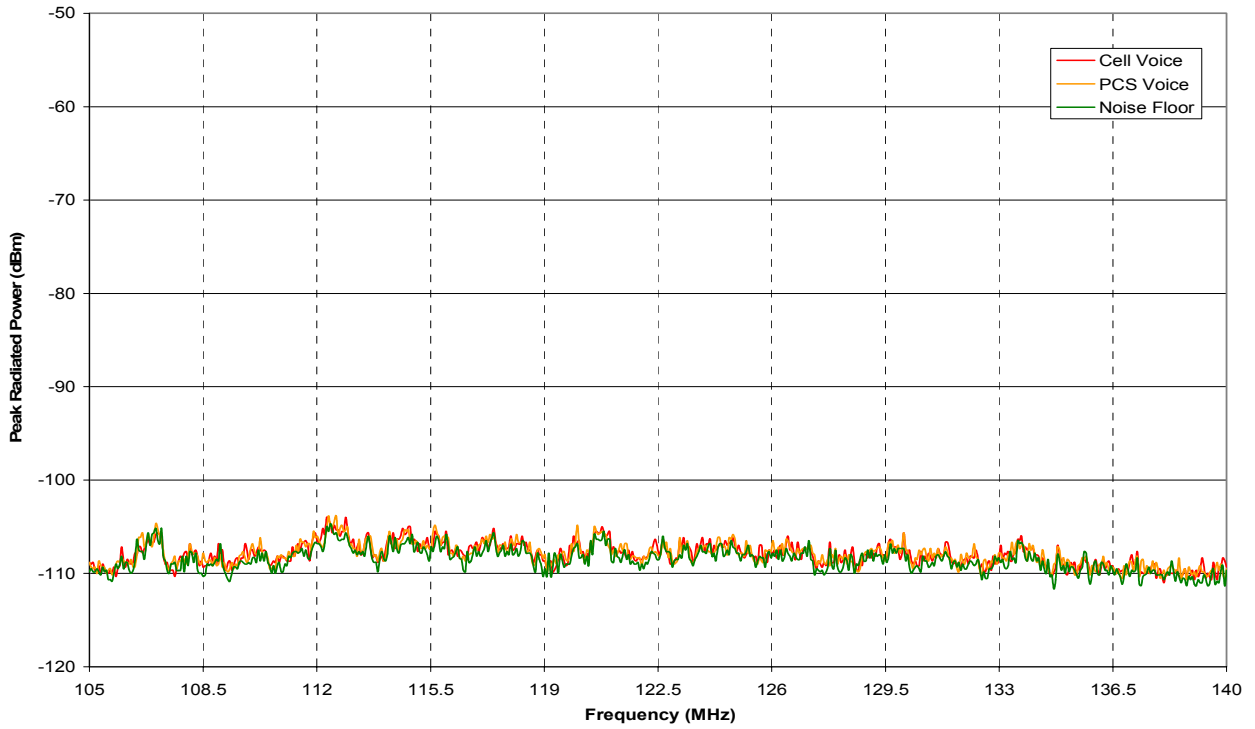


Figure B14: GSM14 two mode envelopes, Band 1.

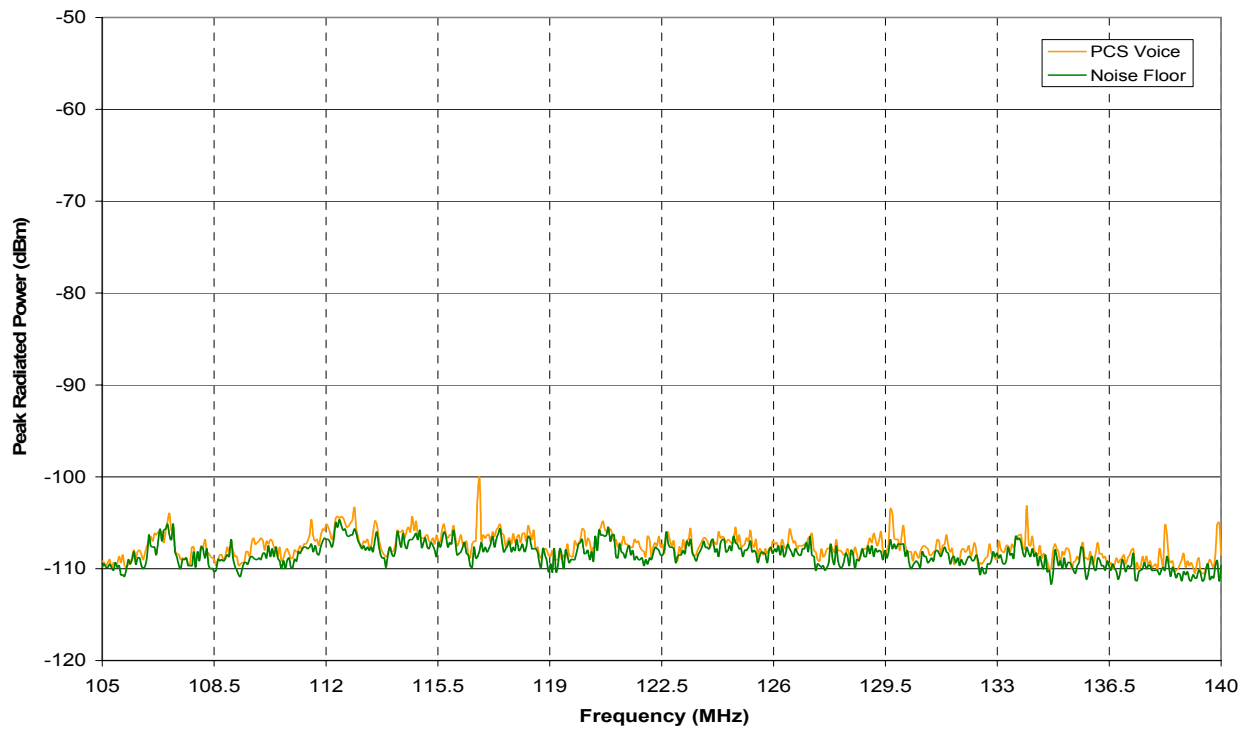


Figure B15: GSM15 one mode envelope, Band 1.

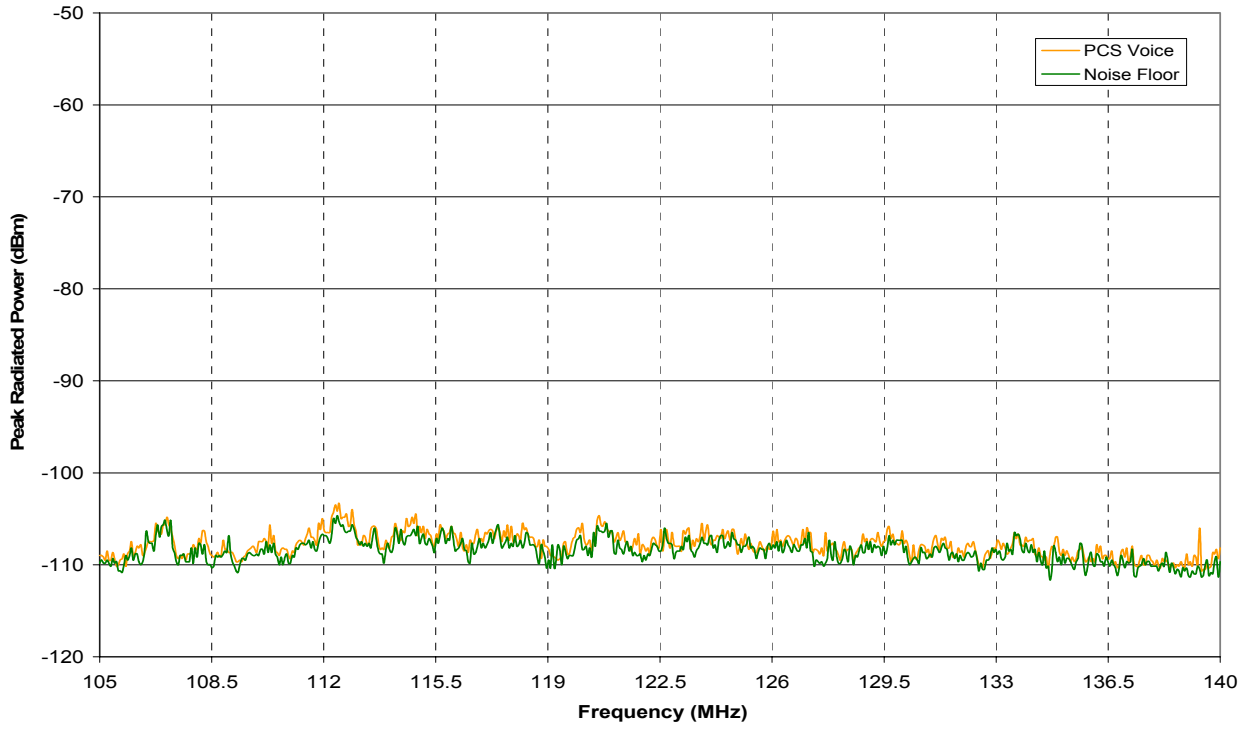


Figure B16: GSM16 one mode envelope, Band 1.

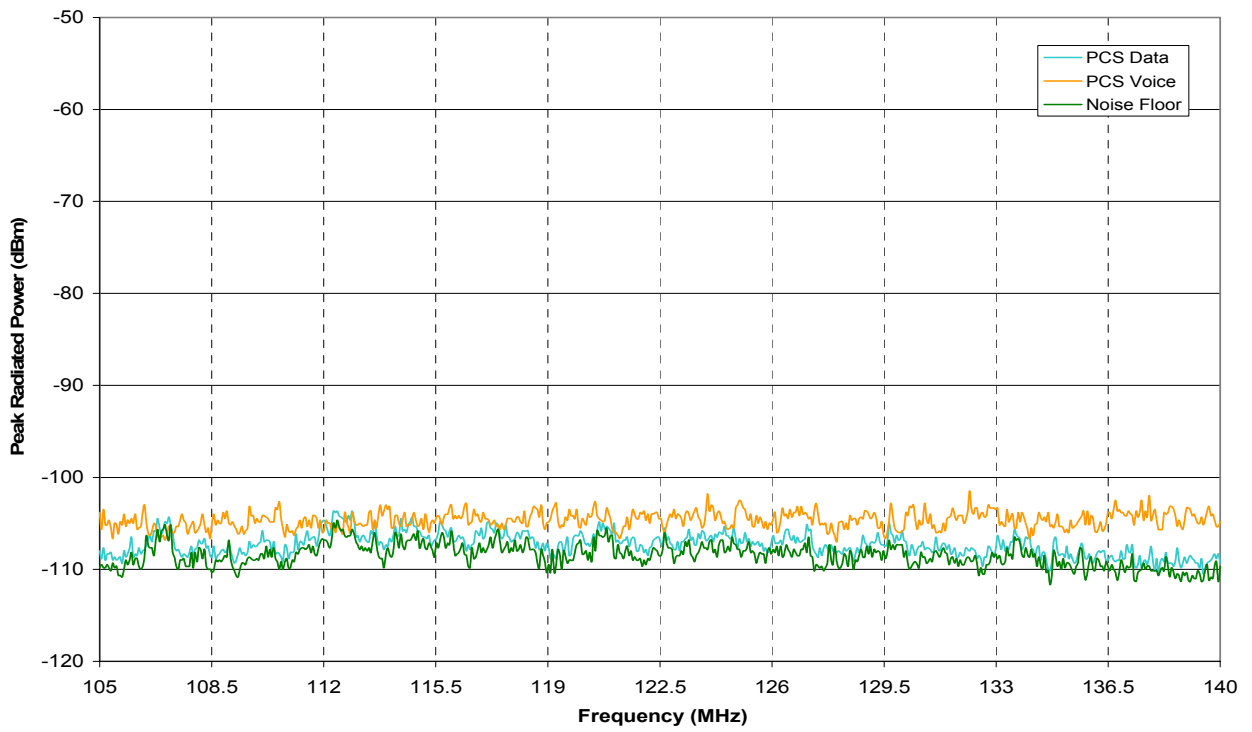


Figure B17: GSM17 two mode envelope, Band 1.

B.2 Band 2

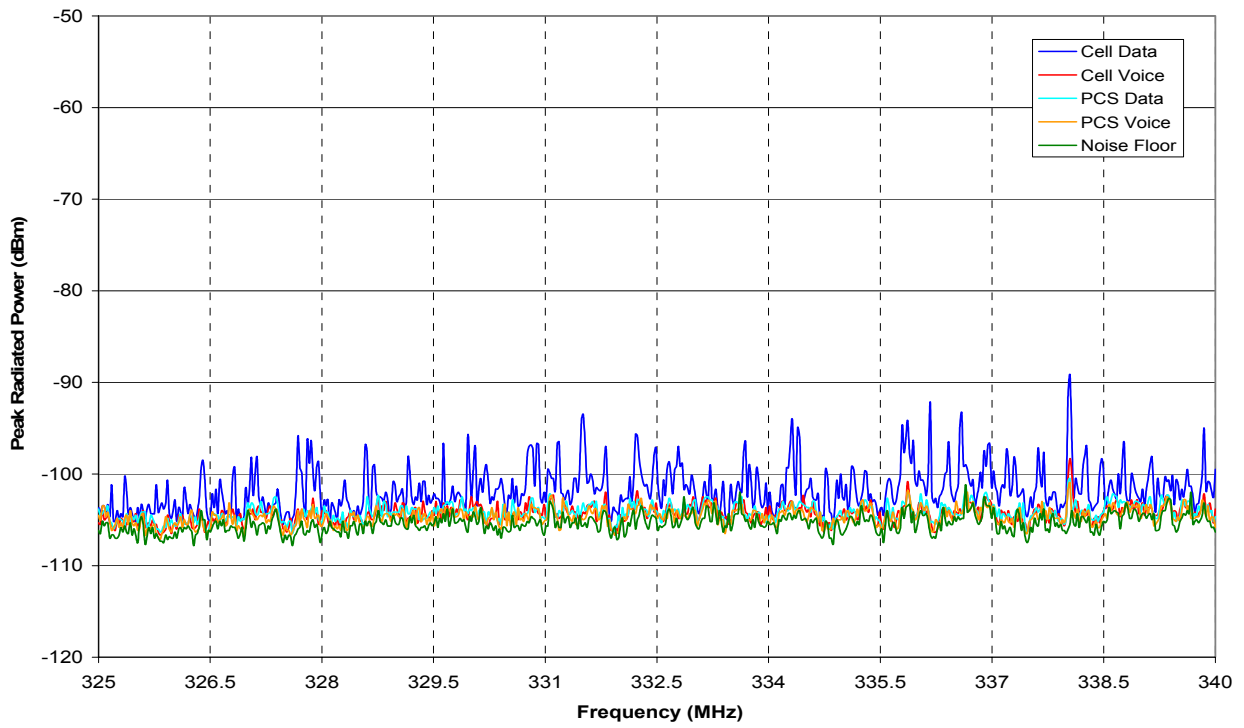


Figure B18: GSM01 four mode envelopes, Band 2.

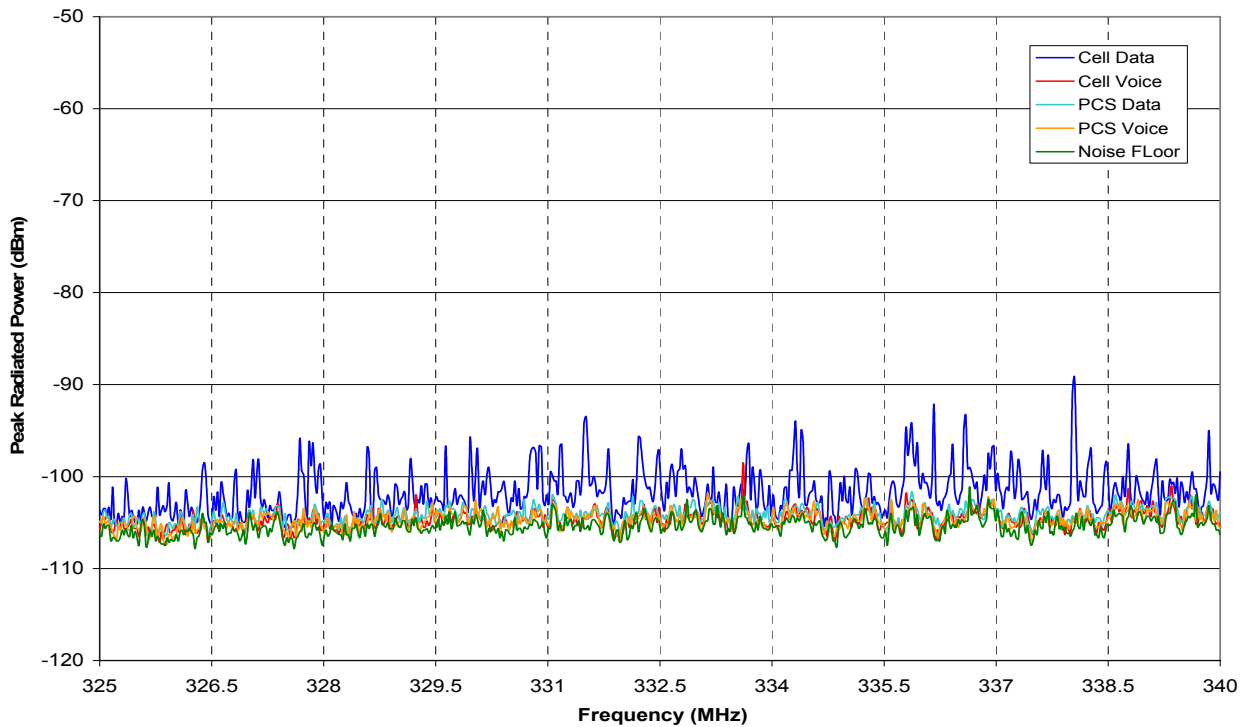


Figure B19: GSM02 four mode envelopes, Band 2.

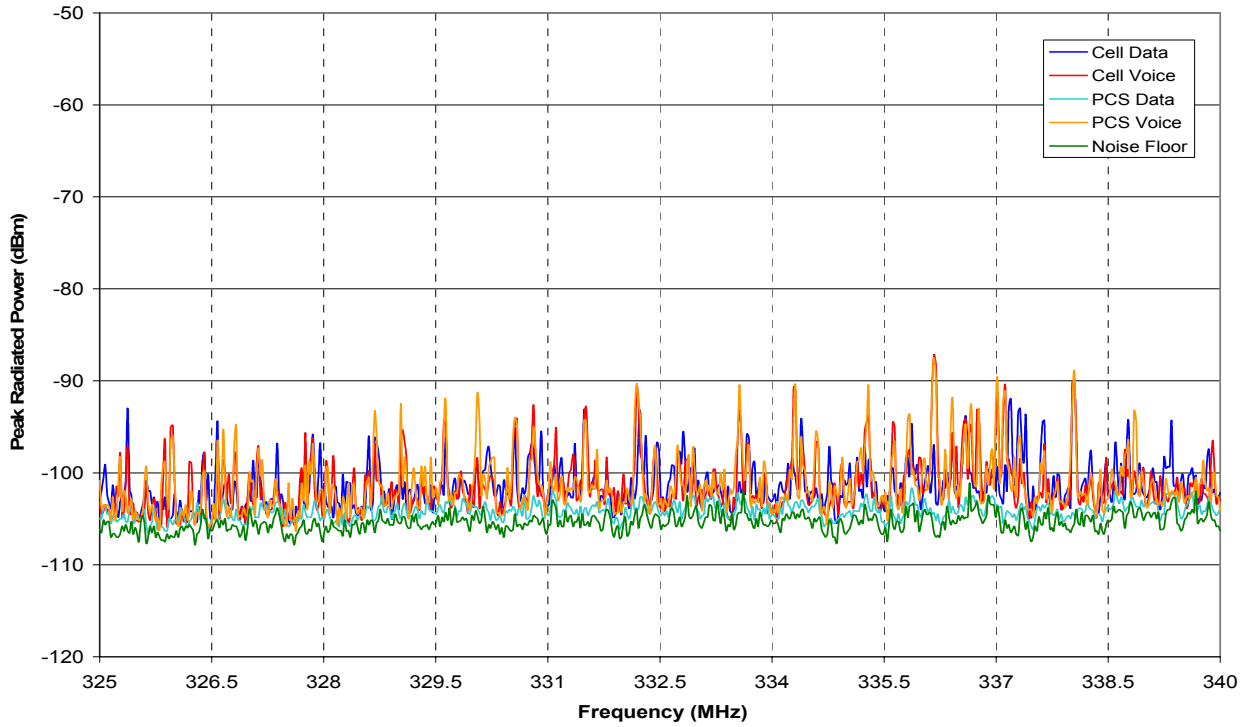


Figure B20: GSM03 four mode envelopes, Band 2.

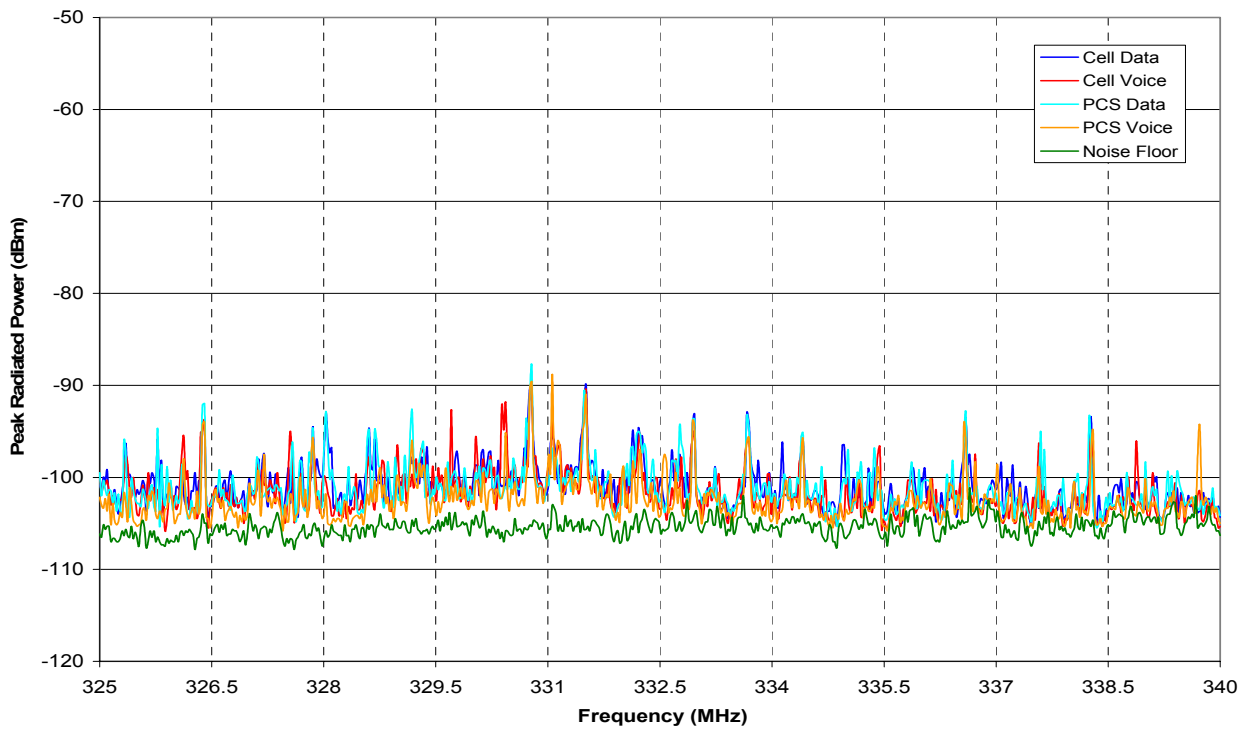


Figure B21: GSM04 four mode envelopes, Band 2.

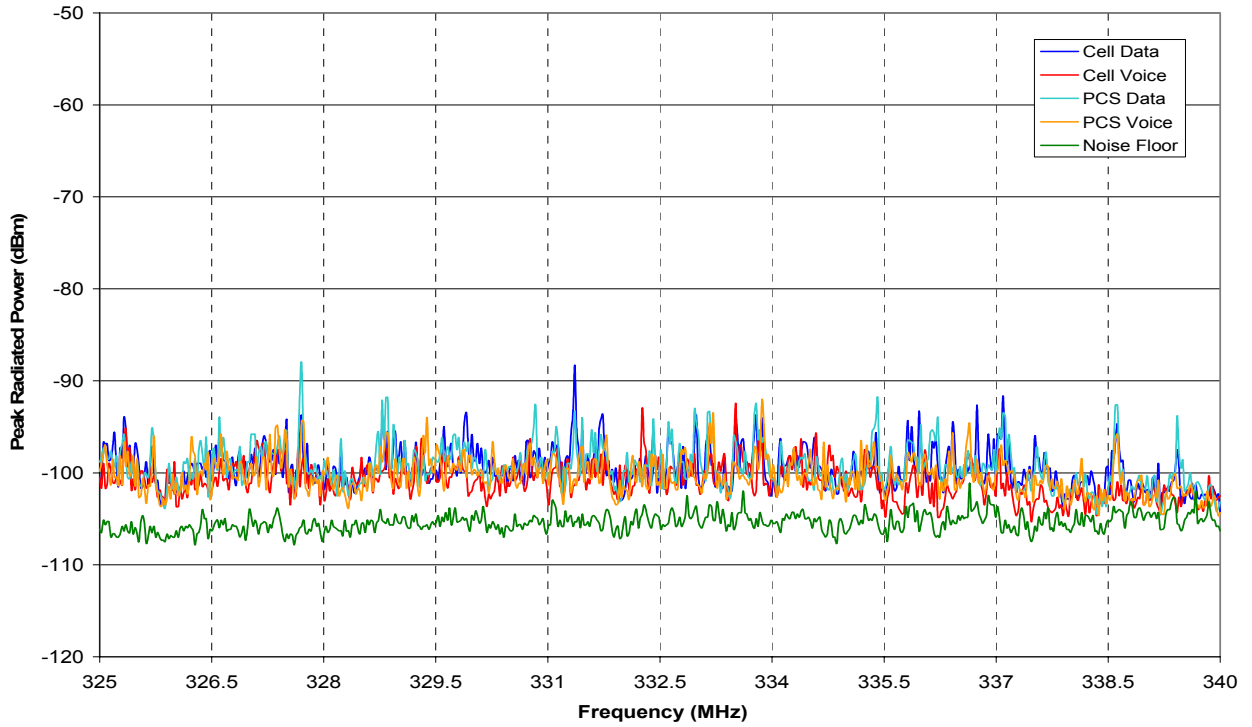


Figure B22: GSM05 four mode envelopes, Band 2.

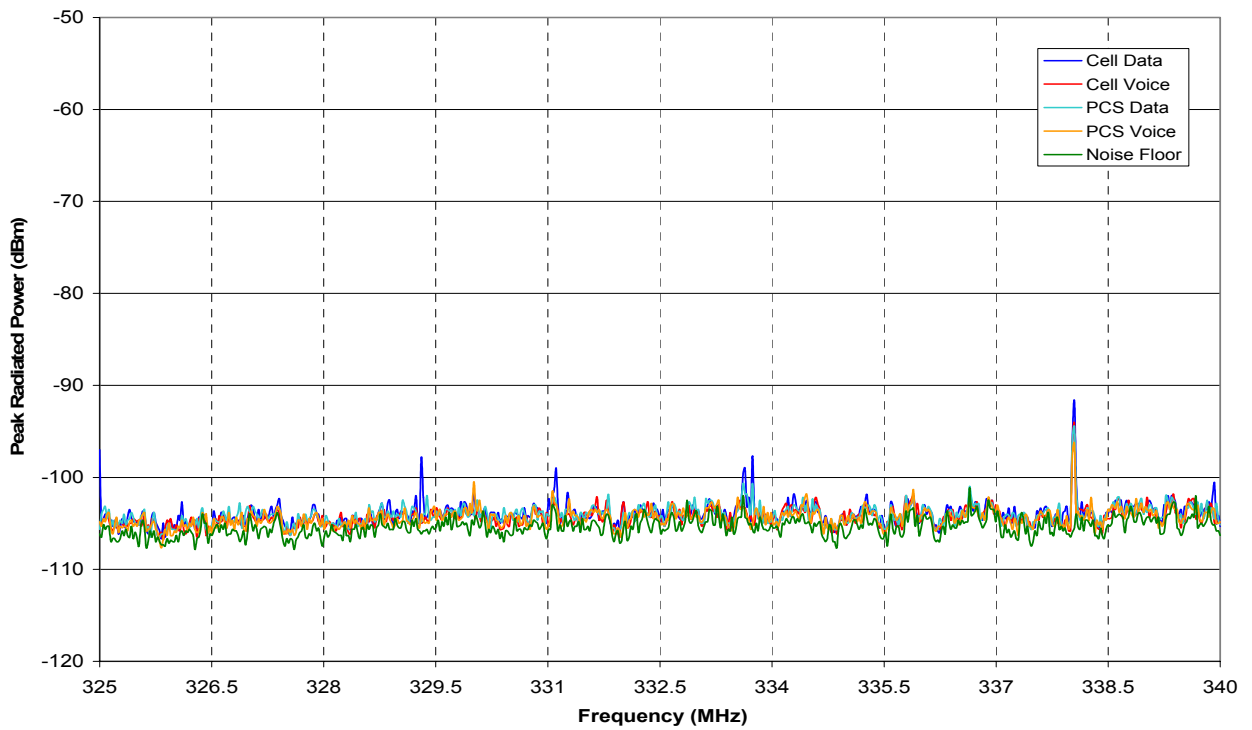


Figure B23: GSM06 four mode envelopes, Band 2.

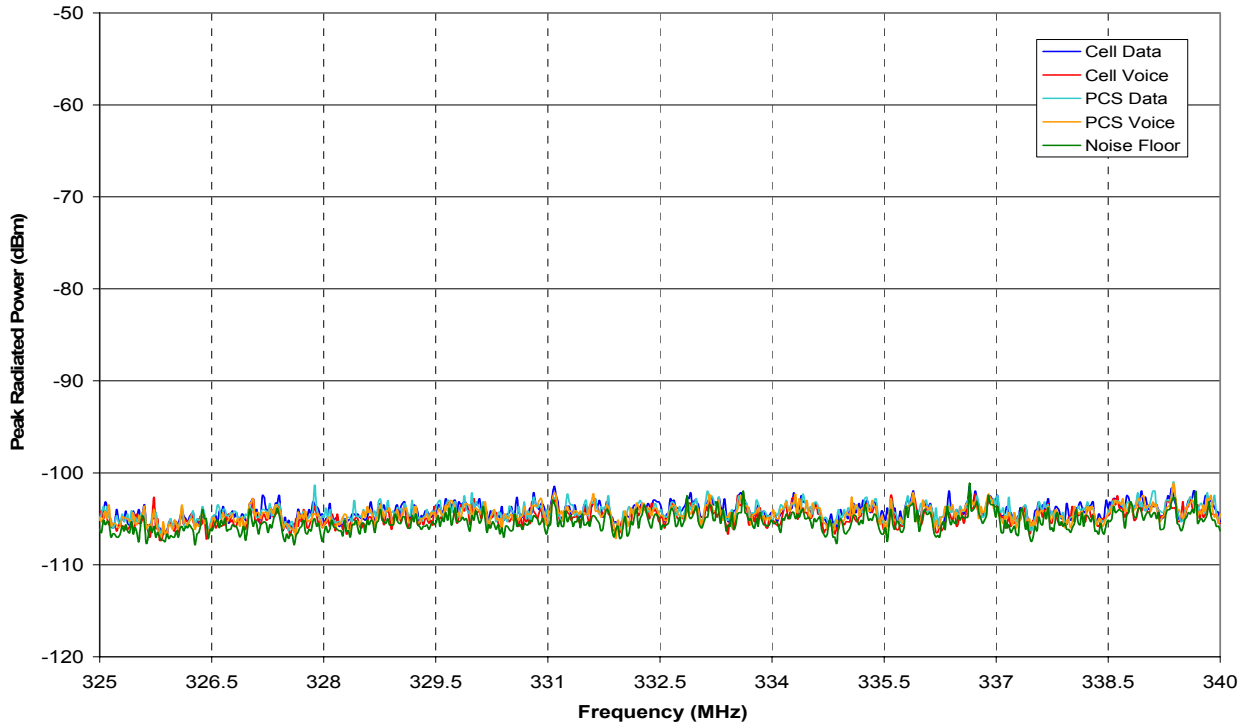


Figure B24: GSM07 four mode envelopes, Band 2.

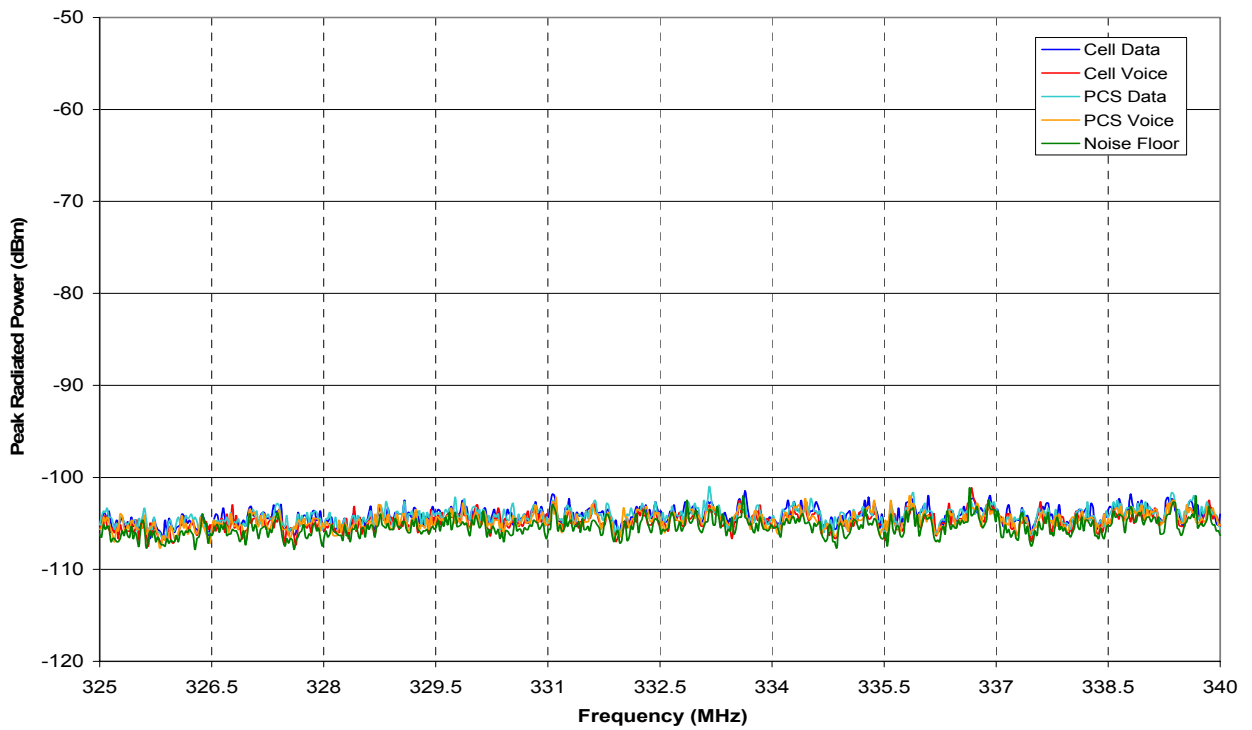


Figure B25: GSM08 four mode envelopes, Band 2.

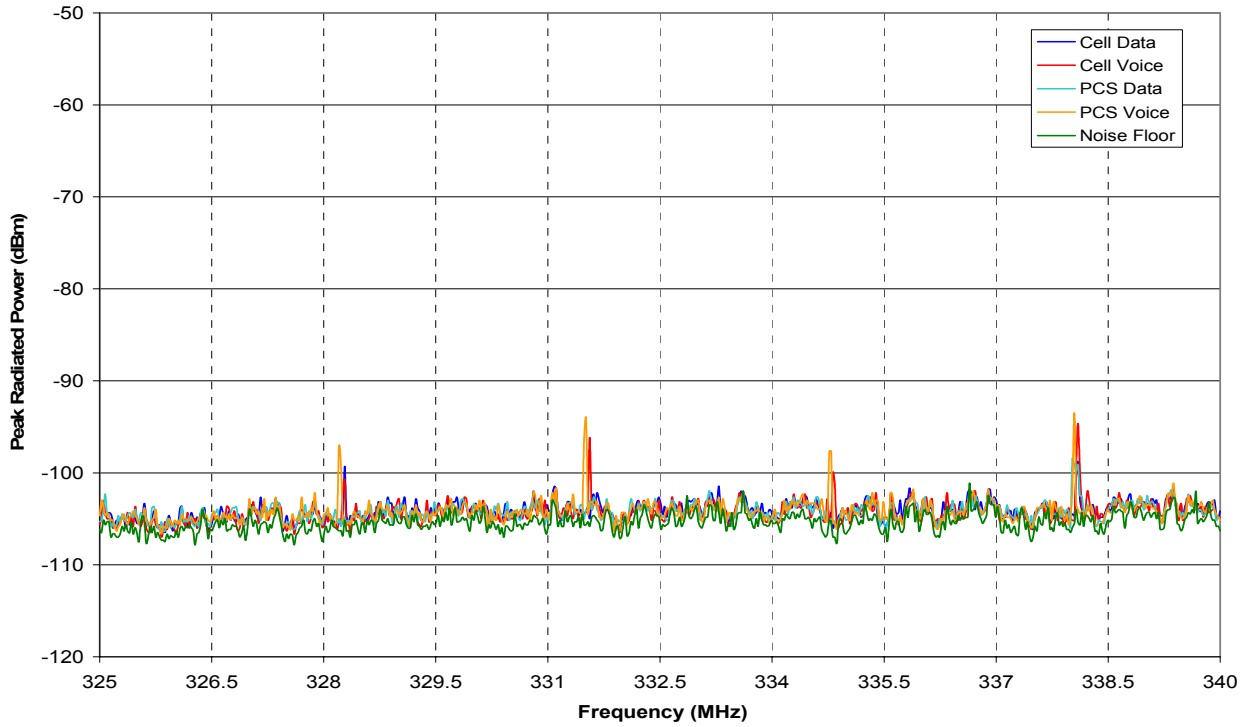


Figure B26: GSM09 four mode envelopes, Band 2.

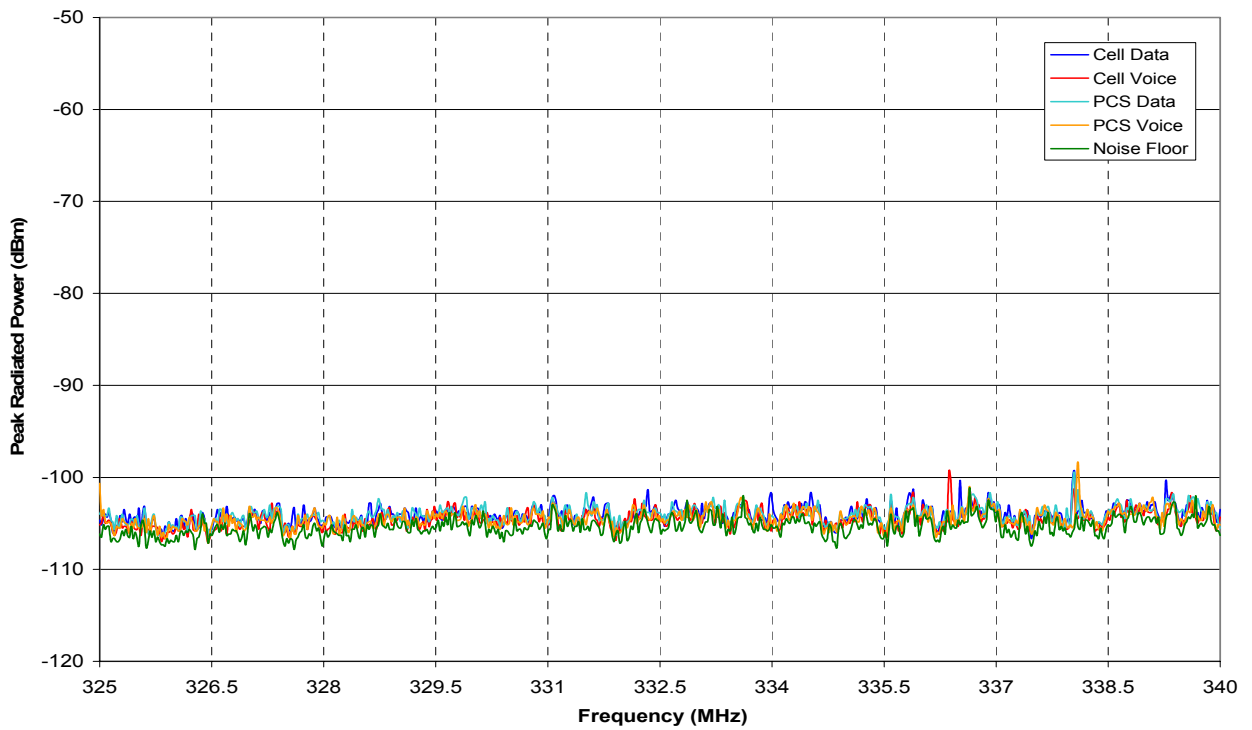


Figure B27: GSM10 four mode envelopes, Band 2.

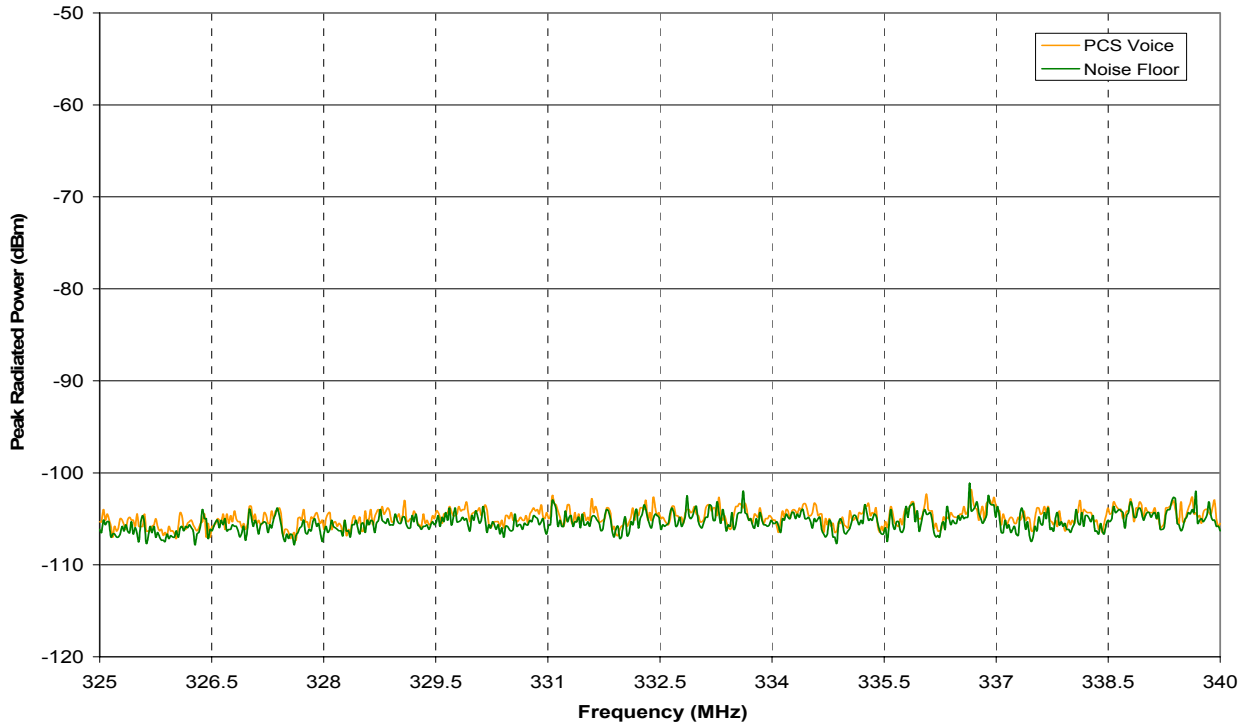


Figure B28: GSM11 one mode envelope, Band 2.

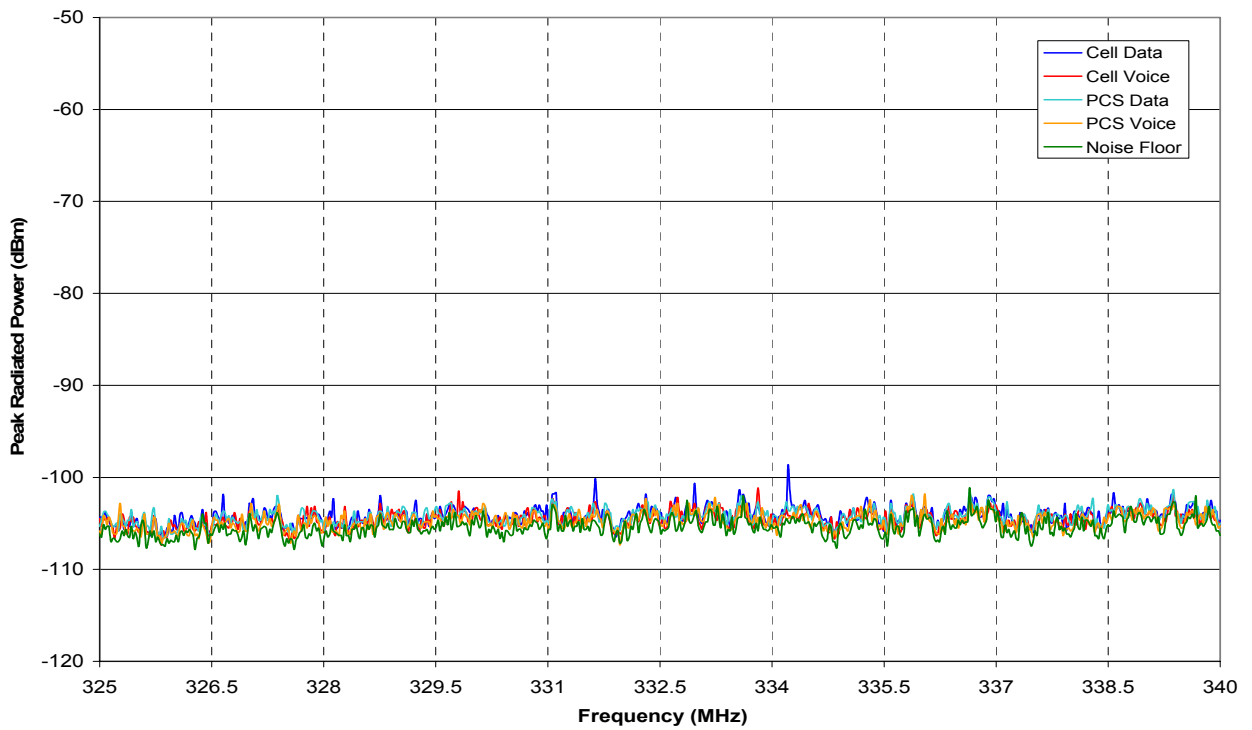


Figure B29: GSM12 four mode envelopes, Band 2.

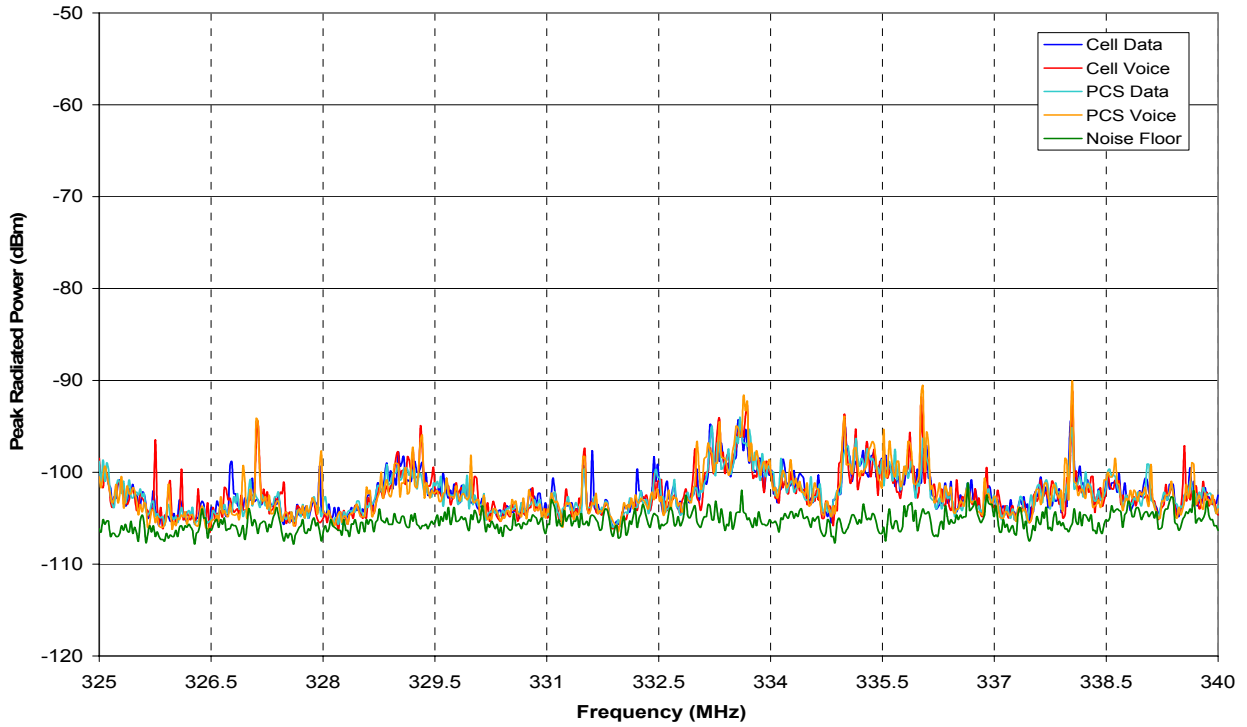


Figure B30: GSM13 four mode envelopes, Band 2.

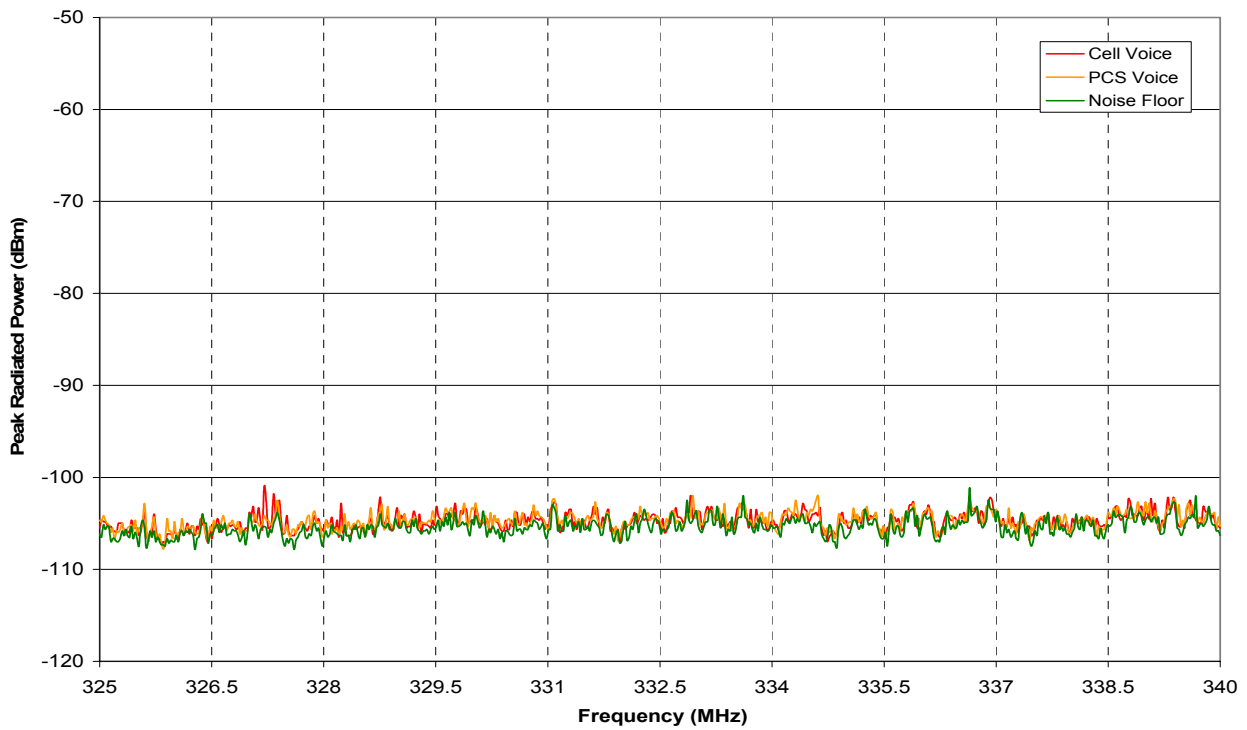


Figure B31: GSM14 two mode envelopes, Band 2.

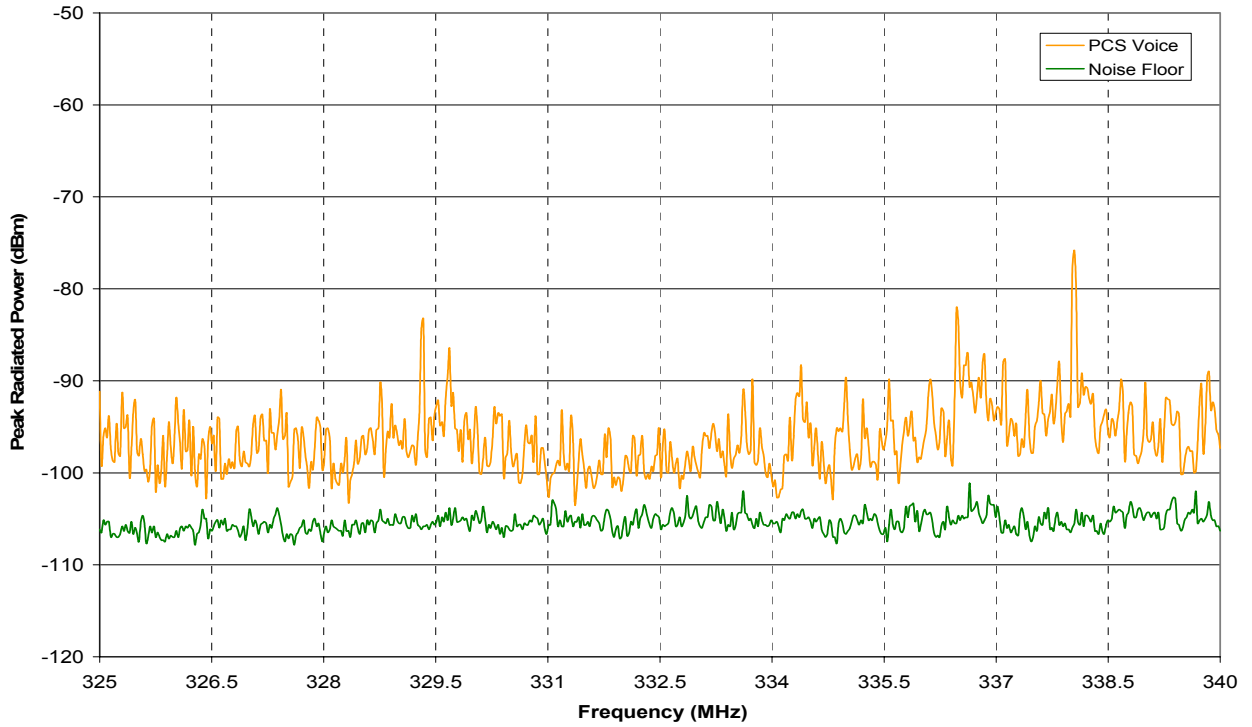


Figure B32: GSM15 one mode envelope, Band 2.

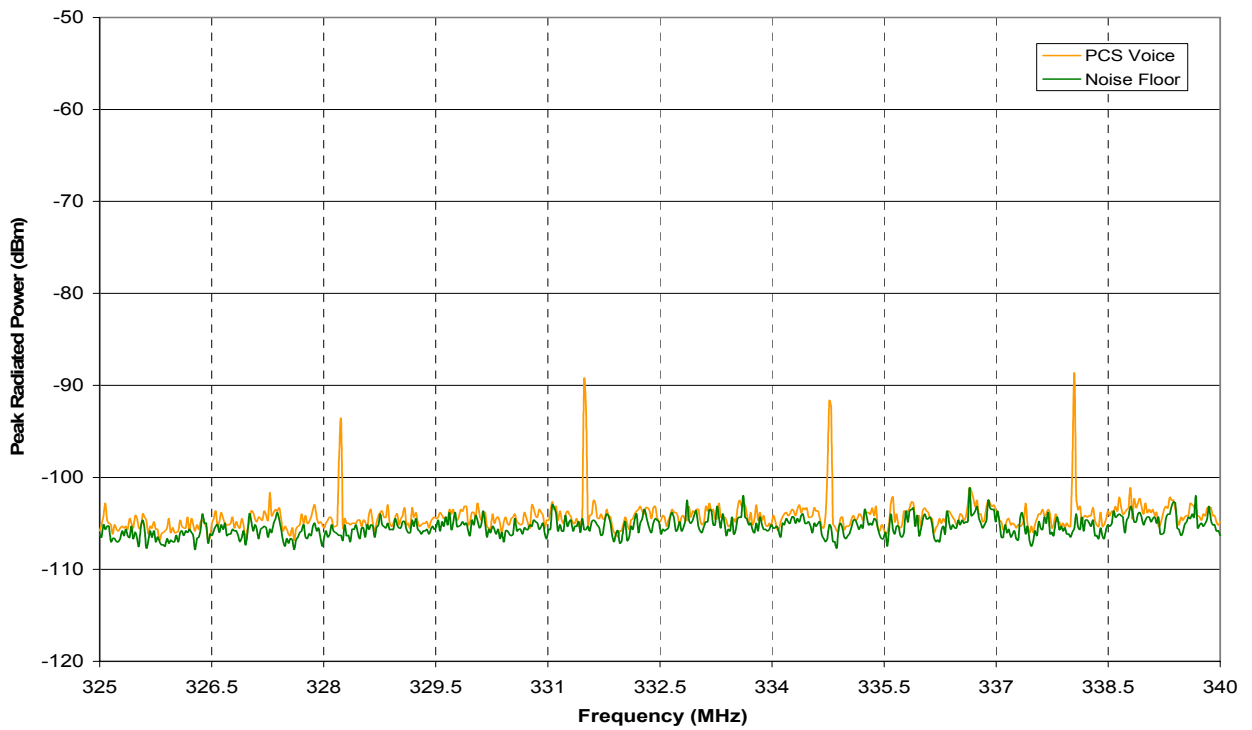


Figure B33: GSM16 one mode envelope, Band 2.

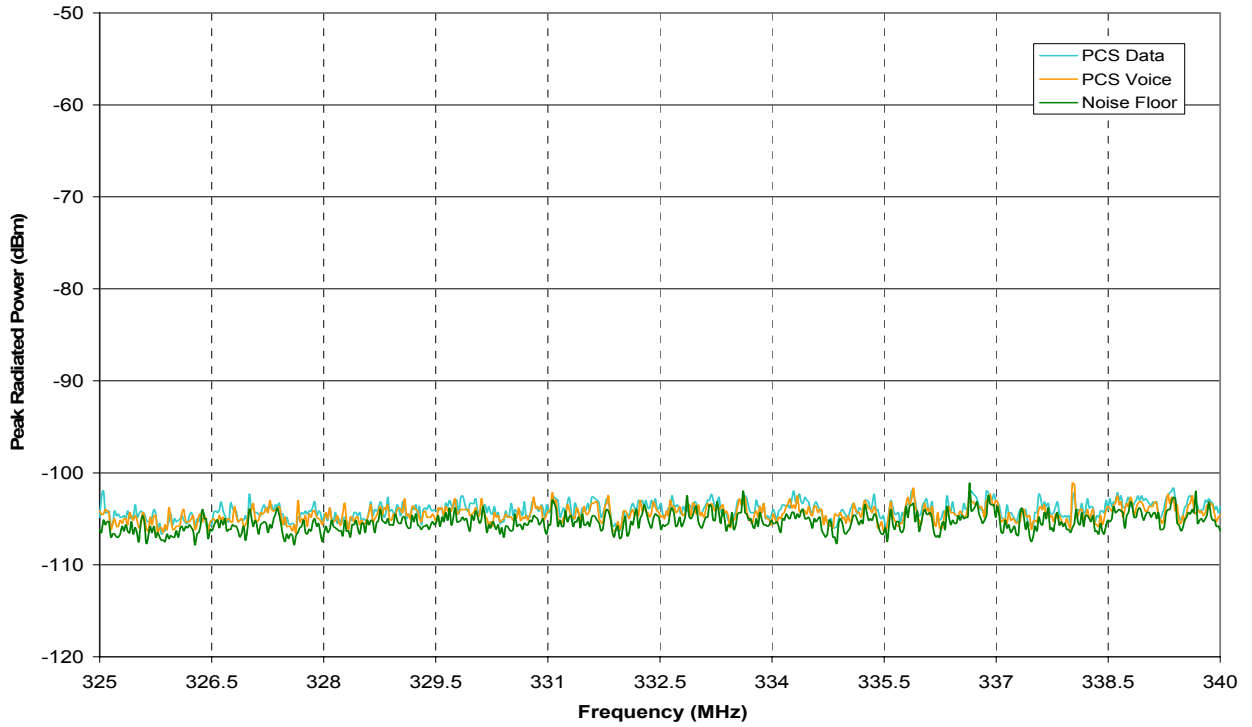


Figure B34: GSM17 two mode envelopes, Band 2.

B.3 Band 3

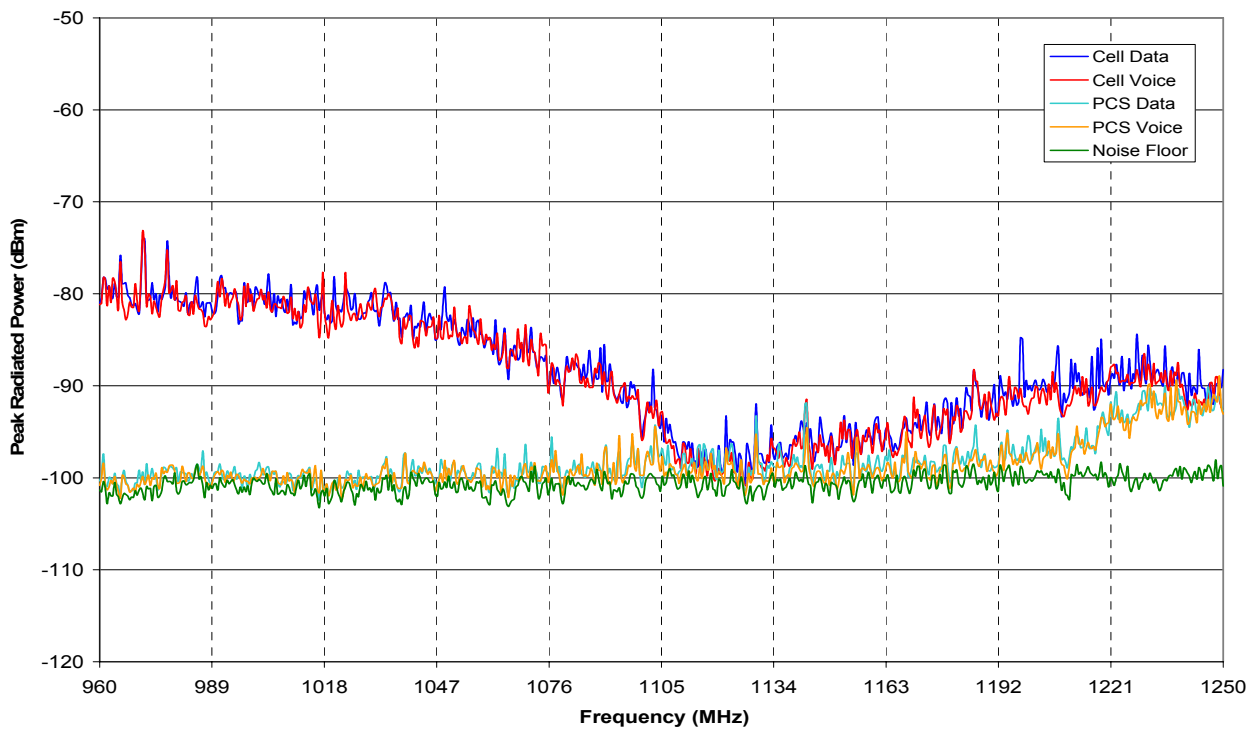


Figure B35: GSM01 four mode envelopes, Band 2.

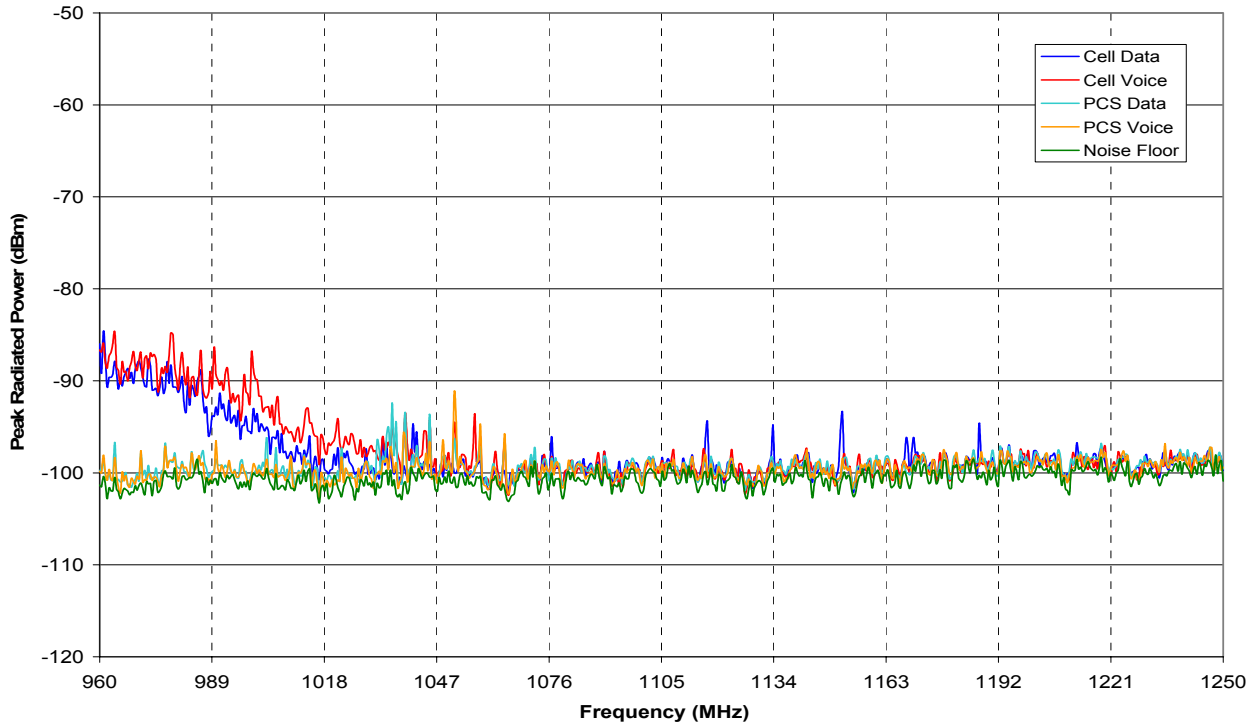


Figure B36: GSM02 four mode envelopes, Band 3.

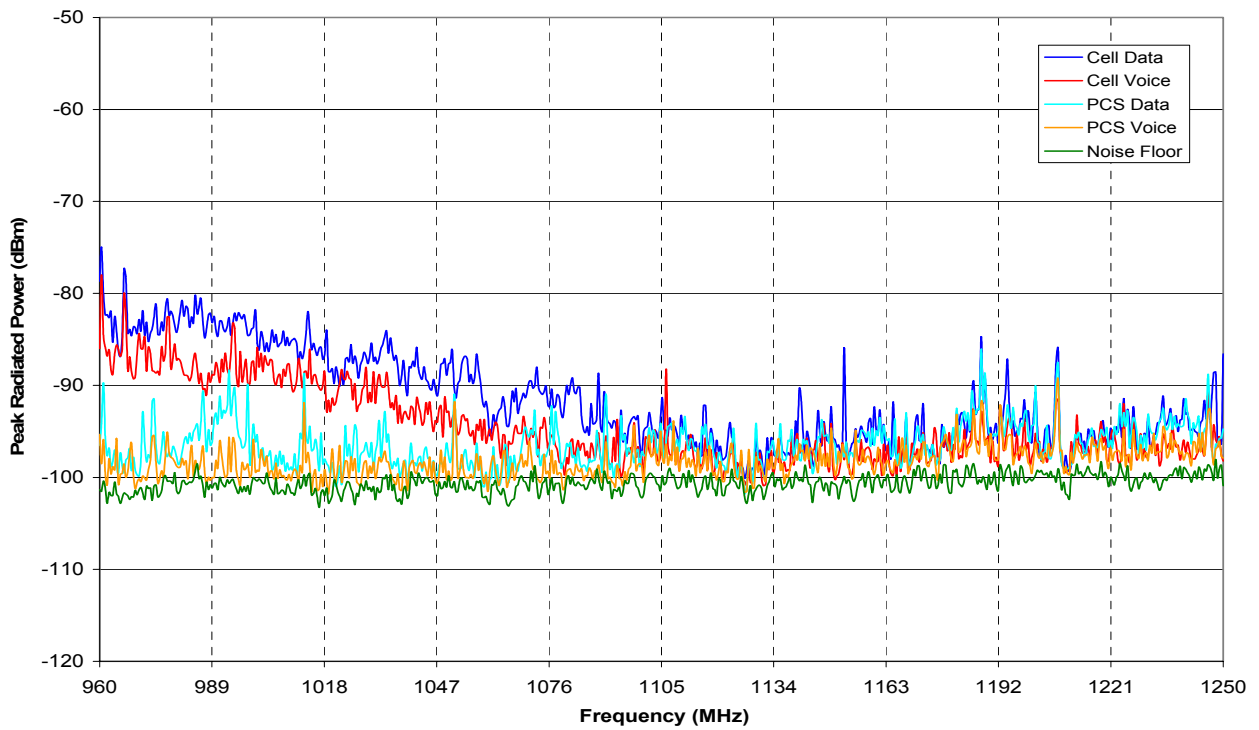


Figure B37: GSM03 four mode envelopes, Band 3.

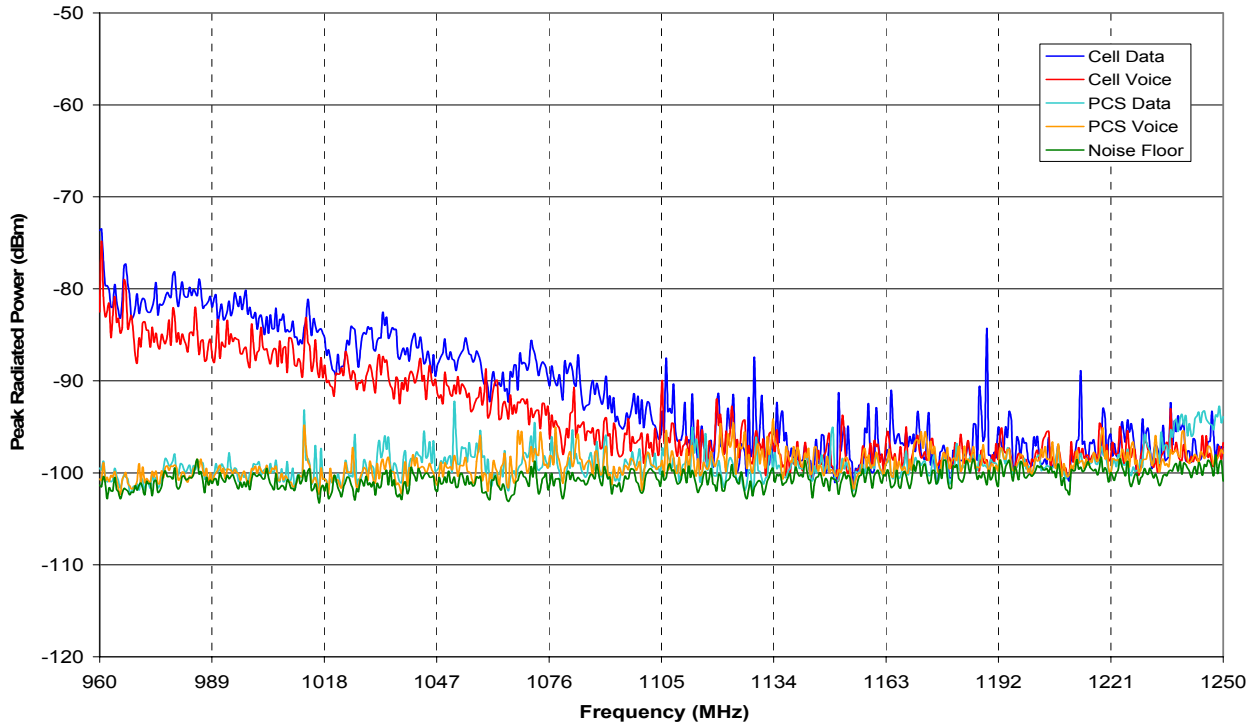


Figure B38: GSM04 four mode envelopes, Band 3.

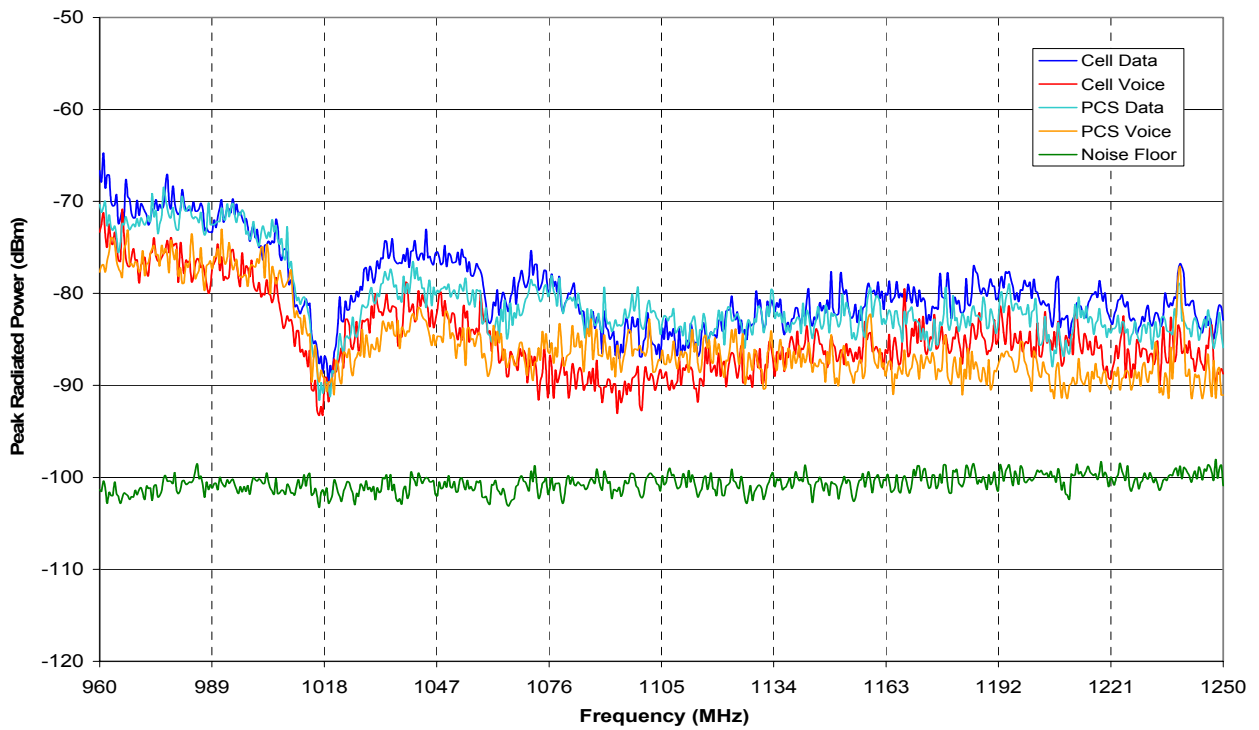


Figure B39: GSM05 four mode envelopes, Band 3.

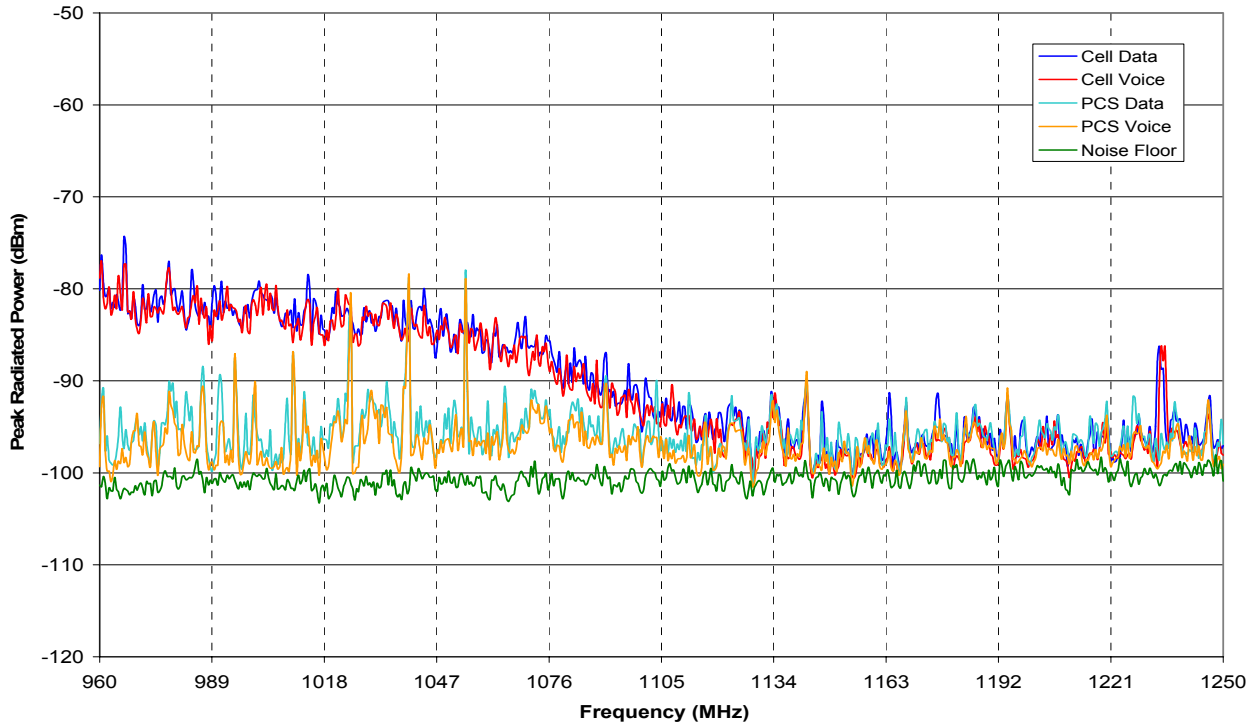


Figure B40: GSM06 four mode envelopes, Band 3.

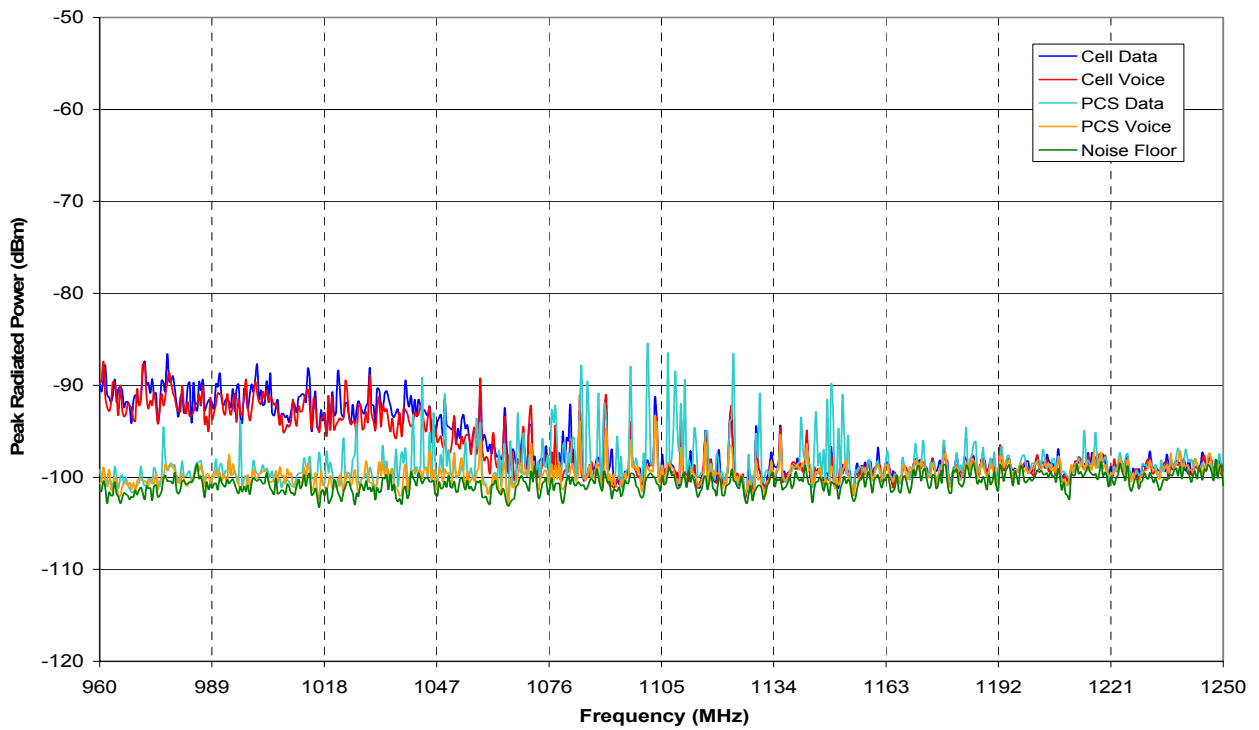


Figure B41: GSM07 four mode envelopes, Band 3.

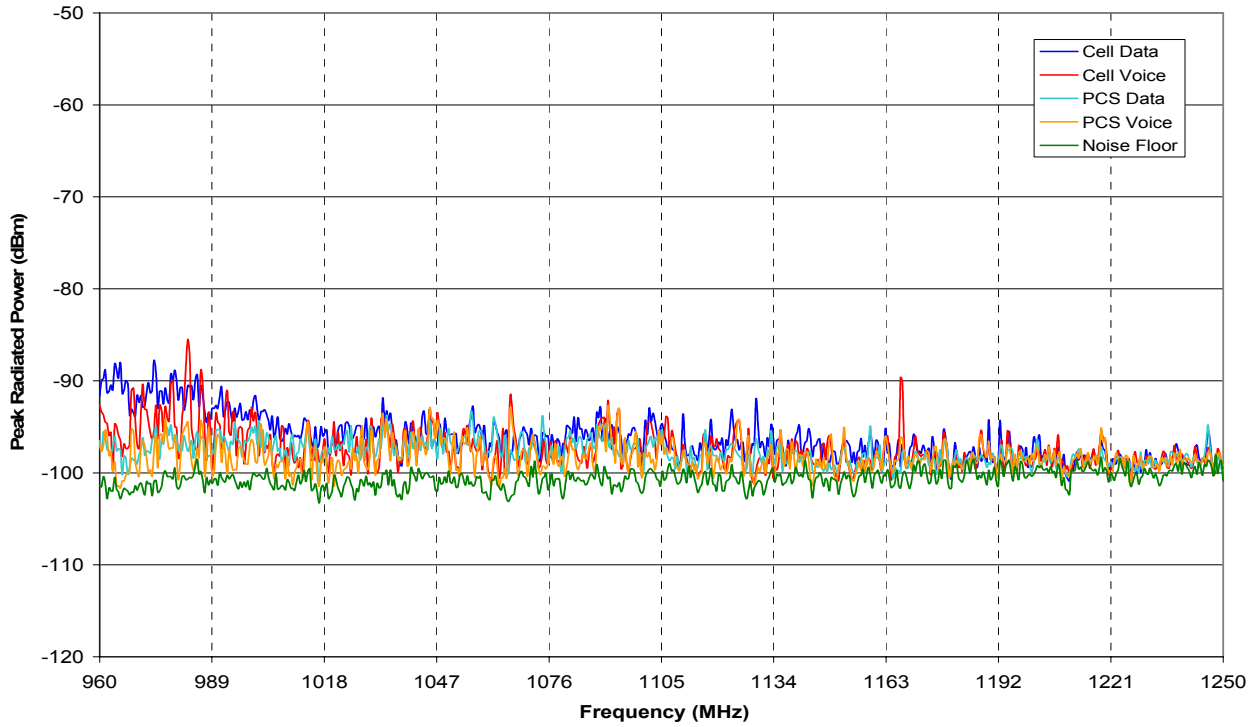


Figure B42: GSM08 four mode envelope, Band 3.

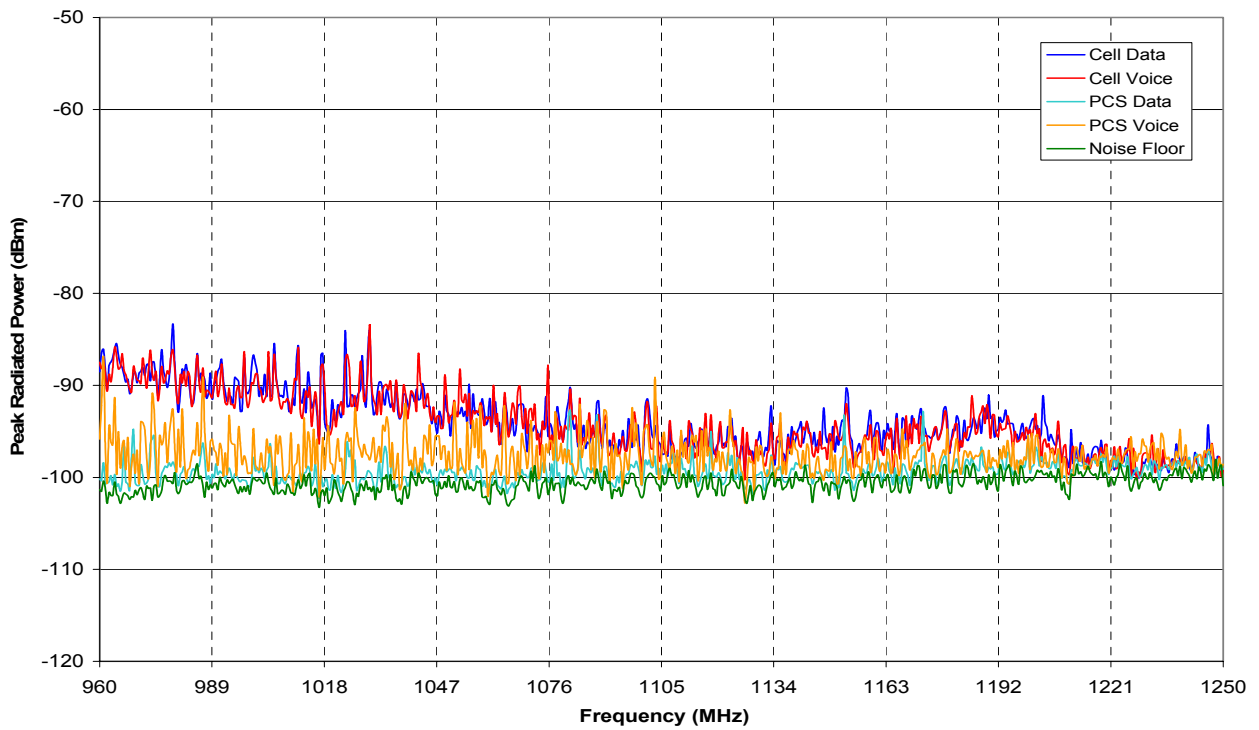


Figure B43: GSM09 four mode envelopes, Band 3.

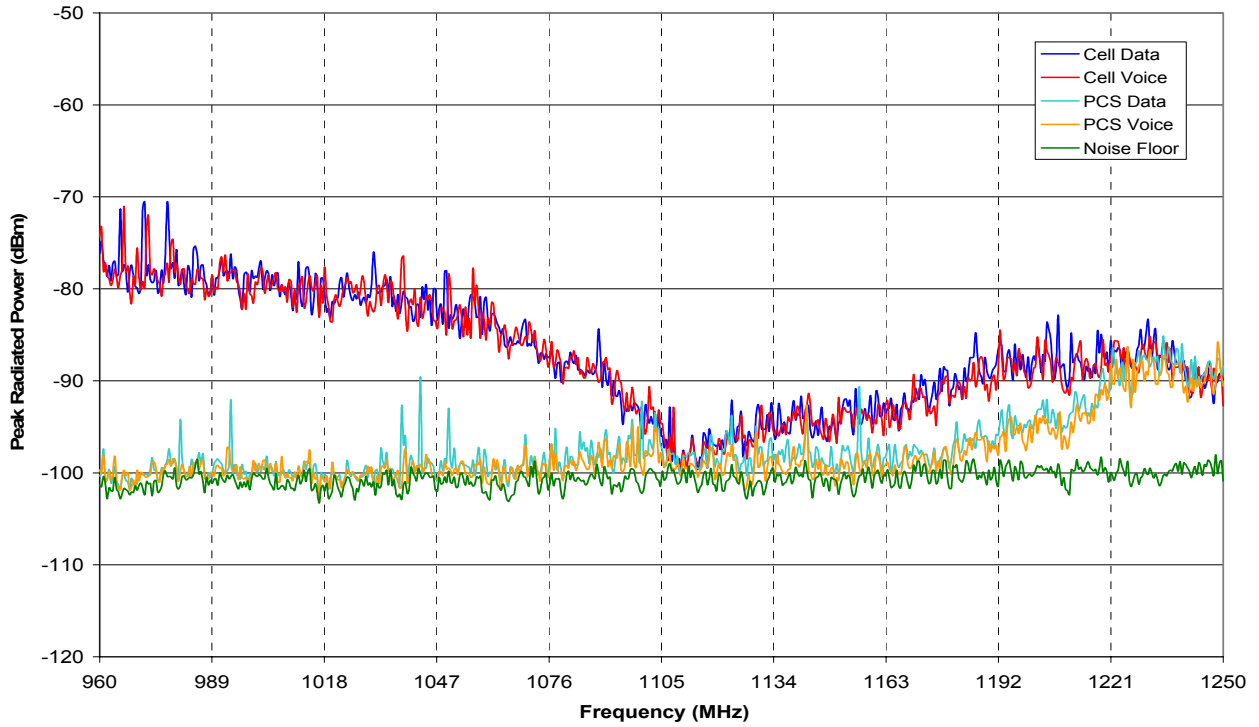


Figure B44: GSM10 four mode envelopes, Band 3.

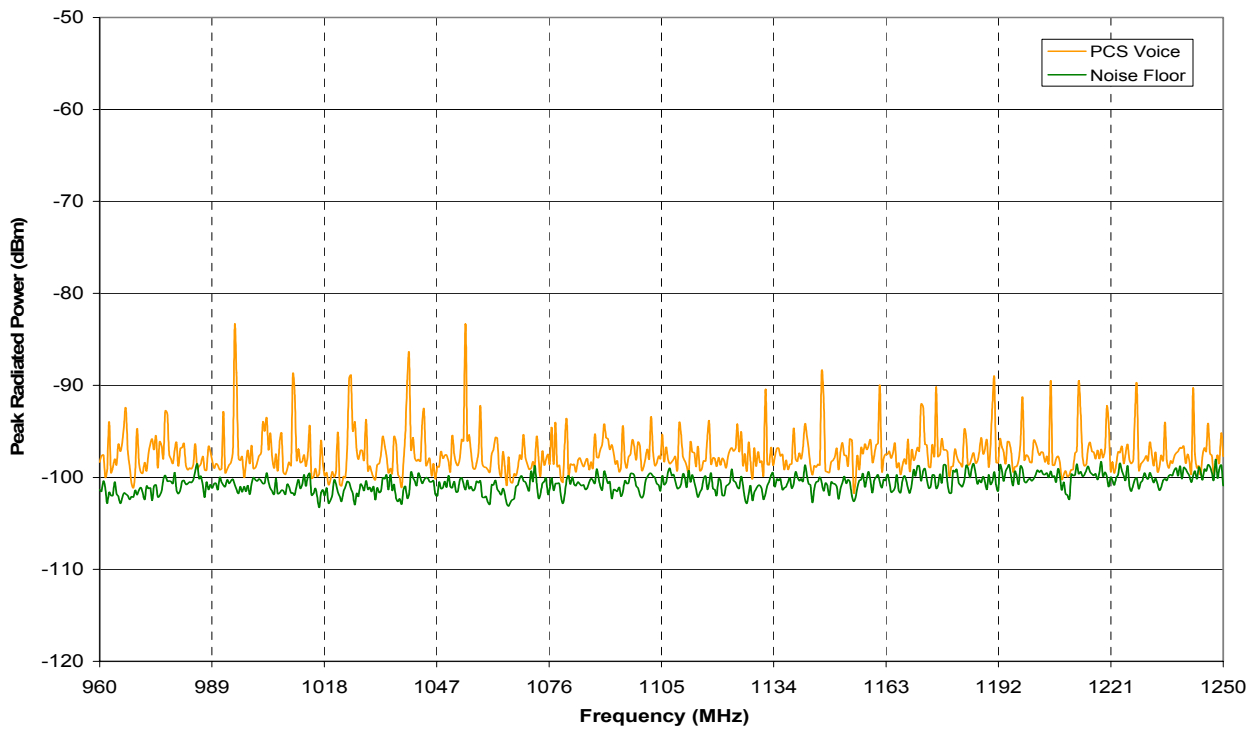


Figure B45: GSM11 four mode envelopes, Band 3.

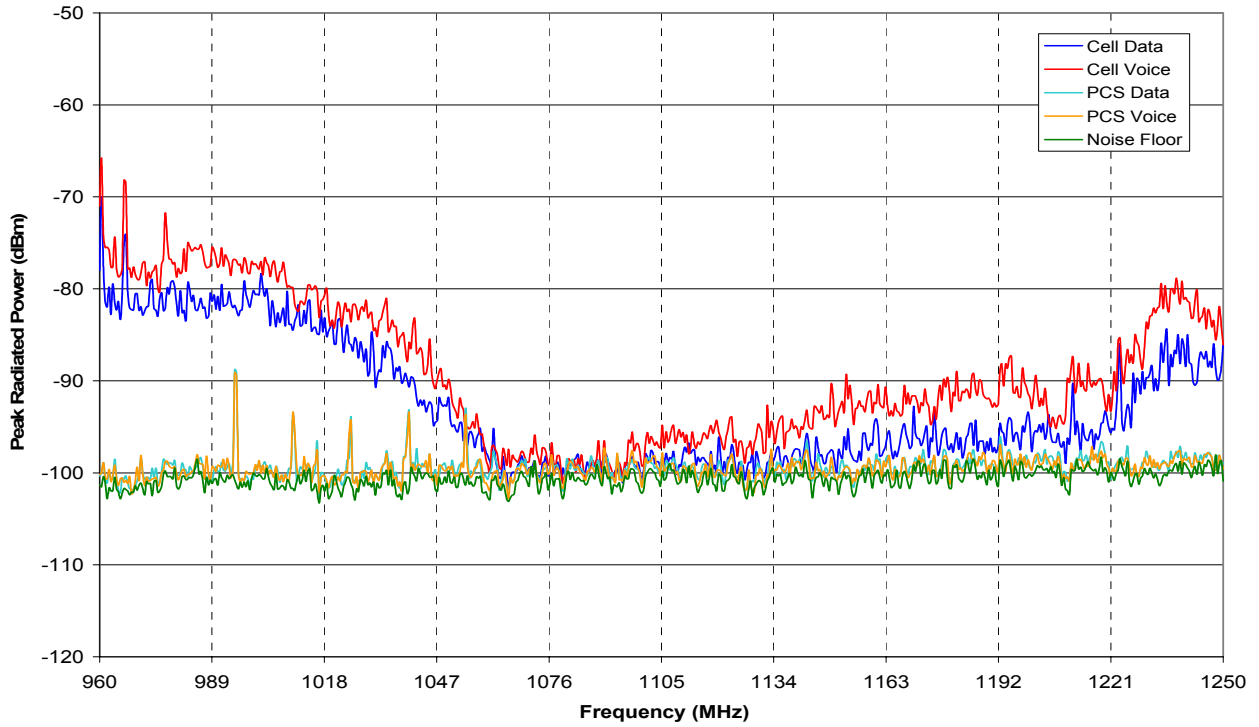


Figure B46: GSM12 four mode envelopes, Band 3.

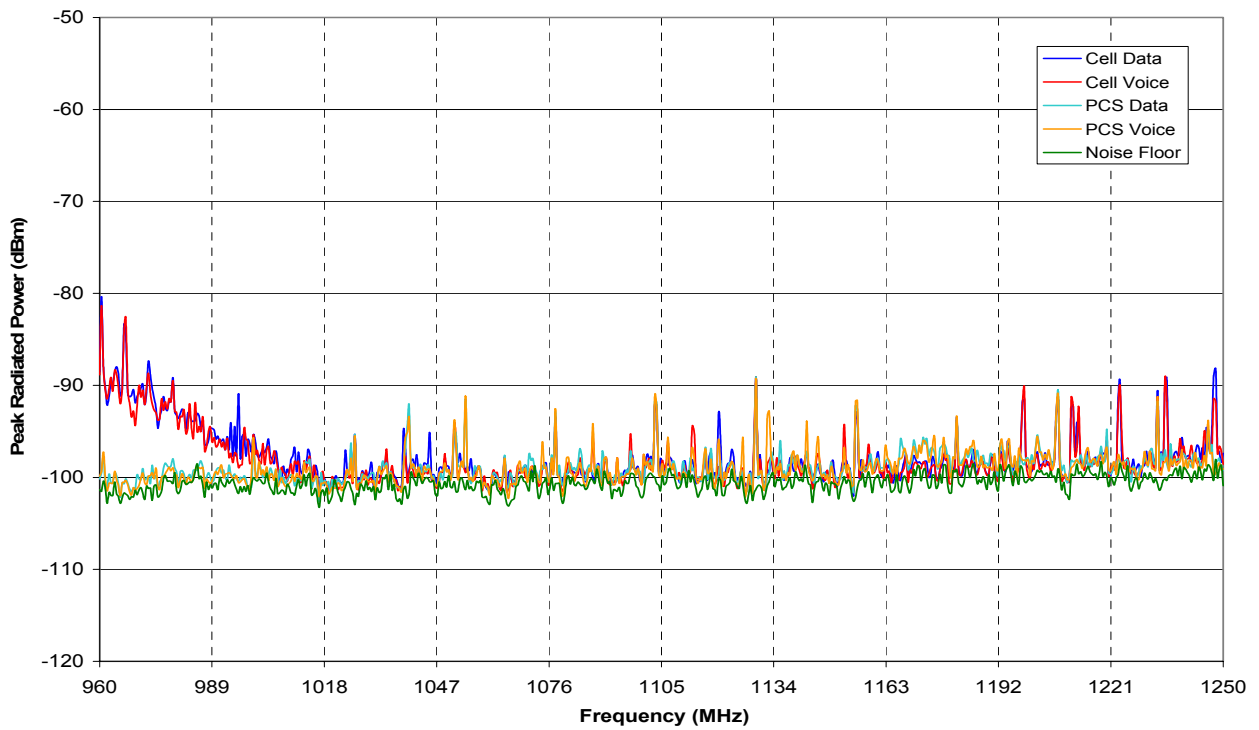


Figure B47: GSM13 four mode envelopes, Band 3.

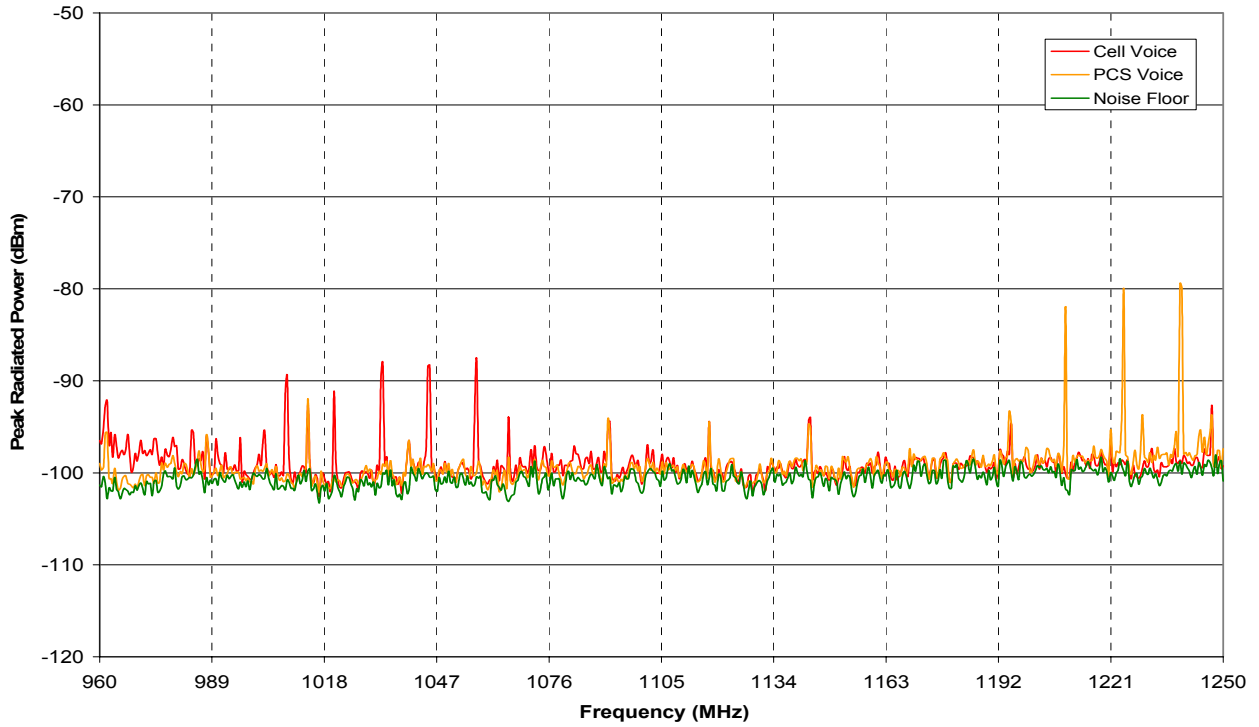


Figure B48: GSM14 two mode envelopes, Band 3.

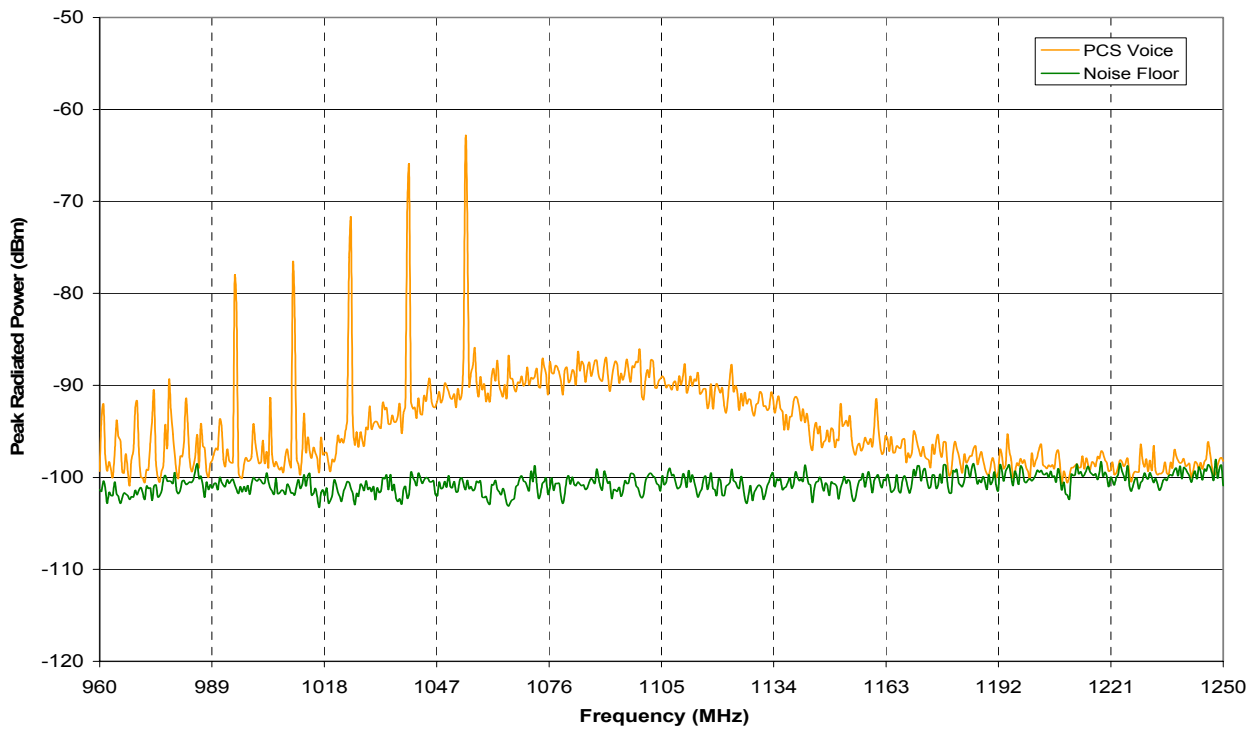


Figure B49: GSM15 one mode envelope, Band 3.

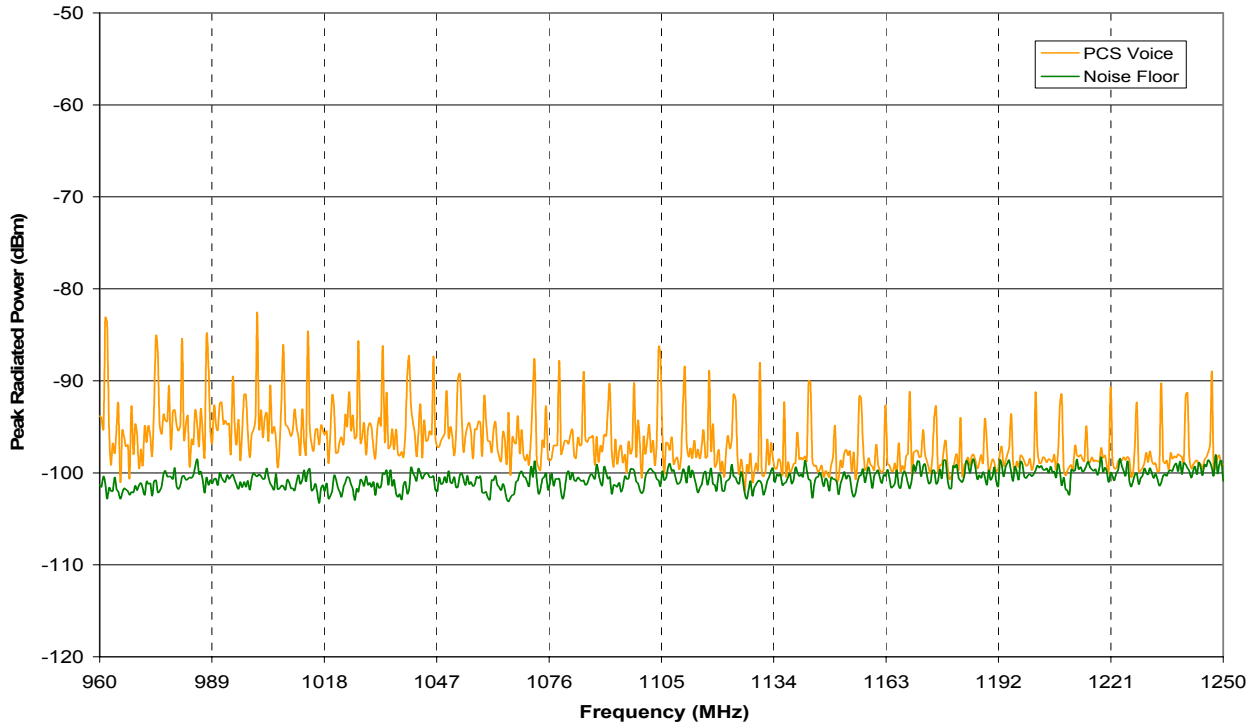


Figure B50: GSM16 one mode envelope, Band 3.

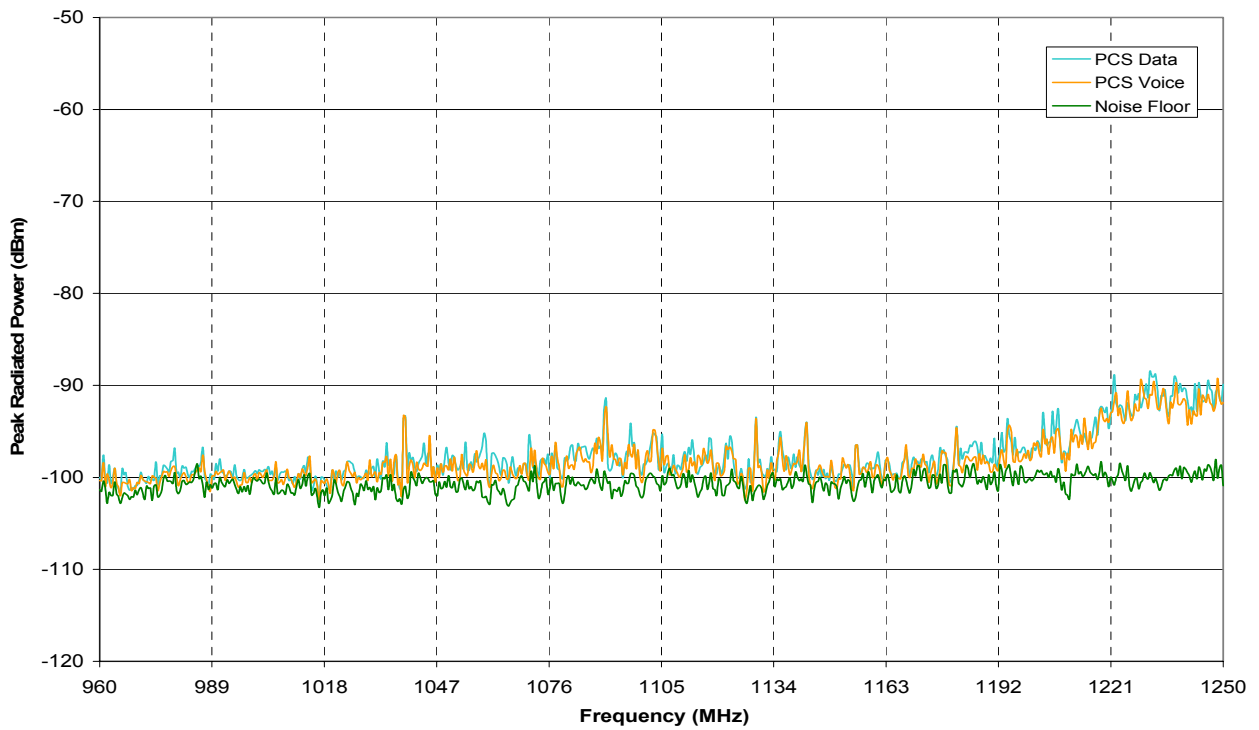


Figure B51: GSM17 two mode envelopes, Band 3.

B.4 Band 4

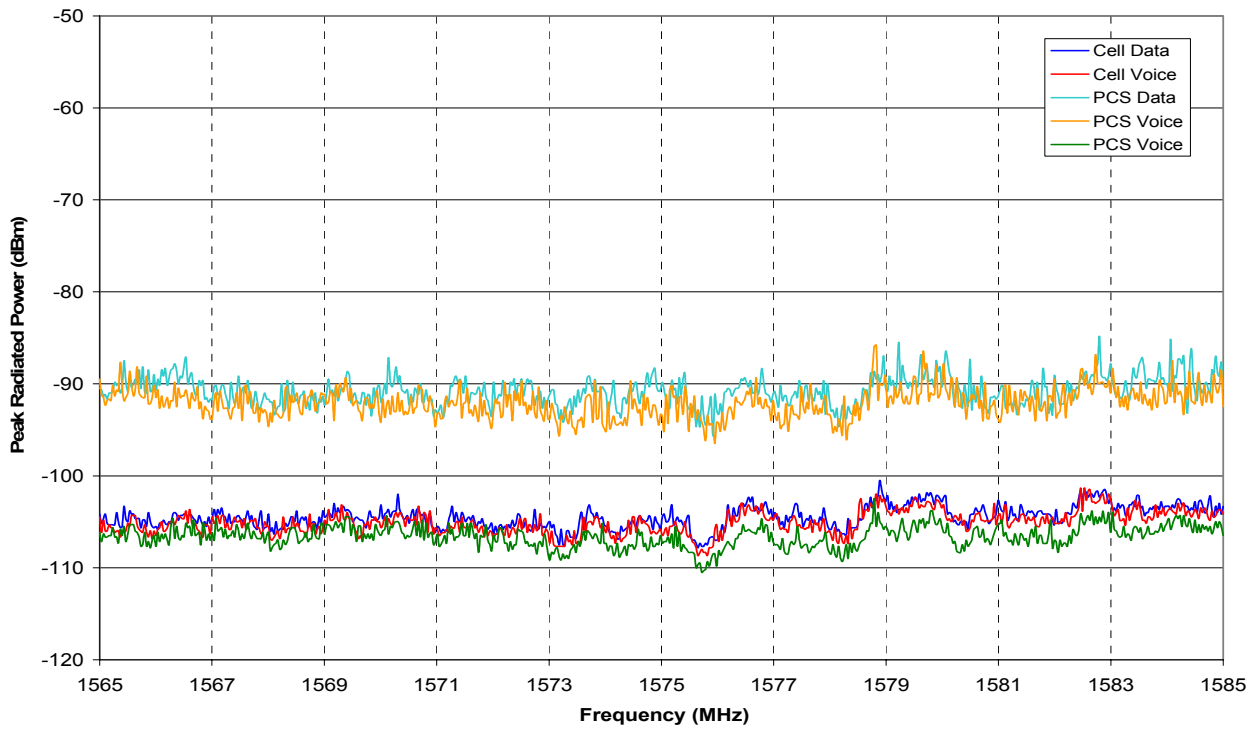


Figure B52: GSM01 four mode envelopes, Band 4.

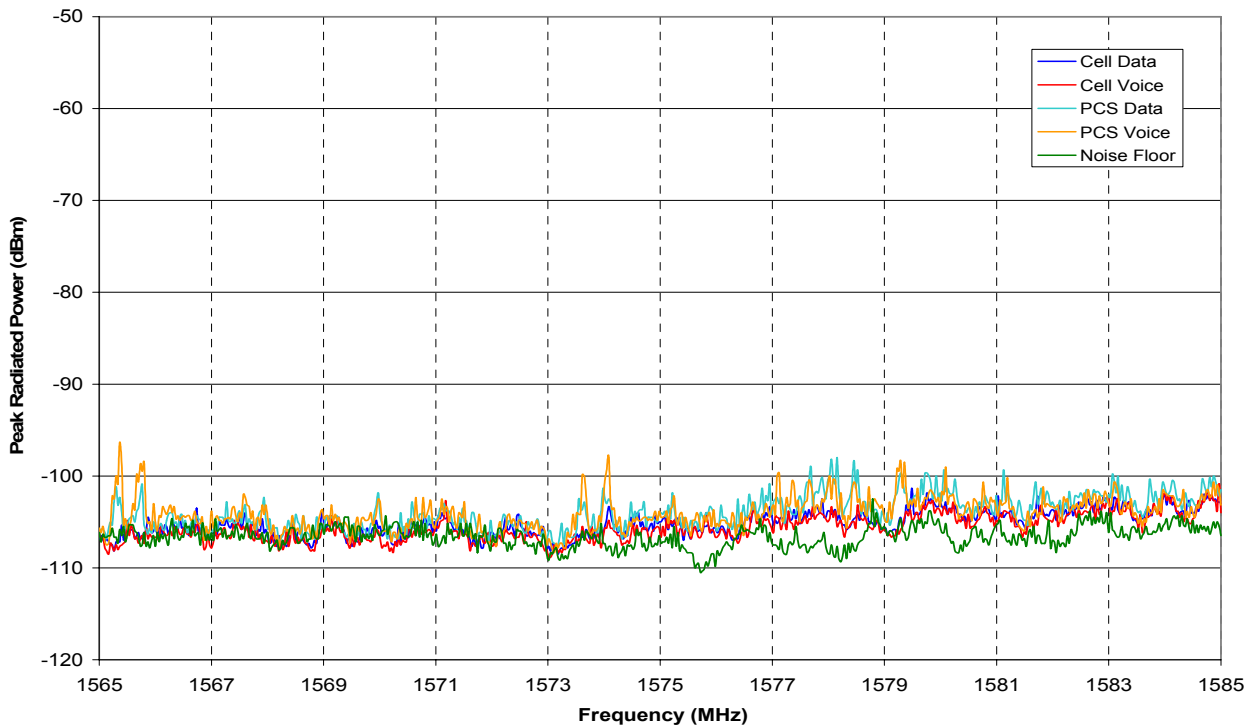


Figure B53: GSM02 four mode envelopes, Band 4.

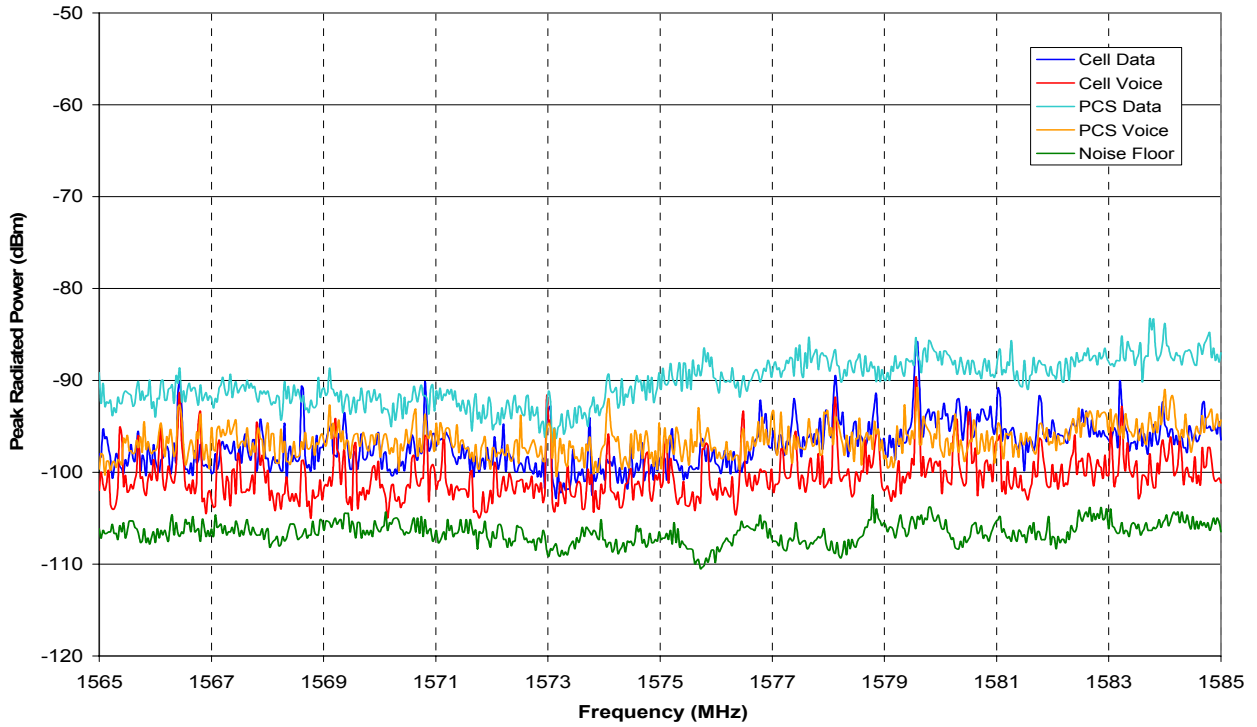


Figure B54: GSM03 four mode envelope, Band 4.

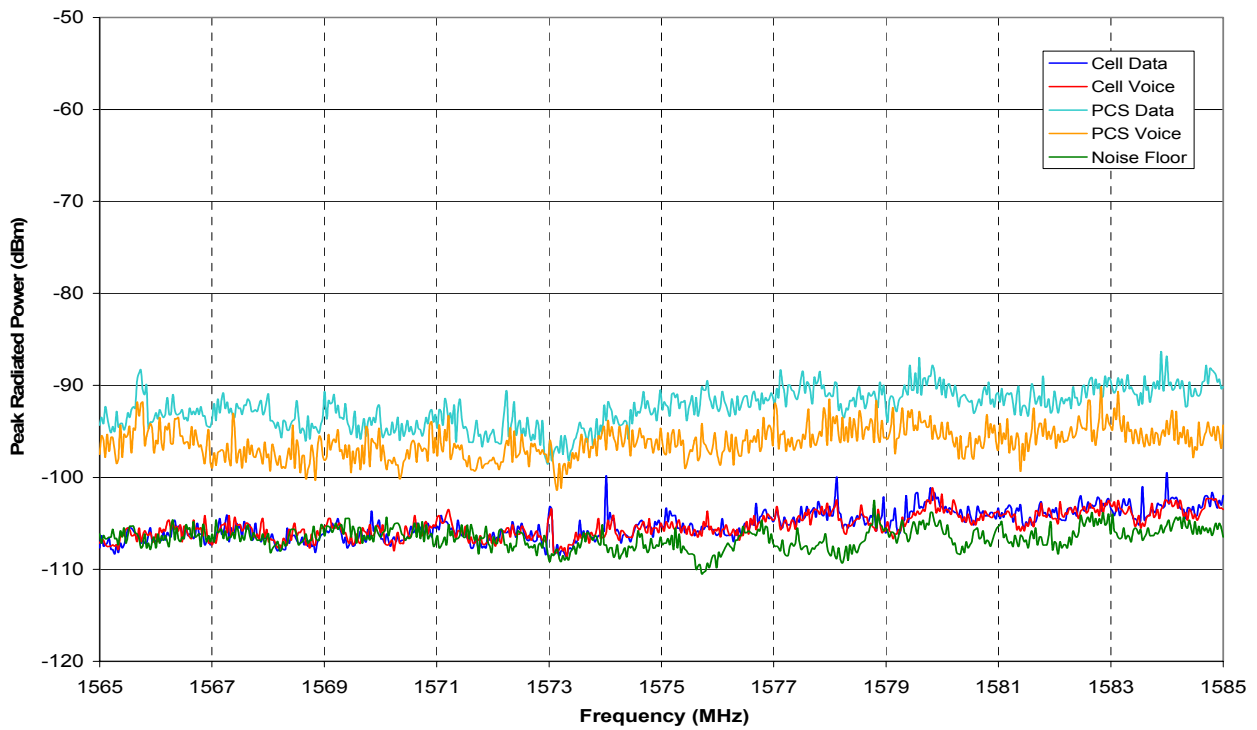


Figure B55: GSM04 four mode envelopes, Band 4.

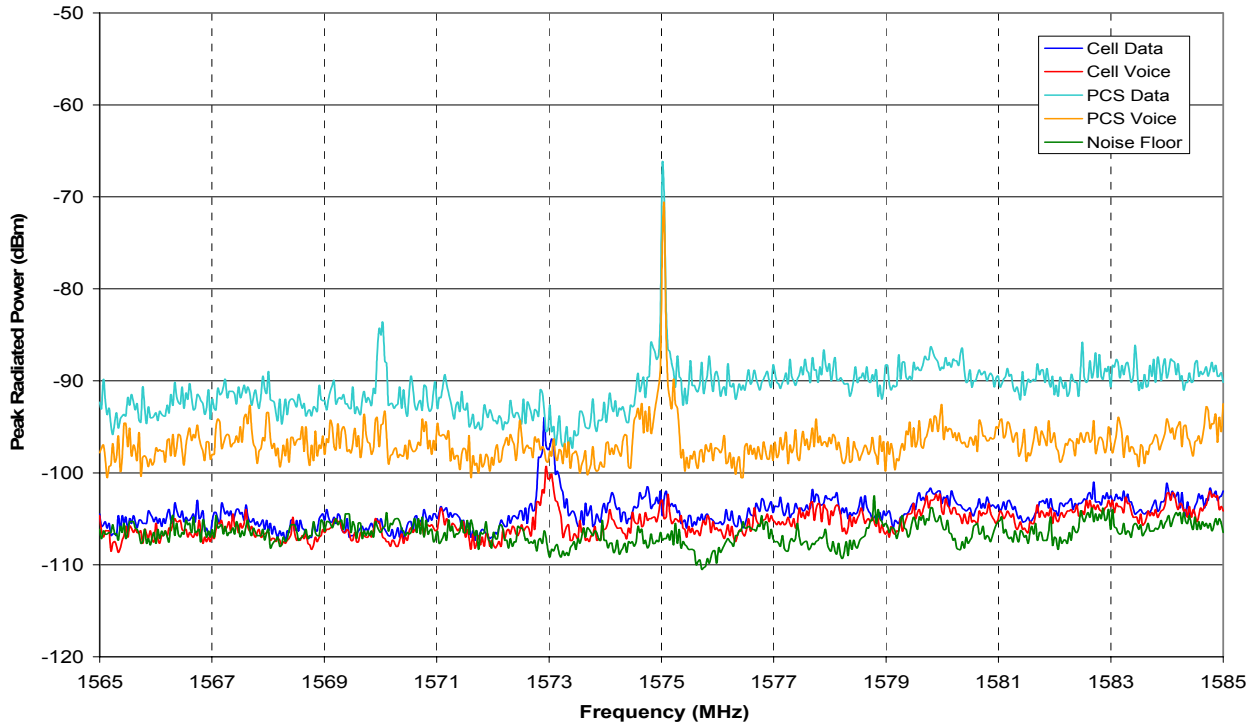


Figure B56: GSM05 four mode envelopes, Band 4.

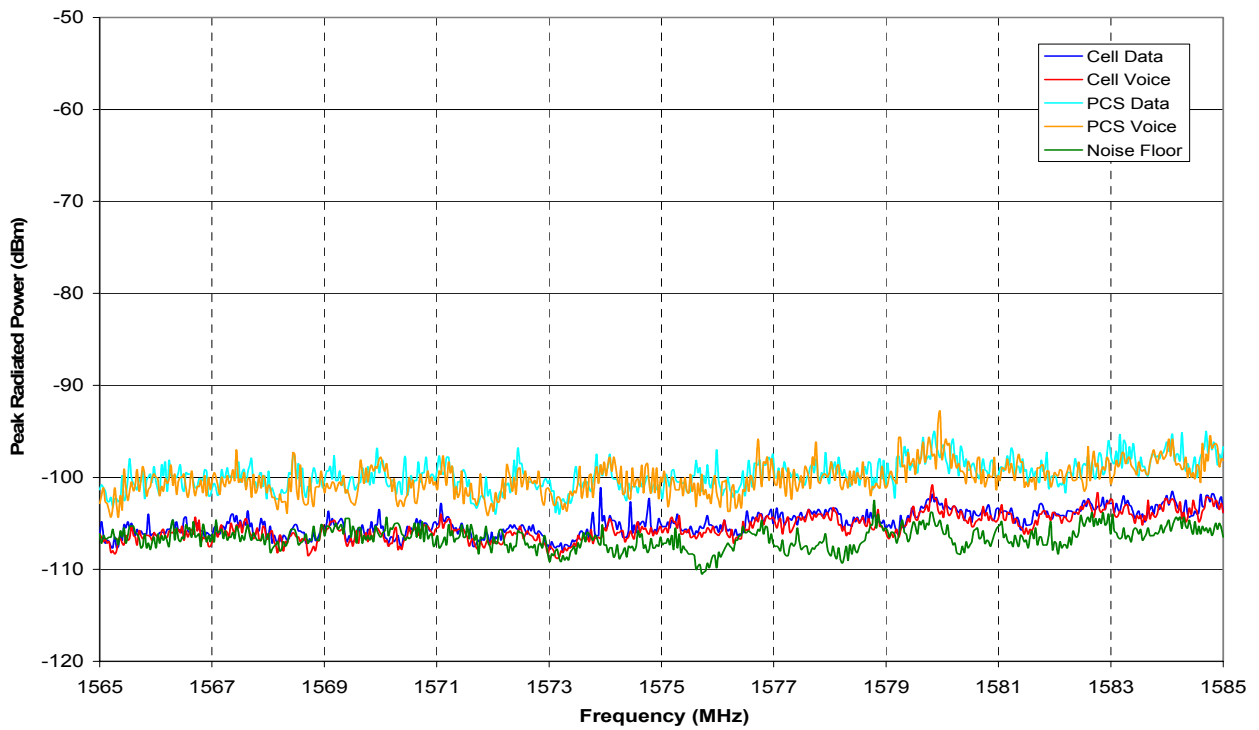


Figure B57: GSM06 four mode envelopes, Band 4.

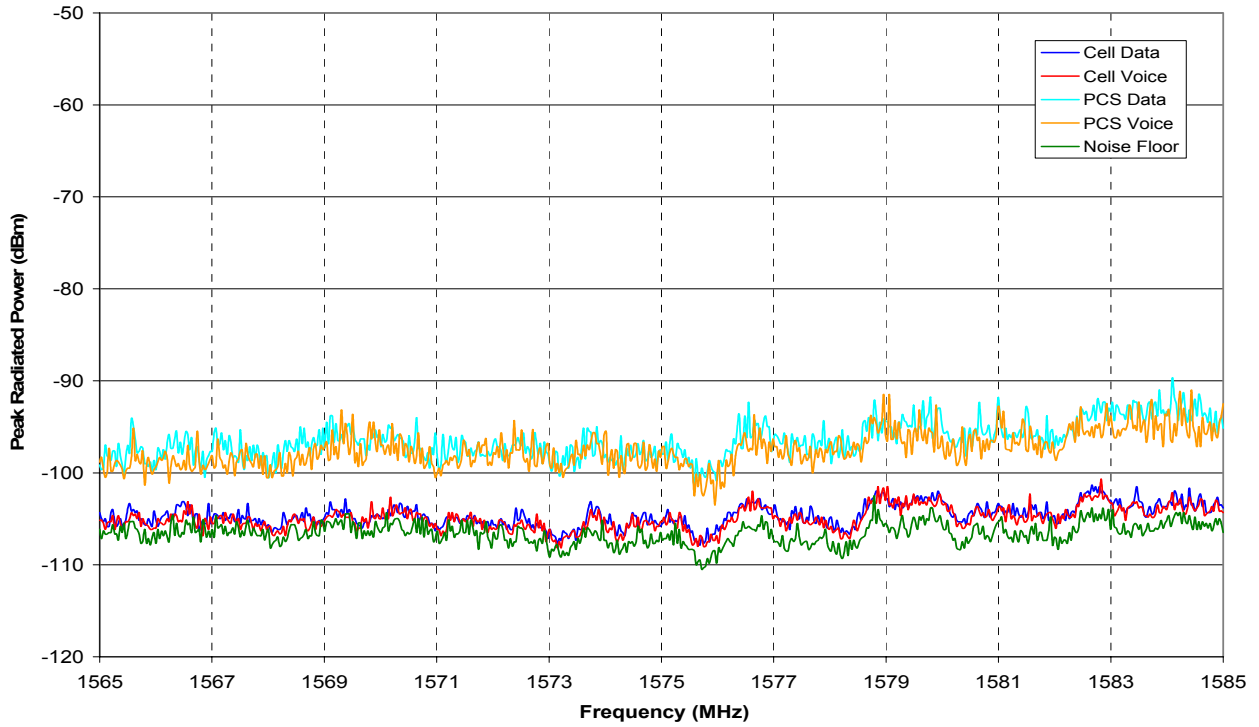


Figure B58: GSM07 four mode envelopes, Band 4.

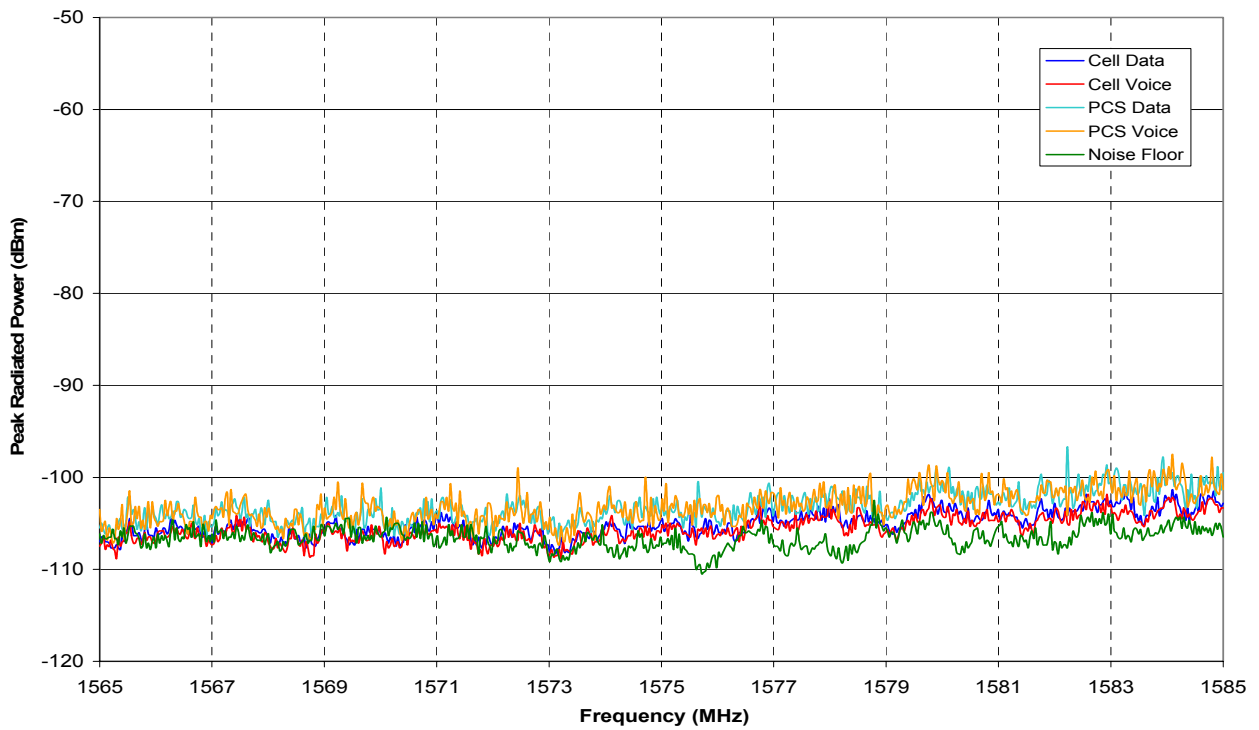


Figure B59: GSM08 four mode envelope, Band 4.

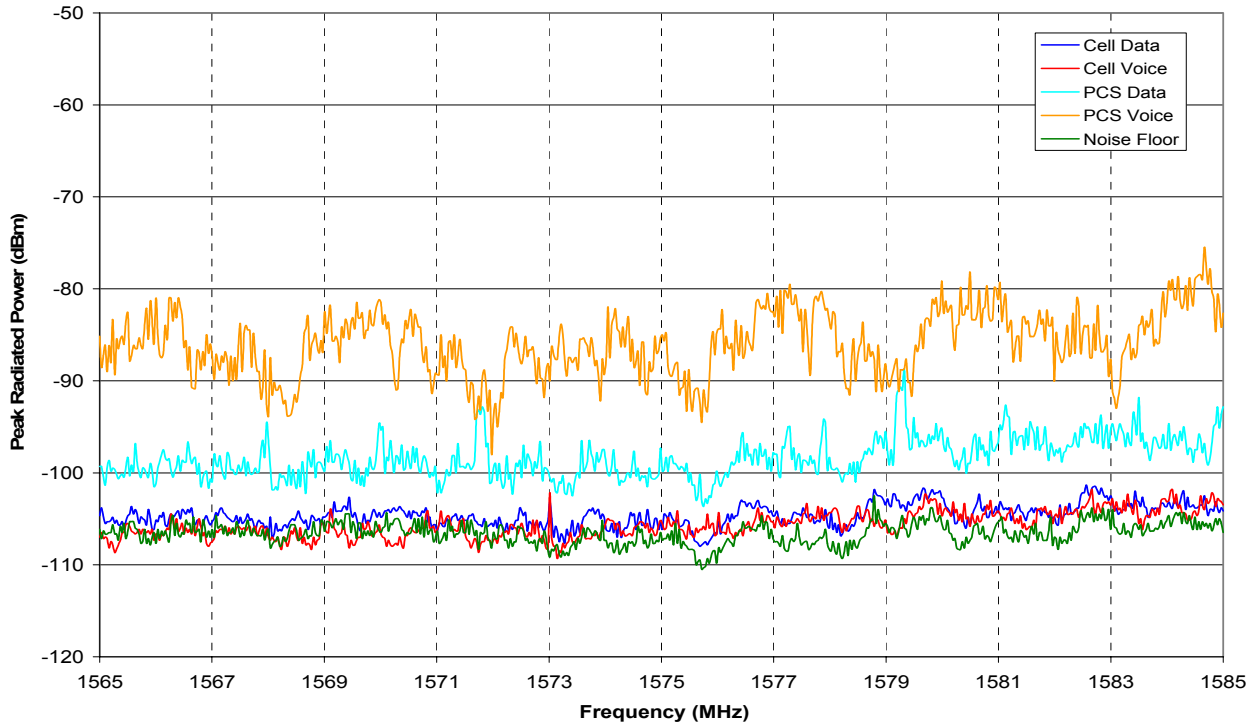


Figure B60: GSM09 four mode envelope, Band 4.

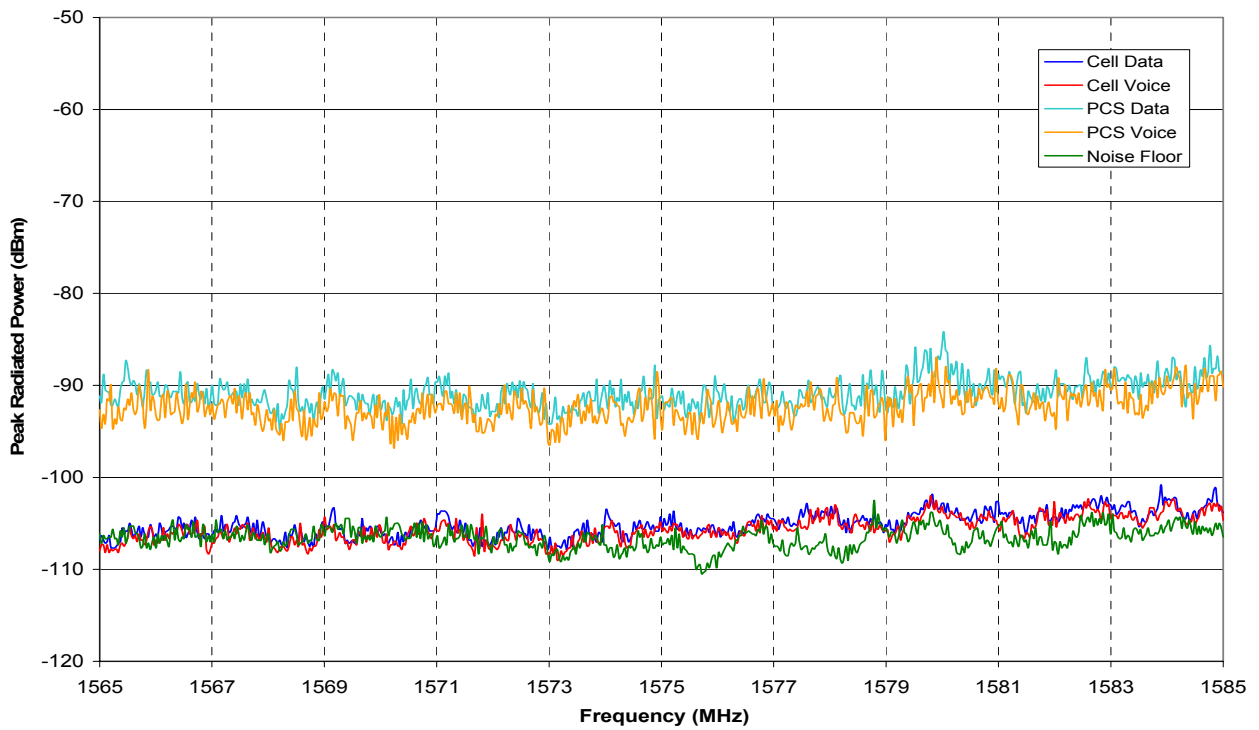


Figure B61: GSM10 four mode envelopes, Band 4.

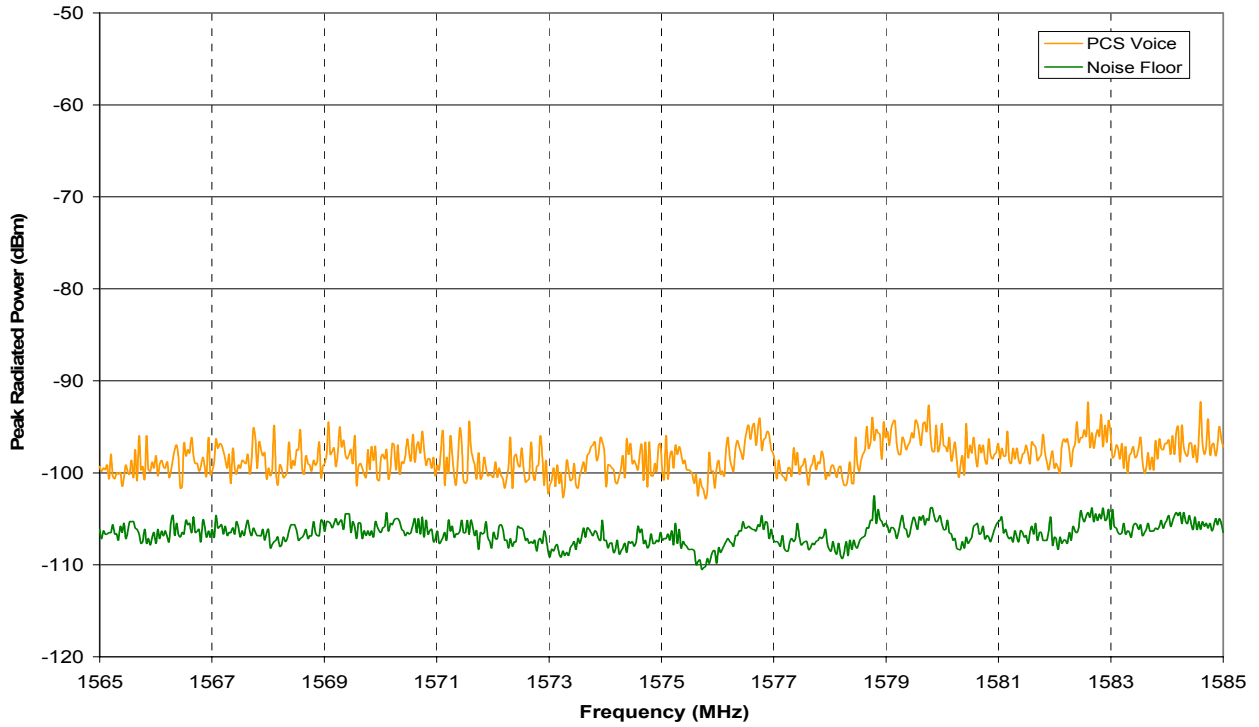


Figure B62: GSM11 one mode envelope, Band 4.

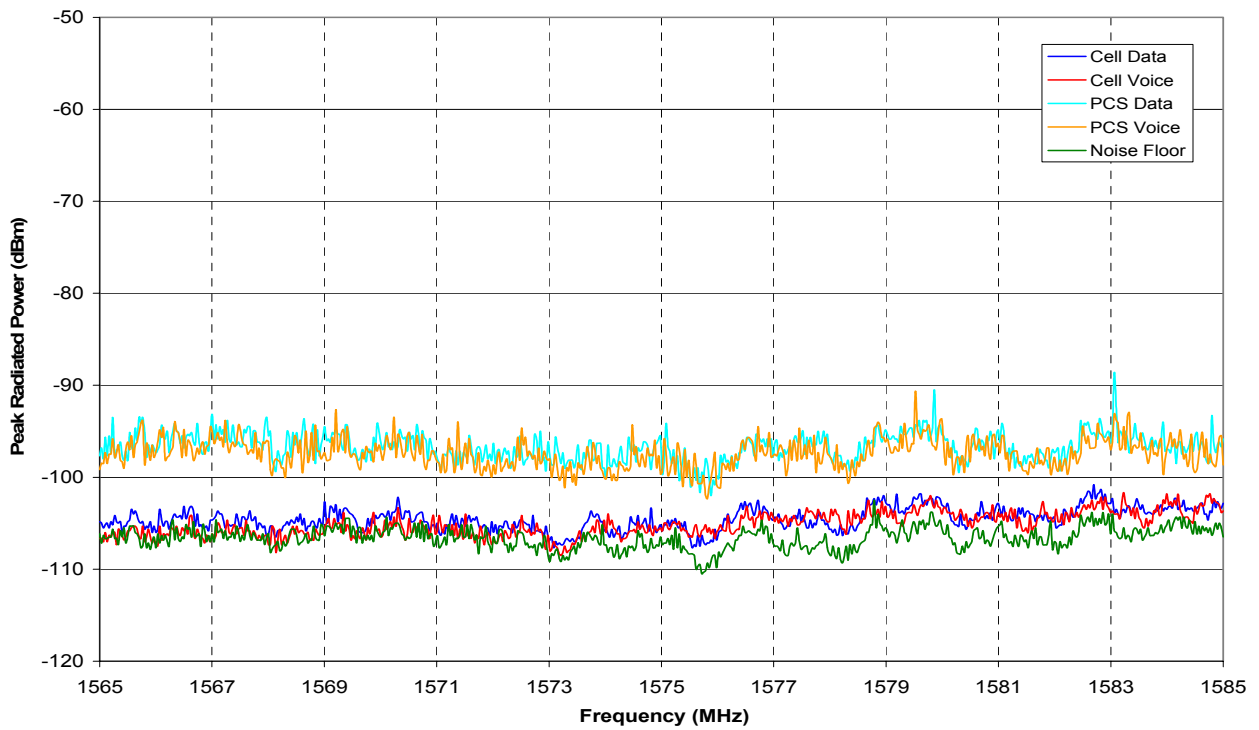


Figure B63: GSM12 four mode envelopes, Band 4.

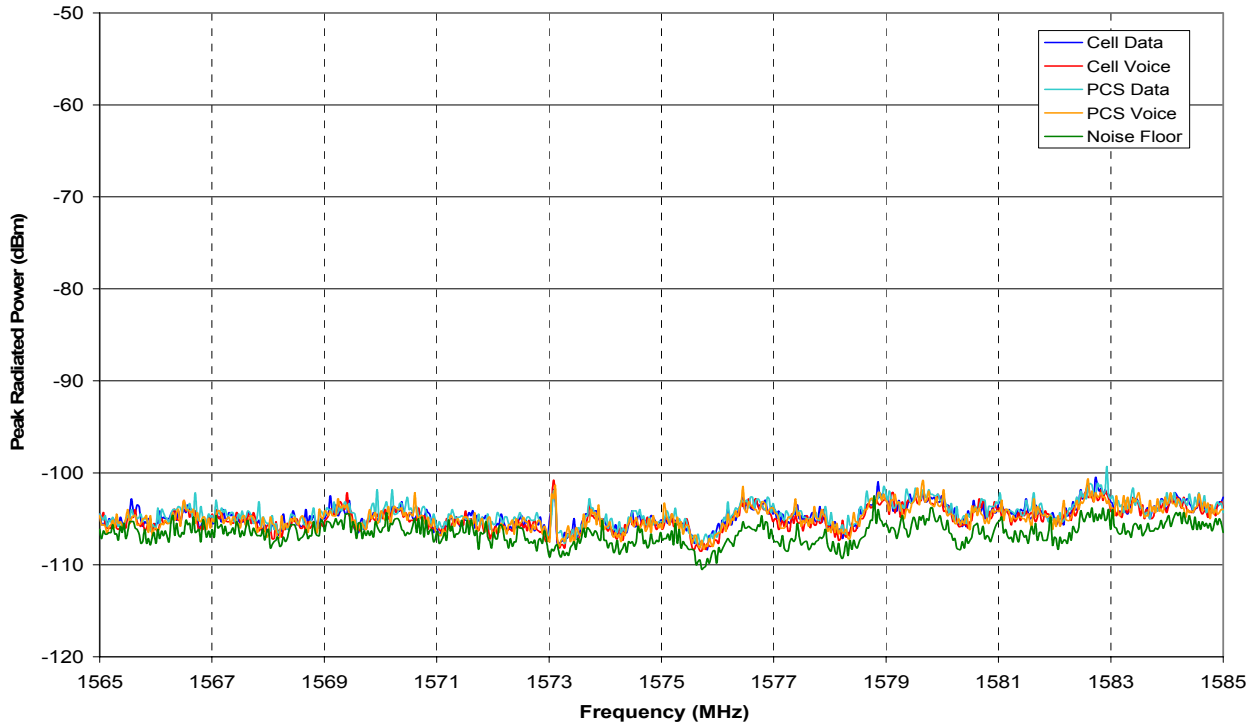


Figure B64: GSM13 four mode envelopes, Band 4.

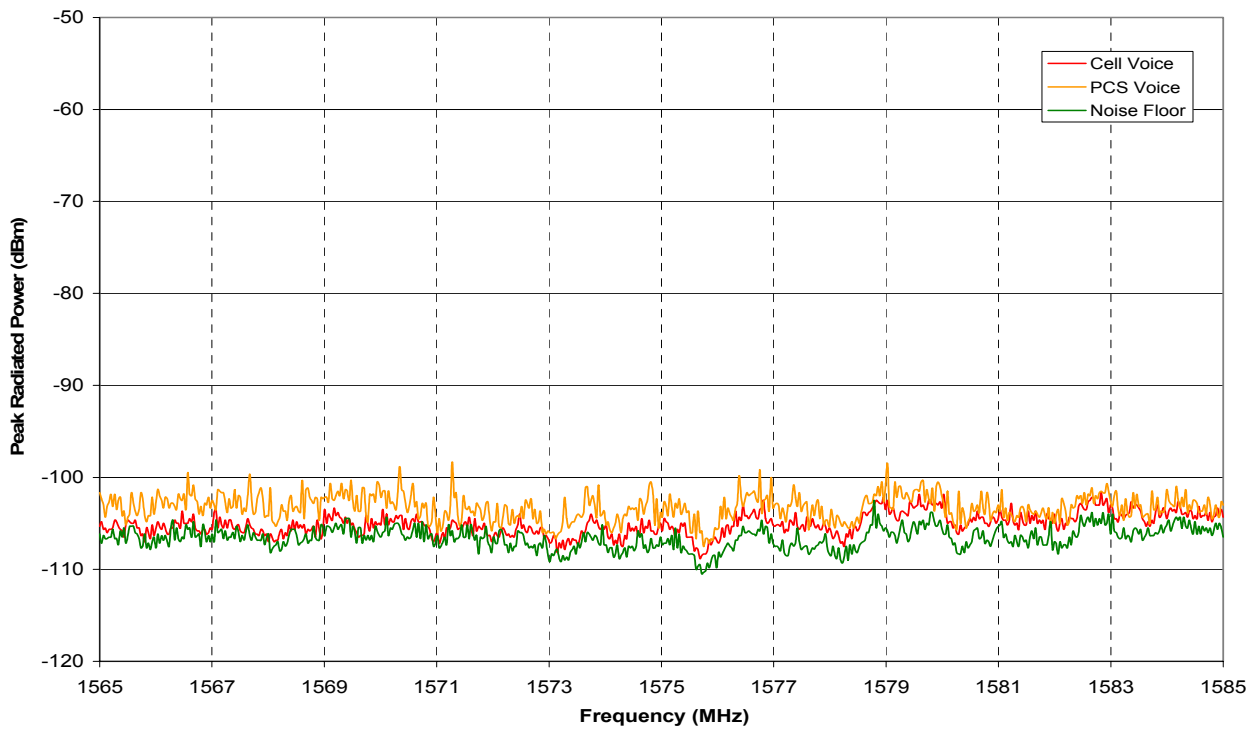


Figure B65: GSM14 two mode envelopes, Band 4.

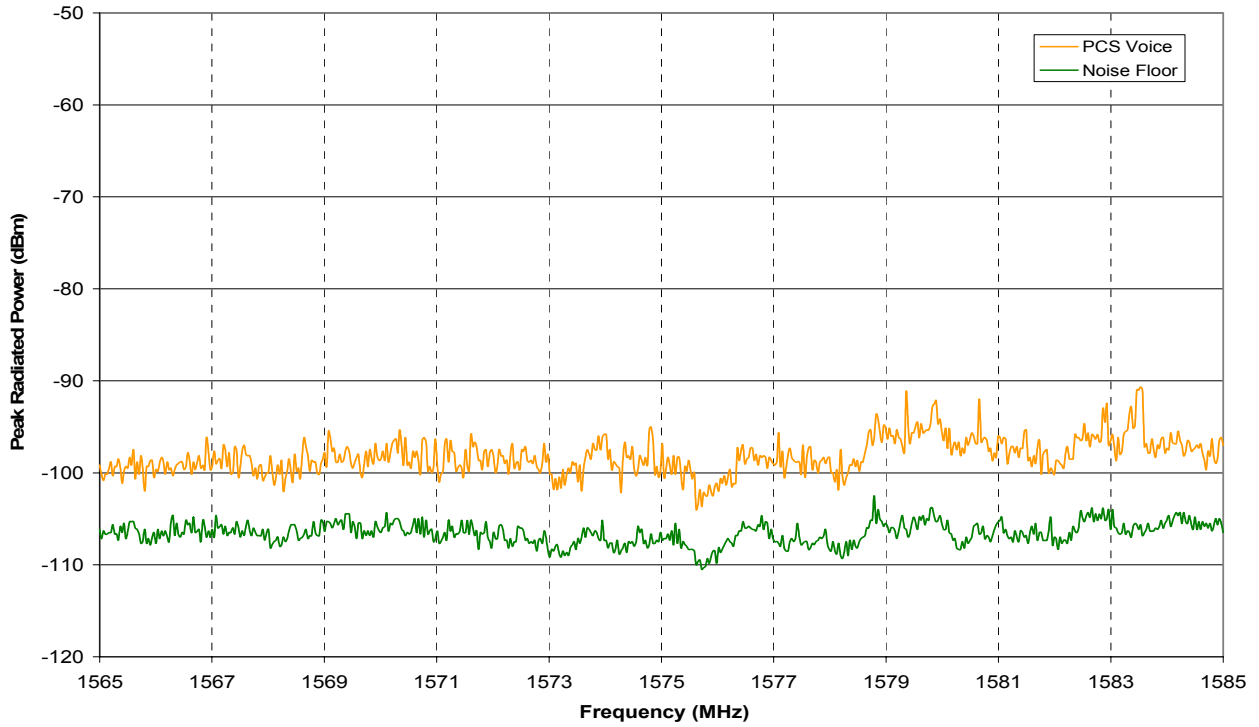


Figure B66: GSM15 one mode envelope, Band 4.

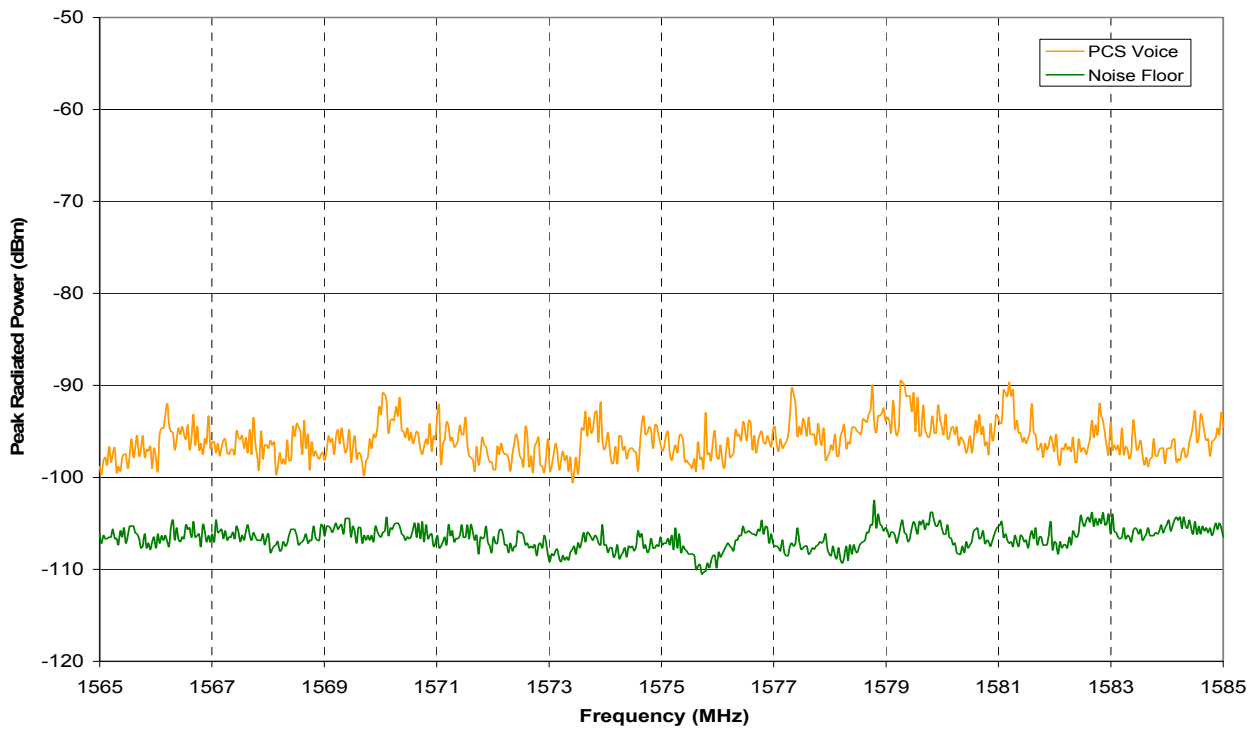


Figure B67: GSM16 one mode envelope, Band 4.

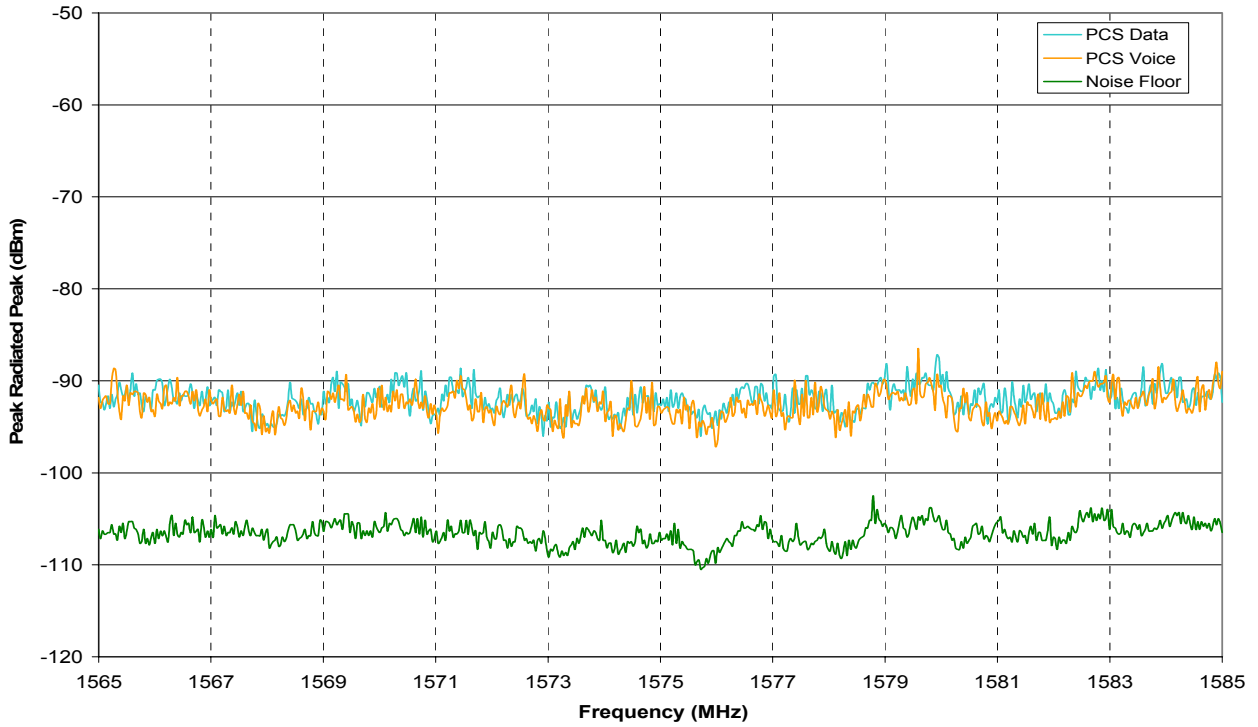


Figure B68: GSM17 two mode envelopes, Band 4.

B.5 Band 5

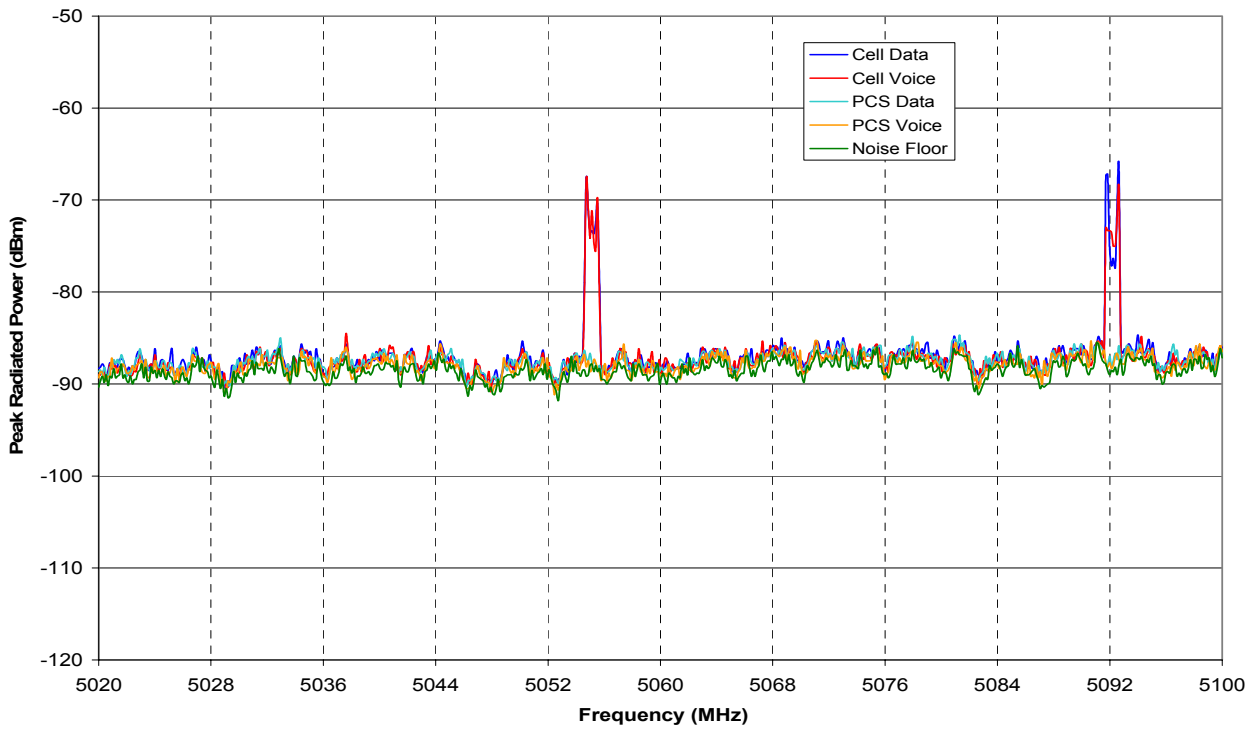


Figure B69: GSM01 four mode envelopes, Band 5.

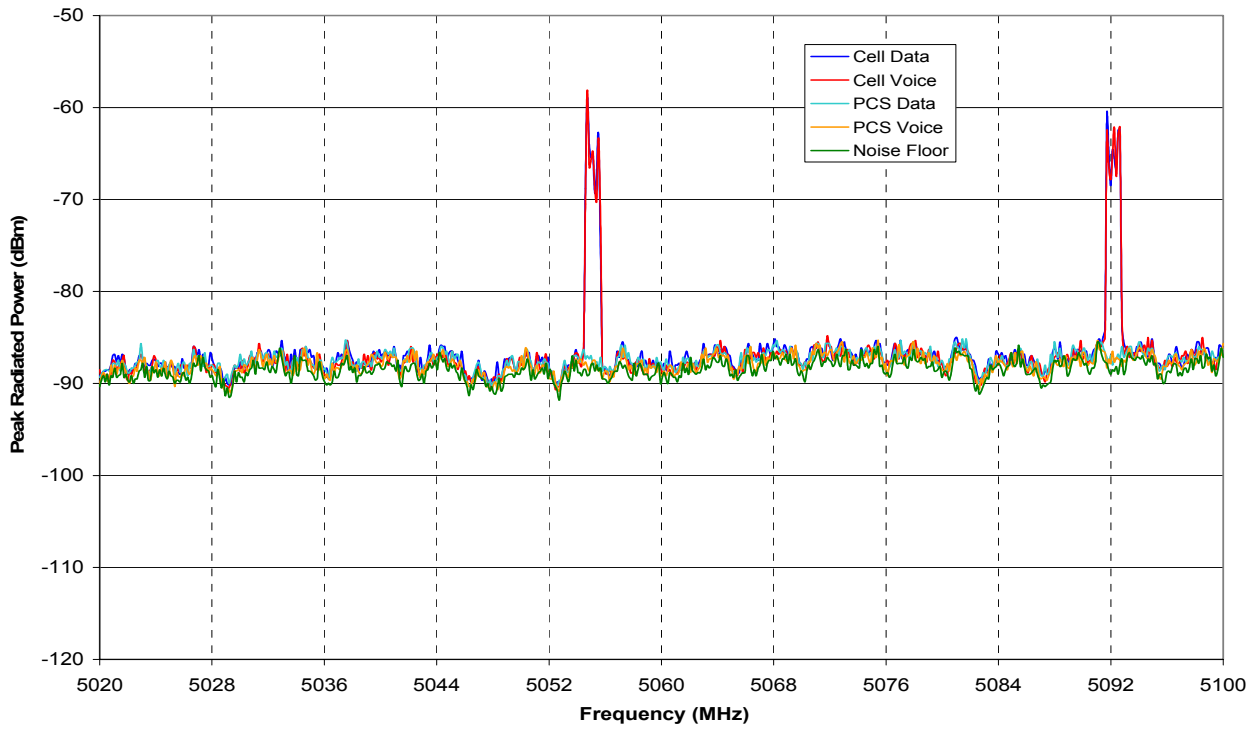


Figure B70: GSM02 four mode envelopes, Band 5.

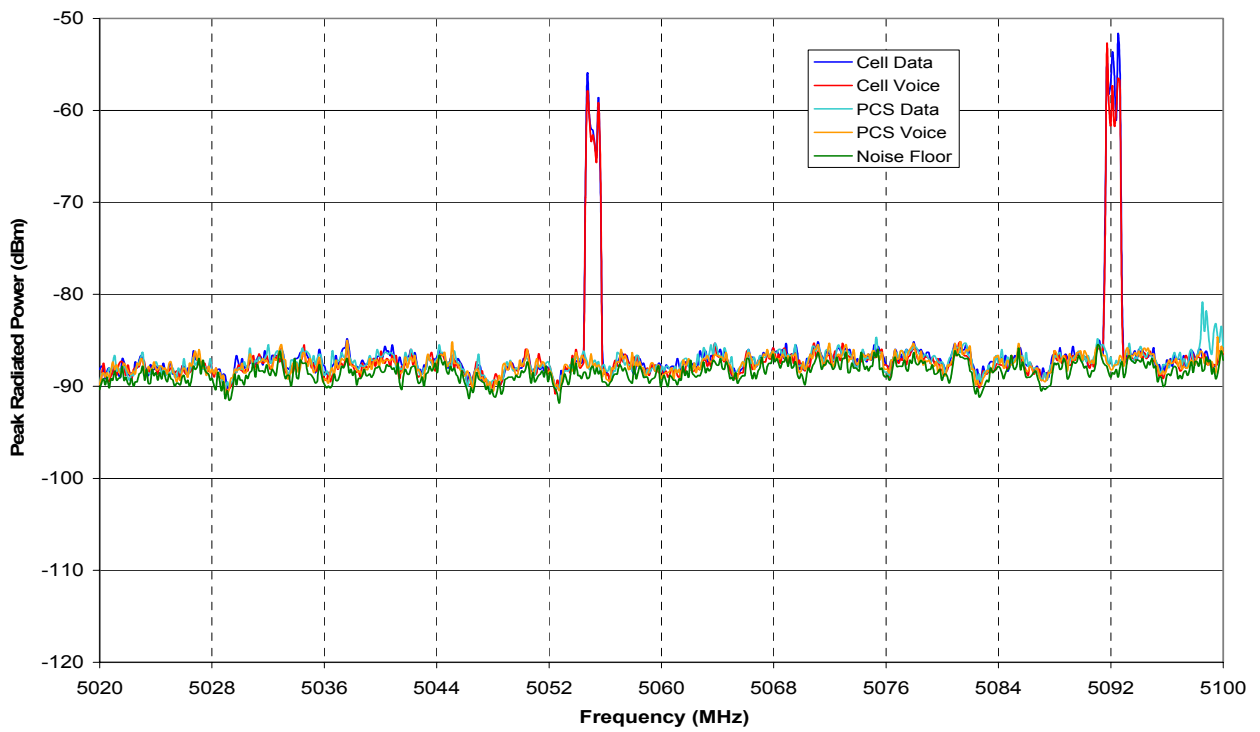


Figure B71: GSM03 four mode envelopes, Band 5.

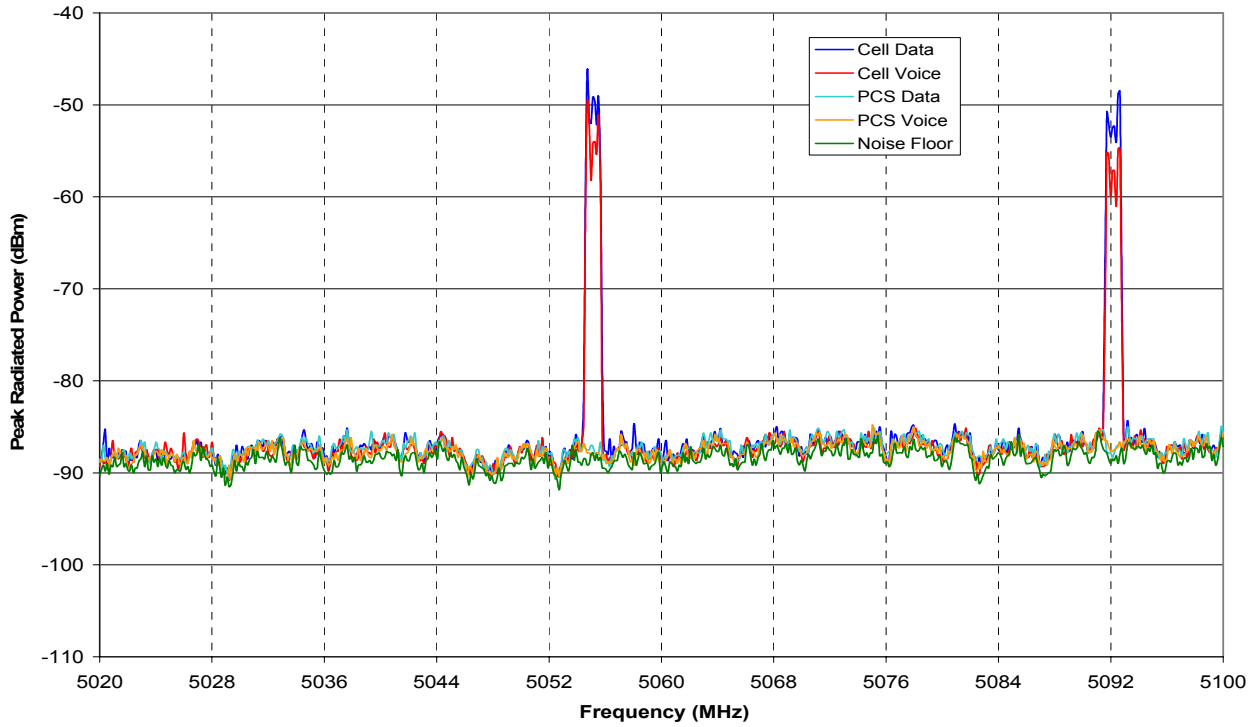


Figure B72: GSM04 four mode envelopes, Band 5.

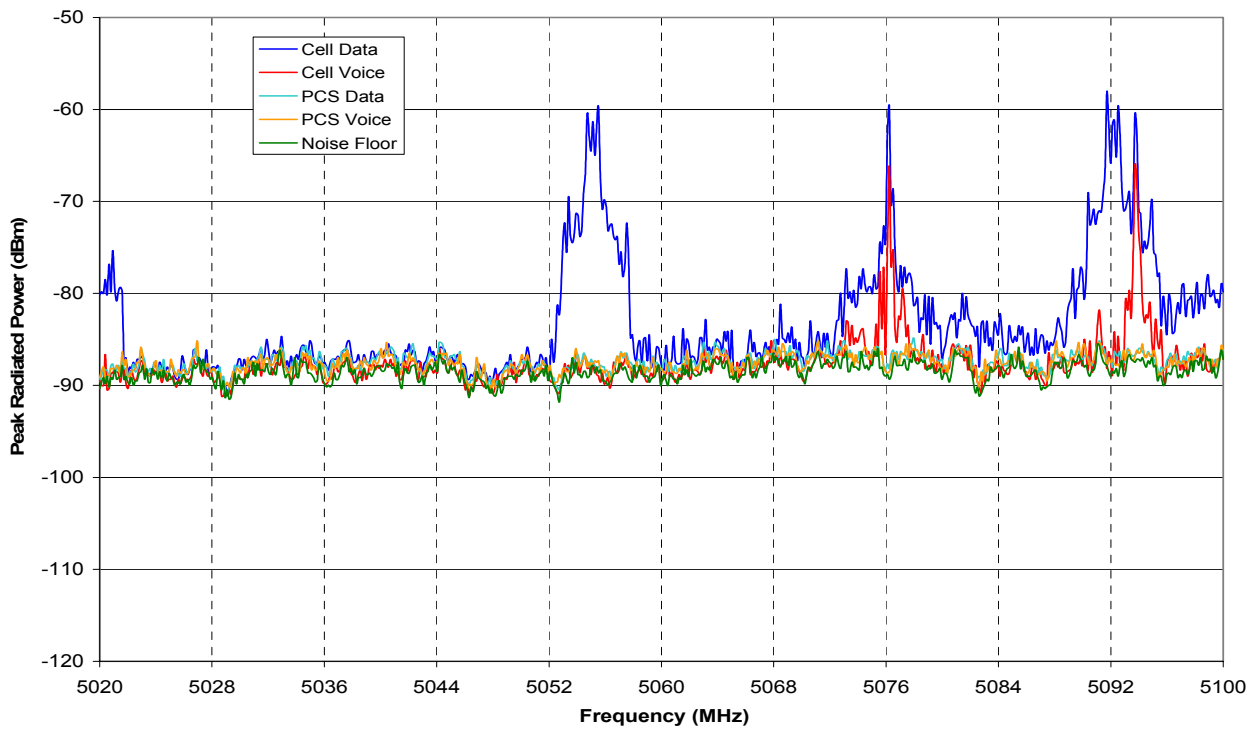


Figure B73: GSM05 four mode envelopes, Band 5.

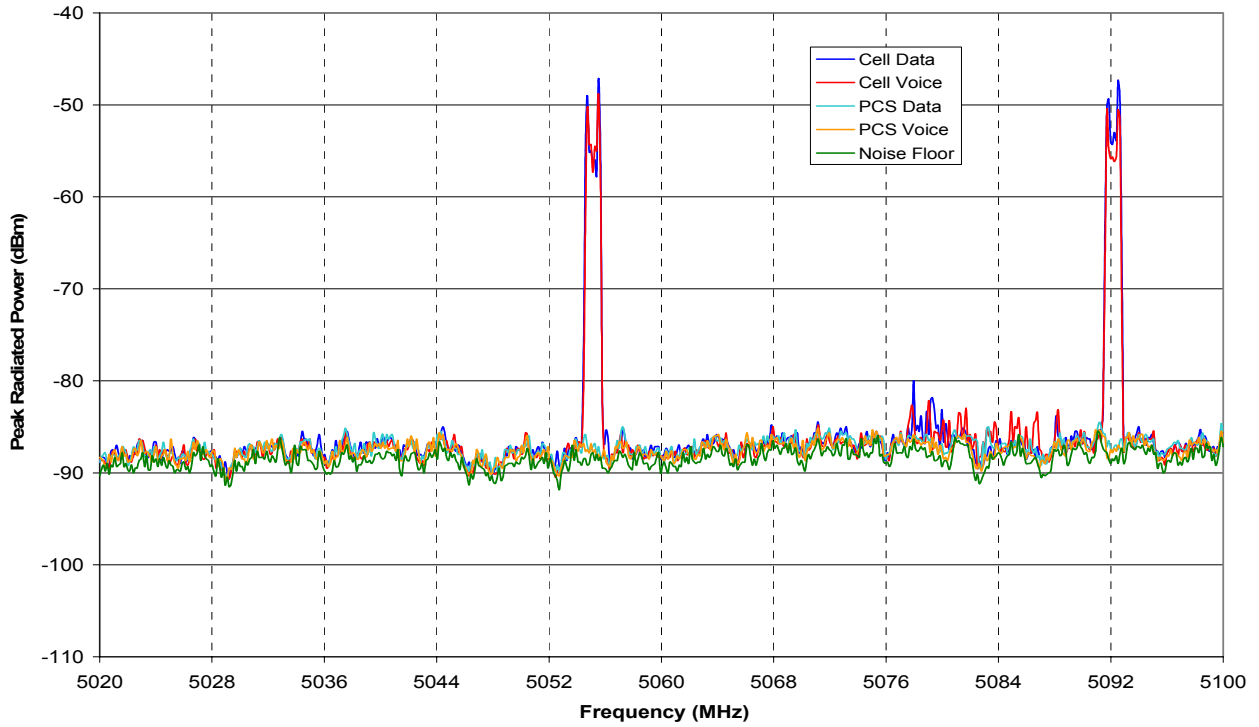


Figure B74: GSM06 four mode envelopes, Band 5.

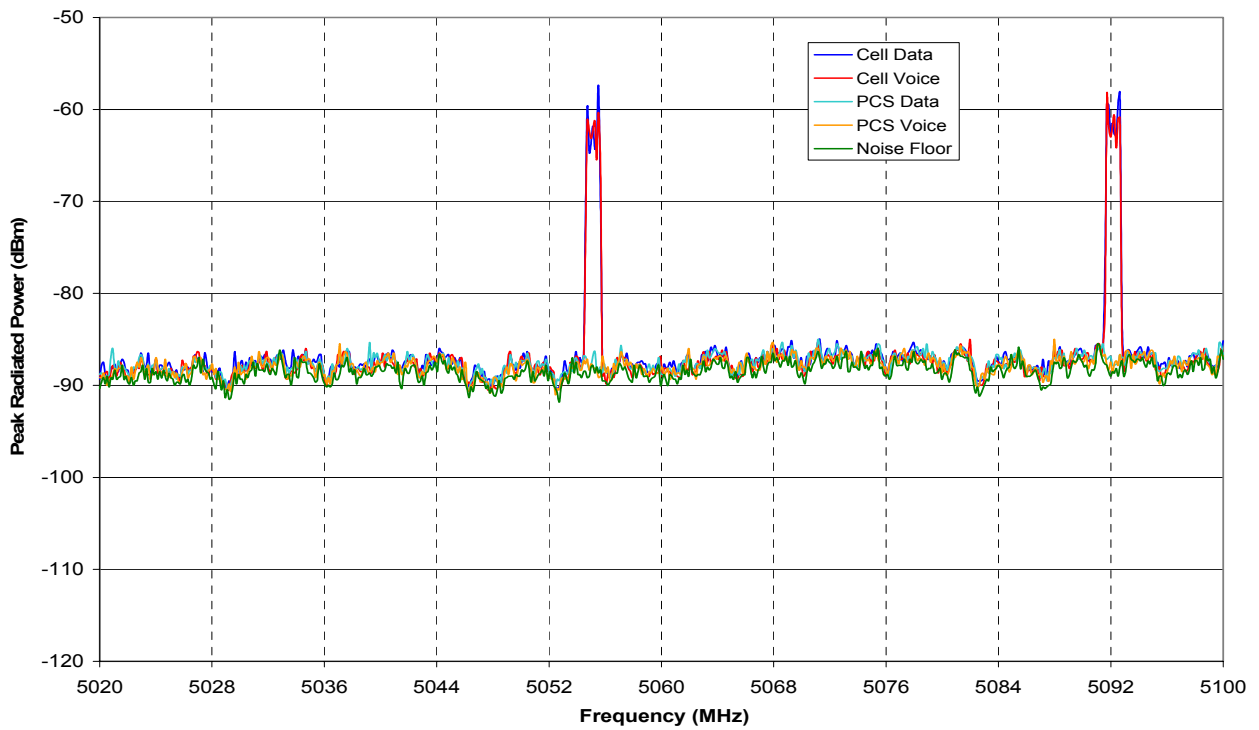


Figure B75: GSM07 four mode envelopes, Band 5.

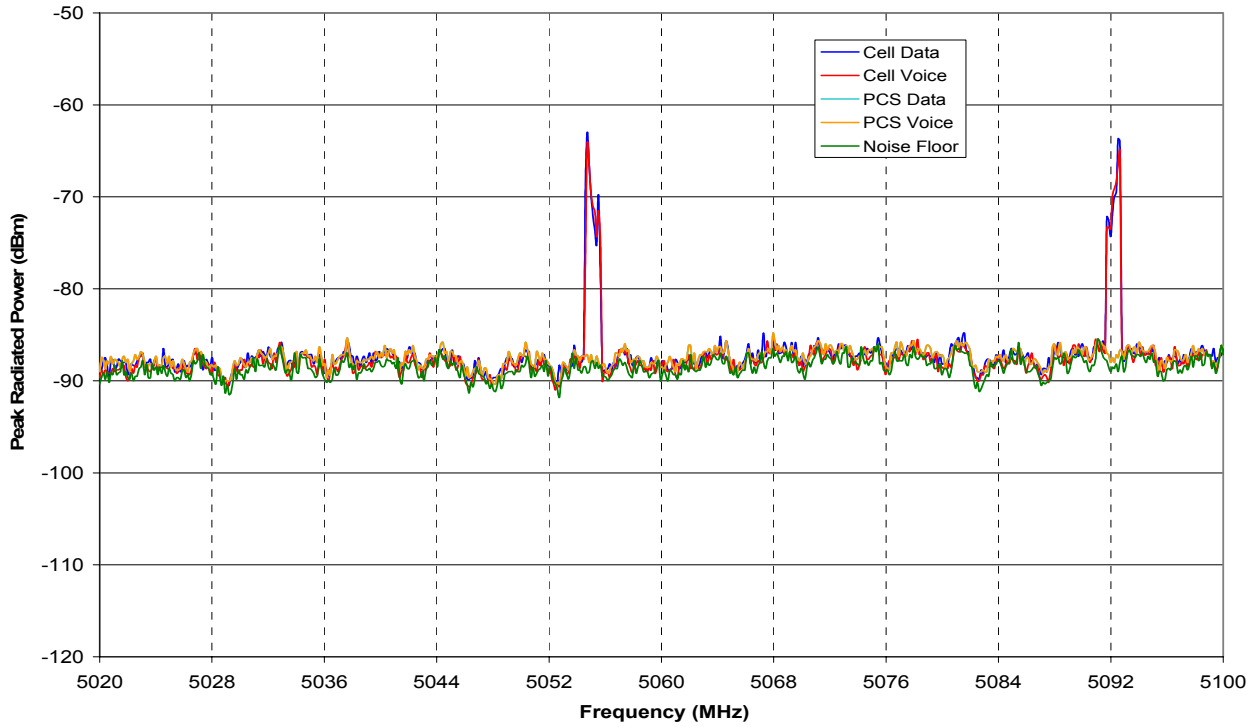


Figure B76: GSM08 four mode envelopes, Band 5.

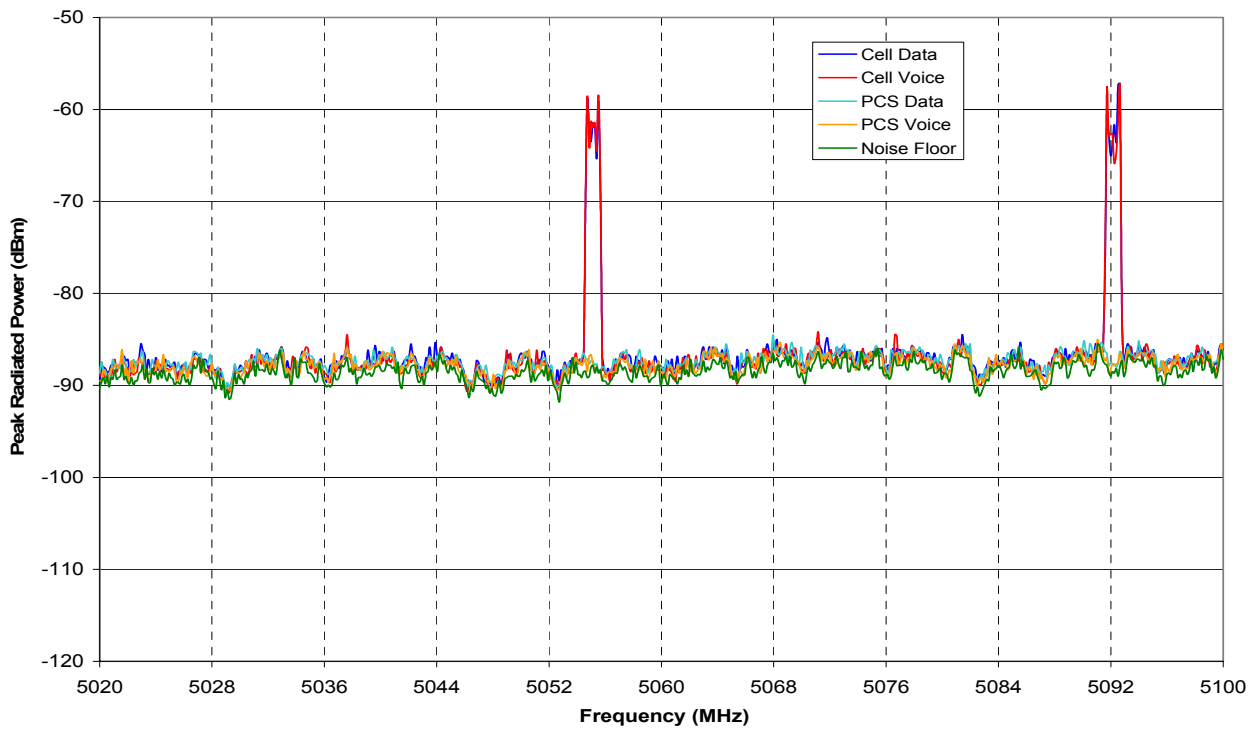


Figure B77: GSM09 four mode envelopes: Band 5.

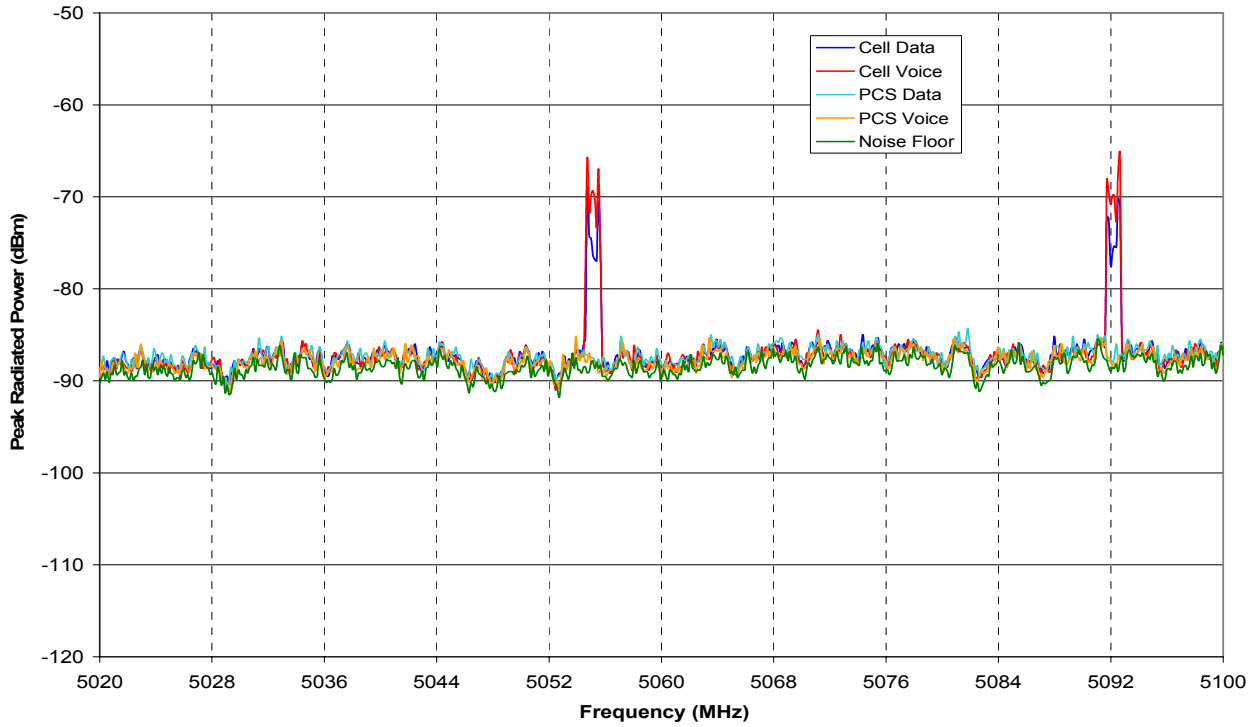


Figure B78: GSM10 four mode envelopes, Band 5.

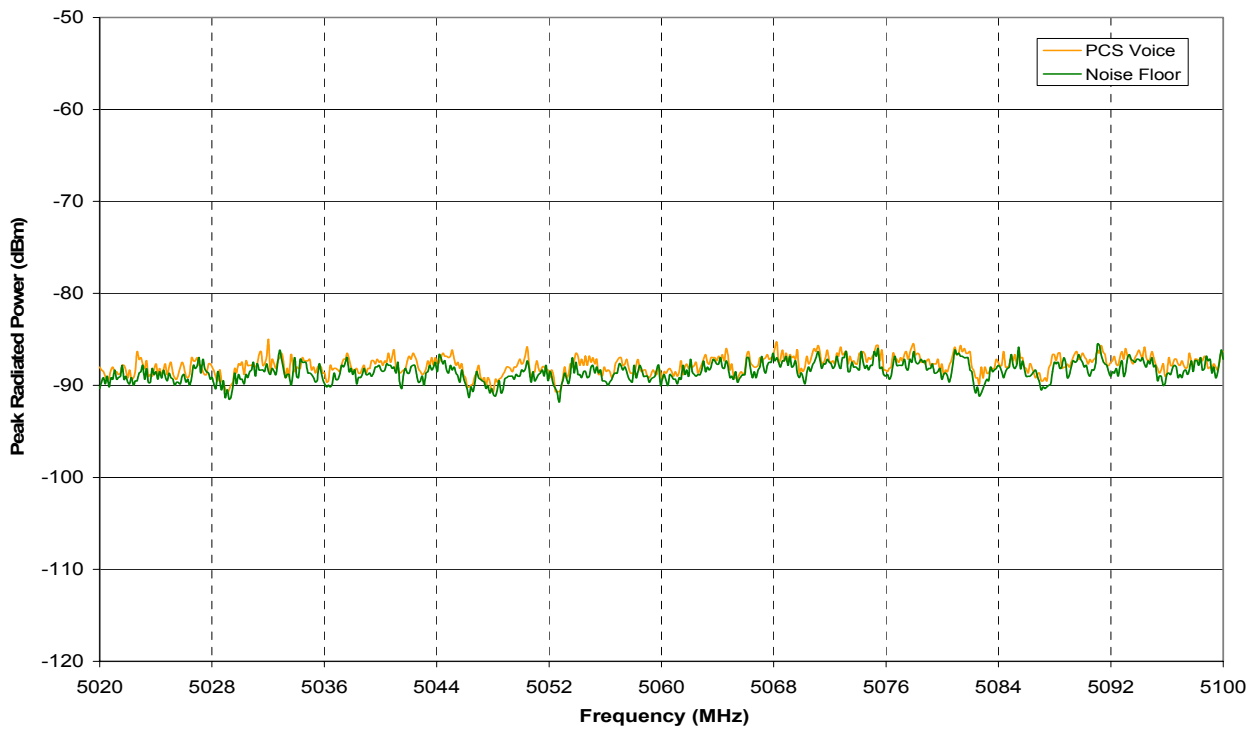


Figure B79: GSM11 one mode envelope, Band 5.

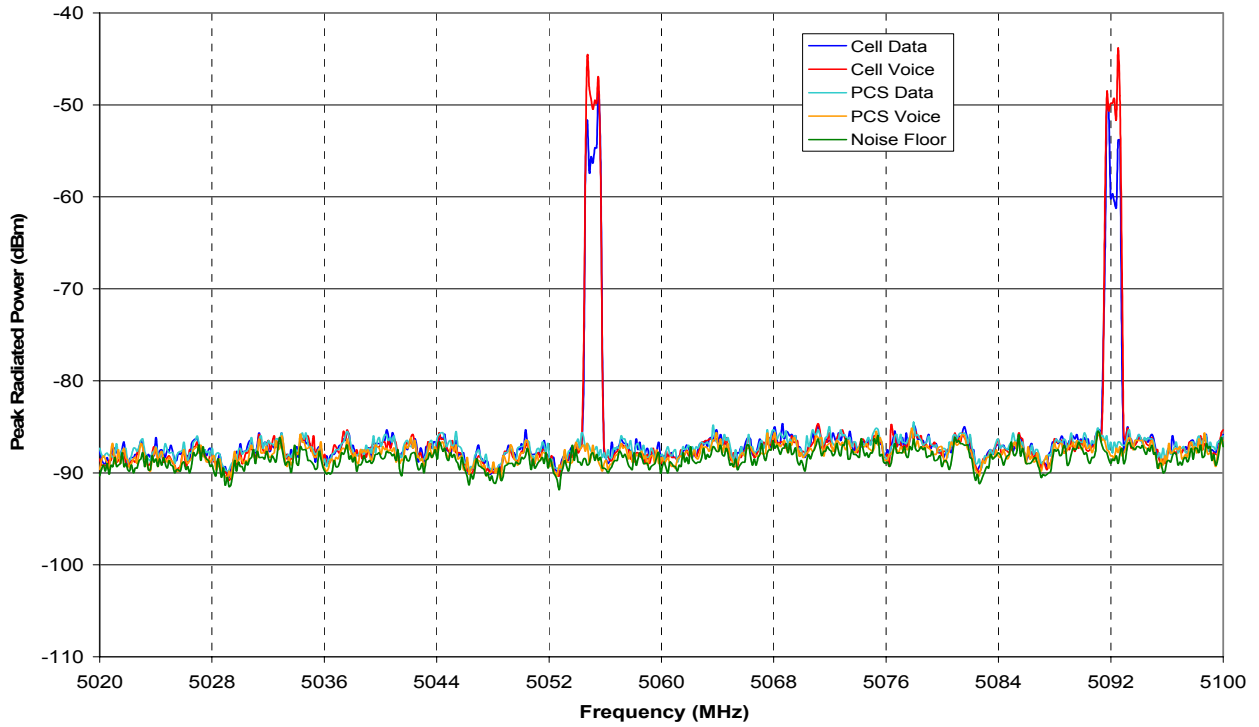


Figure B80: GSM12 four mode envelopes, Band 5.

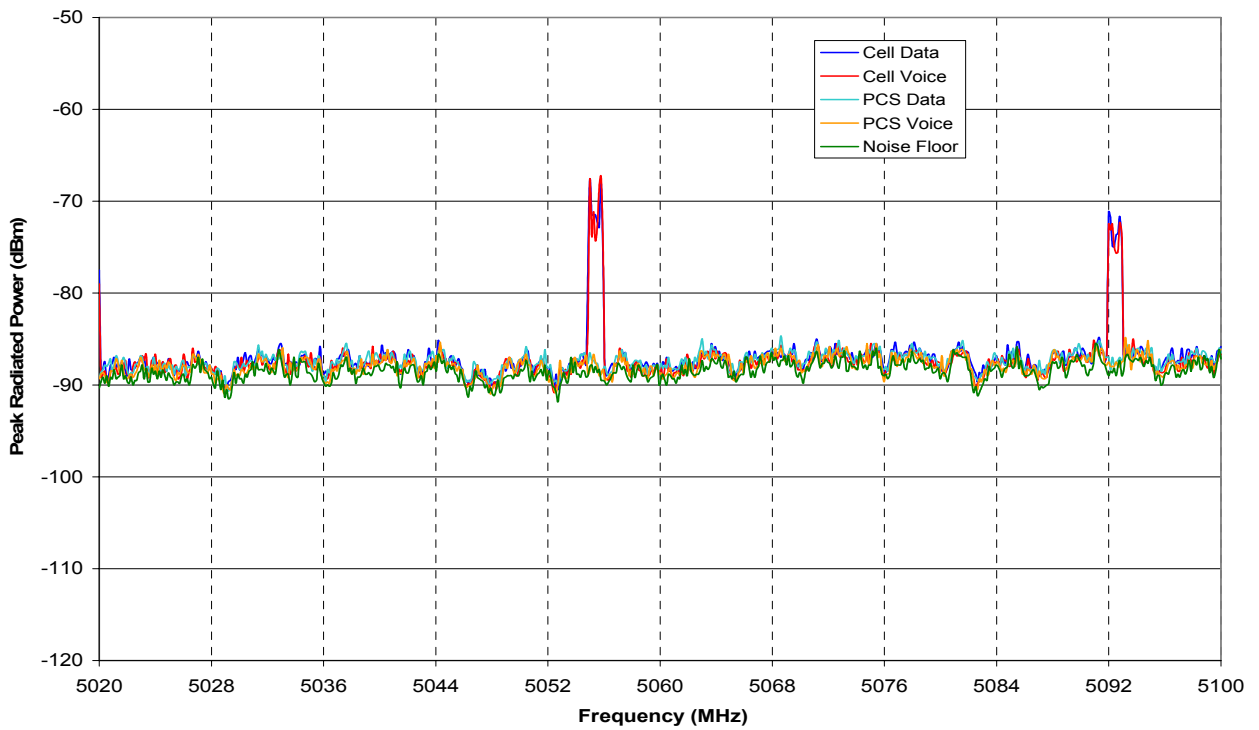


Figure B81: GSM13 four mode envelopes, Band 5.

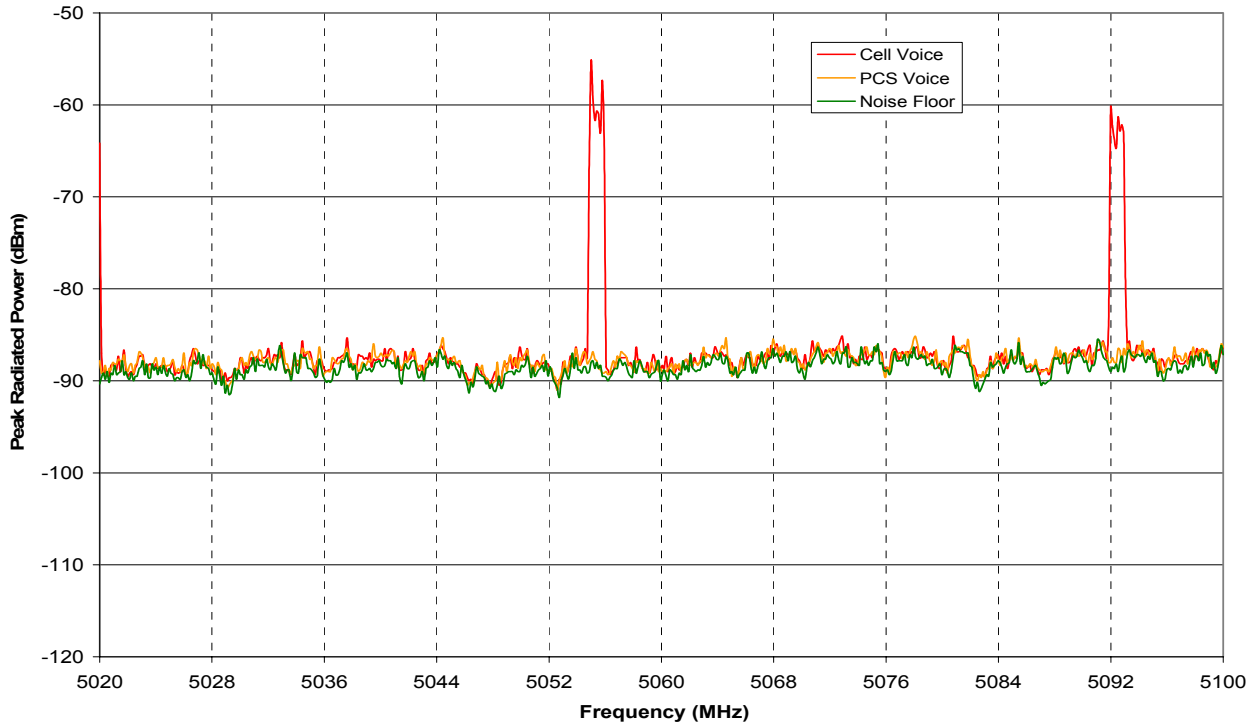


Figure B82: GSM14 two mode envelopes, Band 5.

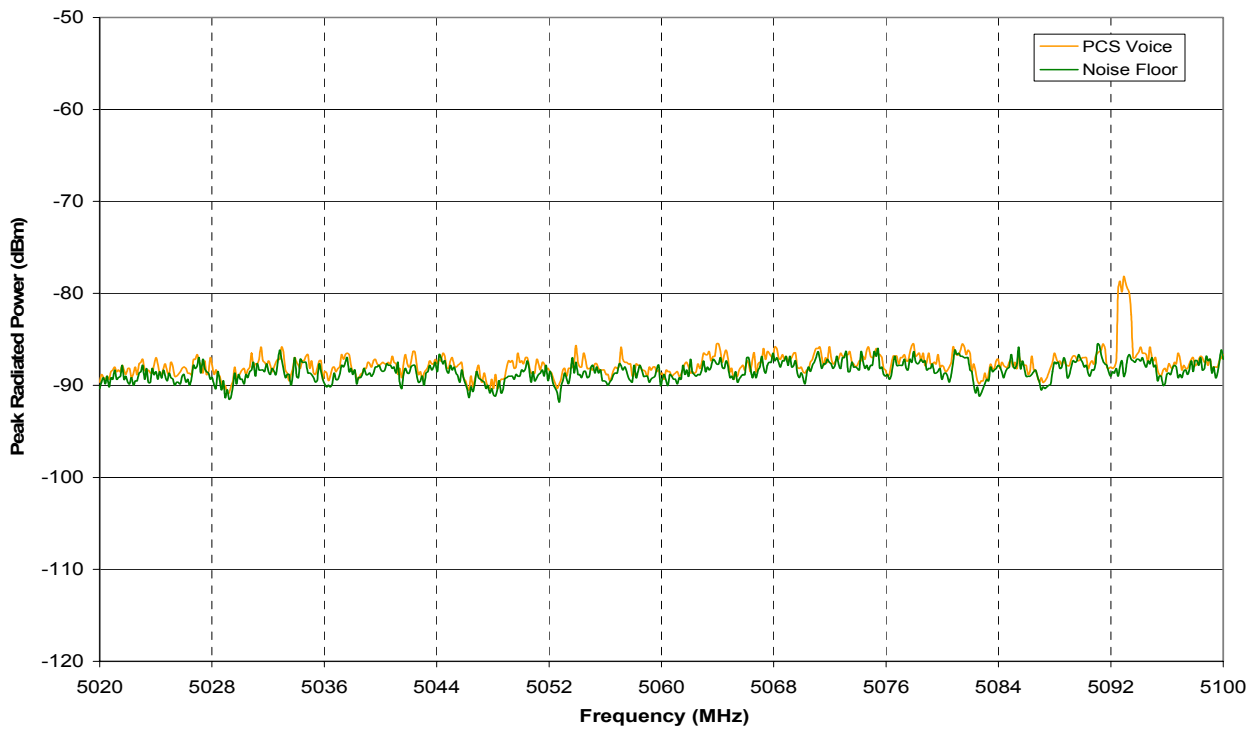


Figure B83: GSM15 one mode envelope, Band 5.

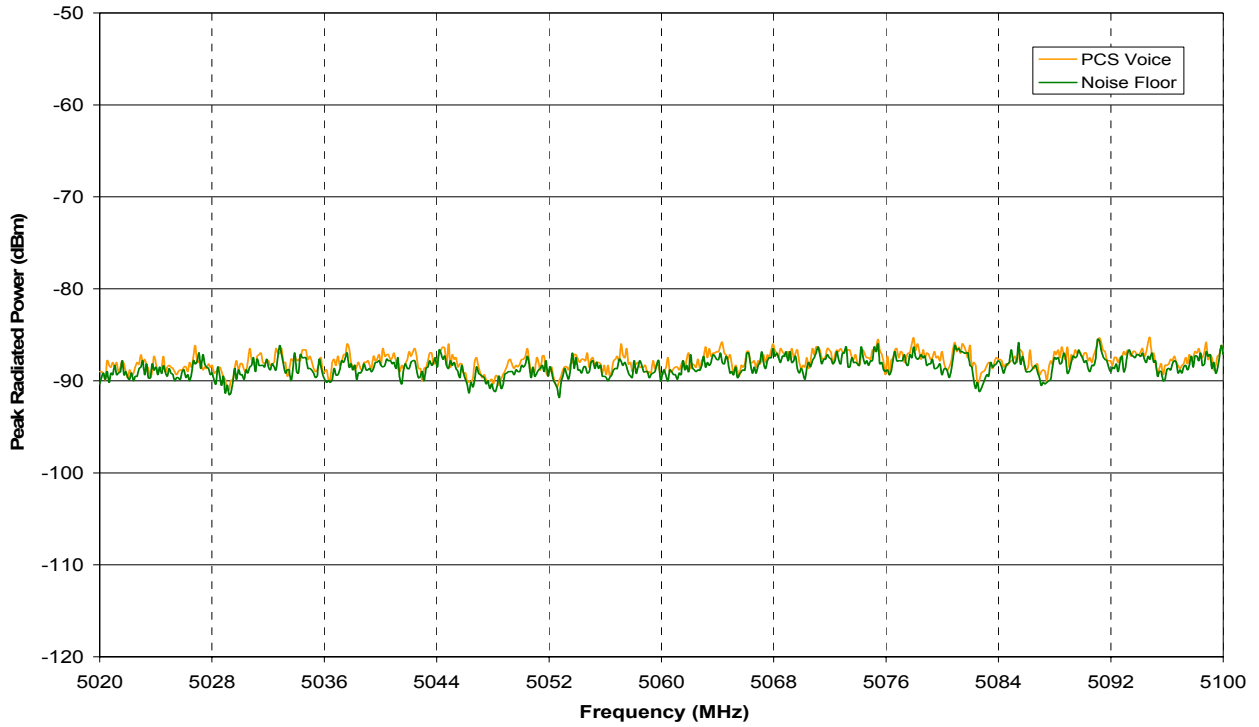


Figure B84: GSM16 one mode envelope, Band 5.

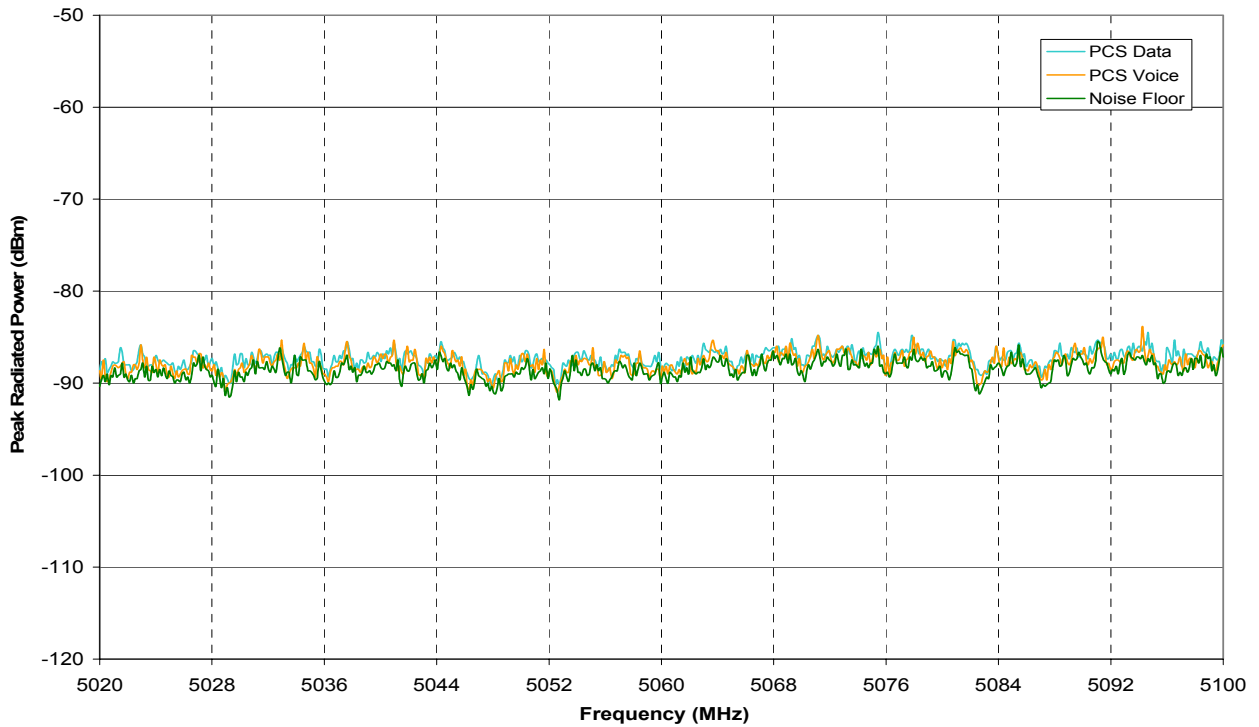


Figure B85: GSM17 two mode envelopes, Band 5.

(This page intentionally left blank)

Appendix C: Comparisons of MEF Using Window IPL

Section 6 data show that *full-aircraft* MEF can be determined within approximately 1 dB by using the *window* IPL data. (For simplicity MEF_{window} refers to MEF computed from window IPL data as described in Section 6). While this observation needs further validation, it would be of interest to compare MEF_{window} for different aircraft. This comparison may provide an insight into of aircraft-to-aircraft variations of the true MEF.

Window IPLs for six B737 aircraft were reported in Section 6. These aircrafts were measured using the same method, thus variations associated caused by test methodology is minimized. Using these data, MEF_{window} are computed and compared in Figures C1 to C4 for LOC/VOR, VHF-Com, and TCAS. In addition, similar comparison for the GPS system is also shown in C-4, even though full-aircraft IPLs were not available for comparison in Section 6.

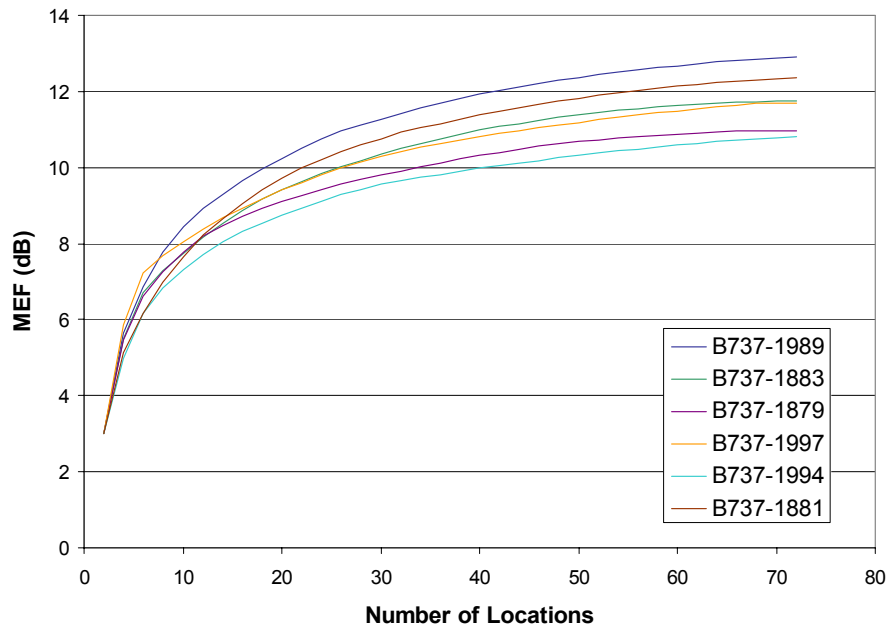


Figure C1: MEF computed using window IPL. LOC/VOR Tail.

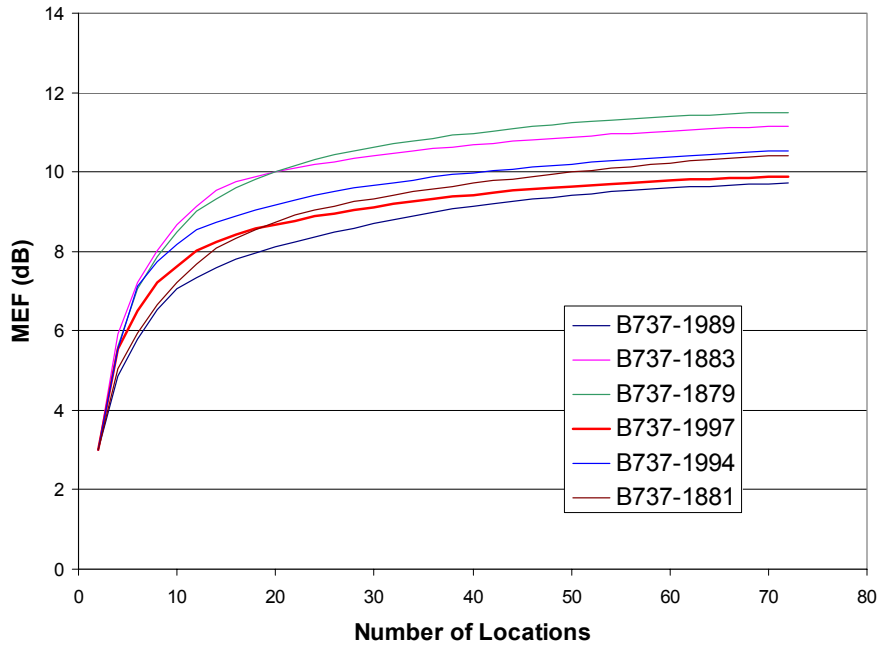


Figure C2: MEF computed using window IPL. TCAS-Top

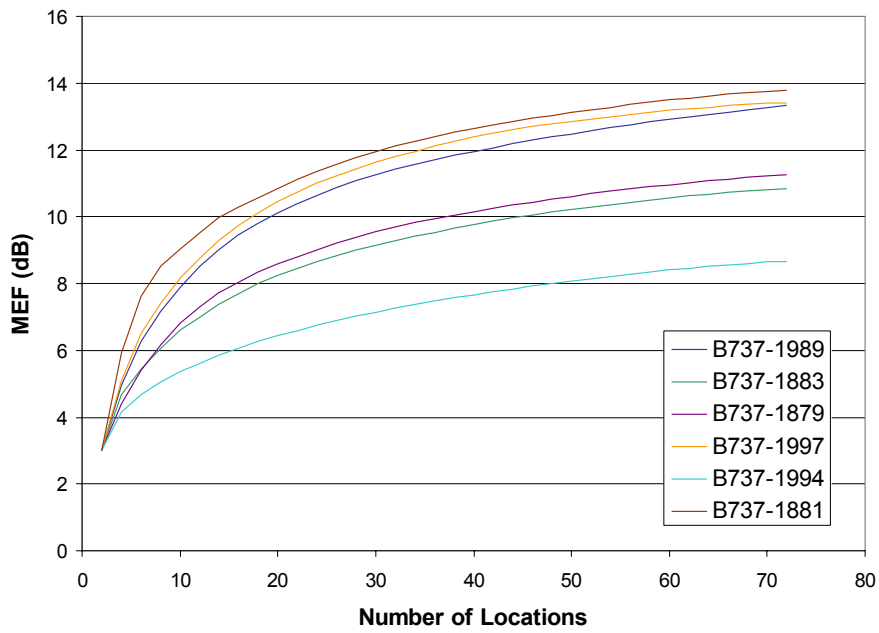


Figure C3: MEF computed using window IPL. VHF-Top.

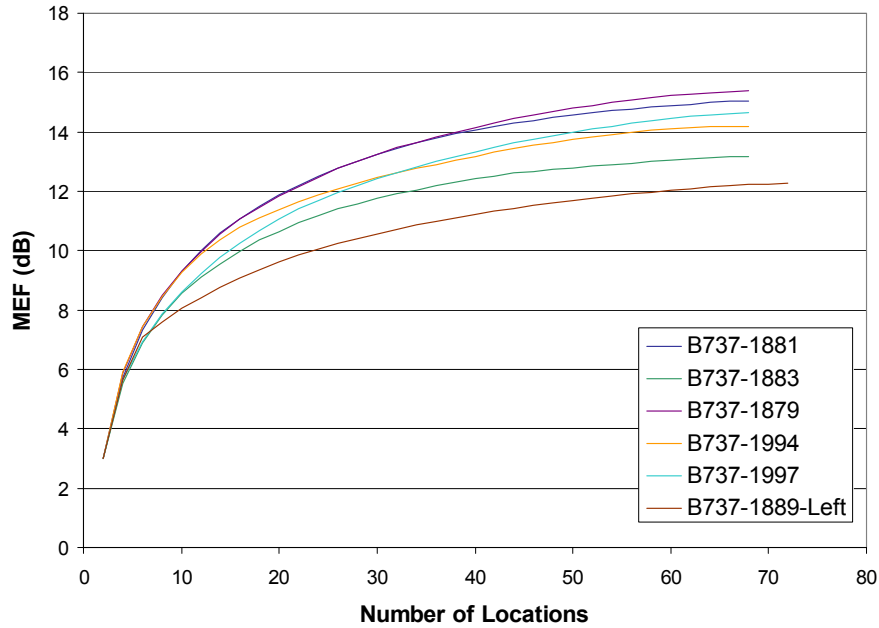


Figure C4: MEF computed using window IPL. GPS-Top.

It is observed that MEF_{window} varies between 2 and 3.5 dB, with the exception of one aircraft in the VHF band (B737-1994). The most likely source of the deviation is suspected to be the differences in airplane configuration. Many of the airplanes were empty (without seats) at the time of measurement. In other cases, seats were blocking the windows that were closest to the aircraft antennas of interest, thereby reducing radiation efficiency out of the windows. It is expected that similar variations would appear in the MEF calculated using the full-aircraft IPL data.

REPORT DOCUMENTATION PAGE				Form Approved OMB No. 0704-0188	
<p>The public reporting burden for this collection of information is estimated to average 1 hour per response, including the time for reviewing instructions, searching existing data sources, gathering and maintaining the data needed, and completing and reviewing the collection of information. Send comments regarding this burden estimate or any other aspect of this collection of information, including suggestions for reducing this burden, to Department of Defense, Washington Headquarters Services, Directorate for Information Operations and Reports (0704-0188), 1215 Jefferson Davis Highway, Suite 1204, Arlington, VA 22202-4302. Respondents should be aware that notwithstanding any other provision of law, no person shall be subject to any penalty for failing to comply with a collection of information if it does not display a currently valid OMB control number.</p> <p>PLEASE DO NOT RETURN YOUR FORM TO THE ABOVE ADDRESS.</p>					
1. REPORT DATE (DD-MM-YYYY)		2. REPORT TYPE		3. DATES COVERED (From - To)	
01- 03 - 2005		Technical Publication			
4. TITLE AND SUBTITLE Third Generation Wireless Phone Threat Assessment for Aircraft Communication and Navigation Radios				5a. CONTRACT NUMBER	
				5b. GRANT NUMBER	
				5c. PROGRAM ELEMENT NUMBER	
6. AUTHOR(S) Nguyen, Truong X.; Koppen, Sandra V.; Smith, Laura J.; Williams, Reuben A.; and Salud, Maria Theresa P.				5d. PROJECT NUMBER	
				5e. TASK NUMBER	
				5f. WORK UNIT NUMBER 23R-722-96-9D11-02	
7. PERFORMING ORGANIZATION NAME(S) AND ADDRESS(ES) NASA Langley Research Center Hampton, VA 23681-2199				8. PERFORMING ORGANIZATION REPORT NUMBER L-19097	
9. SPONSORING/MONITORING AGENCY NAME(S) AND ADDRESS(ES) National Aeronautics and Space Administration Washington, DC 20546-0001				10. SPONSOR/MONITOR'S ACRONYM(S) NASA	
				11. SPONSOR/MONITOR'S REPORT NUMBER(S) NASA/TP-2005-213537	
12. DISTRIBUTION/AVAILABILITY STATEMENT Unclassified - Unlimited Subject Category 33 Availability: NASA CASI (301) 621-0390					
13. SUPPLEMENTARY NOTES Nguyen, Koppen, Smith and Williams: Langley Research Center; Salud: Lockheed Martin. An electronic version can be found at http://ntrs.nasa.gov					
14. ABSTRACT Radiated emissions in aircraft communication and navigation bands are measured from third generation (3G) wireless mobile phones. The two wireless technologies considered are the latest available to general consumers in the US. The measurements are conducted using reverberation chambers. The results are compared against baseline emissions from laptop computers and personal digital assistant devices that are currently allowed to operate on aircraft. Using existing interference path loss data and receivers' interference threshold, a risk assessment is performed for several aircraft communication and navigation radio systems. In addition, cumulative interference effects of multiple similar devices are conservatively estimated or bounded. The effects are computed by summing the interference power from individual devices that is scaled according to the interference path loss at its location.					
15. SUBJECT TERMS 3G; Aircraft; CDMA; Communication; Cumulative effects; GSM; Interference; Navigation; Radiated emission; Wireless phone					
16. SECURITY CLASSIFICATION OF:			17. LIMITATION OF ABSTRACT	18. NUMBER OF PAGES	19a. NAME OF RESPONSIBLE PERSON
a. REPORT	b. ABSTRACT	c. THIS PAGE			STI Help Desk (email: help@sti.nasa.gov)
U	U	U	UU	214	19b. TELEPHONE NUMBER (Include area code) (301) 621-0390